Photochromism of Arylazotetracyanocyclopentadienides and Excited State Activation Barriers of Dihydropyrene Switches

Dissertation

zur Erlangung des akademischen Grades
doctor rerum naturalium
(Dr. rer. nat.)
im Fach Chemie

eingereicht an der
Mathematisch-Naturwissenschaftlichen Fakultät
der Humboldt-Universität zu Berlin

von
Dipl.-Chem. Yves Garmshausen

Präsidentin der Humboldt-Universität zu Berlin
Prof. Dr. Sabine Kunst

Dekan der Mathematisch-Naturwissenschaftlichen Fakultät
Prof. Dr. Elmar Kulke

Gutachter/innen: 1. Prof. Stefan Hecht, Ph.D.
2. Prof. Dr. Emil List-Kratochvil
3. Prof. Dr. Matthew Fuchter

Tag der mündlichen Prüfung: 29.03.2019

Die vorliegende Arbeit wurde in der Zeit von Dezember 2013 bis November 2018 am Institut für Chemie der Humboldt-Universität zu Berlin unter Anleitung von Prof. Stefan Hecht, Ph.D. angefertigt

„Als erstes muss man das Spiel an sich reißen!“

- Rainer Garmshausen über die erste Regel im Skat (und im Leben)

Danksagung

Ich hatte viele Wegbegleiter und Wegbereiter, die zum Erfolg dieser Arbeit beigetragen haben. Zunächst möchte ich mich bei meinem Doktorvater Stefan Hecht bedanken, der die Bezeichnung Doktorvater ernsthaft verdient hat und mich nicht nur beruflich, sondern auch privat immer unterstützt hat. Ich habe in den letzten Jahren immer die richtige Mischung aus Fordern und Fördern erfahren, sodass ich mich zu dem Chemiker entwickeln konnte, der ich heute bin. Ich glaube es gibt kaum ein Umfeld, dass besser geeignet ist, Menschen kreativ, eigenständig und erfolgreich zu machen, als diese Arbeitsgruppe.

Außerdem gilt mein Dank natürlich meiner Familie, insbesondere meinen Eltern, die mir die Möglichkeit gaben, das Leben zu führen, das ich führe. Fine und in den letzten 1 ¾ Jahren Bella haben mir bei allen Anstrengungen so unglaublich viel Freude beschert, dass ich wünschte die Tage hätten mehr als 24 Stunden. Es tut mir leid, dass ich oft unser gemeinsames Abendessen verpasst habe und dass viele Dinge gerade in den letzten Monaten an Fine hängen geblieben sind.

Ein guter Koch geht durch sieben Küchen, bevor er fertig ist. Da die Chemie handwerklich wenigstens ähnlich ist, verhält es sich auch hier so, dass es viele Lehrmeister braucht: Ich hatte die große Freude zum Beginn meiner Zeit im AK Hecht viel von Michael Pätzel und Björn Kobin lernen zu dürfen. Später habe ich von Martin Herder die Grundzüge der Photochemie und von Philipp Viehmann, Antti Senf und Alexis Goulet-Hanssens die Feinheiten der Synthese mitbekommen.

Während meiner Dissertation gab es etliche „Altlasten“ an Sexiphenylen abzuarbeiten und ich möchte Jutta Schwarz und Jana Hildebrandt danken, dass sie mir viel lästige Synthese abgenommen haben. An dieser Stelle sei auch meinen Kooperationspartnern gedankt, die aus meinem ersten Projekt eine ganze Reihe von interessanten Studien gemacht haben. Insbesondere die Arbeit mit Anton Zykov war ein Hochgenuss in vielerlei Hinsicht und hat mir schöne Einblicke in die Physik verschafft. Genauso möchte ich explizit Giovanni Ligorio danken, der von physikalischer Seite die Anwendung meiner Photoschalter auf Oberflächen hochmotiviert vorangetrieben hat.

Ich hatte die große Freude mit vielen hervorragenden Chemikern gemeinsame Projekte zu bearbeiten. Dabei danke ich meinen Bachelorstudenten Stephan Lüdtke, Alexander Arndt und Jonas Becker, wobei letzterer mir auch als studentische Hilfskraft viel geholfen hat. Florian Römpp und Bernd Schmidt danke ich für sämtliche Kristallstrukturen in dieser Arbeit, die ohne die beiden nicht gemessen worden wären. Ebenso danke ich Lutz Grubert, für elektrochemische Untersuchungen meiner Substanzen, auch wenn diese es nicht in die Arbeit geschafft haben. Thanks go to Wenjie Han for starting a project of which I was not convinced in the beginning but which turned out to result in simply amazing molecules. Die Arbeit mit Dennis Chung-Yang Huang und Derk Jan van Dijken hat mir ein tiefgehendes Verständnis von Photoschaltern verschafft, von dem ich noch lange profitieren werde. Ellen Teichmann danke ich nicht nur fürs kritische Korrekturlesen, sondern auch für eine spitzen Zusammenarbeit während ihrer Masterarbeit und viele freundschaftliche Momente. Die Masterarbeit von Kristin Klaue war mir ebenso eine Freude, wie die viele gemeinsame Zeit im Labor und ihr stets offenes Ohr für alle Probleme, die ich beruflich oder privat hatte.

Wie eingangs erwähnt, ist Kreativität ein hohes Gut und es lässt sich nur durch Austausch und Diskussion fördern. Neben den bereits erwähnten Personen, möchte ich hier noch Björn Zyska hervorheben, der mit mir an einem Vorweihnachtsabend drei Stunden Spektroskopieexperimente diskutiert hat um mir dann zu erklären, dass er noch kein einziges von den entsprechenden Molekülen gemacht hat. Aus dieser Diskussion heraus bin ich aber auf die alte Webster Literatur gestoßen, welche

im Azokapitel gemündet ist, sodass es sich jedenfalls für mich gelohnt hat. Johannes Gurke hat mich ebenso in viele Diskussionen genötigt, die sich am Ende aber immer als spannend herausgestellt haben und bis zur sich schließenden S-Bahntür mit aller Härte geführt wurden. Außerdem hatte ich sehr kreative Unterhaltungen mit Michael Kathan, dem ich außerdem für eine sehr gute Korrekturlesung dankbar bin. Leider habe ich zu spät erkannt, wie gut wir miteinander auskommen, sodass es nie ein gemeinsames Projekt gab. Aber wer weiß was die Zukunft noch bringt!

Abstract

The reversible, light induced interconversion between two species (photochromism) offers additional control over a molecular system by an external stimulus. Besides the fact that mother nature frequently uses such interconversions to regulate biological processes, this feature has been widely employed to introduce superior functionality in materials, devices, catalysts, molecular machines or biological systems. To give some examples, it is therefore possible not to just add a catalyst to a reaction mixture, but to switch it on and off on demand, by shining light on the reaction. The conditions under which a device (*e.g.* a field-effect transistor) functions can be changed by the color of light, which is applied as the external stimulus. Specialized polymeric materials can be made which respond to light by a change of their physical properties, resulting in different viscoelasticity or conductivity.

However, any application of photochromism relies on a deep understanding of the structural features which influence the switching. The ability to tailor the photochromic properties to the envisioned application is the basis for developing materials with suitable functions beyond everything chemistry in the ground state offers. It is of special interest to develop photoswitches which work with visible light only, as it is abundant, requires simple, low-cost equipment to work with, and causes no harm to living cells and organisms in contrast to UV-light. After a general background on photochromism from the perspective of definitions and practical aspects, a classification of photoswitches based on their switching mechanism will be given. This work covers two classes of switches, which can be operated with visible light and rely on the main photoreactions used for photochromic materials: 6 π electrocyclization and E/Z isomerization.

For the dihydropyrene system 6 π electrocyclization is usually fast, while the cycloreversion is inefficient, due to an activation barrier in the excited state. It is shown, how substitution with donor and acceptor moieties creates a push-pull system, causing a bathochromic shift of the absorption spectrum to the far red (730 nm onset). The push-pull system induces a dipole in the dihydropyrene, which lowers its excited state activation barrier and therefore increases the quantum yield of the cycloreversion. Further it is shown, how this can be performed in a catalytic fashion, where protonation leads to a species with a lower barrier in the excited state. As dihydropyrenes absorb in the visible and are considered as T-type negative photochromic, they can be switched without the use of UV-light.

In case of the azobenzene class, a new aromatic substitute for one of the benzene rings is investigated and shows superior switching properties. The anionic tetracyanocyclopentadienyl moiety can be synthesized as the corresponding amine or diazonium salt, allowing for direct coupling to the second aromatic substituent. The typical problem of addressability with only visible light is solved by a splitting of the bathochromic absorption bands for both isomers. Band separation of up to 80 nm is shown, along with high photostationary states ≈ 90% favoring each of the two switching directions. Interestingly, the extinction coefficient especially of the E isomer increases to $\varepsilon \approx$ 20000 L $mol^{-1}cm^{-1}$, dramatically enhancing the absorptivity compared to normal azobenzenes. Furthermore, the solubility can be tuned by proper choice of the cation, which is used to investigate solvent effects in nonpolar, polar, and protic (water) solvents as well as in an ionic liquid. With increasing polarity, the absorbance of the E isomer is shifted to longer wavelengths, which is accompanied by a reduced thermal half-life. The half-life of the thermal reverse reaction can be tuned from 3 min to 13 h at ambient temperature. As one of the derivatives is easily protonated, switching of the corresponding azonium species has also been investigated and an astoundingly long thermal half-life of > 2 min at room temperature has been observed.

Zusammenfassung

Die reversible, lichtinduzierte Umwandlung zwischen zwei Spezies (Photochromie) bietet zusätzliche Kontrolle über ein molekulares System durch einen externen Stimulus. Abgesehen von der Tatsache, dass die Natur solche Umwandlungen häufig nutzt um biologische Prozesse zu regulieren, wurden jene Effekte genutzt um verbesserte funktionale Materialien, elektronische Bauteile, Katalysatoren, molekulare Maschinen oder biologische Systeme herzustellen. Um einige Beispiele zu geben, ist es möglich nicht nur einen Katalysator zu einem Reaktionsgemisch zuzugeben, sondern diesen nach Bedarf an- und auszuschalten, indem Licht auf die Reaktionsmischung einwirkt. Die Bedingungen unter denen ein elektronisches Bauteil (zum Beispiel eine Feldeffekttransistor) funktioniert, können abhängig von der Farbe des externen Stimulus Licht modifiziert werden. Spezielle Polymermaterialien, welche auf Lichteinwirkung mit einer Änderung ihrer Leitfähigkeit oder viskoelastischen Eigenschaften reagieren, können ebenso hergestellt werden.

Nichtsdestotrotz basiert jede Anwendung von Photochromie auf einem tiefergehenden Verständnis der Zusammenhänge von Strukturmotiven und den resultierenden Schalteigenschaften. Die Möglichkeit des Anpassens der photochromen Eigenschaften an die entsprechende Anwendung ist die Grundvoraussetzung um neue Materialien mit Funktionen jenseits der Chemie des Grundzustands zu entwickeln. Besonderes Interesse gilt hierbei Schaltern die ausschließlich mit sichtbarem Licht arbeiten, da dieses frei verfügbar, apparativ günstig und nicht zellschädigend ist (im Vergleich zu UV-Licht).

Nach einer generellen Einführung in die Photochromie, bestehend aus Grundbegriffen und praktischen Aspekten, folgt eine Klassifizierung von Photoschaltern nach ihrem allgemeinen Schaltmechanismus. Diese Arbeit umfasst zwei Klassen von Photoschaltern, die auf den gängigsten Photoreaktionen in photochromen Systemen basieren, der $6\,\pi$ Elektrozyklisierung und der E/Z Isomerisierung von Doppelbindungen.

Für Dihydropyrene ist die $6\,\pi$ Elektrozyklisierung für gewöhnlich schnell, wohingegen die Cycloreversion durch eine Aktivierungsbarriere im angeregten Zustand ineffizient wird. Es wird gezeigt, wie durch Substitution mit Donor- und Akzeptorgruppen ein „push-pull“ System aufgebaut wird, welches eine bathochrome Verschiebung der Absorption in den tief roten Bereich (730 nm onset) zur Folge hat. Das „push-pull” System polarisiert den Dihydropyrenkern, was ein Absenken der Aktivierungsbarriere im angeregten Zustand zur Folge hat und in einer erhöhten Quantenausbeute für die Cycloreversion resultiert. Es wird weiter gezeigt, wie dies in nicht-permanenter Art und Weise durch Katalyse vollzogen werden kann, indem eine protonierte Spezies mit einer geringeren Aktivierungsbarriere im angeregten Zustand gebildet wird. Da Dihydropyrene im sichtbaren Bereich absorbieren und im Allgemeinen als T-Typ negativ photochrom betrachtet werden, ist ein Schalten ohne die Verwendung von UV Licht möglich.

Für die Substanzklasse der Azobenzole wird ein neuer aromatischer Substituent anstelle eines der Phenylreste untersucht, welcher verbesserte Schalteigenschaften zeigt. Die anionische Tetracyanocyclopentadienyl Gruppe kann als das entsprechende Amin oder Diazoniumsalz hergestellt werden, was die direkte Kupplung zum zweiten Arylrest erlaubt. Das typische Problem der Adressierbarkeit mit ausschließlich sichtbarem Licht wird durch eine Separation der bathochromen Absorptionsbanden beider Derivate gelöst. Die Bandenseparation von bis zu 80 nm erlaubt hohe photostationäre Zustände von $\approx 90\,\%$ für beide Richtungen. Interessanterweise zeigen die untersuchten Derivate besonders für das E Isomer extrem hohe Extinktionskoeffizienten von

$\varepsilon \approx 20000$ L mol^{-1}cm^{-1}, was zu einer bedeutend gesteigerten Absorption im Vergleich zu herkömmlichen Azobenzolen führt. Weiterhin kann die Löslichkeit der Verbindungen, durch die Wahl des Gegenions moduliert werden, was es ermöglicht Lösungsmitteleffekte in unpolaren, polaren und protischen (Wasser) Lösungsmitteln, sowie einer ionischen Flüssigkeit zu untersuchen. Mit höherer Polarität des Lösungsmittels wird die Absorptionsbande des E Isomers zu längeren Wellenlängen hin verschoben, was mit einer schnelleren thermischen Rückreaktion einhergeht. Die thermische Halbwertzeit der Rückreaktion kann zwischen 3 min und 13 h bei 25 °C eingestellt werden. Da eines der Derivate leicht zu protonieren ist, wurde auch das Schaltverhalten einer Azoniumspezies untersucht und eine erstaunlich lange thermische Halbwertzeit von > 2 min beobachtet.

Table of Content

1 Introduction

Once upon a time, when chemistry was not based on structures but rather on composition and appearance of substances, the mineralogist Robert Allan described a reversible light induced color change in hackmanite minerals in his 1834 “Manual of Mineralogy”.[1,2] Much later in 1867, after Kekulé´s pioneering work on the theory of chemical structure, Fritzsche found that solutions of tetracene would bleach in the sunlight and recover their color in the dark, which marks the first molecular example of photochromism.[3]

After 150 years of photochromic molecules in the scientific literature the number of new photoswitches still increases. While the field started from the attractive phenomenological approach, the color change of a material is a minor aspect of today’s research. Since color is just the most obvious result from the change of many physical properties, photochromism has been applied to various fields. Besides rather general applications of photoswitchable molecules, which include three-dimensional datastorage,[4,5] ion recognition, self-assembly modulation, surface property changes of nanoparticles,[6] and holography,[7–9] major advances have been conducted in the research areas of materials science,[10] devices,[11] catalysis,[12] molecular machines,[13] and life science.[14]

Polymer chemistry offers a broad range of materials with various property combinations. Photochromism has been used to modify these properties by implementing photoswitches into the polymer. Upon light irradiation, diarylethenes switch between a less conjugated and a highly conjugated form. Incorporation of a diarylethene has therefore been shown to allow modulation of the conductivity of polymers depending on the applied wavelength.[15] Attachment of azobenzene end groups results in light induced solubility tuning of polymers based on the higher polarity of the Z isomer.[16] Azobenzene in the E isomer binds well to α-cyclodextrin allowing for the formation of supramolecular hydrogels, when both are attached to different polymers. Switching to the Z isomer interrupts the binding and therefore switches the material from gel to sol. Upon visible light irradiation or heating the material solidifies again.[17] Such an interaction can also be used to provide the functionality of healing mechanical damage (*e.g.* a scratch or rupture) by the means of light.[18] Controlling dynamic covalent chemistry by light has led to other light healable polymers based on the Diels-Alder reaction,[19] imine formation,[20] or trithiocarbonate reshuffling.[21]

Although devices based on inorganic materials, such as silicon solar cells, can profit from low manufacturing costs, the combination of organic and inorganic materials enhances the possibilities for specialized and tailored applications dramatically. Given the huge amount of polymeric and small molecule organic semiconductors, it is still challenging to produce organic light emitting devices (OLEDs) or organic field effect transistors (OFETs), which can compete with silicon-based technology. Incorporation of photoswitches in such devices, results in an additional level of control, unachievable in purely inorganic devices.[11] It has been shown that doping of an insulating layer in an OFET device with spiropyran molecules can be used to modulate the electric properties. Upon UV irradiation the spiropyran opens to the merocyanine, which has a large dipole moment and causes a change in the dielectric bulk properties of the insulating layer. As a consequence, the source-drain current increases, which is reversible upon visible light treatment or thermal relaxation.[22] Similar effects have been observed using azobenzene switches and their light induced dipole change.[7,23] Conceptually different, the change in the HOMO-LUMO gap of diarylethene photoswitches can be used to reversible switch

the injection barrier for holes in OLED devices. By irradiation with a photomask, the electroluminescence can be shut down in specific areas of the OLED.[24]

The opportunity to switch the activity of a catalyst by light has attracted researchers to investigate various approaches, such as the functionalization of an enzyme with an azobenzene moiety to alter the binding affinity of the substrate depending on the azobenzene configuration.[25] Alternately, the azobenzene can compete with the substrate, blocking the binding site in one state, while the other state leaves the binding site free to enable the catalytic activity.[26] More general, an azobenzene can be used to reversibly block the basic site of an amine and therefore switch on or off general base catalysis.[27,28] By incorporation of the active imidazolium salt into a diarylethene switch rather electronic than steric effects have been used for switching the activity of N-heterocyclic carbenes.[29] A diarylethene ligand has also been utilized to change the coordination to a copper center from chelating to non-chelating, which results in light induced stereoselectivity switching.[30] More advanced applications of photoswitches in catalysis include the light induced aggregation and thereby deactivation of catalytically active nanoparticles,[31] as well as photoswitchable polymerization catalysts.[32]

In a chemical sense, life is a far-from-equilibrium system, which requires a permanent fuel supply. The sunlight can be regarded as primary fuel, from which molecular oxygen is produced by photosynthesis. In the human body, the energy stored in the oxygen is further converted to produce ATP as the main fuel. ATP is used in cells to enable the energy consuming processes in the body such as synthesis of biomolecules, mass transport, or muscle contraction. Molecular machines are the artificial analog to the biomolecules operating on ATP consumption in the cell. As any other machine which is supposed to do work, also a molecular machine has to reach its initial state by not going backwards the same way, which is usually accomplished by a rotation. To overcome the problem of microscopic reversibility, photoswitches provide an elegant way, since they intrinsically change the potential energy surface to undergo isomerization.[33] Utilizing C=C double bond isomerizations, unidirectional rotation of an aryl unit around the double bond has been achieved,[34,35] as well as a catenane, where one ring rotates with respect to the other in only one direction.[36]

The relatively young field of photopharmacology unites two of the oldest fields in organic chemistry: drug development and dye synthesis. Photoswitches offer the opportunity to activate and deactivate a drug in a temporally and locally defined manner, *e.g.* by shining light on a tumor, the drug becomes active in the tumor, but is deactivated thermally when leaving the light focus. Another appealing approach is to design drugs, which are deactivated by sunlight once they leave the body to tackle the problem of antibiotic resistances and active hormones in the environment. Although control over the activity of drugs has been shown for many examples, designing applicable photoswitchable drugs involves multiple challenges, such as low toxicity, metabolic stability, and water solubility. Besides finding suitable targets, light delivery to the place of action within the body is still the main issue. A common way involves a light guide, which requires an incision and is technically not limited to certain wavelengths. However, since UV-light damages cells, drugs should at least rely on visible light photochromism, especially, since the protective skin is not present within the body. The simplest approach is to shine the light through the tissue, which is associated with the problem of penetration depth. Below 600 nm the hemoglobin absorbs, which makes switching in both directions with light of longer wavelengths than 600 nm necessary. Due to scattering effects, near infrared light can penetrate deeper into the tissue, making even longer wavelengths attractive. To give an example, for brain tissue (postmortem) the penetration depth (reduction to 1/e or 37% of the intensity) is 0.92 mm at 633 nm and 2.5 mm at 835 nm.[37–39] Photoswitches that operate above 800 nm are especially difficult to design

and are only know in the dihydropyrene series.[40] Their extensive use as food dyes renders azobenzenes predestinated for photopharmacological applications, as there is a solid knowledge on toxicity and metabolism of these compounds. There are several strategies available to implement azobenzenes in drugs: Azologization resembles the substitution of a structural similar part of a non-switchable drug by an azobenzene moiety, *e.g.* benzyl phenyl ether could be substituted by E azobenzene. The other common approach is to attach an azobenzene to the backbone of an existing drug.[14]

The possibility to activate and deactivate a process with an external stimulus allows for superior control over this process. Light as a stimulus has the undoubted advantage of being non-invasive in contrast to other stimuli such as pH. It further offers the opportunity to decide, when and where a reaction happens, although one has to be honest about the limits. The spatial resolution is usually restricted by the Abbe limit, which would require short wavelengths for a better resolution. On the contrary, current research focusses on the exclusion of UV-light, for it harms tissue, causes side reactions on many photoswitches, and is relatively expensive in application. The temporal resolution highly depends on the application and the number of switches, which are to be operated, as it is much faster to "pour 1 mole of HCl in a beaker, than producing 1 mole of photons with artificial light sources". Too intense light may cause side reactions as well, limiting the temporal resolution further. Within these constrains, light allows to apply a stimulus to a closed system through a window, which is otherwise almost impossible. Furthermore, the sun provides light of a broad range of wavelengths for free and it is therefore the least expensive trigger one can think of.

All the examples mentioned above require reliable and predictable photoreactions with distinct property changes and switching efficiencies. Therefore, it is absolutely necessary to understand the influence of structural changes on the switching behavior for the successful application of photoswitches. A Google Scholar search for "photochromism" results in about 32000 hits, showing the huge amount of literature. However, the substance classes, which are able to undergo reversible light induced reactions, are by far not that many. Considering the underlying photoreactions behind the various types of photochromic systems, leaves only few different mechanisms.

This work deals with two classes of switches, which are based on the two main photochemical reactions in the field of photochromism: The 6 π electrocyclization in dihydropyrenes and the E/Z isomerization of a double bond in azobenzenes.

The 6 π electrocyclization is a quite efficient process, whereas the corresponding 6 π cycloreversion usually requires high light intensities and irradiation times. This process is often inefficient due to an activation barrier on the excited state potential energy surface. For the dihydropyrene class (Scheme 1), which suffers from such a barrier, a general strategy is developed to enhance the switchability by lowering this activation barrier. It is further shown, how this strategy can be used to catalyze the cycloreversion *via* a species with a smaller excited state activation barrier (a concept substantially different from excited state catalysis).

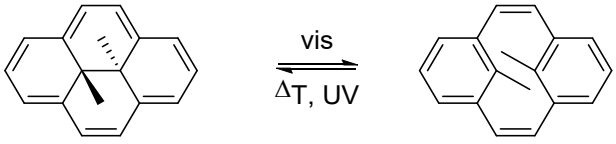

Scheme 1: 6 π electrocyclization and cycloreversion in dihydropyrenes.

The typical representative for an E/Z isomerization switch is azobenzene (Scheme 2), for which a new structural design is examined to overcome a few of the major problems. This study includes the addressability, solubility, absorptivity, as well as photokinetic properties of these switches.

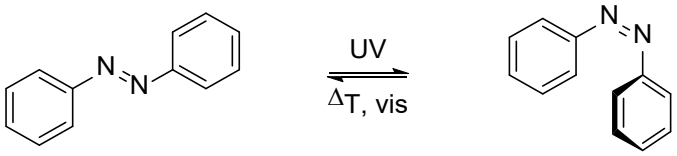

Scheme 2: E/Z double bond isomerization in azobenzene.

To give a theoretical background, some vocabulary about photochromism will be explained first. Thereafter, general and practical aspects are derived from thermodynamic and kinetic considerations and will be differentiated mostly between positive and negative photochromism. A broad overview on classes of photoswitches will be given, structured by the different types of photoreactions. As this work deals with dihydropyrene and azobenzene derivatives, these two classes will be discussed separately in more detail.

2 Theoretical Background

2.1 The Phenomenon of Photochromism

Photochromism describes the reversible interconversion between two species **A** and **B**, which is in at least one direction triggered by light. Since such a system is capable of switching forward and backward several times with light, it is referred to as a photoswitch. The reverse reaction can be induced by various stimuli besides light (P-type), which include oxidation/reduction and thermal energy. If the back reaction occurs thermally at ambient temperature, the system is referred to as T-type. A precise definition for a threshold rate/temperature of a T-type system is not at hand and the term may be used with care, since at a certain temperature most switches revert, or even at ambient temperature most switches revert with a slow rate, yet > 0. Since both species **A** and **B** are different, such an interconversion goes hand in hand with a change of the physical properties, of which the absorption spectrum or color is the most obvious one. If the thermodynamically stable form **A** absorbs light of longer wavelengths than the metastable form **B**, the term negative photochromism is used. “Positive photochromism” describes a thermodynamically stable form **A** which absorbs at shorter wavelengths than the metastable **B** (Figure 1).

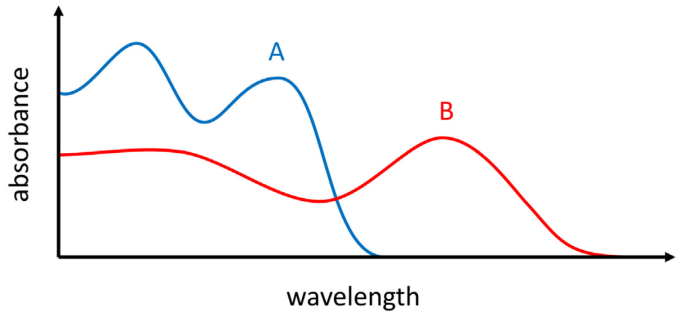

*Figure 1: Absorption spectra of species **A** and **B**, where **A** is the thermodynamically stable form (positive photochromism).*

The absorption spectrum is the first characterization of a photoswitch and obeys the Beer-Lambert law:

$$Abs(\lambda) = \varepsilon(\lambda) \cdot d \cdot c$$

The absorbance *Abs* for each wavelength depends on the pathlength *d* of the sample, the concentration *c,* and the wavelength dependent extinction coefficient ε. The Beer-Lambert law has few limitations, as it applies only for dilute solutions. At a higher concentration the molecules start to interact, leading to different charge distributions and therefore different spectra. The same holds true for additives in large concentrations, such as salts. Furthermore, the refractive index of a liquid changes for high concentrations of solute, leading again to different absorption spectra. Even at low concentrations the Beer-Lambert law may be violated due to dissociation/association of the analyte, as in the case of pH-indicators.

Proper characterization of a photoswitch requires the absorption spectra of both forms **A** and **B** which includes the wavelength with the highest extinction coefficient λ_{max}. The difference between the two

absorption maxima is referred to as the band separation $\Delta\lambda_{max}$, which for "good" photoswitches is obviously large.

$$\Delta\lambda_{max} = \lambda_{max,B} - \lambda_{max,A}$$

Band separation is often referred to, because it is a measurable quantity and gives a hint for high conversions. Ideally, the "perfect switch" requires two wavelengths were only one of the two isomers absorbs. Given that usually one of the isomers absorbs further to the red, the blue form should have an "absorption gap", where the red form has a maximum. This means in general that narrow bands result in better switches as is exemplified in Figure 2, where the band separation for both isomers is the same. In the left example **B** does not feature an absorption gap, which results in similar extinction coefficients and therefore worse addressability compared to the case in the right example, where **A** can be irradiated in the absorption gap of **B**.

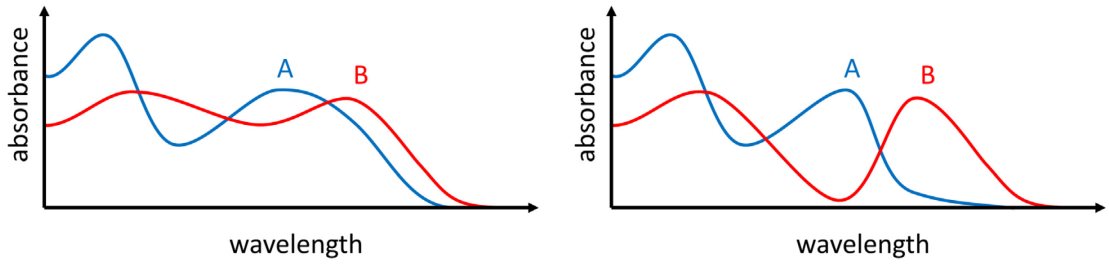

Figure 2: In both spectra the band separation is the same, although the left case will result in worse switching, due to similar extinction coefficients at $\lambda_{max,A}$.

Another parameter characterizing a photoswitch is the quantum yield. It is defined by the fraction of absorbed photons, leading to the desired photoreaction.

$$\Phi = \frac{n_{photo\ reactions}}{n_{absorbed\ photons}}$$

For a neglectable thermal back reaction, the quantum yields and extinction coefficients for both forms define the photostationary state (PSS), representing the ratio of the two forms which is obtained after prolonged irradiation with light of a specific wavelength λ:

$$PSS_\lambda = \frac{A}{B} = \frac{\varepsilon_B^\lambda \Phi_B^\lambda}{\varepsilon_A^\lambda \Phi_A^\lambda}$$

Since the photostationary state depends on the wavelength mainly due to the wavelength dependent extinction coefficient, ideal wavelengths can be found to produce maximum amounts of either **A** or **B**, *e.g.* to achieve as complete as possible switching in both directions. It has to be noticed that the PSS is a dynamic equilibrium, meaning that the system reacts in both directions, although no change in the absorption spectra is visible. In contrast to a thermal equilibrium, the equilibration can be stopped by switching off the light.

For thermally reverting photoswitches, a PSS can only be given for infinite light intensity or at low temperatures, where the thermal back reaction is neglectable. However, care must be taken on comparing such PSSs, since the extinction coefficients (and sometimes the quantum yields as well) are temperature dependent and high light intensities may lead to the formation of side products. The

speed of the thermal reaction is usually characterized by the rate constant *k* or the thermal half-life $t_{1/2}$ at a given temperature for first order kinetics (which is the case for most photoswitches):

$$\frac{dB}{dt} = -k \cdot B$$

After separation of the variables:

$$\frac{dB}{B} = -k \cdot dt$$

Integration gives:

$$\ln\left(\frac{B}{B_0}\right) = -k \cdot t$$

With the concentration *B* being 50% of B_0:

$$\ln\left(\frac{1}{2}\right) = -k \cdot t_{1/2}$$

$$\frac{\ln(2)}{k} = t_{1/2}$$

Measuring rate constants for the thermal back reaction at different temperatures allows for application of an Arrhenius equation, with *A* being a preexponential factor, *R* being the gas constant, and *T* being the temperature:

$$k = A \cdot e^{-\frac{E_A}{RT}}$$

The thereby measured activation energy E_A represents the barrier the molecule has to overcome and can be further differentiated into activation entropy $\Delta S^{\ddagger}$ and activation enthalpy $\Delta H^{\ddagger}$ by application of the Eyring equation, with k_B being the Boltzmann constant and $\hbar$ being the Planck constant.

$$k = \frac{k_B \cdot T}{\hbar} \cdot e^{\frac{\Delta S^{\ddagger}}{R}} \cdot e^{-\frac{\triangle H^{\ddagger}}{RT}}$$

2.2 From General Considerations to Practical Aspects

2.2.1 Thermodynamics

Simplified energy diagrams which explain the difference between positive and negative photochromism are shown in Figure 3. S_0 denotes the ground state of the thermodynamically more stable form **A** and the photoproduct **B** respectively. S_1 resembles the excited state from which the photoreaction can happen, which is usually the lowest excited state. Following the definition of negative photochromism, in such a case S_1–S_0 has to be smaller for **A** than for **B**, resulting in a bathochromic absorption of the thermodynamically more stable form.

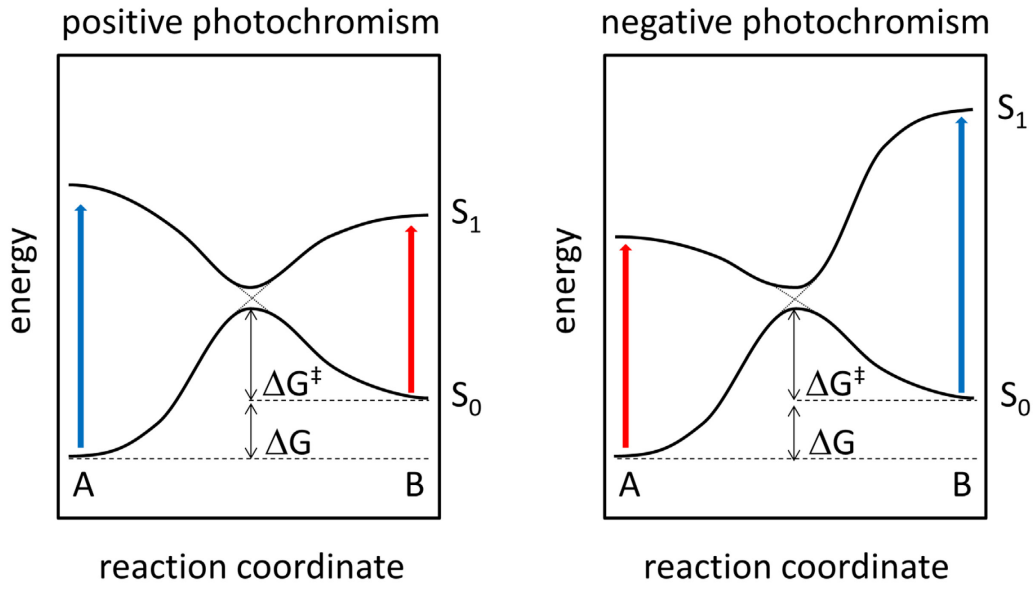

Figure 3: Simplified energy diagrams for positive and negative photochromism.

Where the relative energy differences of the states are given by definition, another very important aspect is unneglectable. For applications which do not rely on the energy stored in the metastable isomer, the relative stability of the ground states of **A** and **B** becomes quasi irrelevant if the activation barrier (denoted as $\Delta G^{\ddagger}$) is high. In the case where no thermal back reaction is apparent, the isolated photoproduct of a positive photochromic compound will behave similar to a negative photochromic material. As an illustrative example, the diarylethene $\mathbf{1}_{open}$ is by definition P-type positive photochromic. However, the isolated closed form behaves as if it was a P-type negative photochromic molecule, as it absorbs at longer wavelengths and does not revert thermally at ambient temperatures.

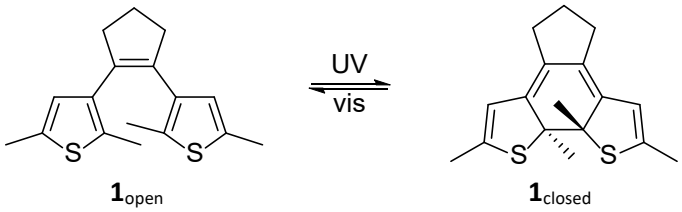

$\mathbf{1}_{open}$ $\mathbf{1}_{closed}$

Scheme 3: Positive P-type photochromism of a diarylethene. The isolated closed form behaves as if it was a negative P-type photochromic molecule.

One of the main goals in developing photoswitchable materials is to shift the irradiation wavelength as far red as possible. In this regard, the implications drawn from simple energy diagrams should be considered: The energy of the light used for irradiation has to be higher in energy than the sum of the thermal barrier for the back reaction and the energy difference of both forms in their ground state (Figure 3):

$$S_1 - S_0 > \Delta G + \Delta G^{\ddagger}$$

According to the Boltzmann distribution, the energy difference between **A** and **B** has to be at least 0.177 eV to assure that at 25 °C 99.9% of the molecules are in their thermodynamically stable form.

$$\frac{B}{A} = e^{-\frac{\Delta G}{k_B T}}$$

The activation barrier is directly linked to the thermal half-life. Application of the Eyring equation, allows to calculate $\Delta G^{\ddagger}$ for different thermal half-lives at 25 °C.

$$k = \frac{k_B \cdot T}{\hbar} \cdot e^{-\frac{\triangle G^{\ddagger}}{RT}}$$

Table 1 gives limits for maximum irradiation wavelengths at 25 °C which are necessary to overcome the sum of ΔG and $\Delta G^{\ddagger}$ depending on the desired thermal half-life.[40]

Table 1: Limits for irradiation wavelengths at 25 °C depending on the thermal half-life.[40]

$t_{1/2}$	ΔG	$\Delta G^{\ddagger}$	λ_{irr}
1 s	0.177 eV	0.766 eV	1314 nm
1 min	0.177 eV	0.871 eV	1182 nm
1 h	0.177 eV	0.977 eV	1074 nm
1 d	0.177 eV	1.058 eV	1003 nm

In practice the S_1 state is usually higher in energy than the minimum of the potential energy surface. Furthermore, activation barriers in the excited state have to be taken into account,[41,42] which limits the irradiation wavelength even more. This is especially important for applications, which rely on high energy gain and a slow thermal back reaction, such as solar energy storage. It is obvious from Table 1 that photoswitches are of limited efficiency for solar energy storage, as a huge amount of energy is lost to assure for a sufficiently high barrier.

2.2.2 Absorption Spectrum of the Photoproduct

One of the most critical aspects for photoswitches concerns the amount of conversion to the photoproduct and linked to this the optical spectra of both isomers. While the spectrum of the stable form **A** is usually known, obtaining the spectrum of **B** often requires additional experiments, such as preparative irradiation and isolation of **B**. For positive photochromism secondary techniques (*e.g.* NMR or HPLC) are usually applied to determine the conversion of an irradiated sample, which is then related to the corresponding UV/vis spectrum. Considering fast thermal back reactions, these techniques either fail or have to be done at low temperature.[43] Since extinction coefficients depend on the temperature, reliable conversion values for ambient conditions are hard to obtain and have to be restricted to *lower limits of conversion*. Otherwise error-prone assumptions can be made to simplify

the problem. This can be that either the photoproduct does not absorb at a wavelength where the starting material absorbs or that the quantum yield is independent of the wavelength.[44] To confirm the latter, the quantum yields have to be determined at different wavelengths, which is often accompanied by side reactions going to the shorter wavelengths or different kinetics from other excited states. Furthermore, light intensity dependent photostationary states must be measured in case of a thermal back reaction, all in all leading to many time consuming experiments.[45]

In the case of negative photochromism, ideally the photoproduct does not absorb in the long wavelength region of the stable form. This implies that the conversion (and the spectrum of the photoproduct) can be directly determined from the absorbance change of the red band. Therefore, no secondary techniques are necessary and even fast thermal back reactions remain no problem anymore. For a good indication that the photoproduct is not absorbing in a certain region, the quotient $\frac{Abs\ (under\ irradiation)}{Abs\ (stable\ form)}$ has to be constant in this region since the absorbance is directly proportional to the concentration and only one isomer absorbs. Under irradiation $Abs_{under\ irradiation}$ resembles the photo thermal equilibrium for fast thermal back reactions, which results in:

$$photo\ thermal\ equilibrium = 1 - \frac{Abs\ (under\ irradiation)}{Abs\ (stable\ form)}$$

2.2.3 Kinetics

Efficient switching is required for any application which makes use of photochromic materials, meaning fast photoreactions and high photostationary states are necessary. In solution the kinetics of a photoreaction of **A** to **B** with a thermal back reaction follow the general rate equation:[46,47]

$$\frac{dA}{dt} = 1000 \cdot \frac{I_0 \cdot d}{v} \cdot \frac{1 - 10^{-Abs'}}{Abs'} \cdot (\varepsilon_B \cdot \Phi_{B\rightarrow A} \cdot B - \varepsilon_A \cdot \Phi_{A\rightarrow B} \cdot A) + k_T \cdot B$$

I_0 denotes the light intensity, d the path length, v the volume of the cuvette, and *Abs'* the absorbance at the irradiation wavelength. This differential equation can only be integrated iterative and for solving it, further experiments are required to determine ε_B. In the case of a negative photochromic compound, where the photoproduct **B** usually does not absorb at the irradiation wavelength, it simplifies a lot:

$$\frac{dA}{dt} = -\frac{1000 \cdot I_0 \cdot d \cdot (1 - 10^{-Abs'}) \cdot \Phi_{A\rightarrow B}}{v} + k_T \cdot B$$

This equation can either be integrated in a closed form and solved, if the thermal back reaction is slow with respect to the irradiation time or an equilibrium between the photoreaction and a thermal back reaction is reached. In the latter, the rate equals zero and the amount of photoproduct in the photo thermal equilibrium can be derived from:

$$[B] = \frac{1000 \cdot I_0 \cdot d \cdot (1 - 10^{-Abs'}) \cdot \Phi_{A\rightarrow B}}{v \cdot k_T}$$

The quantum yield can be calculated from this equation without applying further methods, but moreover this equation shows that the reached equilibrium depends on experimental parameters, such as irradiation wavelength, light intensity, concentration (*via Abs'*), absolute number of molecules (*via* v and *Abs'*), and temperature (*via* Φ, if temperature dependent and k_T). The material properties

including the extinction coefficient, quantum yield, and rate of the back reaction can be designed in a certain frame, although application wise, most of these factors are predefined by the application itself. Apart from that, the light intensity as an external parameter is usually not limited, which should result in higher conversions, making negative photochromic systems good candidates for applied photoswitches.

2.2.4 Concentration

Since the usual rate equations rely on the Beer-Lambert law and extinction coefficients are usually high, they are only valid for highly diluted mixtures (typically 10^{-5} M). Many applications require higher concentrations or photoswitching in bulk, making some general thoughts in this direction necessary: In optically dense matter (*e.g.* a 1 M solution of a switch) all the photons are absorbed by a small fraction of the material. Assuming constant stirring of the solution, this leads to a simple rate equation for the photochemistry:

$$\frac{dA}{dt} = -I_0 \cdot \Phi_{A\rightarrow B} \cdot \frac{\varepsilon_A \cdot A}{\varepsilon_A \cdot A + \varepsilon_B \cdot B} + I_0 \cdot \Phi_{B\rightarrow A} \cdot \frac{\varepsilon_B \cdot B}{\varepsilon_A \cdot A + \varepsilon_B \cdot B} + k_T \cdot B$$

For the case of negative photochromism, ε_B equals zero again which simplifies the equation a lot:[48]

$$\frac{dA}{dt} = -I_0 \cdot \Phi_{A\rightarrow B} + k_T \cdot B$$

Comparing these last two equations results in two important findings: (1) In the case of positive photochromism, the rate of the photoreaction slows down with increasing conversion because $\frac{\varepsilon_A \cdot A}{\varepsilon_A \cdot A + \varepsilon_B \cdot B}$ becomes smaller, whereas $\frac{\varepsilon_B \cdot B}{\varepsilon_A \cdot A + \varepsilon_B \cdot B}$ becomes larger. In contrast, the photoreaction for negative photochromism follows zero order kinetics (given sufficient light intensity) and is therefore constant over the irradiation time until most of the material is switched and transmittance of the sample comes into play, meaning that not all photons are absorbed anymore and the photoreaction slows down. (2) Since switching only makes sense if one can go in both directions, (1) applies exactly the other way around for the backward reaction and for the kinetics of P-type switches it makes no difference whether they display positive or negative photochromism. However, in the case of T-type negative photochromic materials, the thermal reaction helps the backward reaction, whereas for T-type positive photochromic materials it hampers the forward reaction on the one hand but on the other hand accelerates the back reaction which is not really necessary, since it can be regulated by the light intensity.

These facts become even more important moving from solution to the solid state and therefore prevent stirring. Although photochromism in the solid state may be limited due to steric effects, a main issue is that most of the light will be absorbed by the surface, whereby the bulk of the material is in the “shades” of few surface layers. Using negative photochromic molecules, this issue is not apparent, since the surface layers are bleached and become transparent themselves. Therefore, with ongoing irradiation light can penetrate deeper and deeper into the bulk material as long as the light intensity is high enough to overcome thermal back reactions.[49] Generally speaking, the equilibrium between **A** and **B** in optically dense matter can be reached faster for negative photochromic materials and is better if the light intensity is high enough.

The principle difference between a positive and negative photochromic crystal can be seen on a diarylethene co-crystal, which bends upon UV irradiation from one side since only the surface switches. Irradiation with UV-light from the other side straightens the crystal again (both surfaces are switched now) until visible light is applied, which after a while penetrates the whole crystal and therefore induces isomerization to the starting point.[50]

2.3 Classification of Photoswitches

There are several criteria to differentiate between the different classes of photoswitches, *e.g.* sterics versus electronics: Some switches undergo a huge geometrical change while maintaining similar electronic properties, whereas others are characterized by a large modulation of their HOMO and LUMO levels without undergoing substantial geometrical change. Another approach is to categorize by the switching mechanism since many property changes go hand in hand with a certain type of photoreaction. A thorough overview of photochromic systems will be given in this section to illustrate the manifold of possible photoswitches.

2.3.1 Metal Complexes

Although photochromism usually refers to organic compounds some metal complexes are known to undergo an isomerization as well. An excellent overview on inorganic organic hybrid materials has been given by Guo and co-workers, which exploits the different types of reversible photoreactions, involving metal centers and organic ligands.[51] More precisely, a review which focusses on photochromism with structural rearrangements has been written by Nakai and Isobe.[52] In some dinuclear complexes, the metal-metal bond breaks, followed by an insertion into a C-C (Scheme 4) or C-H bond. When the yellow bisruthenium complex $\mathbf{2}_{\text{Ru-Ru}}$ (λ_{max} = 329 nm) is irradiated with 350 nm light, the Ru-Ru bond breaks, followed by rotation and insertion into the C-C bond to yield the colorless high energy isomer $\mathbf{2}_{\text{Ru-C}}$ (λ_{max} = 286 nm) with Φ = 0.15 (Scheme 4). The back reaction occurs with a thermal half-life of 48 min in dioxane (80 °C) and also happens in the crystalline state (208 °C).[53,54]

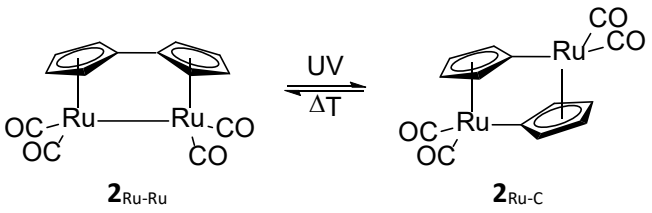

Scheme 4: Isomerization of (fulvalene)tetracarbonyldiruthenium $\mathbf{2}_{\text{Ru-Ru}}$.[53,54]

Instead of a fulvalene ligand the two cyclopentadienyl rings can be separated by a CMe_2 bridge. Here, the ruthenium inserts into the C-H bond upon irradiation with visible light. When a yellow-orange solution of complex $\mathbf{3}_{\text{Ru-Ru}}$ (λ_{max} = 430 nm) is irradiated with > 400 nm, the colorless rearrangement product $\mathbf{3}_{\text{Ru-H}}$ (λ_{max} = 290 nm) forms (Scheme 5). The back reaction occurs thermally with a half-life of 3.5 h (137 °C). Interestingly, the barrier of the thermal reverse reaction is highly dependent on the metal. While the ruthenium complex has a relatively high barrier of $\Delta G^{\ddagger}$ = 27 kcal/mol, the corresponding molybdenum complex has to be irradiated at −60 °C due to a barrier as low as $\Delta G^{\ddagger}$ = 16 kcal/mol.[55]

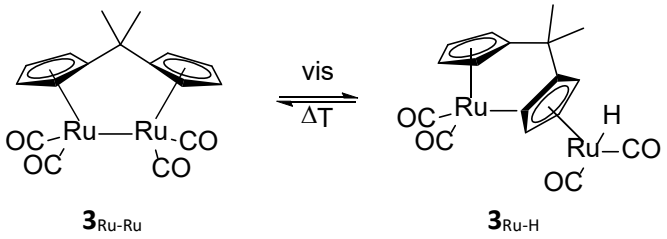

3$_{Ru-Ru}$ **3**$_{Ru-H}$

*Scheme 5: Isomerization of the diruthenium complex **3**$_{Ru-Ru}$ with two bridged cyclopentadienyl ligands.*[55]

In a similar way, coordinative or ionic bonds can be cleaved photochemically, followed by a reorganization of the system or complex. Many examples are known where the binding site of a small ligand, such as dimethylsulfoxide or nitrosyl, changes upon irradiation and reverts back in the dark.[56] Ruthenium is usually complexed by dimethylsulfoxide *via* the sulfur atom. Upon irradiation of a yellow solution of complex **4**$_{S,S}$ (λ_{max} = 348 nm) in dimethylsulfoxide with 354 nm light, the color changes to red, which is attributed to the coordination *via* the oxygen atom of the ligand in **4**$_{O,O}$ (λ_{max} = 507 nm). The back reaction occurs stepwise *via* the O and S coordinated intermediate with half-lives (25 °C) of 2.9 min and 111 min for the first and second step, respectively (Scheme 6).[57]

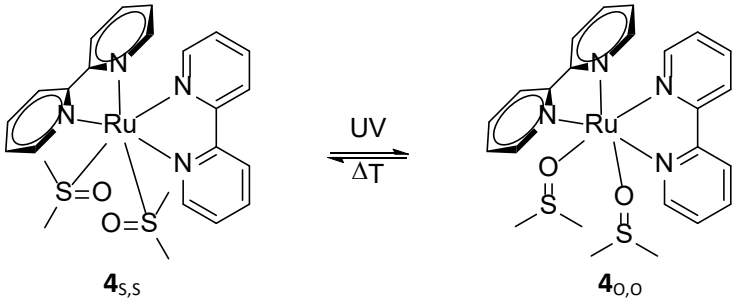

4$_{S,S}$ **4**$_{O,O}$

*Scheme 6: Linkage isomerization of two dimethylsulfoxide ligands of ruthenium complex **4**$_{S,S}$.*[57]

While the isomerization of ligands, such as dimethylsulfoxide, usually requires the presence of free ligand during the irradiation, covalent linkage of a bifunctional ligand circumvents this problem. The purple manganese complex **5**$_N$ is coordinated *via* the pyridine nitrogen atom in the thermodynamically stable form (λ_{max} = 572 nm). Irradiation with visible light causes the isomerization to the blue oxygen coordinated manganese complex **5**$_O$, which features an absorption band around 750 nm and reverts thermally in < 10 min (Scheme 7).[58]

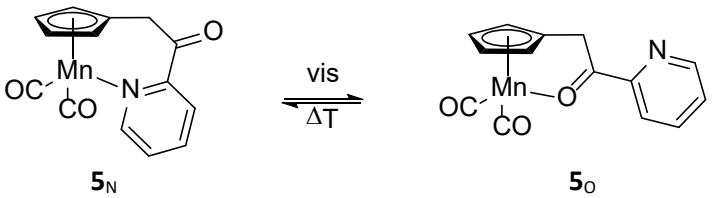

5$_N$ **5**$_O$

*Scheme 7: Linkage isomerization of **5**$_N$ without ligand exchange.*[58]

Other examples of photochromic complexes include clusters of several metal atoms and ligands. Light irradiation can cause the reorganization by changing several metal-ligand and/or metal-metal bonds.[52]

A typical example is the reversible dissociation of the yellow magnesium-iron complex **6**$_{dimer}$ (λ_{max} = 365 nm), which involves the cleavage of four magnesium-bromine bonds and results in the coordination of the magnesium by a fourth tetrahydrofuran in colorless **6**$_{monomer}$ (no absorbance at λ > 280 nm). The dissociation was conducted with UV-light (365 nm) and the reverse reaction showed second order kinetics with a rate constant of 3400 $M^{-1}s^{-1}$, which results in an almost complete recovery after 3 h for a 0.5 mM solution (Scheme 8).[59]

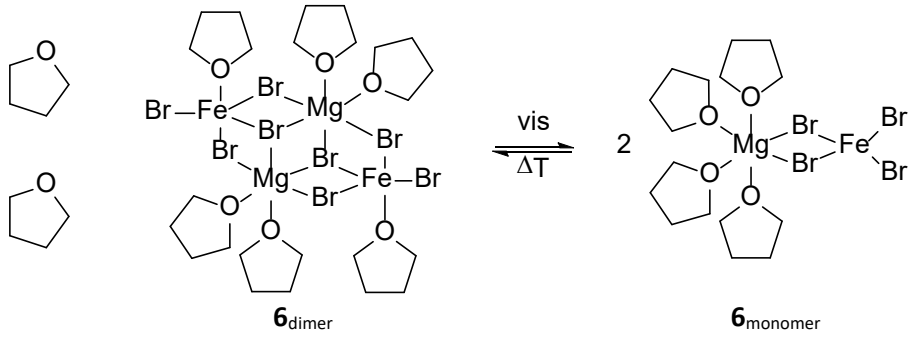

6$_{dimer}$ **6**$_{monomer}$

*Scheme 8: Reversible dimerization and dissociation of a magnesium-iron cluster **6**.[59]*

2.3.2 Dissociation of σ-Bonds

2.3.2.1 Homolytic Cleavage

Some photochromic systems have been based on the homolytic cleavage of a σ-bond, which results in the formation of two radicals. The simplest example is the pale yellow dimer of 2,4,5-triphenylimidizole **7**$_{dimer}$ (λ_{max} = 266 nm), which upon irradiation with UV-light undergoes a cleavage of the C-N bond to form two red violet imidazolyl radicals **7**$_{radical}$ (λ_{max} = 550 nm), which revert rapidly in solution but slowly in the solid state at room temperature (Scheme 9).[60,61]

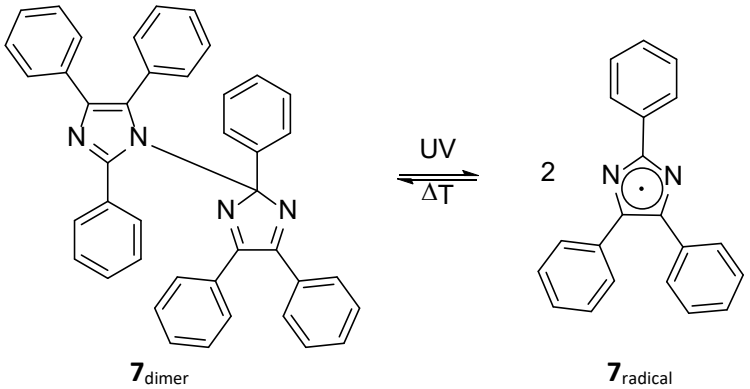

7$_{dimer}$ **7**$_{radical}$

*Scheme 9: Homolytic cleavage of a σ-bond in **7**$_{dimer}$ forming two imidazolyl radicals.[60,61]*

The group of Abe developed bridged hexarylbiimidazole switches, such as **8**$_{dimer}$, which are prevented from unmixing as in the case of the two different imidazol units in **8**$_{radical}$. Irradiation with UV-light of the colorless solid or solution causes an immediate color change to blue, which fades with a half-life of 33 ms at room temperature (Scheme 10). **8**$_{radical}$ features an intense absorption band around 400 nm and a broad band ranging from 500-900 nm. The visible coloration - despite the very short thermal

half-life - is an indication for a high quantum yield and reported values for similar systems reach $\Phi = 1$.[62,63]

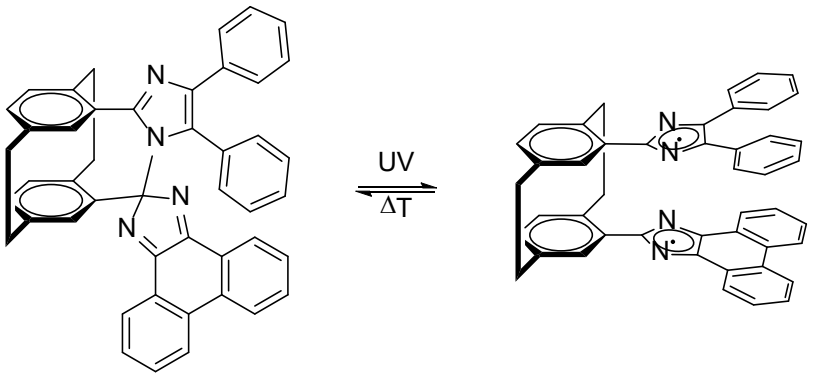

8dimer **8**radical

*Scheme 10: In bridged hexarylbiimidazole switches such as **8**$_{dimer}$ unmixing of the imidazole units is prevented.*[62]

Introduction of 1,1`-binaphthyl as a bridge results in a negative photochromic system, where one of the imidazolyl nitrogen atoms can bind to the other naphthalene, forming a colored but nonradical species **9**nonradical (λ_{max} = 490 nm). In comparison to the previously mentioned hexaarylbiimidazole switches this structure is thermodynamically favored, as it preserves the aromaticity of the bridging unit. Upon irradiation with 517 nm the diradical species **9**radical is build up, which rapidly ($t_{1/2}$ = 9.4 µs at 25 °C) forms the colorless dimer **9**dimer with Φ = 0.03. The dimer reverts back with a thermal half-life of 20 min (25 °C) or UV irradiation (Scheme 11).[64] The system is not limited to imidazole but tolerates other aromatic systems with the capability of stabilizing radicals, such as cyclohexadienone.[65]

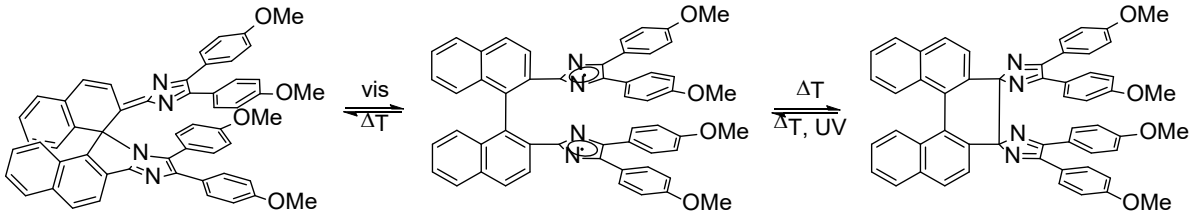

9nonradical **9**radical **9**dimer

*Scheme 11: Negative photochromism of a bridged biimidazole **9**: From the diradical, which is formed upon irradiation the thermal reaction to the imidazole dimer is much faster compared to the attack on the bridging naphthalene.*[64]

2.3.2.2 Heterolytic Cleavage

The heterolytic cleavage of a σ-bond usually requires the formed cation and anion to be stabilized. Therefore, some triarylmethylcyanides such as **10**$_{neutral}$ (λ_{max} = 272 nm) are known to dissociate under UV irradiation to form the stable cyanide anion as well as the stable triarylmethyl cation **10**$_{charged}$ (λ_{max} = 590 nm, Scheme 12). The rate of the thermal recombination is highly dependent on the anion concentration and the substitution of the aryl units. The quantum yields for the forward reaction reach Φ = 1 for donor substituted aryl units as in **10**$_{neutral}$, whereas acceptors lower the quantum yield. This has the dramatic effect that replacement of one dimethylamino group of **10**$_{neutral}$ by a nitro group inhibits the switching almost completely.[66,67]

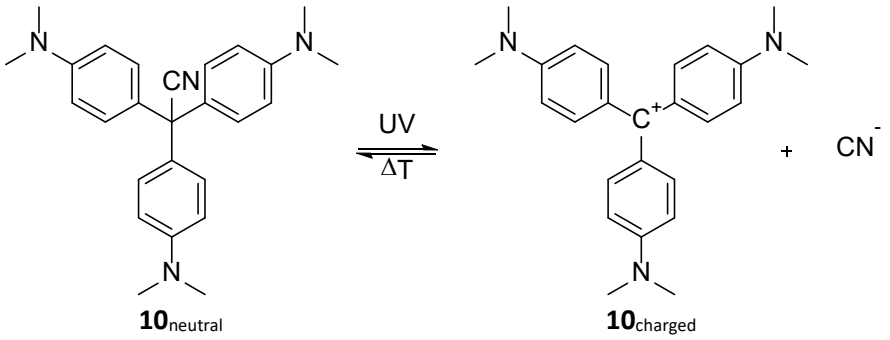

10$_{neutral}$ **10**$_{charged}$

*Scheme 12: Photochemical dissociation of the triarylmethylcyanide crystal violet **10**.[66,67]*

A drawback of these systems lies in the potential substitution with a solvent molecule, *e.g.* water, instead of the cyanide. Covalent linkage of the anion in the form of a carboxylate on rhodamine derivative **11**$_{leuko}$ (λ_{max} = 314 nm) and its photoproduct **11**$_{zwitterion}$ (λ_{max} = 542 nm) has been shown to circumvent this problem and still allows to tune the thermal half-life from 67 ms to 6 min depending on the nature of the linker (amide or sulfonamide) as well as the solvent (Scheme 13).[68]

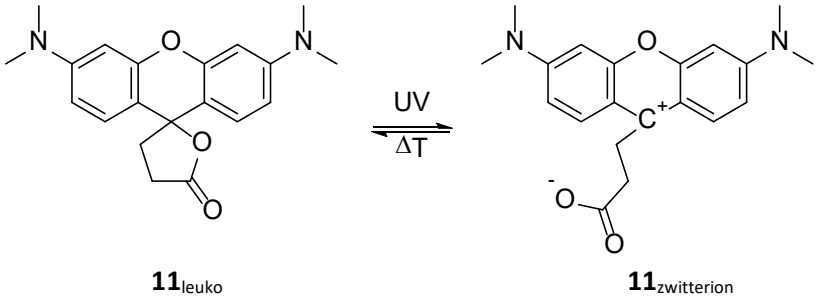

11$_{leuko}$ **11**$_{zwitterion}$

*Scheme 13: Photochromism of a rhodamine derivative **11**$_{leuko}$, where the anionic part is linked covalently.[68]*

Other examples for the light induced heterolytic cleavage of a σ-bond are photoacids, as in the typical photoacid pyranine **12**$_{PyH}$ (λ_{max} = 404 nm) a proton and a stabilized alkoholate **12**$_{Py^-}$ (λ_{max} = 462 nm) are formed. Upon irradiation the molecule reaches the excited state, which has a much lower pK_a and transfers a proton to a solvent molecule (Scheme 14).[69]

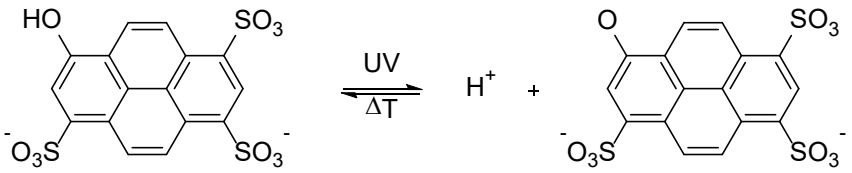

12$_{PyH}$ **12**$_{Py^-}$

*Scheme 14: The photoacid pyranine **12**$_{PyH}$ transfers a proton to a solvent molecule due to the pK_a change upon electronic excitation.[69]*

2.3.3 Redox Photochromism

The phenomenon of redox photochromism has been used to produce sunglasses with photochromic lenses. The most widely applied reaction in this regard is the light induced electron transfer from chloride anions to silver cations. As silver chloride is transparent, upon UV irradiation an electron is transferred from a chloride anion to a silver cation, which results in the formation of elemental silver and causes a darkening of the glass.[70]

Another typical example is the photochemical reduction of viologens, where electron transfer can occur from different sources, such as metal centers[51] or organic counter-ions as for **13**$_{dication}$ which turns green in the solid state upon UV irradiation due to the formation of **13**$_{radicalcation}$ (λ_{max} = 660 nm, Scheme 15).[71]

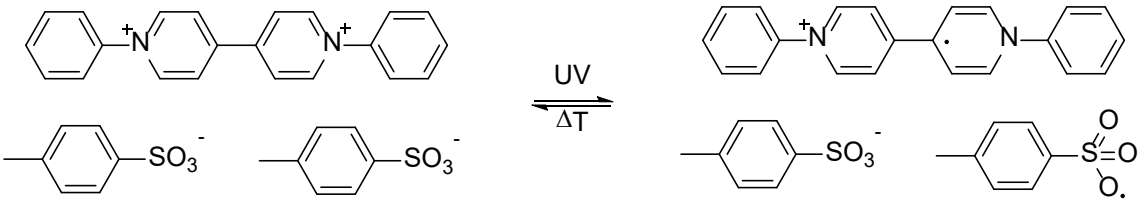

13$_{dication}$ **13**$_{radicalcation}$

*Scheme 15: Solid state photochromism of viologen derivative **13**, where the electron donor is a tosylate counter-ion.[71]*

2.3.4 Light Induced Prototropic Rearrangements

The light induced prototropic rearrangement is a special case of a photoacid, where the proton acceptor is in close proximity to the phenol and where a tautomerization happens upon the light induced proton transfer. Anils are a class of photoswitches, which have been studied quite extensively in this regard. They can be easily obtained from the condensation of anilines with salicylaldehydes and are known to form the E,enol isomer. Although the switching mechanism is still under debate, the enol form **14**$_{enol}$ is usually colorless to yellow, whereas the formed intermediate **14**$_{Z,keto}$ absorbs around 440 nm and the photoproduct **14**$_{E,keto}$ absorbs around 480 nm (Scheme 16). Anils revert back at room temperature with thermal half-lives ranging from minutes to weeks. Beside anilines also aminopyridines and benzothiazole[72] **15**$_{enol}$ can function as the imine part and have been proven photochromic (Scheme 17).[73]

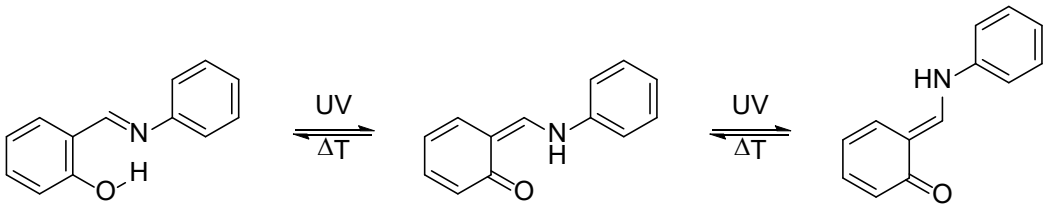

14$_{enol}$ **14**$_{Z,keto}$ **14**$_{E,keto}$

*Scheme 16: Photochromism of anil **14**.[73]*

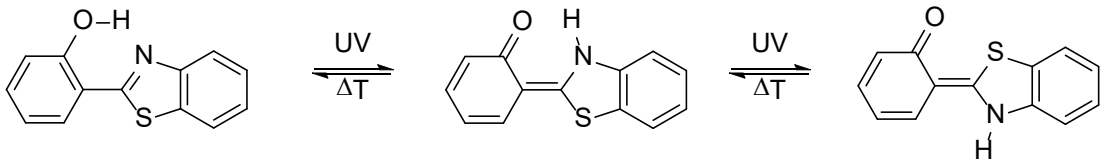

15$_{enol}$ **15**$_{Z,keto}$ **15**$_{E,keto}$

*Scheme 17: Photochromism of the benzothiazole derived anil switch **15**.[72]*

In another case the prototropic rearrangement happens in the last step of the photoreaction. Upon UV irradiation of perimidinecyclohexadienone **16**$_{closed}$ (λ_{max} = 420 nm) the C-N bond breaks heterolytically in the first step followed by a conformational rearrangement to **16**$_{zwitterionic}$ and the proton shift to yield the open form **16**$_{open}$ with Φ = 0.05 (acetonitrile) or Φ = 0.4 (octane). The open isomers also form thermally and absorb in the visible at around 600 nm. The back reaction can proceed either photochemically or thermally with thermal half-lives ranging from minutes to days (Scheme 18).[74]

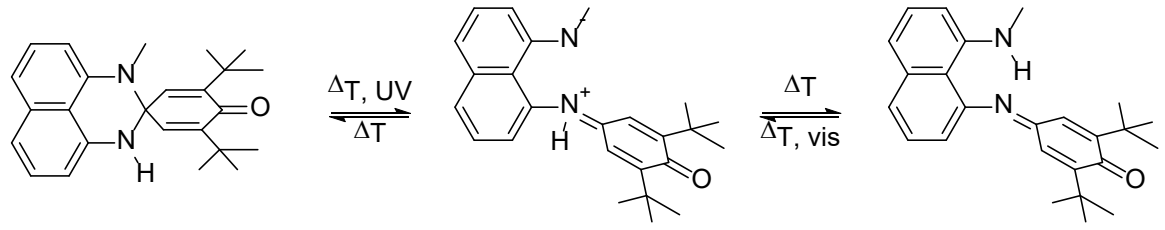

16$_{closed}$ **16**$_{zwitterionic}$ **16**$_{open}$

*Scheme 18: Subsequent heterolytic bond cleavage and prototropic rearrangement in perimidinecyclohexadienone **16**.[74]*

Dinitrobenzylpyridine exists in the stable colorless form **17**$_{CH}$ (λ_{max} = 254 nm) and turns blue upon irradiation with UV-light, which has been shown to be the NH isomer **17**$_{NH}$ (λ_{max} = 600 nm) and occurs *via* an intermediate, where the proton is located on the nitro-oxygen (λ_{max} = 435 nm).[75] The thermal half-life is short in solution (4.7 s at 25 °C), but moderate in the crystalline state (4.6 h, Scheme 19). The rate of the thermal back reaction also depends on the aromaticity of the pyridine moiety, which has been used to increase the thermal activation barrier from 2.8 kcal/mol to 8.2 kcal/mol by changing the pyridine for phenanthroline.[76] Furthermore, the NH isomer can be stabilized by a third nitro group, leading to a tenfold increase of the thermal half-life.[77]

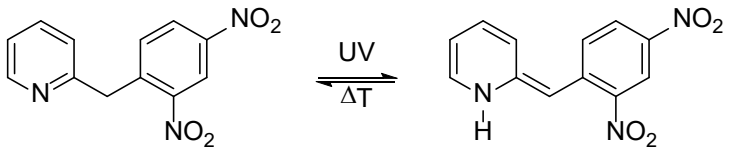

17$_{CH}$ **17**$_{NH}$

*Scheme 19: Dinitrobenzylpyridine **17** forms the N-H isomer upon irradiation.[75]*

2.3.5 E/Z Double Bond Isomerizations

2.3.5.1 Isomerization of C=C Double Bonds

The majority of photochromic reactions involves the isomerization of double bonds with one of the most useful ones to mankind being the isomerization of retinal, which is part of an opsin protein **18**$_{11\text{-}Z}$ and enables vision in the human eye. A lot of effort has been made to restore vision of blind people by the use of photoswitches, where the visual cycle does not work properly.[78] While the Z to E isomerization to **18**$_{all\text{-}E}$ occurs upon absorption of a photon, the back reaction to the Z isomer **18**$_{11\text{-}Z}$ requires several steps (Scheme 20). First, all-E-retinylidene is hydrolyzed from the protein to yield the free all-E-retinal, which is reduced to the corresponding alcohol in the second step. Esterification takes place on the alcohol before isomerization and hydrolysis of the ester are catalyzed by the isomerohydrolase. The 11-Z-retinol is oxidized to 11-Z-retinal, which is then bound to the opsin protein again (**18**$_{11\text{-}Z}$), ready to take up another photon.[79]

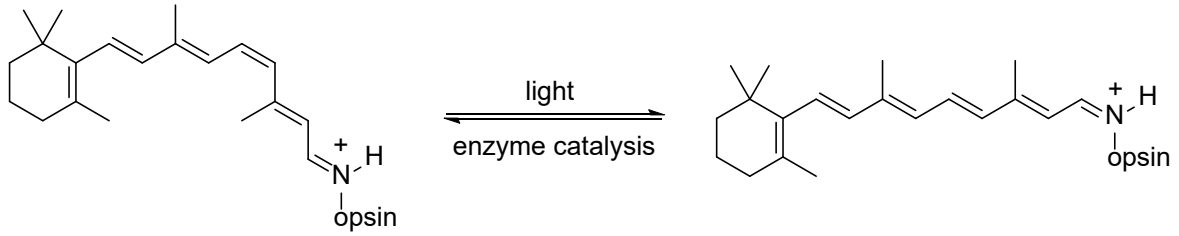

18$_{11\text{-}Z}$ **18**$_{all\text{-}E}$

Scheme 20: Photochemical step in the process of human vision.[79]

Mother nature controls various processes by photochromism such as plant movement or growth, seed germination, circadian rhythms, flowering time, and many others.[80,81] Although the exact mechanism for many systems is still under debate, isomerization of a C=C double bond can be found in several biological systems such as phytochromes.[82,83]

The C=C double bond in unsaturated olefins is often found to establish a photochromic system in analogy to the retinal photoswitch. Whereas cyclohexadiene **19**$_{closed}$ opens quite efficiently under irradiation with 265 nm (Φ = 0.41) to yield hexatriene, a mixture of **19**$_E$ and **19**$_Z$ isomer is found, which can interconvert with low quantum yields (Φ_{ZE} = 0.034 and Φ_{EZ} = 0.016, Scheme 21).[84]

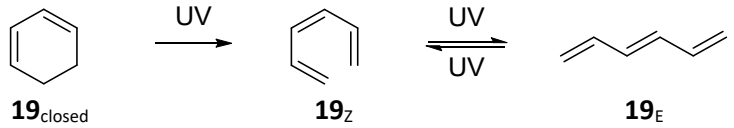

*Scheme 21: E/Z double bond isomerization in the hexatriene system **19**.[84]*

To circumvent the use of deep UV-light as in the hexatriene case, a chromophore can be attached to the double bond system, such as a coumarin dye. The coumarin diene **20**$_E$ (λ_{max} = 505 nm) can be switched to the corresponding Z isomer **20**$_Z$ (λ_{max} = 460 nm) and back using visible light (533 nm and 405 nm) with high quantum yields (Φ_{EZ} = 0.5, Φ_{ZE} = 0.45, Scheme 22). The back reaction is sufficiently slow to consider the system as P-type (175 d at room temperature). It has to be noted that the second double bond also undergoes E/Z isomerization, which leads to two different photoproducts. The corresponding derivative bearing two nitrile groups shows only one photoproduct but less efficient switching in terms of band separation.[85]

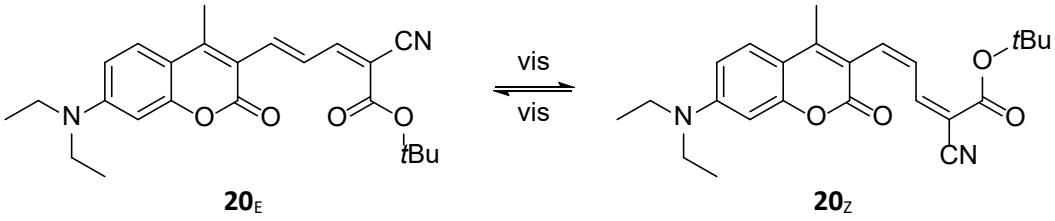

*Scheme 22: Photochromism of coumarin diene dye **20**.[85]*

One of the simplest and arguably most studied artificial systems which can undergo an E/Z isomerization of a C=C double bond is stilbene. Both forms are colorless and interconvert upon irradiation with UV-light (Φ_{EZ} = 0.52 and Φ_{ZE} = 0.35). While the thermodynamically stable E isomer **21**$_E$ (λ_{max} = 300 nm, $\Delta G^{\ddagger}$ > 40 kcal/mol) is planar, the metastable Z form **21**$_Z$ is twisted due to steric interactions, which reduces the conjugation of the π-system and explains the observed hypsochromic shift of the intense π-π* band upon going from E to Z. Besides the disadvantage of harsh irradiation conditions, the Z form can undergo a light induced 6 π electrocyclization (Φ = 0.1) leading to dihydrophenanthrene **21**$_{closed}$, which undergoes subsequent oxidation to phenanthrene **21**$_{ox}$ in many derivatives (Scheme 23).[86–88]

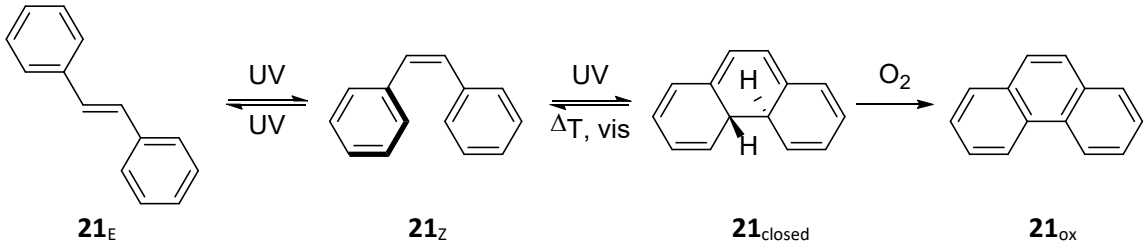

*Scheme 23: Photochemistry of stilbene **21**.[86–88]*

While strategies to circumvent the E/Z isomerization are widely employed, avoiding of the 6 π electrocyclization of Z diarylethenes remains a challenge and requires special substitution patterns.[89] The use of UV-light can be avoided by substitution of one benzene ring by an acridine, which leads to visible light switchable styrylacridine **22**$_E$, although with a low quantum yield Φ = 0.03. The thermal back reaction usually requires high temperatures but can be easily accelerated in polar protic solvents or upon addition of acid (Scheme 24).[90,91]

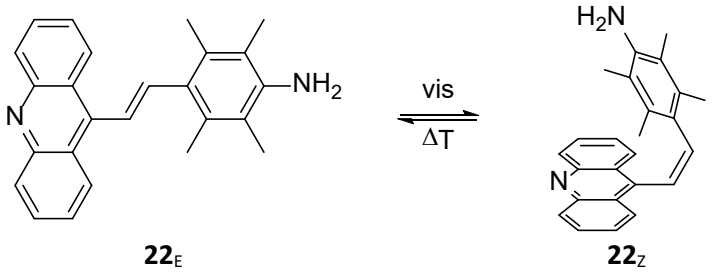

22$_E$ **22**$_Z$

*Scheme 24: Stilbene type photochromism of an acridine derivative **22**.[90,91]*

Other systems featuring the isomerization of a C=C double bond include derivatives of indigo and thioindigo, which show negative photochromism and are highly absorbing in the visible region.[92] By functionalization of one nitrogen atom by at least one alkyl or aryl group, the absorption maximum of the E isomer exceeds 620 nm (Z is above 550 nm) with a tunable thermal half-life from seconds to hours, depending on the substituent on the second nitrogen atom. Furthermore, proper choice of two aryl substituents also allows to tune an equilibrium composition of E and Z form in the ground state. An indigo derivative bearing two nitrobenzene substituents on the nitrogen atoms consists of 88% **23**$_E$ (λ_{max} = 620 nm, Φ_{EZ} = 0.07) and 12% **23**$_Z$ (λ_{max} = 577 nm, Φ_{ZE} = 0.04) in the thermal equilibrium. Irradiation with 660 nm increases the amount of **23**$_Z$ to 82%, which reverts back to the thermal equilibrium with a half-life of 408 min (25 °C, Scheme 25).[93]

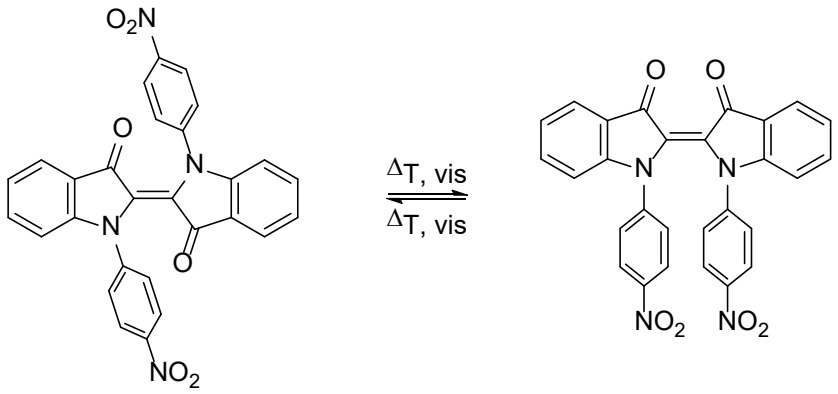

23$_E$ **23**$_Z$

*Scheme 25: Negative photochromism of diarylindigo derivative **23**.[93]*

For the feature of a photoisomerizable double bond one half of the indigo seems to be enough. It has been shown that hemiindigos and hemithioindigos display photochromism as well. In the case of hemithioindigo **24**$_E$ (λ_{max} = 490 nm), the thermal half-life of the photoproduct **24**$_Z$ (λ_{max} = 509 nm) is exceptionally long for this class of switches (35 d at 25 °C), although only moderate PSSs are obtained (82% E or 89% Z, Scheme 26). A general trend which applies for many photoswitches is a reduced thermal half-life, which goes hand in hand with a bathochromic absorption.[94,95]

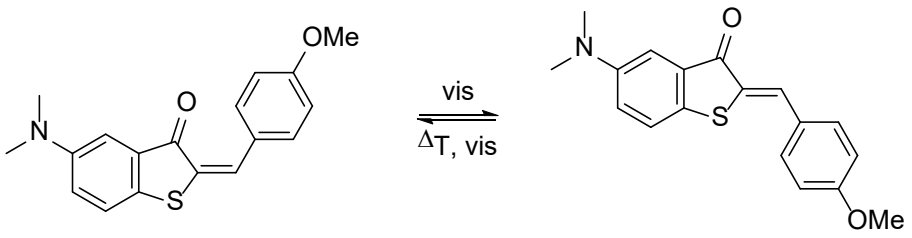

24$_E$ **24**$_Z$

*Scheme 26: Hemithioindigo derivative **24** which is absorbing in the red region and still features a long thermal half-life.[94,95]*

The ketoenamines and ketoenehydrazines are another family of hemiindigos, which displays negative photochromism. Replacing the nitrogen atom of indigo by other groups, such as O, S, NMe, or even CH_2 results in switchable compounds. The main issues in terms of photochromic properties is small band separation and to obtain a high PSS several criteria must be met. It is preferable to utilize benzothiophene based switches in combination with hydrazine and alkyl substituents in the non-indigo half. Ketoenehydrazine **25**$_E$ (λ_{max} = 423 nm) fulfills these criteria and can be completely switched to **25**$_Z$ (λ_{max} = 345 nm). While the forward reaction is fast (Φ_{EZ} = 0.4), the thermal back reaction occurs with a half-life of 3 h (20 °C, Scheme 27).[96]

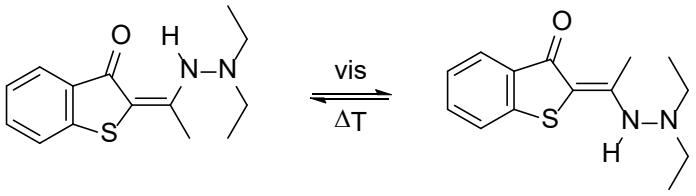

25$_E$ **25**$_Z$

*Scheme 27: Ketoenehydrazine **25** with full switchability in both directions.[96]*

Recently, the field of molecular machines has developed rapidly and the involvement of a photochemical step seems to be key to beat microscopic reversibility.[33] Therefore, the group of Feringa has applied overcrowded alkenes as molecular motors such as **26**, which can undergo a unidirectional 360° rotation in consecutive photochemical and thermal steps (Scheme 28).[34,35]

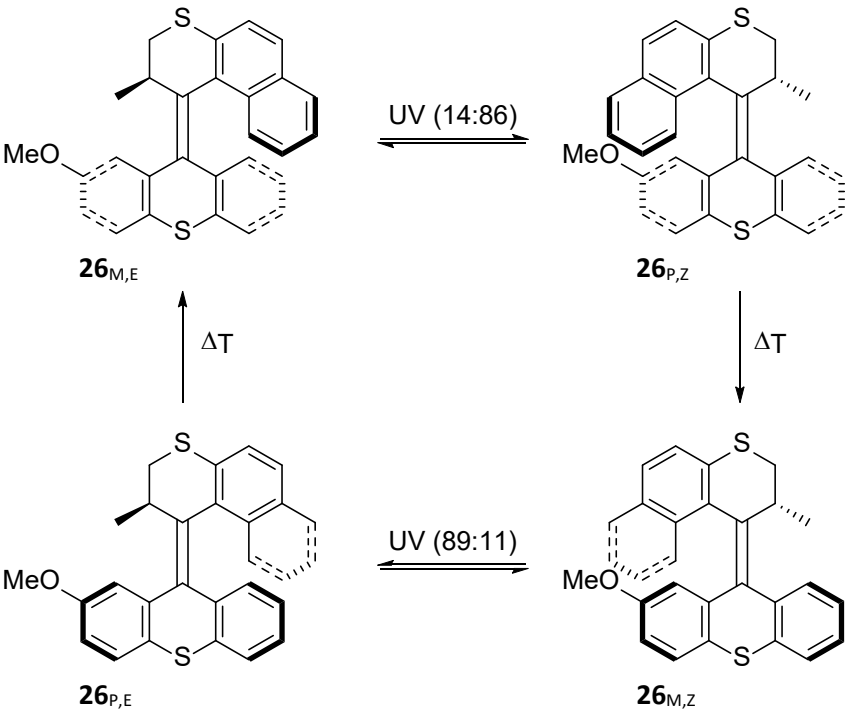

*Scheme 28: Molecular motor **26** based on alternating isomerizations of a C=C double bond and thermal steps to achieve unidirectional rotation.[34,35]*

Leigh´s group used the second widely applied photochromic system in the context of molecular machines: The reversible interconversion of fumaramide to maleamide changes the binding constant of a station in a catenane rotary motor.[36]

2.3.5.2 Isomerization of C=N Double Bonds

In contrast to stilbene, which has a high activation barrier for the thermal Z to E isomerization of 40 kcal/mol and azobenzene of which the barrier is still 23 kcal/mol, N-benzylideneaniline has a small barrier of 16-17 kcal/mol. Thus, irradiation experiments must be conducted at low temperature or on a short time scale. Irradiation of N-benzylideneaniline $\mathbf{27}_E$ (λ_{max} = 368 nm) at −140 °C results in the formation of $\mathbf{27}_Z$ (λ_{max} = 306 nm, Scheme 29).[97] Changing the benzylidene ring for a pyrrole, increases the thermal barrier considerably to almost 20 kcal/mol, which results in switches that can be operated at room temperature with thermal half-lives of several seconds.[98]

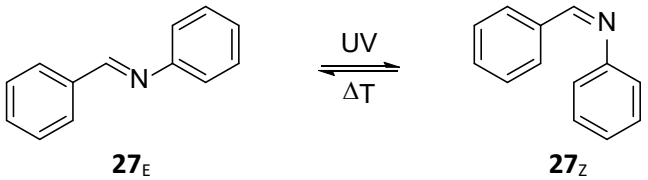

*Scheme 29: Photochromism of N-benzylideneaniline **27**.[97]*

Photochromism does not necessarily require an aryl substituent on the nitrogen atom of the C=N double bond, as oximes and oxime ethers are known to switch as well, although there are only scattered reports in the literature. When the oxime ether **28**$_E$ is irradiated with UV-light, the photoproduct **28**$_Z$ forms (Scheme 30). Although no thermal half-life was given by the authors, a certain stability of Z oximes and oxime ethers is evident, as both isomers can be separated preparatively.[99]

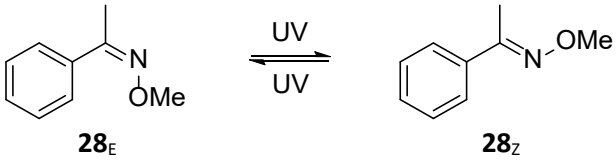

28$_E$ **28**$_Z$

*Scheme 30: Photochromism of oxime ether **28**. The Z form is surprisingly stable.[99]*

In the negative photochromic 2,3-diazabutadienes (azines) both C=N double bonds can undergo an E to Z isomerization,[100] although it is also possible to access the EZ form photochemically, since the EE form absorbs further red then the EZ and the ZZ forms. Both Z double bonds can revert thermally, although the second isomerization is much slower, allowing to access the EZ isomer also *via* the thermal pathway. Azine derivative **29** yields 56% ZZ, 38% EZ, and 6% EE upon irradiation with 436 nm, although an even higher ZZ content would be expected for irradiation at around 450 nm ($\Phi_{EE\ to\ EZ}$ = 0.02, $\Phi_{EZ\ to\ EE}$ = 0.01, $\Phi_{EZ\ to\ ZZ}$ = 0.01, and $\Phi_{ZZ\ to\ EZ}$ = 0.2). Utilization of 480 nm results in the exclusive formation of **29**$_{EZ}$. Whereas the thermal isomerization from ZZ to EZ occurs at room temperature and has a $\Delta G^{\ddagger}$ = 23.3 kcal/mol, the second reaction from EZ to EE requires temperatures > 50 °C due to an activation barrier of $\Delta G^{\ddagger}$ = 26.4 kcal/mol (Scheme 31).[101]

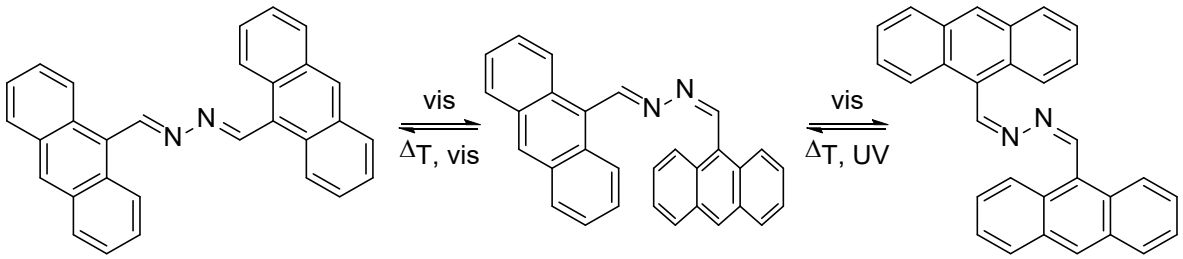

29$_{EE}$ **29**$_{EZ}$ **29**$_{ZZ}$

*Scheme 31: Photochromism of azine **29**, where the EZ isomer is directly accessible via selective irradiation of EE or sufficiently low temperature for the thermal reverse reaction from ZZ.[101]*

Although there is a lot of literature about the biological activity and the metal complex formation of formazanes, their photochromic properties have also been studied. There has been a long debate about the structures of red and yellow formazane, the red ones being stable in non-protic solvents, such as benzene, and the yellow ones being stable in protic solvents like ethanol.[102] Crystal structures proved the red one as a six membered ring, which is formed *via* a hydrogen bond.[103] Going to nonpolar solvents, the C=N bond of **30**$_{EZ}$ (λ_{max} = 500 nm) isomerizes under irradiation first to form the yellow all-trans-formazane **30**$_{EE}$ (λ_{max} = 405 nm, Scheme 32).[104] This one could undergo further E/Z isomerization involving four different species over all, which makes the elucidation of the photoreaction rather complex, although usually no starting material is left. The thermal back reaction follows pseudo first order kinetics and has a half-life of around 4 h at 0 °C, although it highly depends on the purity of the solvent.[105]

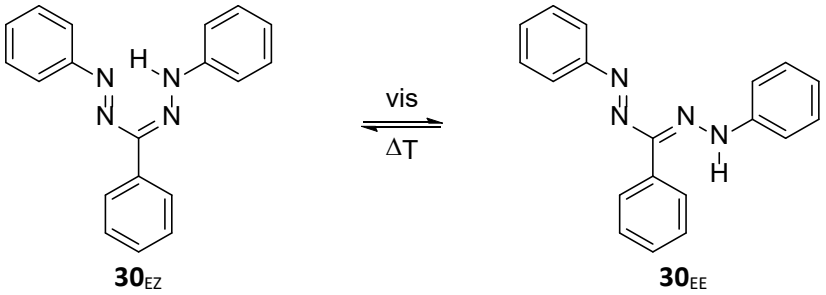

30$_{EZ}$ **30**$_{EE}$

*Scheme 32: Isomerization between the red (EZ) and yellow (EE) form of formazane **30**.*[104]

Shifting the irradiation wavelength further to the red has been accomplished by variation of the aryl units. The blue formazane **31**$_{EZ}$ undergoes the Z to E isomerization under 578 nm irradiation to the yellow **31**$_{EE}$, while the reverse reaction can be conducted either thermally or with 436 nm (Scheme 33). The thermal back reaction proceeds faster compared to the parent **30**$_{EE}$ and interestingly there are only two species present, suggesting that the other isomers revert even faster.[102]

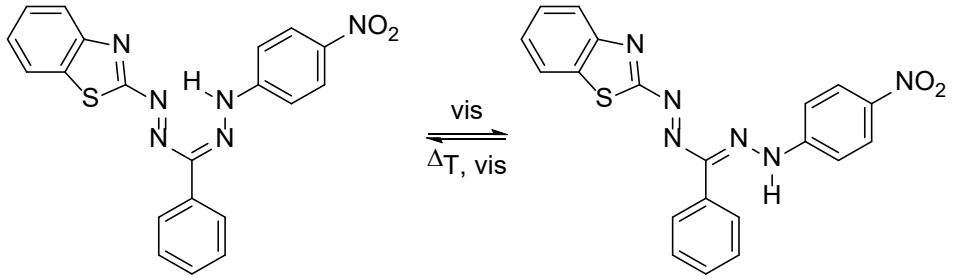

31$_{EZ}$ **31**$_{EE}$

*Scheme 33: Formazane derivative **31** can be switched with 578 nm from Z to E and with 436 nm or heat from E to Z.*[102]

Replacing the azo group of a formazane by a carbonyl group, which can also form a hydrogen bond has a dramatic effect on the switching properties, especially as it can increase the thermal half-life (Scheme 34). The hydrazone **32**$_Z$ (λ_{max} = 398 nm) is converted to the corresponding E isomer **32**$_E$ (λ_{max} = 373 nm) with 442 nm light irradiation (Φ_{ZE} = 0.003, PSS = 91% E). The E isomer has a half-life of 2700 years at 25 °C and the back reaction is conducted with UV-light (340 nm, Φ_{EZ} = 0.024, PSS = 76% Z).[106]

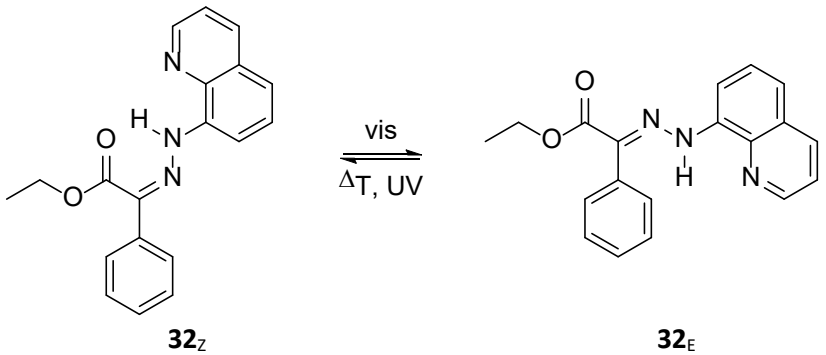

32$_Z$ **32**$_E$

*Scheme 34: Negative photochromic hydrazone based switch **32** with a thermal half-life of 2700 years at 25 °C.*[106]

Acylhydrazones can be easily synthesized from a hydrazide and an aldehyde or ketone, allowing for the simple introduction of various substituents. Although many derivatives were found to be photochromic, including electron donating or withdrawing substituents, heterocycles, and polycyclic aromatic hydrocarbons, most of them require UV-light for both isomerization directions. The biggest effects are observed when changing the ketone/aldehyde half of the switch. In the pyridine derivative **33**$_E$ (λ_{max} = 292 nm) the photochemically produced Z form is considerably stabilized due to hydrogen bonding (Scheme 35). In the case where 2-pyrenyl is used instead of 2-pyridyl the absorption maximum of the E isomer shifts to the visible region (λ_{max} = 403 nm) and renders the system negative photochromic.[107]

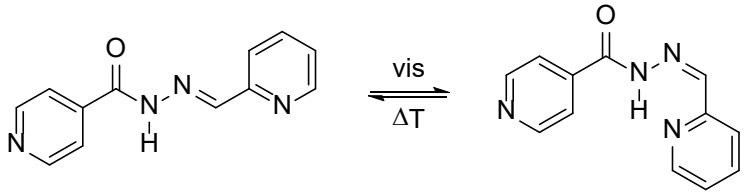

33$_E$ **33**$_Z$

*Scheme 35: P-type photochromism of an acylhydrazone **33**, where the Z isomer is stabilized via a hydrogen bond.[107]*

2.3.5.3 Isomerization of N=N Double Bonds

The most prominent case of the E to Z N=N double bond isomerization is azobenzene, which will be discussed separately in section 3.2.1. Nevertheless, some systems are known, where at least one aryl unit is substituted by a nonaromatic substituent. In the case of azoalkanes, both substituents are aliphatic and, in most cases, undergo the photoisomerization with quantum yields of around 0.5 in both directions. Despite very low extinction coefficients (usually < 200 L mol^{-1}cm^{-1}), there are two main issues: a) the decomposition to nitrogen and the two corresponding radicals and b) the tautomerization to the more stable hydrazone. Both side reactions are much more serious for the Z isomers, whereas the E isomers are relatively stable. It is not surprising that with decreasing stability of the formed radical the nitrogen release pathway is hampered. Therefore, the best aliphatic azo switches in terms of photochemical stability bear either unbranched alkyl chains, such as *n*-propyl or polycyclic substituents, where at least one ring is five membered and the bridge head is connected to the N=N double bond. One of the best studied examples is azonorbornane **34**$_E$ (λ_{max} = 364 nm), which upon irradiation of UV-light forms the Z isomer **34**$_Z$ (λ_{max} = 423 nm) and reverts back thermally only at high temperatures with a half-life of 10 min at 100 °C (Scheme 36).[108–110] Few studies report on molecules with one aryl unit and one alkyl substituent, which results in an enhanced stability towards decomposition, accompanied with a bathochromic shift of the absorption maxima.[111,112] The combination of a phenyl substituent and a cyclohexene ring results in similar properties compared to azobenzene.[113]

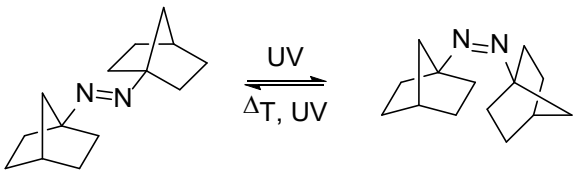

34$_E$ **34**$_Z$

*Scheme 36: P-type photochromism of azonorbornane **34**, where the typical side reactions do not occur.*[108–110]

2.3.6 Pericyclic Reactions

Relevant pericyclic reactions in this context are electrocyclizations and cycloadditions. The electrocyclization reduces the amount of double bonds by one and results in one new single bond, which can be accompanied by the formation of two stereocenters. The cycloaddition reduces the amount of double bonds by two and forms two new single bonds. Given the right symmetry criteria, this will result in 4 new stereo centers built up by the action of a single photon. It should be mentioned here that the Nobel Prize-rewarded Diels-Alder reaction is still widely applied in organic synthesis of drugs and natural products since it is also capable of building up 4 stereo centers in a single reaction. On the contrary, light induced dimerization reactions are only scarcely applied in natural product synthesis[114] although the photochemical dimerization of tetracene has been described already in 1867 by Fritzsche, and was the first molecular photochromic system.[3]

2.3.6.1 4 π-Electrons

4 π-electrons can react in a pericyclic reaction either in terms of a 4 π electrocyclization or a [2+2] cycloaddition. The main issue of photochromic molecules based on only 4 π-electrons is their absorption band, which usually lies in the deep UV. Therefore, the by far biggest amount of literature dealing with light induced electrocyclizations concerns the 6 π electrocyclizations, such as in diarylethenes, dihydropyrenes, fulgides, and so forth. Conceptually, photochemical 4 π electrocyclizations are different in that, according to the Woodward-Hoffmann rules,[115,116] the substituents at the periphery would point towards each other in the photoproduct, leading to very different possibilities for applications. A class of molecules which can undergo such 4 π electrocyclizations is derived from cycloheptatriene. Cycloheptatriene itself could undergo various photoreactions, one of them being the cyclization to bicyclo[3.2.0]heptadiene. Although this reaction is thermally reversible it requires temperatures as high as 400 °C.[117] Similar observations were made for monocyclic troponoids and azepines,[118] however among the cycloheptatriene systems, some display not only negative photochromism, but can be switched back thermally at rather moderate or low temperatures. In this context, it was found that the absorption of 2,5-disubstituted tropones usually reaches the visible region, providing a maximum little above 400 nm for amino substituents in the 2-position. The rate of the thermal return reaction increases with the donor strength in the 2-position or the acceptor strength in the 5-position and can be tuned over a wide range (2 min at 80 °C to 2 min at −75 °C). Tropone derivative **35**$_{open}$ (λ_{max} = 409 nm) is converted to the bicyclic **35**$_{closed}$ and reverts with a thermal half-life of 2 min at −75 °C (Scheme 37).[119]

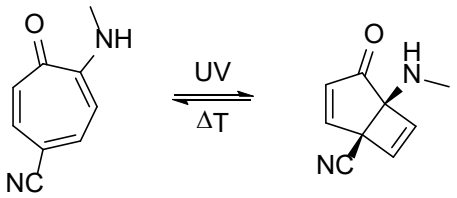

35open **35**closed

*Scheme 37: Reversible 4 π electrocyclization of tropone derivative **35**.[119]*

The similar cycloheptatrienes with a donor in the 1-position and any aryl substituent in the 4-position are capable of undergoing the 4 π electrocyclization via excitation to the S_1 state with reasonable thermal half-lives of few minutes at 50 °C as well. The absence of the carbonyl moiety also allows for a photochemical sigmatropic hydrogen shift, although it only occurs from higher excited states.[120,121] Other systems which undergo a 4 π electrocyclization, are three-membered heterocycles, such as oxiranes, oxaziridines, or aziridines.[122,123] Upon irradiation with UV-light, a single bond is cleaved heterolytically and the corresponding 1,3-dipoles are being formed (carbonyl ylides, nitrones, and azomethine ylides respectively). The reversion proceeds either by irradiation or thermally. The colorless aziridine derivative **36**closed (λ_{max} = 283 nm) undergoes the ring opening to the blue **36**open (λ_{max} = 605 nm) upon UV irradiation either in solution or the crystalline state (Φ_{CO} = 0.85). The ring closure occurs thermally with a half-life of 12 h at 25 °C or photochemically by visible light irradiation (Scheme 38).[124]

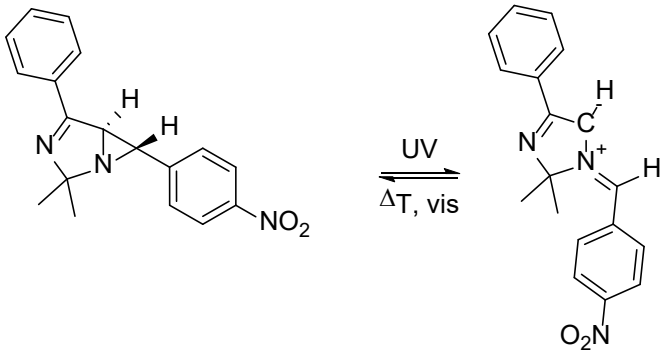

36closed **36**open

*Scheme 38: Photochemical ring opening of aziridine **36** to yield a zwitterion.[124]*

The light induced [2+2] cycloaddition of norbornadiene resulting in quadricyclane is mostly discussed in solar energy storage applications,[125–127] since many prerequisites come together in this system: Besides its high energy capacity (ΔH = 21 kcal/mol)[128] it is a liquid of low molecular weight, therefore allowing for high energy densities. Furthermore, the thermal back reaction is slow (2.5 h at 161 °C)[129] but can be accelerated by various catalysts.[125] One of the main drawbacks of norbornadiene is its transparency over most of the solar spectrum and a rather low isomerization quantum yield (Φ = 0.05).[130] Although sensitizers, such as acetophenone, may help to increase the quantum yield close to unity, a sufficient bathochromic shift of the absorption spectra matching the sunlight remains not easy-to-reach.[125] To achieve visible light switching the spectral properties of norbornadienes can be adjusted by substitution at one of the double bonds, reaching absorption onsets up to 700 nm.[131] Efficient ways to modify the photochromic properties are elongation of the π-system,[132] donor-acceptor substitution,[132,133] introduction of methyl groups in the bridge head,[127] or substitution of the

second double bond with CF_3-groups.[134] Norbornadiene derivative **37**$_{open}$ (λ_{max} = 365 nm) can be converted with UV-light (Φ_{oc} = 0.46) to the quadricyclane **37**$_{closed}$, which reverts with a half-life of 1.9 h at 25 °C (Scheme 39). The [2+2] cycloaddition is not necessarily limited to norbornadienes but can also proceed in other cage forming reactions. To overcome the high barrier for the reverse reaction usually catalysts, such as base or transition metals, are applied.[135] Other typical reversible [2+2] cycloadditions in the sense of a dimerization reaction have been described for naphthoquinones, coumarines,[136] cinnamic acid derivatives,[137] thiophosgene, and others.[138]

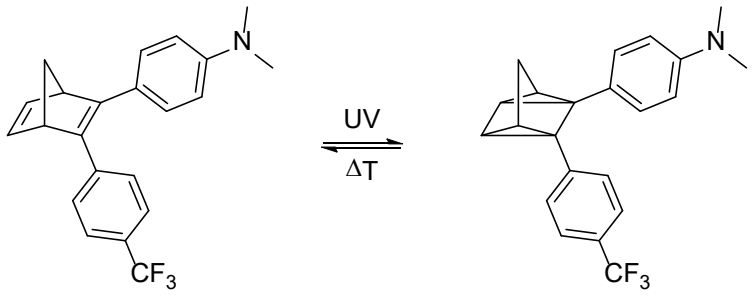

37$_{open}$ **37**$_{closed}$

*Scheme 39: Donor-acceptor substitution shifts the spectrum of the norbornadiene **37** to the visible region.[132,133]*

2.3.6.2 6 π-Electrons

In principle, any hexatriene system can undergo a 6 π electrocyclization to a cyclohexadiene and even photochromic systems have been described, where the 6 π electrocyclization leads to five membered heteroaromatic rings.[123] However, since all three double bonds of a hexatriene system are also capable of undergoing an E/Z isomerization, usually at least two of them are fixed in a cycle or substituted symmetrically. Since the hexatriene systems absorbs in the deep UV, it is preferred to utilize aromatic systems instead of plain double bonds. During the electrocyclization the aromatic character is lost, which leads to a reduced thermal stability of the ring closed isomer. By proper choice of aromatic stabilization of the open isomer, the thermal half-life can be tuned. Although 6 π electrocyclization based switches are usually considered to be P-type, terarylenes have been described, which revert with a half-life of < 2 s at 25 °C.[139,140] Nevertheless, the 6 π electrocyclization can only occur when the inner double bond is in the Z configuration as has been discussed earlier for Z stilbene. There are two main strategies to inhibit the Z to E isomerization of the inner double bond: In many cases proper choice of substituents can strongly decrease the Z to E quantum yield, diminishing the Z to E isomerization to such an extent that virtually only the open Z and the closed form are present. This strategy has been largely applied to fulgides: While the **38**$_E$ (λ_{max} = 360 nm) isomerizes to the Z isomer **38**$_Z$ (λ_{max} = 347 nm) at 366 nm irradiation (Φ_{EZ} = 0.06), the back reaction does not occur. Instead, **38**$_Z$ is further isomerized to the closed **38**$_{closed}$ (λ_{max} = 510 nm, $\Phi_{Z,closed}$ = 0.62) with a PSS close to 100%. The system is thermally stable and the back reaction is induced with visible light (492 nm, $\Phi_{closed,Z}$ = 0.04, Scheme 40). When the same molecule bears a methyl group instead of the bulky isopropyl, the Z to E isomerization becomes a concurrent reaction (Φ_{ZE} = 0.13, $\Phi_{Z,closed}$ = 0.19).[141,142]

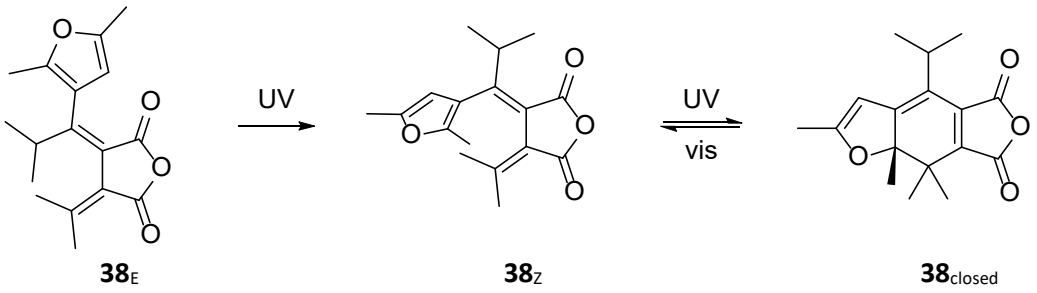

38$_{E}$ **38**$_{Z}$ **38**$_{closed}$

Scheme 40: The bulky isopropyl group prevents the Z to E isomerization of fulgide switch ***38****$_{Z}$.*[141,142]

The second strategy to prevent the Z to E isomerization of the inner double bond has been applied for diarylethenes with cyclopentene bridges. The closed form of diarylethenes is prone to form a rearrangement side product upon UV irradiation and only few fatigue resistant switches have been described. A thorough study on various derivatives revealed that electron-deficient substituents are preferable: The colorless open isomer **39**$_{open}$ (λ_{max} = 284 nm) cyclizes to the closed isomer **39**$_{closed}$ (λ_{max} = 548 nm) upon 313 nm light irradiation with Φ_{OC} = 0.44 with a PSS of 97%. The reverse reaction is conducted with visible light at 546 nm and usually suffers from a low quantum yield (Φ_{CO} = 0.005 for **39**), which on the other hand results in a high PSS for the forward reaction and can be compensated for with broad range irradiation in the visible for the back reaction (Scheme 41). The quantum yield for the byproduct formation in **39** is exceptionally low ($\Phi_{byproduct}$ = 0.0004).[143] The dihydropyrene to *meta*-cyclophanediene isomerization is also regarded as a 6 π cycloreversion and will be discussed separately in section 3.1.

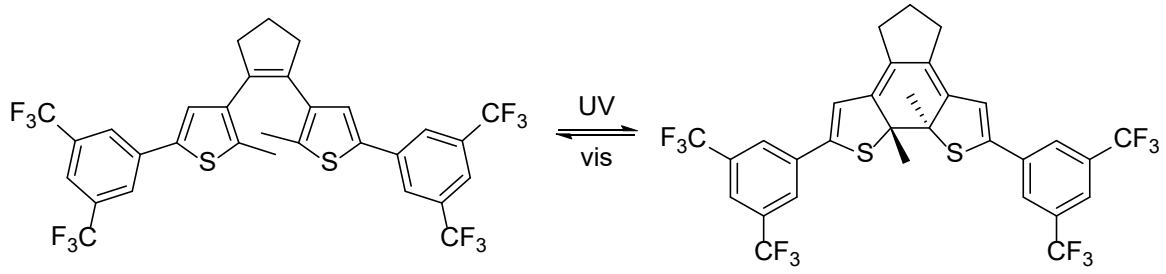

39$_{open}$ **39**$_{closed}$

Scheme 41: P-type photochromism of a fatigue resistant dithienyl ethene ***39****.*[143]

Besides the electrocyclization, 6 π-electrons can undergo the [4+2] cycloaddition. Reaction-type wise there is a certain similarity to the Diels-Alder reaction, although a Diels-Alder reaction does not involve the excited state. An often observed photochemical [4+2] cycloaddition happens in polycyclic aromatic hydrocarbons, which react with oxygen to endoperoxides. Mechanistically, the aromatic system acts as a triplet sensitizer, which then produces singlet oxygen. The singlet oxygen reacts with an aromatic system in the ground state. In cases where the endoperoxide cannot open to a stable intermediate, the release of singlet oxygen becomes favorable, which renders the system photochromic. Typical systems are based on the structure of 9,10-diphenylanthracene, where the phenyl rings are fixed in plane with the anthracene by an additional bridge. **40**$_{DPA}$ (λ_{max} = 539 nm) can be oxidized by irradiation in air saturated solution to **40**$_{EPO}$ (λ_{max} = 307 nm), which is greatly stabilized by the increased aromaticity of the two newly formed benzene rings versus the former anthracene. The reverse reaction proceeds either thermally at high temperatures and at a neglectable rate at room temperature (4 years half-life at 20 °C) or photochemically by UV-light irradiation (Scheme 42). In addition to the

cycloreversion, splitting of the endoperoxide and successive reaction is a competing process. Interestingly, both processes happen from different excited states, so that the ratio of cycloreversion and decomposition is wavelength dependent.[144,145]

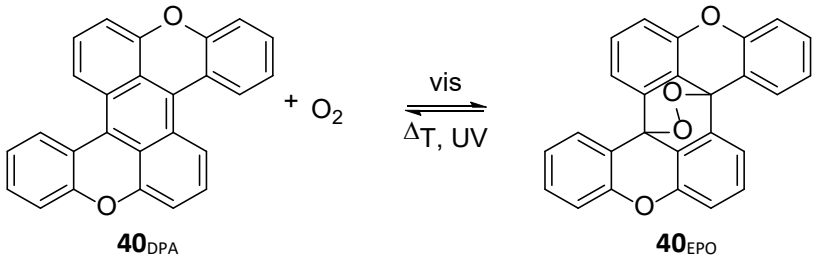

40$_{DPA}$ **40**$_{EPO}$

*Scheme 42: Reversible oxidation of the polycyclic aromatic hydrocarbon **40**.[144,145]*

2.3.6.3 8 π-Electrons

The dimerization of anthracene derivatives has been studied since the discovery of molecular photochromism. An interesting aspect of dimerization reactions is the option of two different products when non-symmetrically functionalized derivatives are in question. The possibility to obtain either head to head or head to tail dimers, depending on the substitution pattern has been shown.[146–148] Since the dimerization efficiency is highly dependent on the concentration, bridged anthracene dimers have been synthesized and the dependence of the quantum yield on the distance between the two moieties has been investigated.[149] The negative photochromic **41**$_{monomer}$ (λ_{max} = 388 nm) dimerizes upon irradiation with 366 nm (Φ_{MD} = 0.32) to **41**$_{dimer}$ (λ_{max} = 255 nm) and reverts upon irradiation with 254 nm (Φ_{DM} = 0.64, Scheme 43). With an increasing quantum yield for the dimerization, the fluorescence quantum yield decreases (Φ_{fluo} = 0.03 for **41**$_{monomer}$).[150] Other systems undergoing a reversible [4+4] cycloaddition are 2-pyridones, triazolopyridines,[114] and some pyrane derivatives.[114]

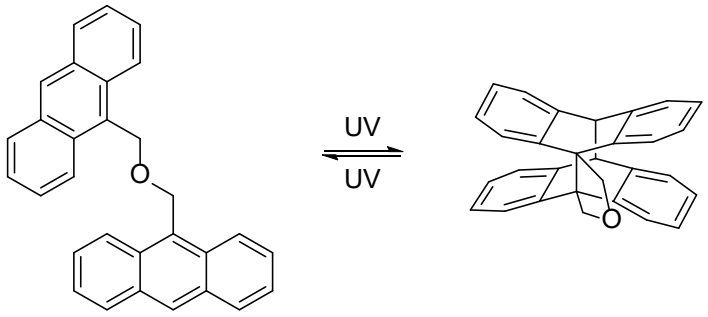

41$_{monomer}$ **41**$_{dimer}$

*Scheme 43: [4+4] cycloaddition of a bridged anthracene dimer **41**.[150]*

2.3.6.4 10 π-Electrons

With an increasing number of π-electrons, the number of photochromic systems decreases. Most systems, which consist of more than 6 π-electrons, prefer to undergo an E/Z isomerization or a 6 π electrocyclization instead of a 10 π electrocyclization or a [6+4] cycloaddition. In the dihydroazulene system these reactions are impossible and it is therefore an example for this unusual photoreaction. Dihydroazulene **42**$_{DHA}$ (λ_{max} = 381 nm) undergoes a 10 π cycloreversion upon irradiation with UV-light (Φ_{MD} = 0.15, 366 nm) to form the vinylheptafulvene **42**$_{VHF}$ (λ_{max} = 450 nm). Complete conversion to the vinylheptafulvene is achieved since the back reaction does only proceed thermally with a half-life of 4 h at 20 °C (Scheme 44). The photochromic properties of the switching system are only slightly influenced by substitution effects or solvents and although various derivatives have been synthesized, the dihydroazulene shows only an absorption tail in the visible region, quantum yields up to 0.6, and thermal half-lives from few minutes to hours.[151,152]

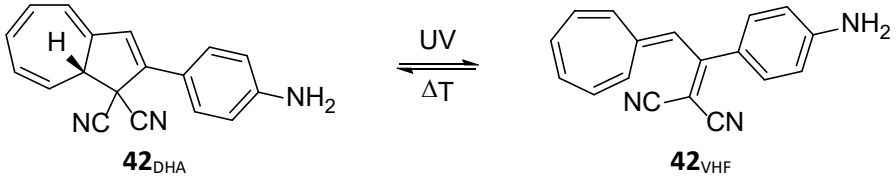

42$_{DHA}$ **42**$_{VHF}$

*Scheme 44: 10 π cycloreversion of dihydroazulene switch **42**.[151,152]*

2.3.7 Photochromism with a Consecutive Reaction

Many switches show more than a simple photochromic reaction but have a consecutive reaction, leading to a different product. Such a consecutive reaction can be either thermal or photochemical and allows for the design of even more complex systems as it enhances the variety of photochemical reactions. Typical systems undergo an E to Z isomerization, followed by a photochemical 6 π electrocylization or the attack of a donor moiety on an acceptor.

The simplest and best understood system is again stilbene, where the E to Z isomerization is followed by a 6 π electrocyclization to dihydrophenanthrene (see section 2.3.5.1). Similar systems are fulgides, where the 6 π electrocyclization drives the system away from the photochemical E/Z equilibrium,[141,142,153] as well as dithienylethenes with non-cyclic bridges. Upon irradiation of **43** with 405 nm light, three different isomers are found in the mixture: **43**$_{E}$ (λ_{max} = 325 nm), **43**$_{Z}$ (λ_{max} = 304 nm), and **43**$_{closed}$ (λ_{max} = 522 nm), which interconvert. In comparison to the stilbene system, the internal methyl groups prevent oxidation and diminish the major fatigue path (Scheme 45).[154,155]

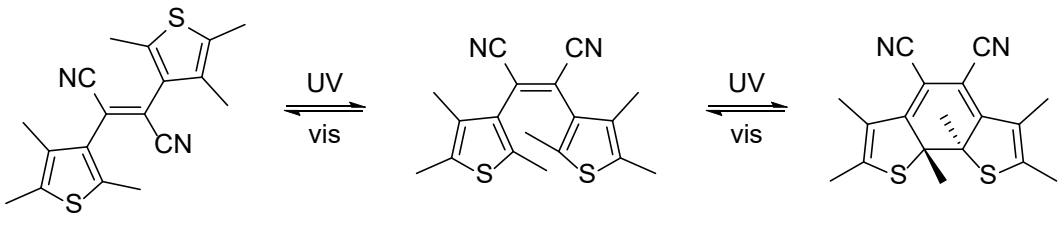

43$_{E}$ **43**$_{Z}$ **43**$_{closed}$

*Scheme 45: E to Z isomerization followed by a 6 π-electrocyclization of diarylethene **43**.[154,155]*

An E/Z double bond isomerization can also enable the photoproduct to undergo a cycloaddition as in the case of 9,9'-azoanthracene. Irradiation of **44**$_E$ with 350 nm light results in the formation of the closed species **44**$_{closed}$ (λ_{max} = 247 nm), which does not revert photochemically, but thermally upon heating to 280 °C.[156]

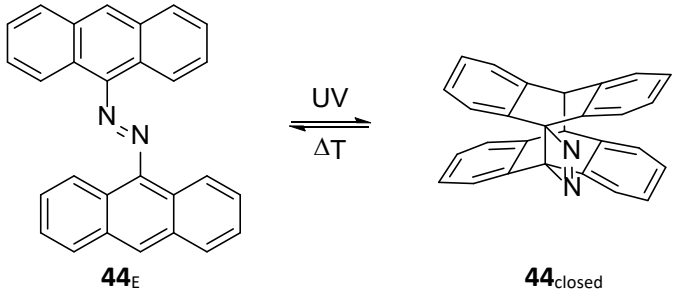

44$_E$ **44**$_{closed}$

*Scheme 46: E to Z isomerization 9,9'-azoanthracene **44**, followed by a [4+4] electrocyclization.[156]*

A special case of the C=C or C=N double bond isomerization are photoswitches, like spiropyrane or spirooxazine. Although the exact mechanisms are under debate, in the current picture the opening of spiropyrane occurs *via* a 6 π cycloreversion, which is followed by a thermal Z to E isomerization of the double bond,[157] whereas the closing happens *via* an E to Z isomerization in the excited state (without relaxation to the ground state), followed by ring closure. In the case of strong acceptors attached to the ketone part, such as nitro in **45**$_{SP}$ (λ_{max} = 350 nm), the merocyanine form **45**$_{E,MC}$ (λ_{max} = 560 nm) is stabilized and is therefore present in a thermal equilibrium (Scheme 47).[83,158,159]

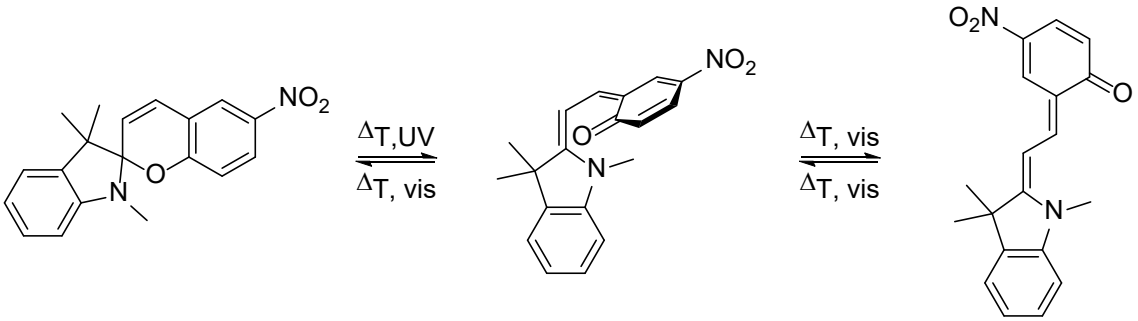

45$_{SP}$ **45**$_{Z,MC}$ **45**$_{E,MC}$

*Scheme 47: The spiropyrane and merocyanine system **45**.[157]*

Design-wise the merocyanine connects a donor and an acceptor *via* a system of conjugated double bonds, which are in principle able to undergo an E to Z isomerization. It is therefore plausible that other systems with of similar nature show the same stepwise switching property. An example is given where tricyanofuran acts as the acceptor and phenol as the donor.[160] Interestingly, the acceptor strength of the tricyanofuran moiety is sufficient to allow the nitrogen atom of a quinoline to act as the donor as well. The strong acceptor stabilizes the open form rendering the system negative photochromic. The yellow solution of **46**$_{open}$ (λ_{max} = 428 nm) decolorizes upon irradiation with 470 nm by forming the closed isomer **46**$_{closed}$ (λ_{max} = 310 nm) with Φ_{OC} = 0.2 and reverts with a half-life of 102 min (Scheme 48).[161]

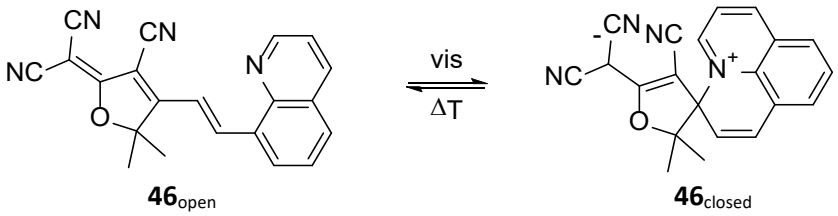

46$_{open}$ **46**$_{closed}$

*Scheme 48: Negative T-type photochromism of tricyanofuran system **46**.*[161]

The open form of donor-acceptor Stenhouse adducts displays the same structural motif as merocyanines and tricyanofuran switches. Upon irradiation of **47**$_{E,open}$ (λ_{max} = 545 nm) a C=C double bond isomerizes to **47**$_{Z,open}$ (λ_{max} = 600 nm), followed by a rapid thermal ring-closure to **47**$_{closed}$ (λ_{max} ≈ 270 nm), which reverts back with a thermal half-life of 40 s (Scheme 49). The thermal ring-closure is believed to proceed in a 4 π electrocyclization, although the attack of an enol on the imine should be as likely.[162] Donor-acceptor Stenhouse adducts are negative photochromic (considering the ring closure is fast) and are usually limited to nonpolar solvents. Although a thorough study on their photochromic properties in terms of quantum yields is still missing, absorption spectra show an interesting feature, as they exhibit a "gap" of more than 150 nm (300-450 nm for **47**), where both isomers essentially do not absorb. Such a rare property has high potential in applications which require orthogonal switching.[163]

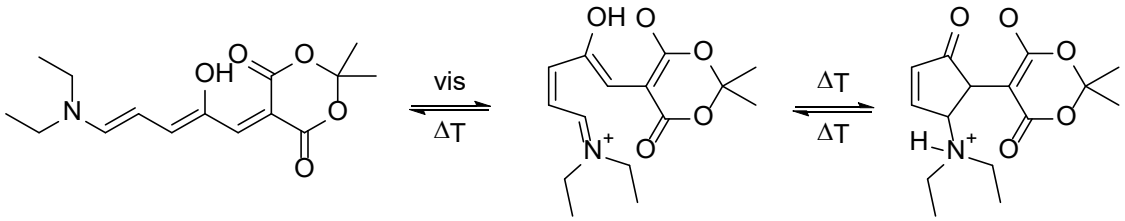

47$_{E,open}$ **47**$_{Z,open}$ **47**$_{closed}$

*Scheme 49: Photochromism of donor-acceptor Stenhouse adducts. The ring closure of **47**$_{E,open}$ is believed to occur via a thermal 4 π electrocyclization, although the attack of the enol **47**$_{Z,open}$ on the iminium carbon is as likely.*[163]

During the ring closure of diarylethenes the former (hetero)aryl units become nonaromatic. In case of phenol as one aryl unit **48**$_{OH,open}$, an enol is formed **48**$_{OH,closed}$ upon UV irradiation, which can undergo keto-enol tautomerization to **48**$_{keto,closed}$ (Scheme 50).[164,165] This additional feature, which cannot be accomplished with the "classic" photoreactions, leads to new applications such as light controlled dynamic covalent chemistry[165] or a photoswitchable polymerization catalyst.[32]

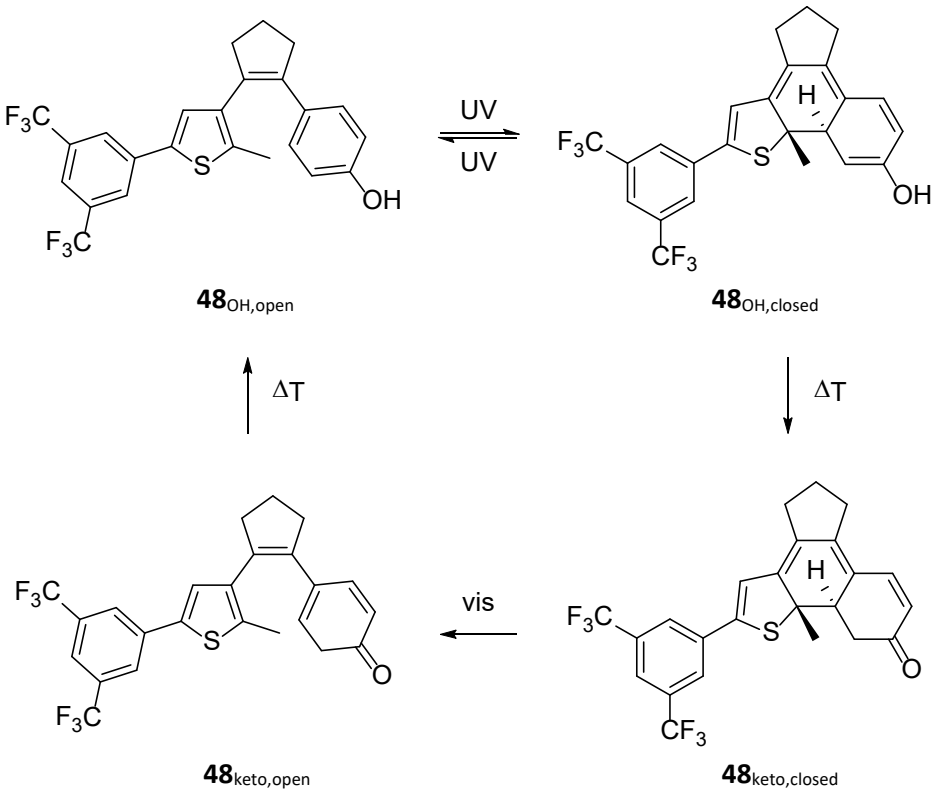

*Scheme 50: 6 π electrocyclization of diarylethene **48** with a consecutive keto-enol tautomerism.*[165]

3 Results and Discussion

3.1 Dihydropyrenes

Among the examples of negative photochromic molecules in the literature, the dihydropyrene class is probably the best studied, since its negative photochromism does not depend on the environment and therefore substitution can be very effective. The planar parent molecule consists of 14 π-electrons, which are delocalized in a π-conjugated cycle and it is therefore aromatic. This fact is revealed by the ^{1}H-NMR signal of the internal methyl protons of **49**$_{closed}$, appearing at −4.2 ppm.[42] Upon irradiation of the green **49**$_{closed}$ (λ_{max} = 466 nm) with visible light (> 430 nm) a 6 π cycloreversion takes place, resulting in the bleached *meta*-cyclophanediene system **49**$_{open}$ (λ_{max} = 276 nm, Φ_{CO} = 0.006, Scheme 51).[42,166] The backward reaction can be induced photochemically using UV-light with high quantum yields, *via* a Woodward-Hoffmann-forbidden thermal pathway (42 h at 20 °C),[42,167] or reductively.[168]

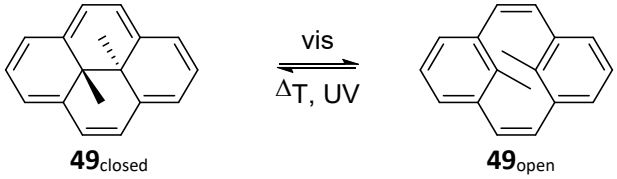

49$_{closed}$ **49**$_{open}$

*Scheme 51: Photochromism of the parent dihydropyrene **49**.*

Interestingly, the photoisomerization does not take place from the lowest excited state, but after excitation to the second, which is in most cases the reason if quantum yields are low.[41] The first three excited states are involved in the photochromism of dihydropyrene. The S_1 state is a locally excited state (LE) similar to the S_1 state of benzene and is depicted as a structure where all bonds are slightly stretched. Although the transition S_0-S_1 is forbidden (as in benzene), there is still a fine structured absorption with low extinction coefficients (≈ 300 L mol^{-1}cm^{-1}) visible around 640 nm. The S_2 state is of zwitterionic nature, where the charges are separated between the two benzene rings, resulting in a dipole along the long axes. The S_3 state is a singlet biradical state, where the radicals are localized on the inner carbon atoms. No characteristic feature for this state is observed in the UV/vis spectrum, as the transition from the ground state is symmetry forbidden. After excitation to the S_2 state the molecule moves along the reaction coordinate to a conical intersection with the S_1 state. The main deactivation takes place through this conical intersection. From the S_1 state the molecule mainly relaxes thermally, although weak fluorescence without Stokes shift is observed (Φ_{fluo}=0.0006).[166] The molecules, which do not relax *via* the S_1 state, move further along the reaction coordinate and pass the biradical state. From the biradical state a conical intersection to the ground state was found, which then leads to the formation of open and closed isomer, although the exact transition from the zwitterionic to the biradical state remains unresolved (see chapter 3.1.4 for further discussion and Figure 4).[41]

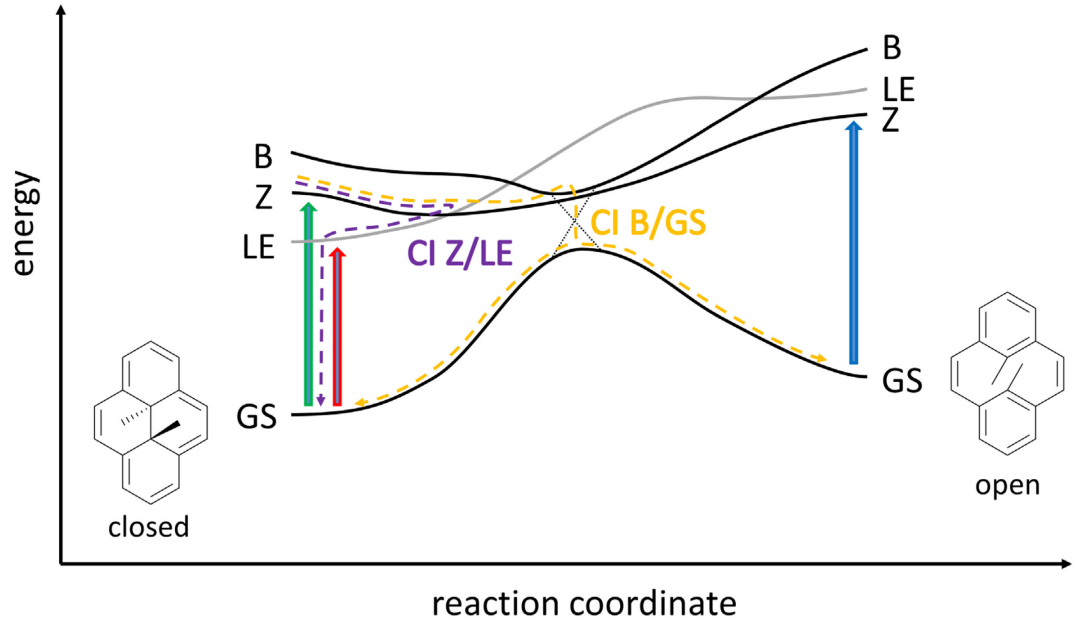

*Figure 4: Switching mechanism of the parent dihydropyrene **49**: Excitation to the S_1 state (LE, red arrow) in the long wavelength region above 600 nm does not lead to switching. After excitation to the S_2 state (Z, green arrow), the molecule can either change to the LE state via the conical intersection CI Z/LE and relax thermally (purple dashed line) or overcome an excited state activation barrier to the conical intersection CI B/GS from the B state, which leads to the formation of the open isomer (identical to Figure 9 and Figure 28).*[41]

Back in 1963, the first derivative of dimethyldihydropyrene was synthesized in 18 steps *via* the corresponding saturated cyclophane by Boekelheide and Phillips.[169,170] A breakthrough was accomplished, when Mitchell and Boekelheide invented the thiacyclophane route in 1968, which is used until today and yields about 2 g of unsubstituted dihydropyrene in 10 steps starting from dichlorotoluene.[171,172] By introducing *t*-butyl groups in the 2- and 7-position, the synthetic effort can be reduced and 8-9 g of switch **56** can be obtained in 6 steps starting from *t*-butyltoluene **50** (Scheme 52).[49,173,174]

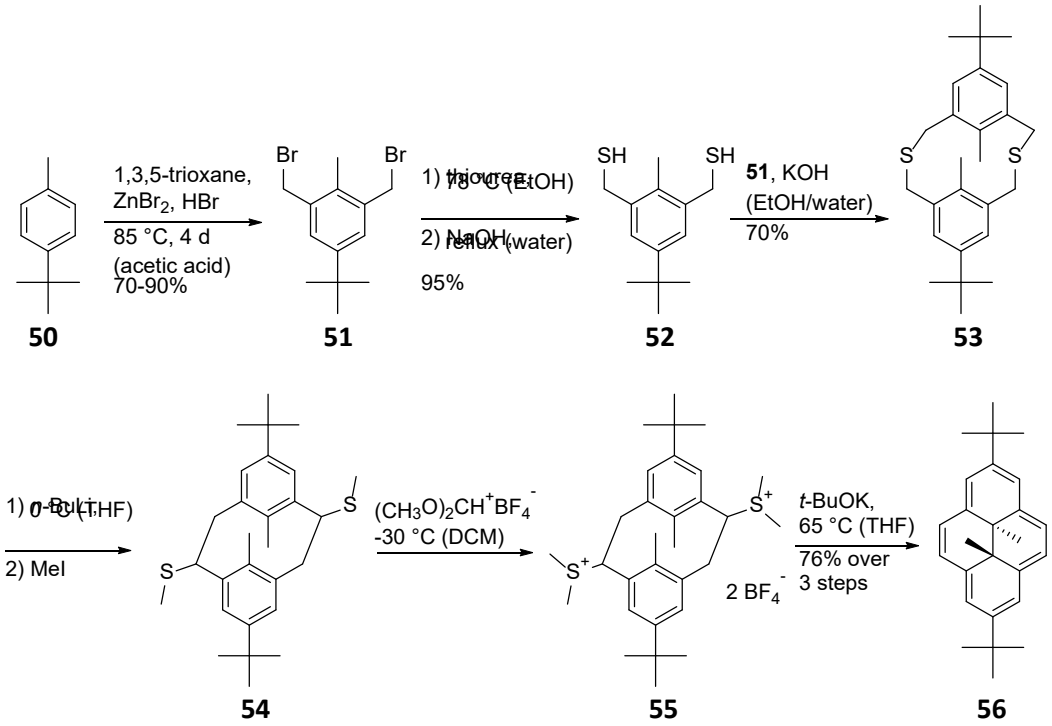

*Scheme 52: The 6 step synthesis yields 8 g of 2,7-bis(t-butyl)-dihydropyrene **56**.* [48]

Since classic reactions known for aromatic rings can be performed very well on dihydropyrenes,[175] typical functional groups have been attached, such as nitro, acyl, benzoyl, formyl, or halides and reversible oxidation to the corresponding 2,7-quinone, or Birch reduction are possible.[175] Electron donating substituents have not been introduced due to the instability of the resulting compounds. The most reactive position in unsubstituted dihydropyrene **49** is the 2-position. In the case of **56**, where the most reactive positions are blocked, electrophilic aromatic substitution goes selectively to the 4-position. The 1-position, which is the most reactive in pyrene, is hardly accessible and only few derivatives have been described where an intramolecular functionalization has been applied. The difference in reactivity already points at the better comparability with benzene than with pyrene. The possibility of trapping arynes with furan followed by deoxygenation made benzannelated dihydropyrenes accessible.[176] The dihydropyrene only reacts as an aromatic compound, therefore, other internal substituents then methyl have to be introduced from the very beginning. A synthetic way to transform the inner positions late in the synthesis was introduced by Mitchell as a Wittig reaction on an internal formyl group can be performed on the thiacyclophane stage.[177]

As most dihydropyrenes show a weak absorption corresponding to the S_0-S_1 transition, from which the opening does not occur, λ_{max} values given in this thesis ignore this transition. The photochromism of dihydropyrene switches highly depends on the substitution pattern. Already in 1970 Blattmann and Schmidt found that strong acceptors in the 2-position increase the quantum yield and the rate of the thermal back reaction dramatically. Therefore, 2-nitrodihydropyrene **57** (λ_{max} = 598 nm, Figure 5) has a quantum yield of 0.37 compared to 0.02 for the parent in this study. On the contrary, acceptor substitution at the 4-position has only little effect on the switching efficiency, whereas the 1-position is least studied due to synthetic reasons.[42] A lot of research was undertaken to increase the quantum yield without accelerating the thermal back reaction. One of the most important findings in this regard was the effect of benzannulation to stabilize the open form. Benzannulation in the 1,2-position

resulted in no observation of switching, which is ascribed to a very fast thermal back reaction, since in the open form the aromatic stabilization of a naphthalene ring and a benzene ring is smaller than that of two benzene rings. In contrast to that, the 4,5-benzannulated derivative **58** (λ_{max} = 504 nm) exhibits a long thermal half-life (7.3 d at 20 °C in toluene),[49,167] since three benzene rings are formed, stabilizing the open isomer. Moreover, the quantum yield for the opening reaction is increased slightly by a factor of 7 to 0.042.[166] Since the benzene ring has a bond localization effect on the dihydropyrene core, the aromaticity of the dihydropyrene is decreased. This is resembled by a huge shift of the ^{1}H-NMR signal for the internal methyl groups from -4.06 ppm (**56**) to -1.58 ppm (**58**) and can be used as an aromaticity probe if other aromatic systems are annulated and compared in terms of their bond localizing effect.[178] In case of double benzannulation in the 4,5 and 9,10-position, the open form **59** (λ_{max} = 287 nm) consists of four benzene rings and becomes more stable than the closed one.[43]

The by far largest effects on the photochromic properties can be reached by changing the internal substituents. It has to be considered that a 1,5-sigmatropic rearrangement of the internal substituent can be a problem. Whereas this requires temperatures as high as 200 °C for internal methyl groups, 15,16-dicyano-dihydropyrene undergoes the rearrangement already at 50 °C.[167] Although internal cyano groups increased the thermal half-life to 36 years at 20 °C, other internal conjugated substituents have been investigated to overcome the rearrangement issue. Among these, isobutenyl proved to be the best (16 years at 20 °C) and in combination with an electron withdrawing group **60** (λ_{max} = 557 nm, Figure 5) switches with high quantum yield and still long thermal half-life (Φ = 0.66, $t_{1/2}$ > 2 years at 20 °C).[179]

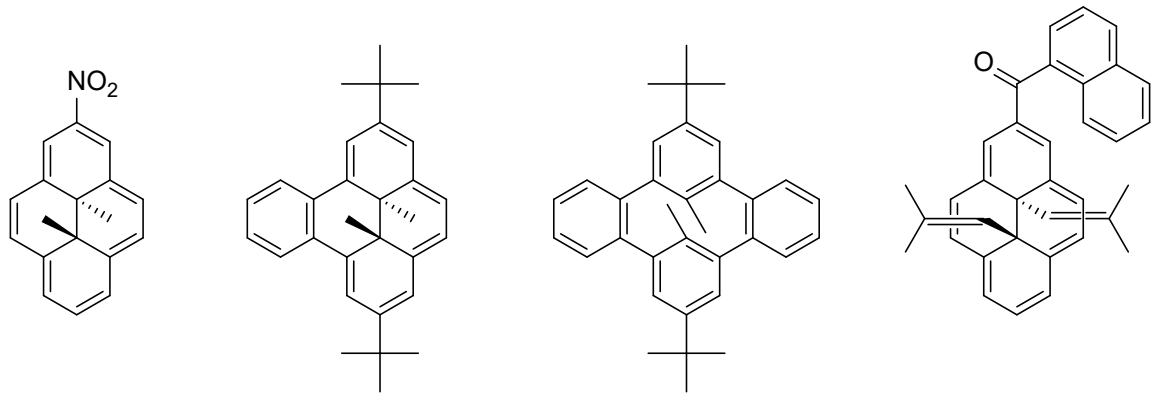

*Figure 5: 2-Nitrodihydropyrene **57**, 4,5-benzodihydropyrene **58**, and the open form of 4,5,9,10-dibenzodihydropyrene **59**. Internal isobutenyl groups increase the thermal half-life of **60** dramatically.*[42,43,166,179]

Due to the synthetic effort, only few heterocyclic derivatives are known (Figure 6) of which the azaderivative **61** (λ_{max} = 472 nm) has been shown to undergo reversible isomerization. Upon irradiation with visible light **61** opens to the corresponding *meta*-cyclophanediene and reverts with a half-life of 60 h at 30 °C. This conversion also happens with the protonated form **61-H$^+$** (λ_{max} = 640 nm), accelerating the thermal back reaction dramatically ($t_{1/2}$ = 8 s at 17 °C).[180] The sulfur containing derivative **62**, was not investigated in terms of switching but was reported to be unstable under light.[181]

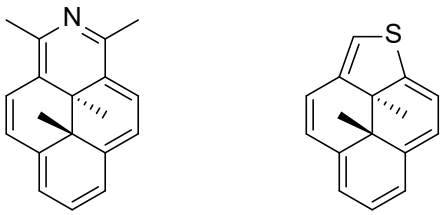

61 **62**

*Figure 6: Heterocyclic derivatives of dihydropyrenes **61** and **62**.*[180,181]

3.1.1 Motivation

Although dihydropyrenes can be used in rather physical applications such as logic gates,[182] the fact of negative photochromism and therefore the use of red light renders them promising candidates for photopharmacology. This was shown by a ribozyme with an aptamer which would bind only a closed dihydropyrene derivative. Switching the dihydropyrene causes a decrease in catalytic activity by a factor of 900.[183] Recent investigations were done on dihydropyrenes as red light activated singlet oxygen-sensitizer and -carrier in one molecule, which has potential application in cancer therapy.[184,185] However, one of the major problems in photopharmacology is the limited penetration depth in tissue, due to scattering and the absorbance of heme in blood. Shifting the switching wavelength to the near infrared would lead to a substantially enhanced penetration depth, but goes for most switches hand in hand with an extremely short thermal half-life or is limited to a special substituent. In contrast, it has been shown earlier, that dihydropyrenes bearing the general substitution pattern of a donor and acceptor moiety in the 4- and 9-position **63** (λ_{max} = 690 nm) bear NIR absorption due to a partially quinoid character **63$_{quin}$**.[186] Therefore, it was possible to switch with light > 800 nm with useful quantum yields and thermal half-lives, an accomplishment never made before and opening the door to true NIR photochromism.[40] Here, it is shown how donor and acceptor substituents in the 2- and 7-position can be chosen to modulate the photochromic properties of dihydropyrenes *via* manipulation of ground state and excited state activation barriers.

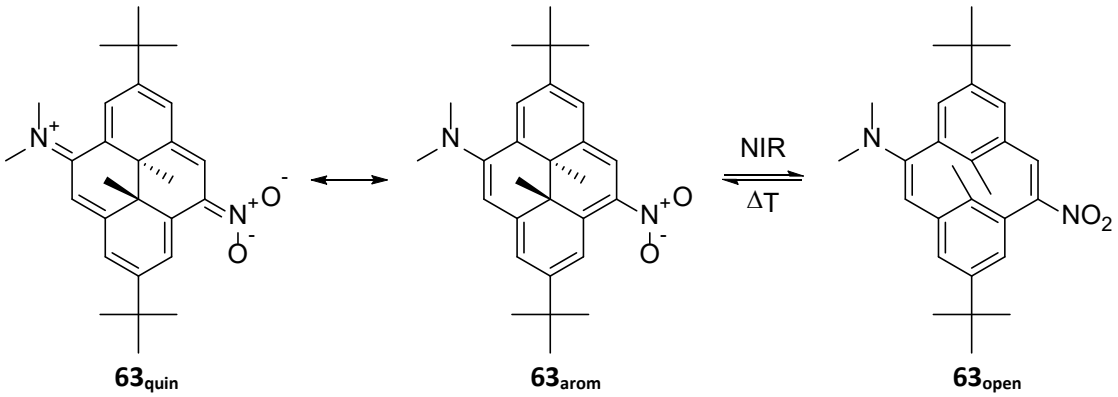

63$_{quin}$ **63$_{arom}$** **63$_{open}$**

*Figure 7: Push-pull system **63** results in true NIR switching.*[40,186]

3.1.2 Synthesis[i]

It has been shown earlier that the switching properties are only slightly affected by substituents in the 4-position. On the contrary, substituents in the 2-position have a dramatic effect on absorption maxima, extinction coefficient and quantum yield. Furthermore, 2-substituted or 2,7-substituted dihydropyrenes are highly symmetric, which could be advantageous in some applications and is rarely observed in other classes of photoswitches. For further functionalization of dihydropyrenes in the 2- and 7-positions, a different synthetic strategy is required, which does not utilize the *t*-butyltoluene precursor. Starting from readily available 2,6-dichlorotoluene **64**, the palladium catalyzed cyanation with $K_4[Fe(CN)_6]$ to yield 2,6-biscyanotoluene **65** has been investigated, which makes the earlier described use of CuCN in a Rosenmund-von Braun reaction on a large scale unnecessary.[187] The originally described further steps of DIBALH reduction to yield the bisaldehyde and subsequent reduction with $NaBH_4$ to the corresponding bisbenzyl alcohol were found to be tedious during the work-up and purification.[187] The strategy was changed to hydrolysis of the nitrile groups to the corresponding acids **66** with KOH, which is a quantitative reaction and allows precipitation of the product by acidification. The subsequent reduction to the bisbenzyl alcohol **67** by $LiBH_4/SiMe_3Cl$ does not form insoluble side products, which allows for simple crystallization of the product and therefore circumvents the tedious extraction procedure. The bisbenzyl bromide **68** is obtained in a quantitative reaction with aqueous HBr. A portion of the bisbenzyl bromide is transferred to the bisbenzyl thiol **69** *via* the corresponding thiouronium salt and subsequent hydrolysis. Although this type of reaction is usually done in one pot, for the synthesis of unsubstituted dihydropyrene isolation of the salt improves the yield of this two-step process considerably. The following steps are carried out as described for the 2,7-bis-*t*-butyl-dihydropyrene: Under high-dilution conditions, the thiacyclophane macrocycle **70** is formed, which is the scale limiting step of the complete synthesis. The Wittig rearrangement, which causes the ring contraction, was only described for other derivatives but worked as well in the unsubstituted dihydropyrene route. Methylation of the exocyclic thioether **71** with Borch reagent to the bissulfonium salt **72** and subsequent Hoffmann elimination yields the unsubstituted dihydropyrene **49** *via* the open form (Scheme 53).

[i] Conditions for synthesis of **66** and **67** (Scheme 53) were developed by Jonas Becker.

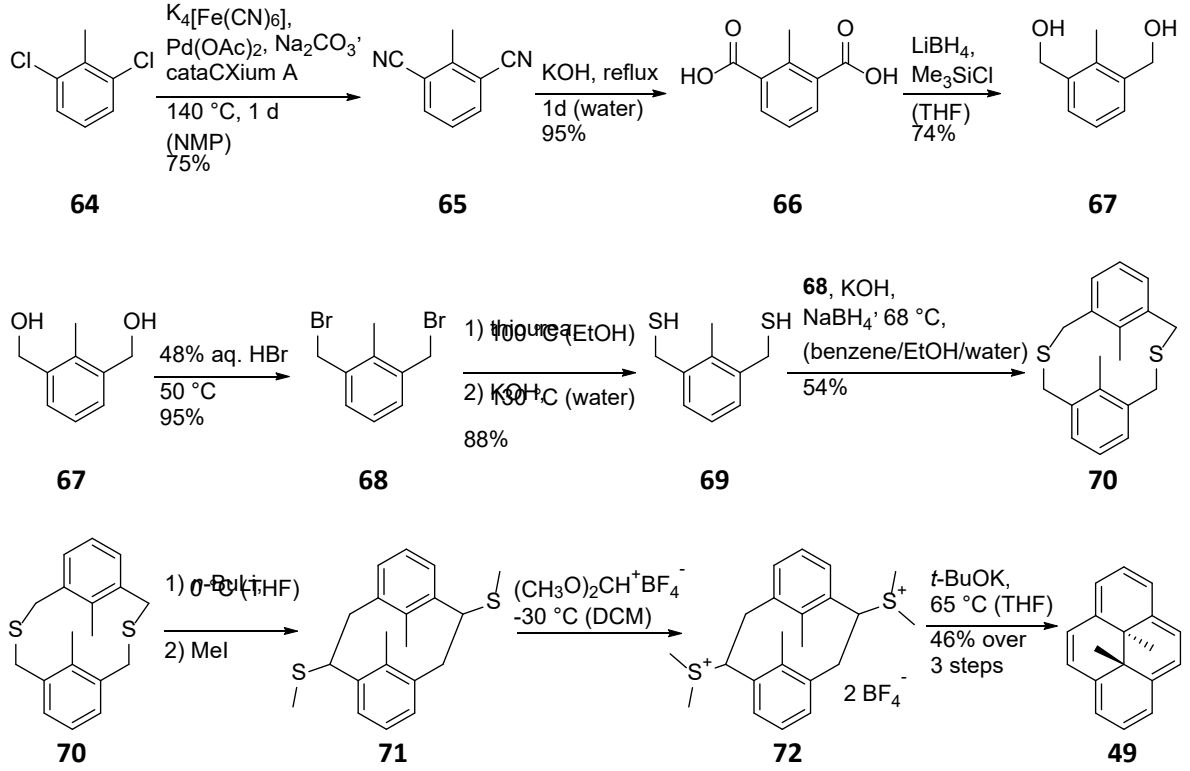

*Scheme 53: Synthesis of unsubstituted dihydropyrene **49**.*[187]

The unsubstituted dihydropyrene is selectively brominated in the 2-position with NBS in DMF.[49] The second bromination with NBS in DMF occurs in the 7-position.[188] Conditions developed in the group of Knochel[189] were found to efficiently couple boronic acids to the bromodihydropyrenes, which allows for the synthesis of various 2,7-diaryldihydropyrenes.

3.1.3 Catalysis of the 6 π Cycloreversion in Pyridine Substituted Dihydropyrenes

Among the general concepts in chemistry, the manipulation of reactions by utilization of a catalyst is one of the most applied and has influenced almost every field of chemistry. A catalyst increases the rate of a reaction without influencing the standard Gibbs energy change of the reaction itself.[190] Mechanistically, such a catalyst lowers the activation barrier of the rate limiting step by opening a new pathway on the ground state potential energy surface, involving additional or different intermediates in *thermal* reactions.

Reactions can also proceed on the excited state surface, which requires an initial excitation source, typically a photon.[191] Activation barriers can also exist on the potential energy surface of the excited state and it would be advantageous to reduce this barrier, for example with the aid of a catalyst, to enhance the efficiency of the photoreaction. Such a barrier gives rise to quantum yields that are dependent on both wavelength and temperature as excess vibrational energy facilitates excited molecules to overcome it. If a photoreaction is reversible, the substance is called photochromic, regardless of whether the back reaction is conducted photochemically (P-type), thermally (T-type), or with other stimuli (electrochemically, mechanically…).[192] The existence of excited state activation barriers is known for some light induced 6 π cycloreversion reactions as in the ring opening of

photochromic diarylethenes (Figure 8) but their quantification usually requires time consuming measurements.[193–195] Unfortunately, excited state activation barriers are quite ambitious to predict from theory since the calculation of reaction pathways in the excited state is notably more complicated than in the ground state, especially if multiple excited states of different multiplicity are involved.[41]

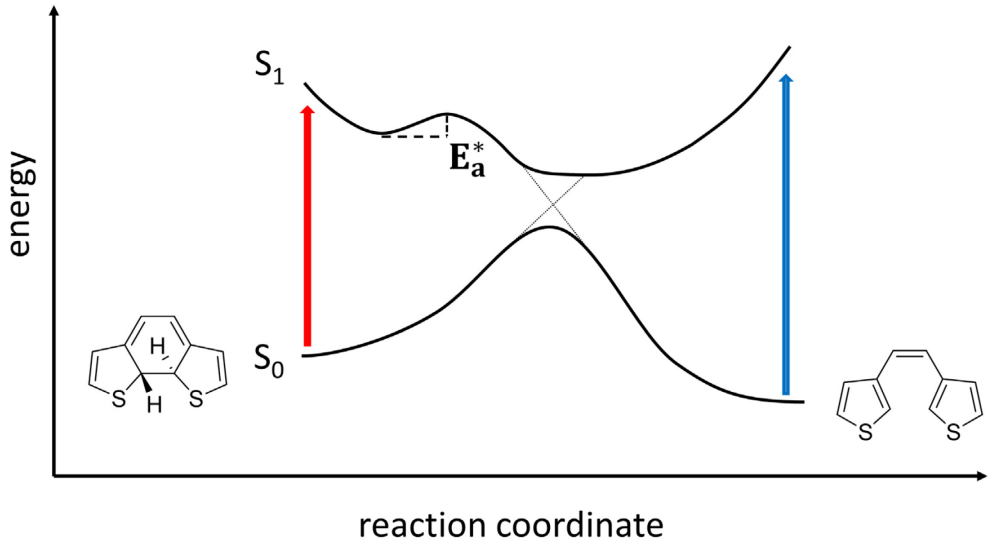

Figure 8: Simplified energy diagram for the 6 π cycloreversion of a diarylethene: After excitation to the S_1 state (red arrow), the molecule has to overcome a barrier on the excited state potential energy surface to reach the conical intersection. If this barrier is high, other deactivation pathways, such as thermal relaxation or fluorescence dominate.

Considering all the different classes of photochromic molecules, several conditions have to be met to qualify as a "good switch" and only few of them are (1) switchable with visible light only, (2) show a large spectral separation, (3) have reasonable quantum yields, (4) are fatigue resistant, and (5) are not restricted to specific working conditions such as special solvents or pH. Furthermore, this work focusses on negative photochromic materials, an often underappreciated feature where upon irradiation with light the compound is bleaching, meaning that for the metastable form a hypsochromic shift is observed in UV/vis spectroscopy. Conceptually, negative photochromism has several advantages such as the potential to use only visible light for switching (T-type) and simpler analysis of the spectroscopic properties. Negative T-type photochromism is advantageous in optically dense matter due to an intrinsically higher switching efficiency and penetration depth (ideally the photoproduct does not absorb at the irradiation wavelength) and the possibility to switch in both directions *quantitatively*.

The dihydropyrene photoswitch **49**$_{closed}$ (Scheme 51), which would open to the colorless *meta*-cyclophanediene form **49**$_{open}$ upon irradiation with visible light, fulfills these requirements, except for the high quantum yield, a challenge which will be met by taking advantage of a catalyst allowing to switch *via* a different excited state potential energy surface as a new concept.[196] Boggio-Pasqua *et al.* have shown in calculations that unsubstituted dihydropyrene opens after excitation to the zwitterionic S_2 state,[41] which is rather inefficient since, in agreement with Kasha´s rule,[197] most of the excitation energy is lost by thermal relaxation *via* the locally excited S_1 state. Moreover, an excited state activation barrier seems to be present, which further decreases the quantum yield as is also indicated by a low temperature experiment (Figure 9).[42] Interestingly, the ring opening quantum yield seems to increase with the acceptor strength of a substituent in the 2-position of the dihydropyrene. For

instance, the nitro group in 2-nitrodihydropyrene **57** increases the quantum yield from 0.02 for the parent **49** to 0.37.[42] It can be assumed that the zwitterionic state becomes the S_1 state and the deactivation *via* the locally excited state is shut down.

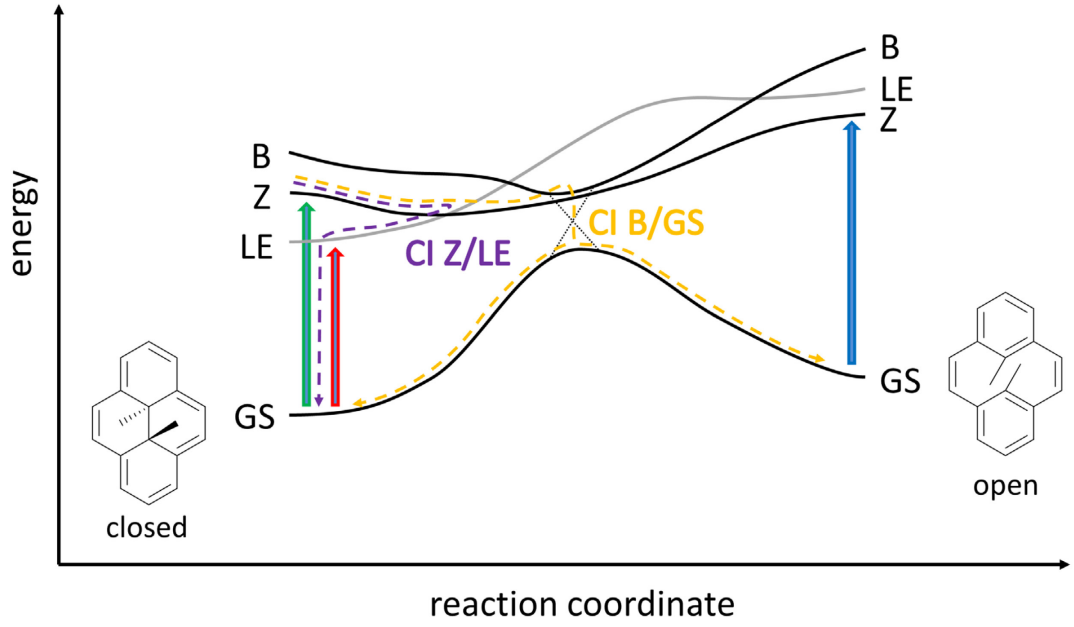

*Figure 9: Switching mechanism of the parent dihydropyrene **49**: Excitation to the S_1 state (LE, red arrow) in the long wavelength region above 600 nm does not lead to switching. After excitation to the S_2 state (Z, green arrow), the molecule can either change to the LE state via the conical intersection CI Z/LE and relax thermally (purple dashed line) or overcome an excited state activation barrier to the conical intersection CI B/GS from the B state, which leads to the formation of the open isomer (identical to Figure 4 and Figure 28).*[41]

Until now, it remains unknown how the substitution pattern influences the excited state activation barrier and it would be desirable to lower this barrier in a non-permanent way by an external chemical trigger – the catalyst.

Here, it is demonstrated how the photochromic properties of pyridine substituted dihydropyrenes **73** and **74** (Scheme 54) can be influenced by protonation, which turns the pyridine into a pyridinium and therefore increases the acceptor strength considerably. Furthermore, it is shown that catalytic amounts of protons are sufficient to enhance the light induced conversion to the open form by switching *via* a species with a lower excited state activation barrier.

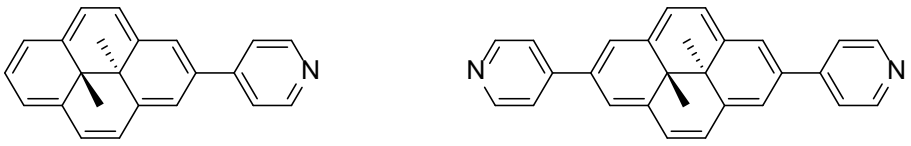

73 **74**

*Scheme 54: The pyridine substituted dihydropyrene derivatives **73** and **74** investigated in this study.*

There are two versions of the dihydropyrene, the first having *t*-butyl groups in the 2- and 7-position **56** which allows for an easier synthesis in six steps and has been developed by Tashiro,[173,174,198,199] following the general thiacyclophane route which has been invented by Mitchell and Boekelheide earlier.[49,171,200] Reactions on this molecule will take place in the 4-position although it has been shown

that substituent effects on the photochemistry in this position are in general limited.[201] Royal´s group has shown that the quantum yield for the ring opening can be increased by protonation/methylation of 4-pyridine dihydropyrenes, with the highest value being Φ = 0.042.

Starting from unsubstituted dihydropyrene **49**, which can be synthesized in 10 steps from 2,6-dichlorotoluene[200,171,202] allows for substitution in the 2-position, which is known to have a bigger impact on the photo- and thermochromic properties. Comparing UV/vis spectra of the parent **49** and the pyridine substituted dihydropyrenes **73** and **74**, the maximum absorption wavelength and extinction coefficient increases with the length of the π-system.

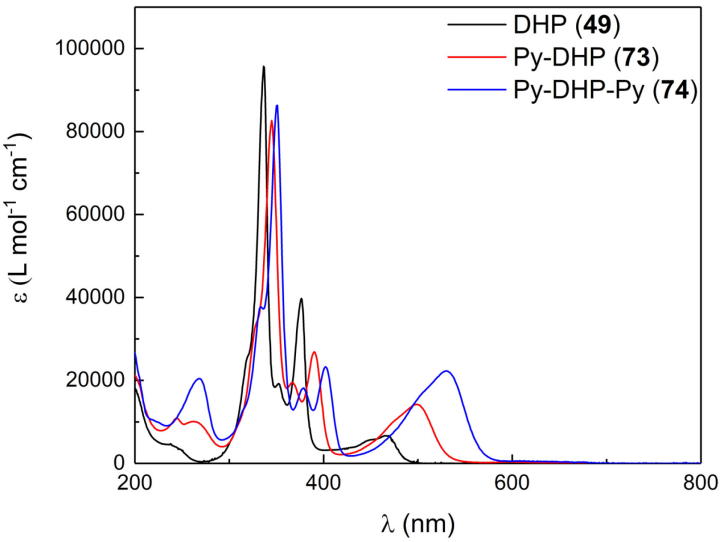

*Figure 10: UV/vis absorption spectra of parent dihydropyrene **49**, 2-(4-pyridyl)-dihydropyrene **73**, and 2,7-bis(4-pyridyl)-dihydropyrene **74** in acetonitrile (25 °C): With an increasing length of the π-system a bathochromic and hyperchromic shift is observed.*

On the contrary, the quantum yield for the ring opening reaches 0.02[203] for parent **49** and 0.018 for monopyridine **73** (Figure 11), whereas no switching of bispyridine **74** has been observed at the applied low light intensity.

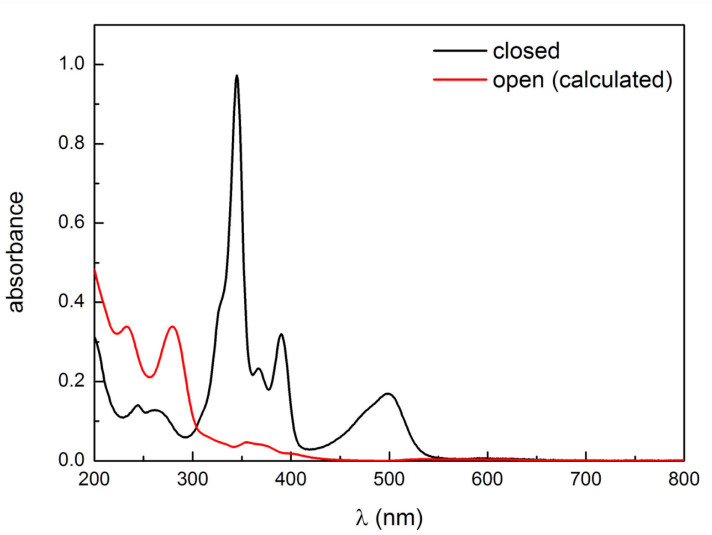

*Figure 11: UV/vis absorption spectra of open and closed form of 2-(4-pyridyl)-dihydropyrene **73** in acetonitrile ($1.1 \cdot 10^{-5}$ M, 25 °C): Since the open form does not absorb around 500 nm, the conversion and hence open form spectrum can be calculated from the absorbance in this region in the photothermal equilibrium and the initial spectrum.*

Methylation of the pyridine substituted switches with methyl iodide or treatment with methane sulfonic acid leads to a bathochromic shift (Figure 12 and Figure 13) and more importantly to an increase of the quantum yields to 0.18 (**73-Me**$^{+}$), 0.22 (**73-H**$^{+}$), 0.014 (**74-Me$_2$**$^{2+}$), and 0.016 (**74-H$_2$**$^{2+}$). Protonation or methylation of the switches also accelerates the thermal return reaction distinctively (Table 2), which results in photo-thermal-stationary states, where an equilibrium between the forward photoreaction and the backward thermal reaction is reached.

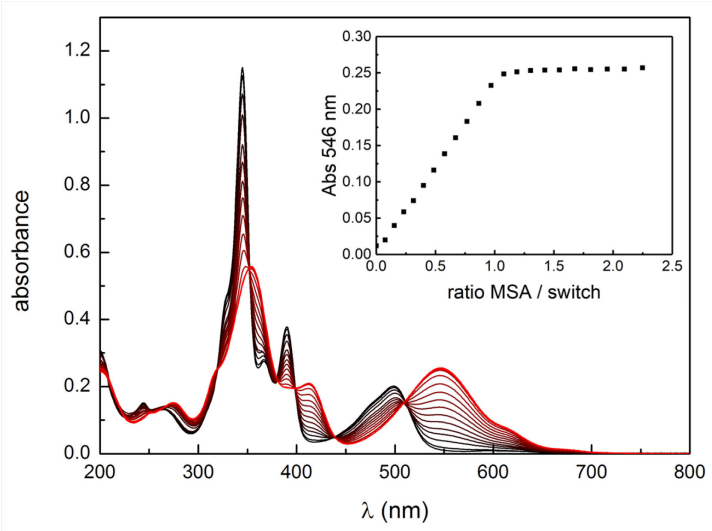

*Figure 12: Titration of 2-(4-pyridyl)-dihydropyrene **73** with methanesulfonic acid in acetonitrile ($1.3 \cdot 10^{-4}$ M, 1 mm cuvette, 25 °C).*

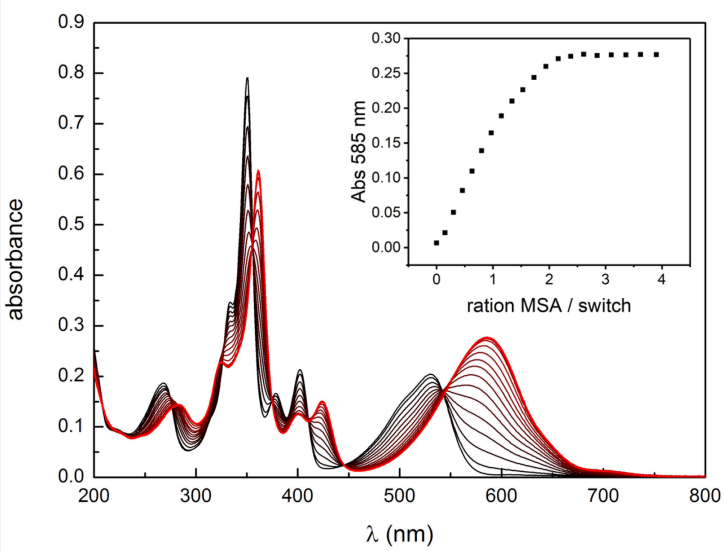

*Figure 13: Titration of 2,7-bis(4-pyridyl)-dihydropyrene **74** with methanesulfonic acid in acetonitrile ($7.5 \cdot 10^{-5}$ M, 1 mm cuvette, 25 °C).*

Table 2: Absorption maxima, quantum yields (579 nm), thermal half-lives, and activation parameters in the ground state for the pyridine substituted dihydropyrenes at 25 °C in MeCN.

No.	Derivative	λ_{max} (ε)	Φ_{co}	$t_{1/2}$ (min)	E_A	ΔH	ΔS
73	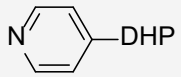	499 (14200)	0.018[a]	117			
73-Me$^+$	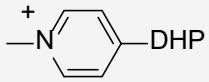	551 (25300)	0.18	12	21.6	21.0	−1.7
73-H$^+$	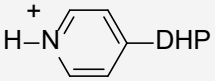	549 (18700)	0.22	10	21.7	21.2	7.1
74		530 (22300)	–	12			
74-Me$^+$	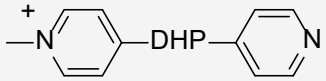	571 (32300)	0.10	1.4	18.9	17.3	−10.1
74-Me,H^{2+}	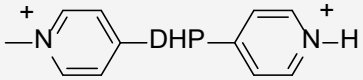	592 (37900)	0.018	0.7	17.3	16.7	−9.8
74-Me$_2^{2+}$	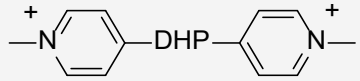	593 (39600)	0.014	0.6	18.2	17.7	1.0
74-H$_2^{2+}$	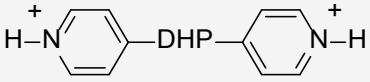	590 (36500)	0.016	0.4	20.6	20.0	9.4

Counter-ion is PF_6^- for methylated derivatives and $MeSO_3^-$ for protonated derivatives, λ_{max} in nm, ε in L mol^{-1}cm^{-1}, E_A in kcal/mol, [a] Quantum yield measured at 500 nm.

Irradiation of a solution of protonated **74-H$_2^+$** to the photo thermal equilibrium, followed by deprotonation with NEt_3 made it possible to determine the thermal half-life of **74** to 12 min.

To investigate the catalytic effect of protonation, substoichiometric amounts of acid have been added to a solution of **73** before irradiation to the photothermal equilibrium. Deprotonation of these mixtures allowed to calculate the conversion, which was above the degree of protonation (Figure 14).

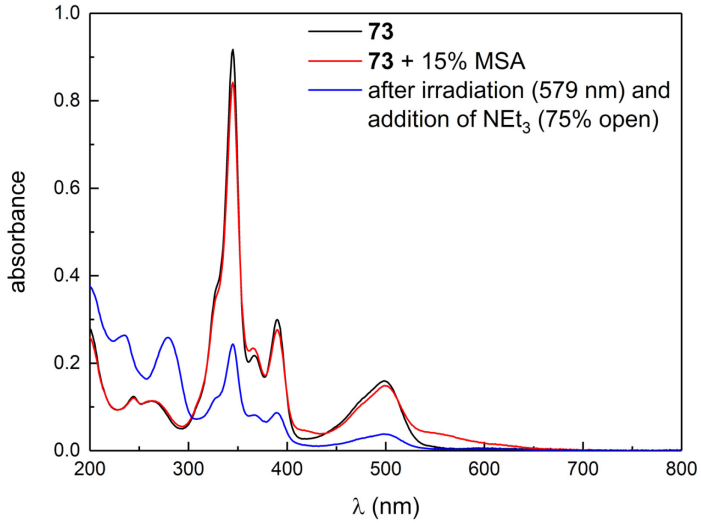

*Figure 14: Proton catalyzed switching of **73** in acetonitrile ($1.3 \cdot 10^{-5}$ M, 25 °C): 15% of the molecules are protonated before irradiation (calculated from the absorbance around 500 nm, to correct for the concurrent protonation of the solvent). After irradiation and deprotonation 75% of the switches are in the open form.*

The proton clearly acts as a catalyst by a) increasing the quantum yield of the photoreaction and b) increasing the extinction coefficient at the irradiation wavelength. A catalytic cycle as outlined in Scheme 55 is proposed. Pyridine substituted dihydropyrene **73** opens and closes slowly in the non-protonated form. Upon protonation, the quantum yield for the ring opening increases, together with a higher extinction coefficient at the irradiation wavelength. Despite the also accelerated thermal back reaction, the photoreaction is efficient enough to produce more open isomer than the amount of protonated dihydropyrene before irradiation.

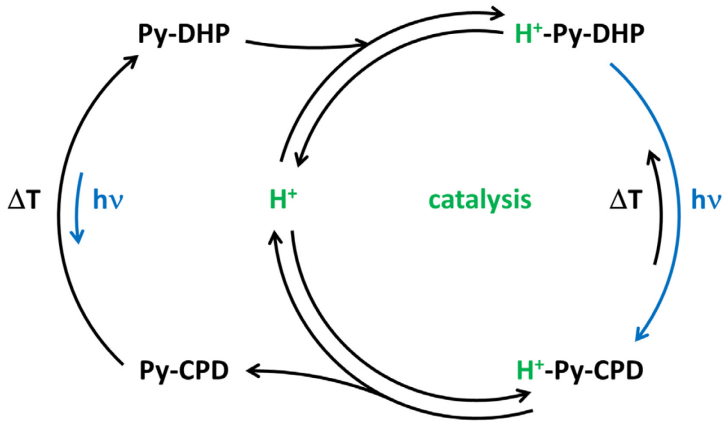

*Scheme 55: Catalytic cycle for the opening of pyridine substituted dihydropyrene **73**: Upon protonation, the pyridine becomes a stronger pyridinium acceptor, which accelerates the photoreaction. After the ring opening, the proton can either catalyze the thermal back reaction or another photoreaction. A conversion higher than the degree of protonation requires sufficient light intensity to compensate for the also accelerated thermal back reaction.*

In the case of **74** the single and double protonated species have to be considered, which is why the conversion in dependency of the degree of protonation has been investigated (Figure 15). Although such a dependence of the photo thermal equilibrium will be different for other light intensities, temperatures, concentrations, or cuvette volumes, it is evident that a small number of protons accelerates the photoreaction. However, too many protons result in lower conversions. To exclude

effects such as different rates for thermal back reactions or the fact that the deprotonated form does not absorb at the irradiation wavelength, quantum yields were determined.

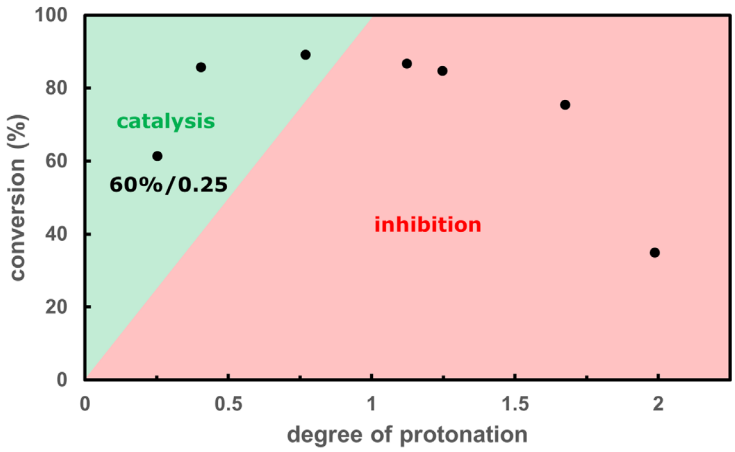

*Figure 15: The conversion of **74** to its open form depends on the degree of protonation, where small amounts of protons catalyze the photoreaction (green area), while bigger amounts of protons rather inhibit the photoreaction (red area).*

For a small proton concentration, the single protonated **74-H$^+$** will dominate the efficiency of the system. Since single protonation of **74** for a quantum yield measurement is virtually impossible, the singly methylated **74-Me$^+$** and the methylated versions of the pyridine-substituted dihydropyrenes **73-Me$^+$** and **74-Me$_2^{2+}$** have been prepared as model systems.

The investigation of **73-Me$^+$** and **74-Me$_2^{2+}$** showed almost no difference with respect to the spectroscopic properties of their protonated versions, therefore **74-Me$^+$** seems to be a good substitute to study the properties of the single protonated species. Surprisingly, the quantum yield for **74-Me$^+$** was 0.10 and therefore six times higher than the quantum yield for the fully protonated **74-H$_2^{2+}$**, which explains why small amounts of acid accelerate the photoreaction while excess of acid decreases the quantum yield.

Further insights can be gained from temperature dependent measurements of quantum yields. The temperature dependence of the photoreaction rate has been shown to correlate with the barrier in the excited state *via* an Arrhenius type equation.[193] However, this study neglects two important facts: a) The temperature dependence of the extinction coefficient has not been taken into account, which results in an overestimation of the rate at lower temperatures, due to a higher absorptivity of the sample. To overcome this problem, it is suggested to measure the quantum yield Φ instead of overall rates as a function of temperature, since Φ is directly connected to the rate which leads to the formation of the photoproduct.[204] b) After excitation, the molecule is supposed to relax to a THEXI-state (thermally relaxed excited state), which can be only partially the case, since it would imply that the height of the barrier is always the same, no matter which excitation wavelength has been applied. It has been shown in previous studies that the quantum yield at shorter wavelengths is higher, which can be explained by a reaction happening from a higher vibronic state.[203] However, since the measured barrier is still highly related to the actual barrier and has a practical importance, it will be referred to in the following as “effective activation barrier” $E^*_{A,eff}$ and all derivatives are compared at the same irradiation wavelength (546 nm).

The apparent barrier in the excited state can be extracted from an Arrhenius plot of ln(Φ) versus inverse temperature, since for low quantum yields the ratio of the small rate constant of the thermal reaction in the excited state $k_{CO}(T)$ and the sum of all rate constants is proportional to the quantum yield. This approximation implies, that all other rate constants have much smaller barriers and therefore neglectable dependency on the temperature (Figure 16):[193]

$$\Phi = \frac{k_{co}(T)}{k_{co}(T) + k_{thermal\,relaxation} + k_{fluorescence} + \dots}$$

With the approximation:

$$k_{co}(T) \ll k_{thermal\,relaxation} + k_{fluorescence} \cdots$$

$$\Phi \approx \frac{1}{k_{thermal\,relaxation} + k_{fluorescence} + \dots} \cdot k_{co}(T)$$

$$k_{co}(T) \approx const \cdot \Phi$$

In the Arrhenius equation, $k_{CO}(T)$ can be substituted for the quantum yield. Since the reaction on the excited state potential energy surface does not happen from a THEXI state and depends on the irradiation wavelength, the quantum yield is correlated to an effective activation barrier:

$$k_{co}(T) = A \cdot e^{-\frac{E_A^*}{RT}}$$

$$\Phi \approx const \cdot e^{-\frac{E_{A,eff}^*}{RT}}$$

$$\ln(\Phi) \approx const - \frac{E_{A,eff}^*}{RT}$$

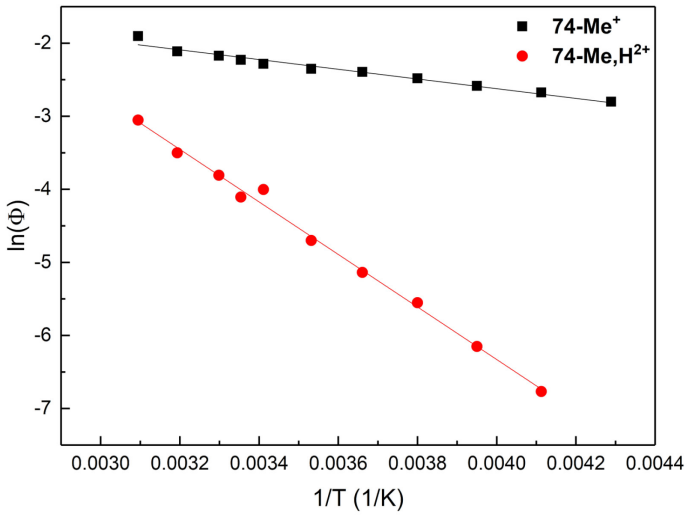

*Figure 16: Arrhenius Plots for the ring opening quantum yields of **74-Me⁺** and its protonated analog in acetonitrile.*

Examining this relation, the measured effective excited state activation barrier for protonated **74-Me,H^{2+}** (7.1 kcal/mol) is five times bigger than for the singly methylated switch **74-Me^{+}** (1.3 kcal/mol), which explains very well the higher quantum yield for deprotonated **74-Me^{+}** and shows how protons can be used as catalysts or inhibitors. It is noteworthy that protonation also catalyzes the thermal back reaction by lowering the activation barrier in the ground state, although this effect is overcompensated by the higher quantum yield at low concentrations and sufficient light intensity. An overall mechanism involving two interconnected acid dependent pathways to explain acceleration and inhibition is proposed in Scheme 56. Whereas at a low proton concentration the photoreaction becomes much more efficient and results in catalysis, a high proton concentration has the opposite effect of a diminished photoreaction and a fast thermal back reaction.

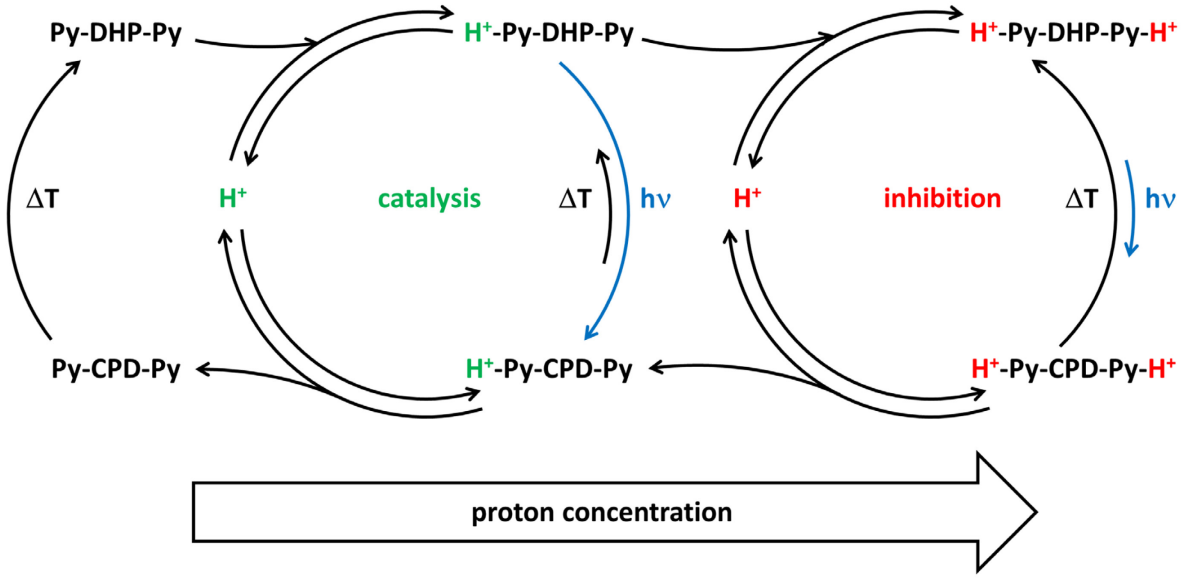

*Scheme 56: Catalysis-Inhibition cycle for the bispyridine substituted dihydropyrene **74**: The closed and deprotonated switch does not open under the low light intensities, which were applied here, although a slow thermal back reaction occurs in the deprotonated form. At low proton concentrations, **74** is protonated only on one side, which results in a high quantum yield and efficient opening to a greater extent than degree of protonation, despite a faster thermal back reaction (left side). When the proton concentration increases, the ring opening becomes less efficient and the thermal back reaction is accelerated even more, which results in inhibition and therefore lower conversions than the degree of protonation (right side).*

Since Royal and coworkers found pyridinium substituted dihydropyrenes to form the endo peroxide of the open isomer as well,[185] **73-Me^{+}** (Figure 17) has been examined with respect to this side reaction.

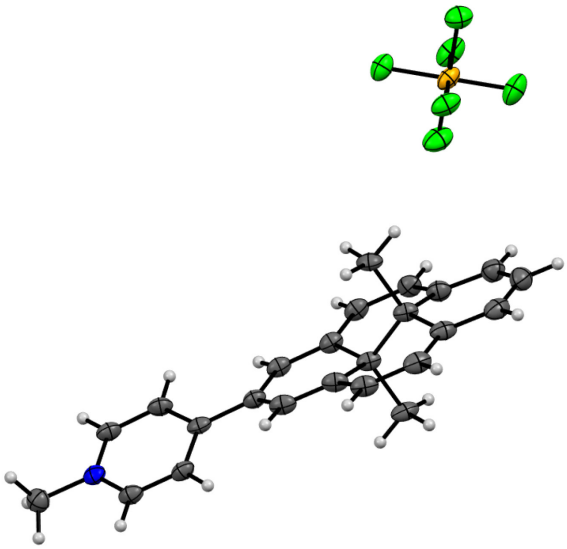

*Figure 17: Molecular structure of **73-Me**⁺. Ellipsoids are set at a 50% probability.* [ii]

A solution of **73-Me**⁺ was irradiated with and without degassing and the photokinetics of both experiments are essentially the same (Figure 18). Besides the starting material, only a single product is found by UPLC analysis. The thermal back reaction follows a first order kinetics and clean isosbestic points are observed for forward and backward reactions in both cases. It is likely that the endo peroxide formation depends on the light intensity, as will be discussed in chapter 3.1.4 where such an observation is made and simply does not occur at the low light intensity and concentrations applied here.

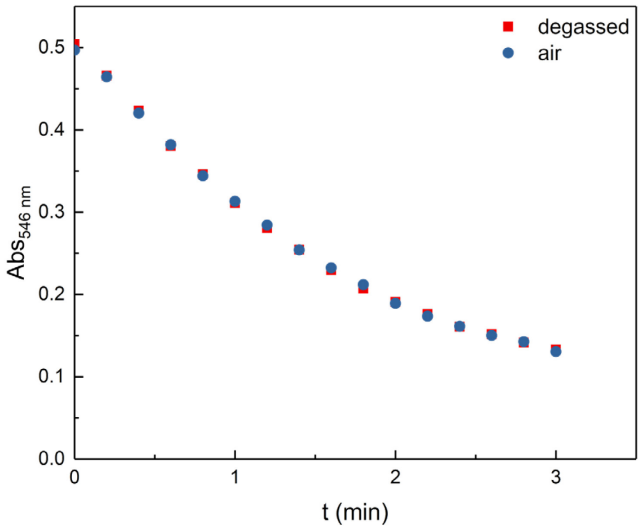

*Figure 18: Irradiation of **73-Me**⁺ in degassed and in non-degassed solution under the otherwise same conditions in acetonitrile (25 °C).*

A strategy has been shown, which allows to manipulate the efficiency of a photoreaction by general acid catalysis on one and the same molecule. Mechanistically, catalytic amounts of the protonated

[ii] X-Ray analysis of **73-Me**⁺ performed by Florian Q. Römpp.

species are produced which have a lower activation barrier on the excited state potential energy surface and a higher quantum yield. The quantum yields of dihydropyrenes substituted with pyridine moieties in the 2- or 2- and 7-position increase by protonation or methylation of one pyridine ring. In contrast to that, the protonation or methylation of a second pyridine leads to lower switching efficiencies. This effect can be ascribed to a higher activation barrier in the excited state, which was obtained from temperature depended quantum yield measurements. Finally, the catalytic effect of protons is reflected in higher conversions to the metastable isomer in the ground state. It can be concluded that acceptor strength is not the only criterion for efficient ring opening of dihydropyrenes. Moreover, a certain polarization seems to be necessary to obtain high quantum yields, which will be discussed in the next chapter 3.1.4. A similar effect has also been shown for a dihydropyrene which bears strong donor and acceptor substituents in the 4- and 9-pseudo *para* position.[40]

3.1.4 Excited State Activation Barriers in Donor-Acceptor Dihydropyrenes

Many modern applications rely on smart materials, which are able to respond to an external stimulus such as light by changing their physical properties.[192] For example, donor-acceptor substituted switches change their dipole moment upon isomerization, which has been used to control photoswitchable devices.[7,11,22,23] Although many photochromic systems are known,[123,192] in applications most of them are based on either an E/Z isomerization of a double bond or a 6 π electrocyclization reaction.[205] While the typical examples of E/Z switches are azobenzenes or stilbenes, the 6 π electrocyclization/-reversion occurs in many systems, such as diarylethenes or dihydropyrenes. Where the photochemical 6 π electrocyclization is usually very efficient, oftentimes the cycloreversion suffers from a low quantum yield and requires long irradiation times or high light intensities. In many cases the reason for the slow cycloreversion is due to an activation barrier on the excited state potential energy surface (Figure 8). Unfortunately, only little effort has been made to measure such barriers and even less to manipulate them. While in the case of dihydropyrenes such a barrier has been predicted by quantum chemical calculations, there are also few experimental studies on diarylethenes, relying on temperature dependent irradiation kinetics.[194,204,206–210] However, clear structure property relationships are still missing to understand and manipulate this barrier, especially for the dihydropyrene switches. Dihydropyrenes are of interest since they show T-type negative photochromism, minor geometrical changes upon switching, and high symmetry if substituted in the 2- and/or 7-position which is otherwise difficult to achieve and makes them good candidates for applications relying on densely packed solid-state structures. Furthermore, it has been shown that 4,9-substituted push-pull dihydropyrenes can efficiently switch *via* irradiation at a charge-transfer band in the near-infrared region, which in many other switching classes leads to loss of the photochromic property.[40]

In the previous chapter 3.1.3 it has been shown, how the pyridine substituted dihydropyrene **73** can only switch efficiently under acidic conditions. The corresponding pyridinium species **73-H$^+$** with its strongly electron withdrawing nature seemed to have a lower activation barrier in the excited state. On the contrary, in **74** a second pyridinium in the pseudo *para* position caused an increase of the barrier resulting in a lower quantum yield. It has been assumed that the photoswitching happens *via* a zwitterionic state, which should become the lowest excited state in strongly polarized dihydropyrenes, resulting in high quantum yields. Here, different donor-acceptor substituted dihydropyrenes are examined in terms of their excited state activation barrier to better understand this phenomenon.

A decision has been made to undertake the investigation on 2,7-diaryl substituted dihydropyrenes, since they lead to higher extinction coefficients in the visible compared to the typically used **56** which bears *t*-butyl groups in the 2- and 7-position. This substitution pattern would further allow to utilize already developed synthetic methods such as brominating and cross coupling reactions, especially for introducing donor substituents. Furthermore, comparability to the previously synthesized pyridine derivatives is assured. In analogy to the pyridine study, the symmetrically substituted derivatives diphenyl **75**, dibenzonitrile **76**, and di(3,5-bistrifluoromethyl)phenyl **77** (Figure 19 and Figure 20) have been chosen as a starting point, of which **76** gave crystals of satisfying quality for X-ray analysis (Figure 21).

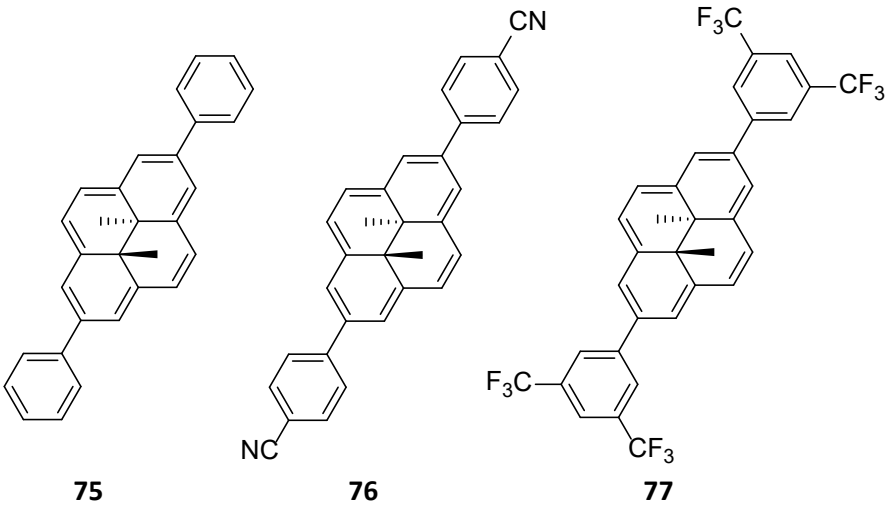

Figure 19: Symmetrically substituted dihydropyrenes investigated in this study.

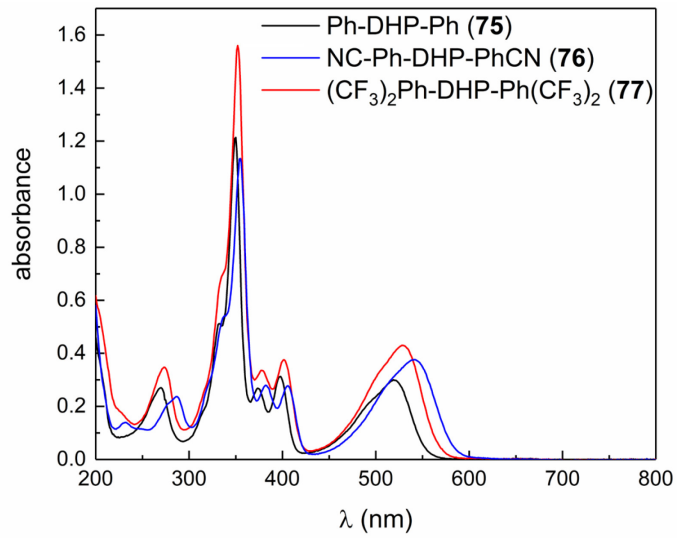

Figure 20: UV/vis absorption spectra of symmetrically substituted dihydropyrenes investigated in this study in acetonitrile ($1\text{-}2 \cdot 10^{-5}$ M, 25 °C).

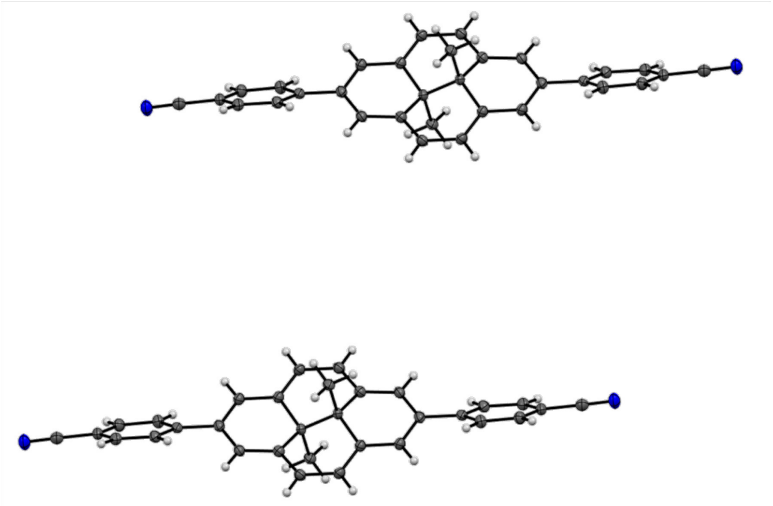

*Figure 21: Molecular structure of **76**. Ellipsoids are set at a 50% probability.* [iii]

The expectation was a better switching for the more electron-deficient derivatives **76** and **77**, as has been observed for pyridinium versus pyridine. Surprisingly, switching in all three cases required high light intensity LED irradiation and resulted in mixtures of the open forms and their corresponding oxygen adducts, as determined by UPLC. The open forms, as well as the endo peroxides, revert to the closed form at room temperature. As expected, neither forward nor backward reaction show isosbestic points and the thermal back reaction does not follow an overall first order kinetics. A completely different behavior was observed going to donor-acceptor substituted molecules (Figure 22), where decent switching has been found for the pair anisole/benzonitrile in **78** with a quantum yield of Φ_{co} = 0.0048. No isosbestic point was observed when **78** was irradiated with an LED at high light intensity and the endo peroxide was identified by UPLC. The low light intensity irradiation experiment, which was used to determine the quantum yield resulted in isosbestic points and did not show any endo peroxide in the subsequent UPLC analysis. Therefore, all quantum yield determinations have been performed at low light intensities.

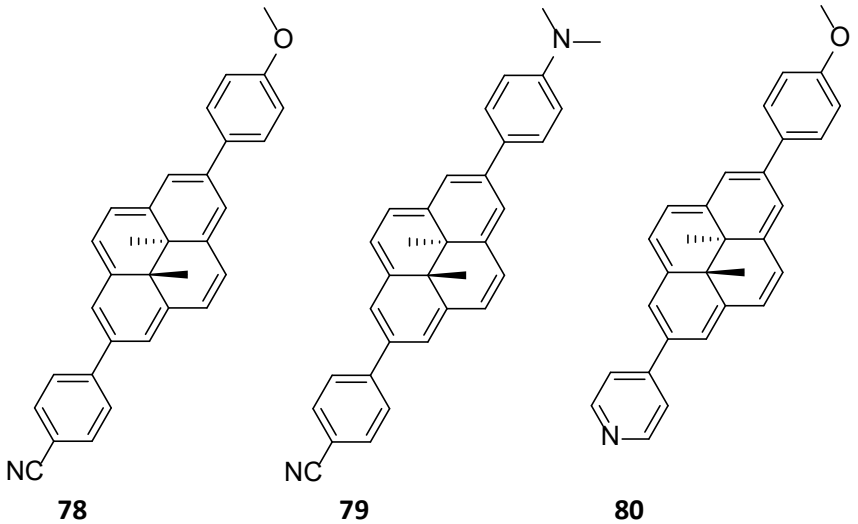

78 **79** **80**

Figure 22: Donor-acceptor substituted dihydropyrenes with efficient ring opening quantum yields.

[iii] X-Ray analysis of **76** performed by Bernd M. Schmidt.

Changing the donor to *N,N*-dimethylaniline in **79** (Figure 23) increases the quantum yield by a factor of 12 to Φ_{co} = 0.058, while addition of acid protonates the aniline **79-H**$^+$ and causes a low quantum yield of Φ_{co} = 0.00016. The donor-acceptor derivate **79** also crystallized well and was subjected to X-ray analysis (Figure 24).

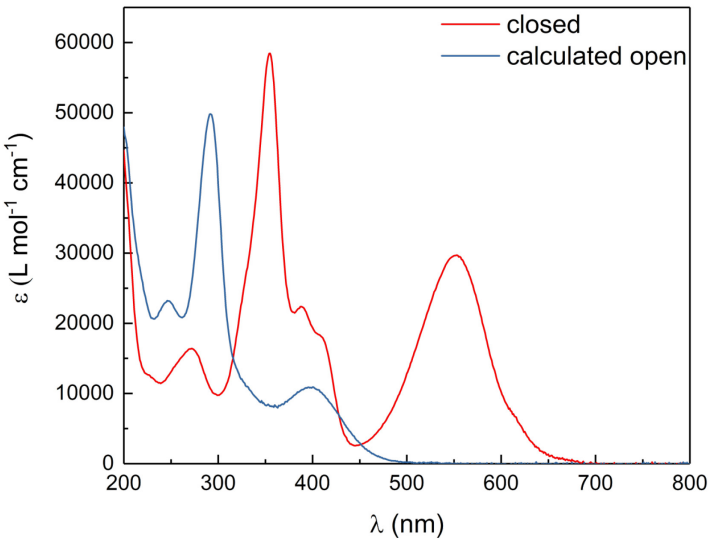

*Figure 23: UV/vis absorption spectra of open and closed form of the aniline/benzonitrile substituted dihydropyrene **79** in acetonitrile (20 °C): Since the open form does not absorb > 550 nm, the conversion and hence open form spectrum can be calculated from the absorbance in this region in the photo thermal equilibrium and the initial spectrum.*

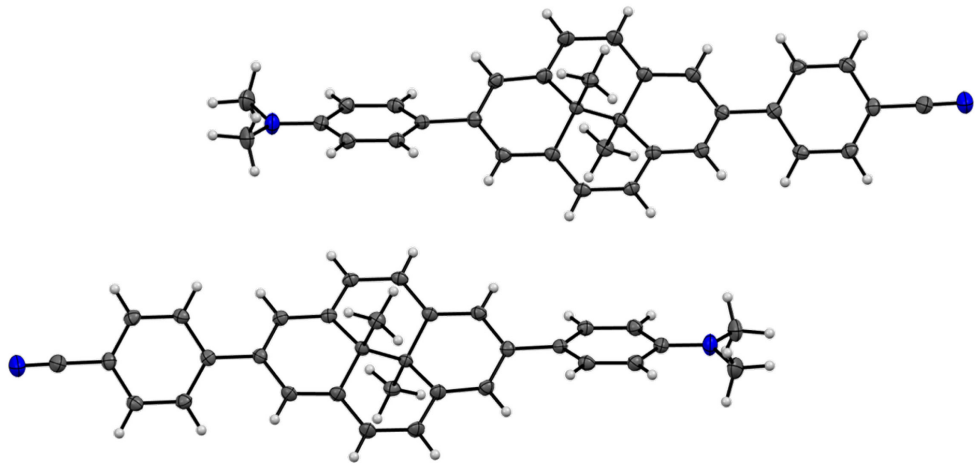

*Figure 24: Molecular structure of **79**. Ellipsoids are set at a 50% probability.* [iv]

Maintaining anisole as the donor and changing the acceptor from benzonitrile to pyridine **80** results in only little change to Φ_{co} = 0.0056. Since the effect of pyridine and benzonitrile on the quantum yield seemed to be similar, this result is in good agreement with the previous study, where the bispyridine substituted dihydropyrene **74** would not undergo switching similar to the dibenzonitrile substitued dihydropyrene **76**. Upon protonation of the anisole/pyridine pair **80-H**$^+$, the quantum yield increased

[iv] X-Ray analysis of **79** performed by Florian Q. Römpp.

by a factor of 10 to Φ_{co} = 0.053 (Figure 25), which is also in agreement with the efficient switching of the pyridinium substituted dihydropyrenes **73-Me**$^{+}$ and **74-Me$_2$**$^{2+}$.

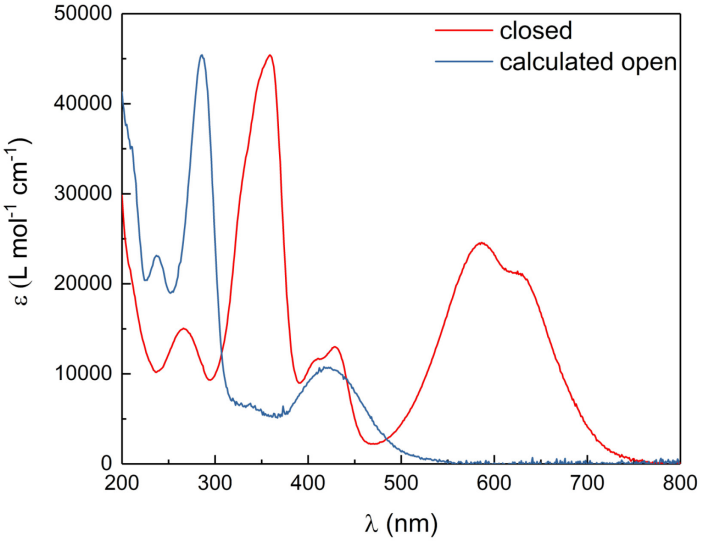

*Figure 25: UV/vis absorption spectra of open and closed form of the anisole/pyridinium substituted dihydropyrene **80-H**$^{+}$ in acetonitrile (20 °C): Since the open form does not absorb > 650 nm, the conversion and hence open form spectrum can be calculated from the absorbance in this region in the photo thermal equilibrium and the initial spectrum.*

Irradiation experiments were conducted at temperatures ranging from −40 °C to +60 °C to obtain activation barriers and the results are summarized in Table 3. From Arrhenius plots of ln(Φ) versus 1/T (see Figure 16 and Figure 26) $E^{*}_{a,eff}$ values have been obtained and it is evident that a high quantum yield goes hand in hand with a low excited state activation barrier. Strong donors and acceptors create a push-pull system, which on the one hand increases the quantum yield for ring opening but on the other hand lowers the barrier for the thermal ring closure back to dihydropyrene. As expected, going to stronger donors or acceptors also causes a bathochromic shift (Figure 27), which places the onset in case of the protonated anisole/pyridine pair **80-H**$^{+}$ at 730 nm (5% of the maximum absorbance at λ_{max} = 587 nm). As the *N,N*-dimethylaniline/benzonitrile pair **79** shows good switchability over the whole temperature range (Φ_{co} = 0.014 (−40 °C) to Φ_{co} = 0.12 (+60 °C)) in combination with a moderate thermal half-life, it has been investigated in different solvents as well. As can be seen from Table 3, a nonpolar solvent, such as toluene, increases the excited state activation barrier, which causes a reduction of the quantum yield by a factor of 7. Surprisingly, the ground state activation barrier, as well as the λ_{max}, seem to be almost unaffected by the polarity of the solvent, implying that the polarity of the environment can be used to manipulate the quantum yield, without affecting the thermal back reaction.

Table 3: Photo- and thermochromic properties of 2,7-diaryldihydropyrenes in acetonitrile at 20 °C.

No.	Derivative	λ_{max} (ε)	Φ_{co}[a]	$E^*_{A,eff}$	$t_{1/2}$ (min)	E_A GS[b]
75		520 (28400)				
76	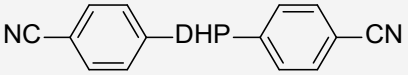	542 (36000)				
77	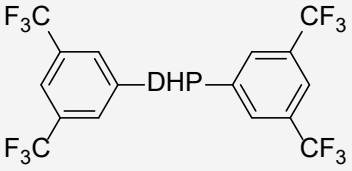	529 (28300)				
74		530 (22300)[c]			12[c]	
74-Me$^+$	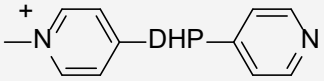	573 (32700)	0.10	1.3	2.7	18.9
74-Me,H^{2+}	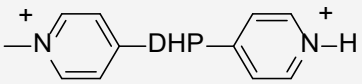	592 (38800)	0.018	7.0	0.8	17.3
78	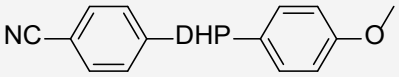	537 (28500)	0.0048	5.9	21	20.4
80	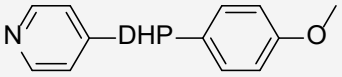	532 (23200)	0.0056	5	25.8	20.3
80-H$^+$	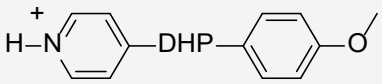	628 (21100) 587 (24600)	0.053	1.6	1.5	15.6
79	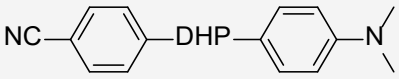	553 (29700) 550 (35600)[c] 555 (34600)[d]	0.058 0.027[d] 0.0085[e]	3.1 3.6[d] 5.6[e]	10.3 9.2[d] 10.2[e]	19.8 20.1[d] 19.8[e]
79-H$^+$	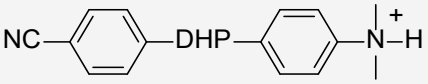	534 (29500)	0.00016		13.4	

λ_{max} in nm, ε in L mol^{-1}cm^{-1}, E_A in kcal/mol, [a]Although the thermal half-lives for the symmetric derivatives are in the order of several minutes, the quantum yields are too low, to obtain a measurable conversion at the low light intensities required for the quantum yield measurement. [b]ground state, [c]25 °C, determined by deprotonation of an irradiated solution of **74-H$_2^{2+}$**, [d]ethanol, [e]toluene.

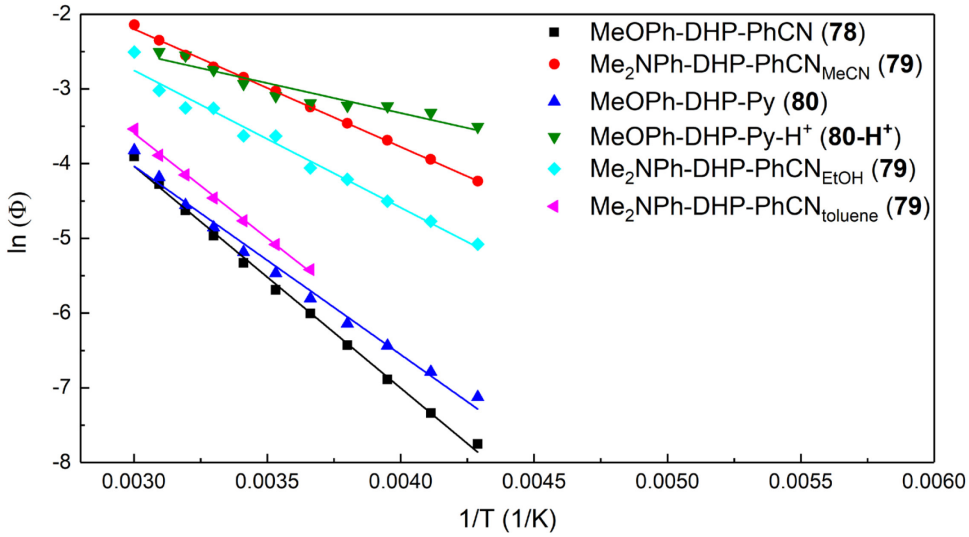

Figure 26: Arrhenius plots for the ring opening quantum yield of donor-acceptor substituted dihydropyrenes in acetonitrile unless otherwise noted.

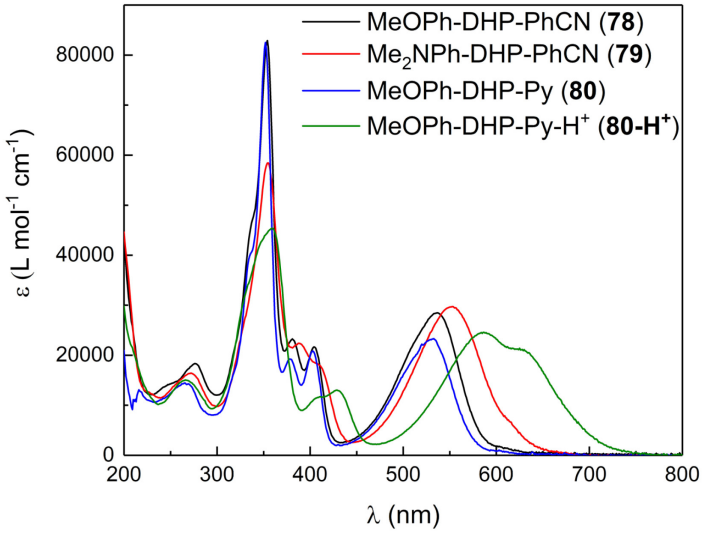

*Figure 27: UV/vis absorption spectra of donor-acceptor dihydropyrenes in acetonitrile (25 °C): For the weaker donor-acceptor substituted dihydropyrenes **78** and **80** a weak band at 600 nm is observed, which presumably belongs to the forbidden transition to the S_1 locally excited state. Stronger donors and/or acceptors cause a bathochromic shift, which results in an overlap of the allowed transition to the S_2 zwitterionic state from which the switching happens.*

Theoretical investigations of the dihydropyrene system have shown that the switching starts with an excitation to the S_2 state (Z). From there, two pathways have been found, of which the dominant one leads to the S_1 state (LE) and causes mainly thermal relaxation, while the other is an activated process which passes the singlet biradical state S_3 (B) and results in switching to the open form and relaxation to the closed form (identical Figure 9 or Figure 28).

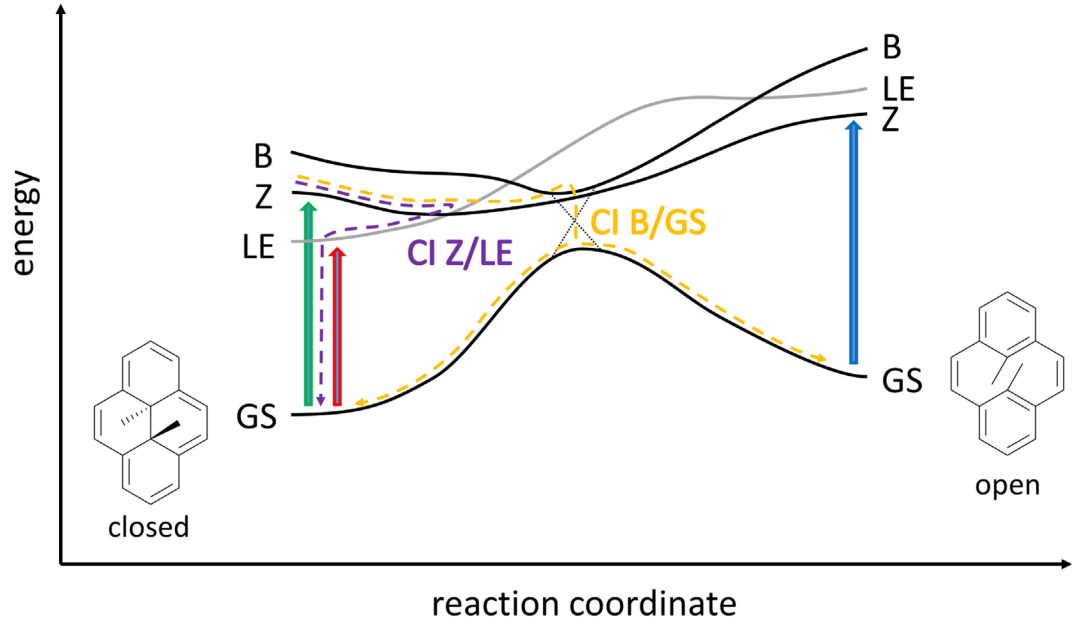

*Figure 28: Switching mechanism of the parent dihydropyrene **49**: Excitation to the S_1 state (LE, red arrow) in the long wavelength region above 600 nm does not lead to switching. After excitation to the S_2 state (Z, green arrow), the molecule can either change to the LE state via the conical intersection CI Z/LE and relax thermally (purple dashed line) or overcome an excited state activation barrier to the conical intersection CI B/GS from the B state, which leads to the formation of the open isomer (identical to Figure 4 and Figure 9).*[41]

The direct excitation to the LE state is forbidden and causes a fine structured, weak absorbing band usually between 600 and 700 nm, which is also apparent in the switches with low quantum yields, but is overlapping with the band corresponding to the Z state in the donor-acceptor substituted switches. Looking at the tail of the spectra in Figure 27, the absorption which presumably belongs to the S_0-S_1 transition is visible at 600 nm for **78** and **80**. From a theoretical point of view, there are two cases which improve the quantum yield of dihydropyrenes: a) The conical intersection between Z and LE is located at the valley of the Z potential energy surface. Shifting this conical intersection would decrease the probability of deactivation, which is the case for dihydropyrenes with internal isobutenyl groups or acceptors in the 2-position. b) The Z state becomes the lowest excited state and no deactivation *via* other excited states is possible, which is the case for 4,5-benzofused dihydropyrenes.[211] From this study, it is concluded that the latter is the case here and the push-pull system lowers the Z state, making it possibly the S_1 or close to it (Figure 27), so that thermal relaxation *via* LE becomes less likely. Furthermore, a donor-acceptor system causes a capto-dative effect[212–214] which possibly stabilizes the B state as well, lowering the excited state activation barrier, therefore facilitating the transition to the B state and improving the switchability.

In conclusion, a series of dihydropyrenes has been shown, which allowed investigation of substituent effects on the basic switching parameters, such as quantum yield, thermal half-life and absorption maximum. It has been found that the excited state activation barrier is lower in push-pull systems, presumably caused by a lower lying Z and B state. It is evident that this is not just an effect of acceptor strength, as an amino group produces a lower barrier than a methoxy group. The general capability of polar solvents to enhance the push-pull effect supports this assumption, since a much higher excited state activation barrier and lower quantum yields have been found going to nonpolar solvents.

3.2 Arylazotetracyanocyclopentadienide Photoswitches

3.2.1 Azobenzenes

Although azobenzene **81** has been synthesized already in 1834,[215] the light induced isomerization to the Z form has not been found until 1937 (Scheme 57).[216]

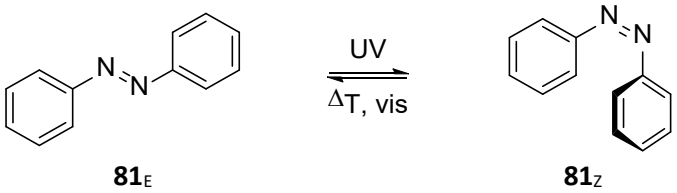

81$_E$ **81**$_Z$

*Scheme 57: Photochromism of the parent azobenzene **81**.[216]*

Given their use as dyes in many industrial applications, various synthetic routes have been developed to establish the azo bond. The original synthesis works *via* the reductive homocoupling of nitrobenzene, which is a general method today for symmetric azobenzene derivatives. On the contrary, oxidative coupling of anilines can be used as well where the reduction interferes with other moieties. Starting from aniline, two classical ways for the synthesis of unsymmetrically substituted azobenzene derivatives are established: The diazotation and subsequent azo coupling to electron-rich aromatic molecules, such as phenolates or aniline derivatives or the partial oxidation to the corresponding nitroso species and subsequent Mills reaction with aniline derivatives. The latter allows the introduction of electron poor aromatic systems (Scheme 58). Other methods include the oxidation of hydrazo species or the reduction of azoxy species to azobenzene.[217]

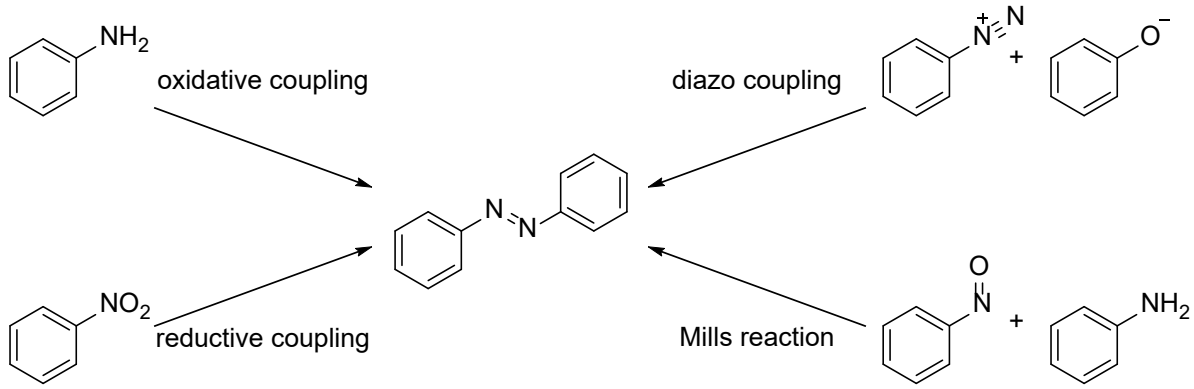

Scheme 58: Main routes for the synthesis of azobenzene derivatives. While oxidative and reductive coupling are used for symmetric substitution, the diazo coupling and the Mills reaction are utilized for unsymmetric substitution patterns with either electron-rich or electron-deficient coupling partners.[217]

Regarding the photochromic properties of azobenzene several substitution patterns have to be discussed. In the spectrum of the parent azobenzene **81**$_E$ two main absorption bands are visible, of which the one at 316 nm (21000 L mol^{-1}cm^{-1}) belongs to the π-π* transition, whereas the one at 445 nm belongs to the n-π* transition. Since the n-π* transition is forbidden, a low extinction coefficient of 550 L mol^{-1}cm^{-1} is observed. The E to Z isomerization causes a twist of the benzene rings leading to a less conjugated system and therefore hypsochromic and hypochromic shift of the π-π* band to 279 nm (4300 L mol^{-1}cm^{-1}). The position of the n-π* band is not affected as much, although it becomes less forbidden (428 nm, 1200 L mol^{-1}cm^{-1}). The more intense π-π* band at longer wavelengths makes UV-light of 347 nm the best wavelength for the E to Z isomerization (Figure 29),

whereas visible light at 413 nm gives the highest E content in the PSS. In general, the quantum yield is higher for Z to E isomerization and for switching *via* the n-π* band than *via* the π-π*band: ($\Phi_{EZ\pi\pi^*}$ = 0.14; $\Phi_{EZn\pi^*}$ = 0.31; $\Phi_{ZE\pi\pi^*}$ = 0.35; $\Phi_{ZEn\pi^*}$ = 0.55). The half-life for the thermal back reaction is about 7 d.[113,218]

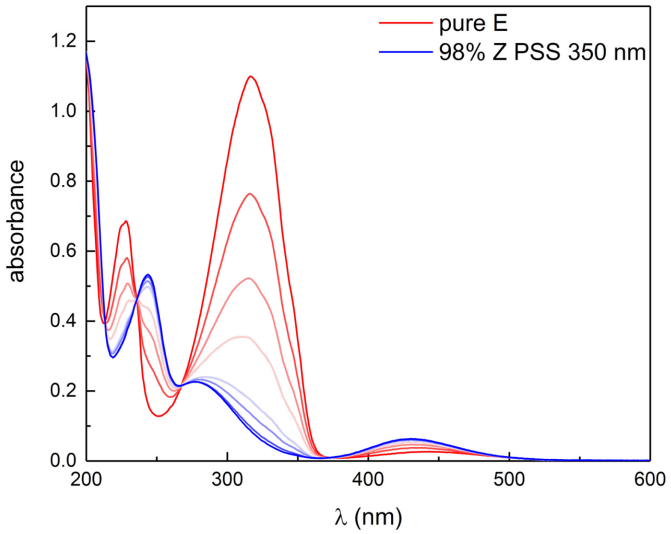

*Figure 29: UV/vis absorption spectra of the parent azobenzene **81** ($5.2 \cdot 10^{-5}$ M, 25 °C) in acetonitrile: The low extinction coefficient and small separation of the n-π* bands make UV light necessary for switching.*[v]

In terms of substituent effects in the 4- and 4'-position, many switches behave similar to azobenzene, with two exceptions of which the typical representatives are 4-aminoazobenzene **82** and 4-amino-4'-nitroazobenzene **83** (classification of Rau, Figure 30). Azobenzene derivatives decorated with an amino group in the 4-position show a bathochromic shift of the π-π* band and absorb in the blue region with high extinction coefficients. Interestingly, the n-π* band does not seem to be affected by these substitutions, so that π-π* and n-π* band are closer and start to overlap in these systems. Compared to the parent azobenzene, the n-π* band of aminoazobenzenes is more intense due to a stronger mixing with the π-π* state, "borrowing intensity". While the quantum yields are similar to the parent azobenzene, the thermal half-life of aminoazobenzenes is much shorter and usually lies in the region of few minutes.[219,220]

The 4,4'-donor-acceptor substituted azobenzene derivatives are referred to as "pseudo-stilbenes" and absorb even further in the visible due to the charge-transfer character of the π-π* band. The π-π* transition becomes lower in energy than the n-π* transition, which results in completely overlapping absorption bands. Since the weak n-π* band is not visible under the intense π-π* band, the absorption spectrum appears like the one of a bathochromic stilbene derivative. Due to the short thermal half-life at room temperature, donor-acceptor azobenzene derivatives are usually characterized at low temperatures or by ultrashort time-resolved spectroscopy. [219,220]

[v] Spectroscopy of parent azobenzene **81** by Lutz Grubert.

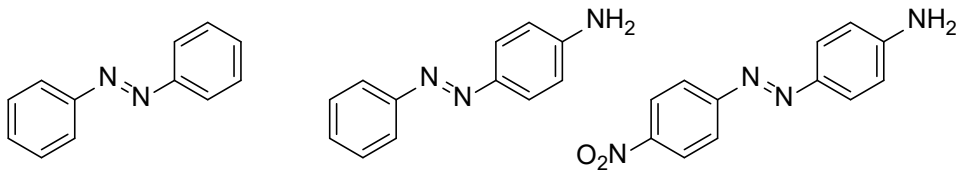

81 **82** **83**

*Figure 30: Classification of azobenzenes according to Rau: azobenzene-type molecules **81**, aminoazobenzenes **82**, and pseudo-stillbenes **83**.*[221]

Rau classified the three azobenzene types in 1990 according to the separation of π-π* and n-π* band[221] and since then, many new structural motifs on azobenzene derived switches have been investigated of which few will be discussed here. Whereas substituents in the 4- and 4'-position of the azobenzene have been investigated for decades, the last 10 years brought several advances on *ortho* substitution with hetero atoms and some more sophisticated derivatives.[222,223] It has been shown that introduction of amino groups in the *ortho*-positions resulted in the aminoazobenzene case in switches with half-lives between < 1 s and 2 min, which could be switched with blue light, although the π-π* and n-π* band strongly overlap.[224] Introducing four methoxy groups in the *ortho* positions leads to a hypsochromic shift of the π-π* band and bathochromic shift of the n-π* band, which is attributed to twisting of the aryl units in the E isomer, as well as an interaction of the oxygen and nitrogen lone pairs, which raises the n-orbital in energy. In the Z isomer, the n-π* band is not affected, which leads to a good band separation of both n-π* bands (36 nm for **84**, Figure 31) and allows switching in both directions with visible light. The negative photochromic tetra-*ortho*-methoxy azobenzene **84** (λ_{max} = 480 nm) undergoes efficient E to Z isomerization upon irradiation at 635 nm (PSS = 93% Z). The thermal back isomerization is slow (14 d at 25 °C) and back switching is conducted with blue light (450 nm, PSS = 86% E). A similar but less pronounced effect is observed for the corresponding tetra-*ortho*-chloro and tetra-*ortho*-bromo derivatives of **84**.[225,226] In the tetra-*ortho*-thioether azobenzene derivatives the separation between the n-π* bands is even less pronounced and leads together with thermal half-lives in the region of minutes to moderate switching. On the contrary, extinction coefficients in the visible of around 10000 L $mol^{-1}cm^{-1}$ have been observed.[227]

In contrast to bromo or chloro substituents, the tetra-*ortho*-fluoro azobenzene **85** features an even larger band separation between the n-π* bands of 53 nm together with a thermal half-life of 2 years. The *ortho*-fluoro substituents lower the energy of the n-orbital in the Z isomer and to a minor extent the π*-orbitals in both isomers, which leads to a hypsochromic shift of the n-π* band in the Z isomer and a bathochromic shift in the E isomer. **85**$_E$ (λ_{max} = 474 nm) can be converted with light > 500 nm to the Z isomer **85**$_Z$ (λ_{max} = 421 nm, PSS = 90% Z) and back with 410 nm (PSS = 97% E).[228]

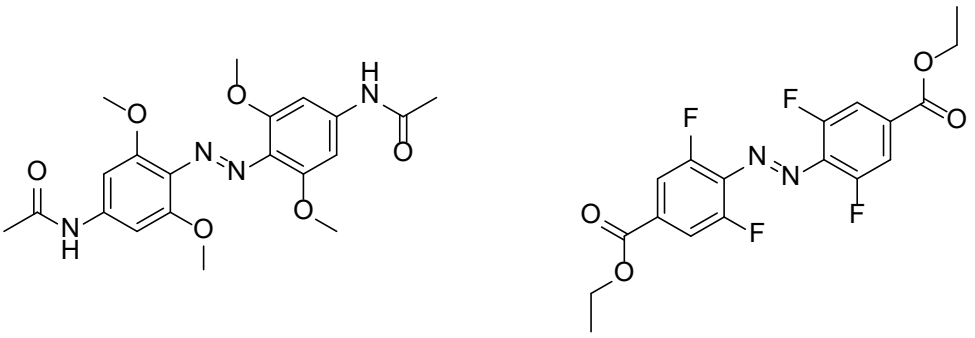

84 **85**

Figure 31: Tetra-ortho-methoxy or -fluoro substituted azobenzenes provide separated n-π bands, which makes the use of UV-light unnecessary.*[225,226,228]

An interesting effect was observed by the group of Woolley, when they investigated the pH dependent switching of tetra-*ortho*-methoxy substituted azobenzenes. Whereas even the electron-rich 4-aminoazobenzenes require a pH < 3.5 to be protonated and suffer from thermal half-lives in the range of microseconds, *ortho*-methoxy groups stabilize the azonium ion, allowing for protonation around neutral pH. They observed that upon switching the pK_a of the Z isomer is reduced, which leads to deprotonation in the neutral pH region. Since the deprotonated Z isomers exhibit a much longer thermal half-life, they were able to observe reasonable switching with red light of up to 720 nm.[229,230]

In a similar way to the azonium ion, the group of Aprahamian used coordination of the azo group by BF_2 to synthesize azobenzene derivatives, which can be operated with visible light (Scheme 59). The coordination by a Lewis acid inverts the order of n-π* and π-π* transition, similar to the "pseudo-stilbene" case but prevents a fast relaxation. **86**$_E$ (λ_{max} = 680 nm) has an extinction coefficient of 36000 L mol^{-1}cm^{-1} and undergoes E to Z isomerization with 710 nm. In comparison to donor-acceptor azobenzenes the thermal half-life is quite long (4 min at 20 °C), but still too short to determine further switching parameters (PSS > 63% Z). The classic phenomenon of a bathochromic shift with a decreased thermal half-life has been observed for these coordination compounds as well. Replacing the *N,N*-dimethylaniline by benzene increases the thermal half-life to 12.5 h and shifts the $\lambda_{max,E}$ to 570 nm, which results in good PSSs. It has to be mentioned that in thermal equilibrium both isomers are present. Whereas the dark E content is above 90% for most derivatives, 42% Z have been found for 1,3-dimethoxybenzene instead of the *N,N*-dimethylaniline **86**.[231,232]

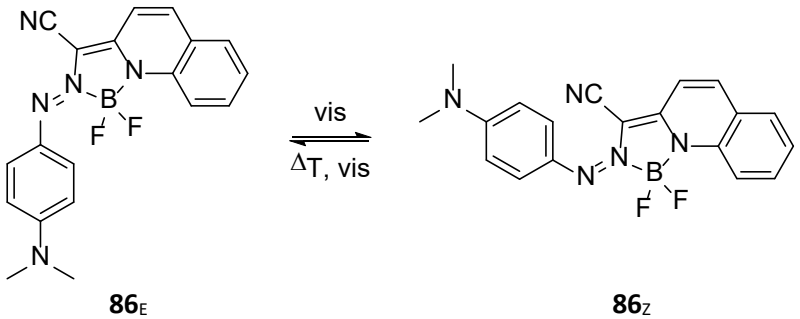

86$_E$ **86**$_Z$

Scheme 59: BF_2 coordinated azo switches with high extinction coefficient in the visible.[231,232]

Although the diazocine **87**$_Z$ has been synthesized decades ago,[233] in 2009 the group of Herges investigated its photochromic properties for the first time and extended their work to several derivatives (Scheme 60). In contrast to unbridged azobenzenes, the Z form is more stable than the E isomer and both forms have well separated n-π* bands in the visible region. **87**$_Z$ (λ_{max} = 404 nm) undergoes efficient Z to E isomerization (Φ_{ZE} = 0.72, 385 nm). The back reaction of **87**$_E$ (λ_{max} = 490 nm) happens under irradiation (Φ_{EZ} = 0.5, 520 nm) or thermally with a half-life of 4.5 h at room temperature.[234] By substitution of the benzene rings with amides/amines or introduction of hetero atoms in the bridge, the thermal half-life can be tuned from 90 s to 3.5 d. Similar to unbridged azobenzenes the n-π* bands of both isomers seem to be quite unaffected by these substitutions.[235,236]

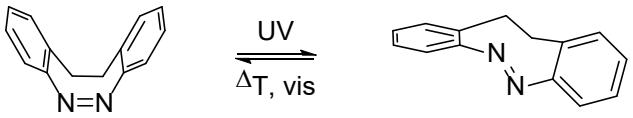

87$_Z$ **87**$_E$

Scheme 60: Photochromism of diazocine.[234]

Changing the phenyl moieties of the parent azobenzene for heteroaromatic compounds has been done for decades in dye industry. Their photochromic properties, however, remained unregarded. Intensive studies on nitrogen containing five membered aromatic rings in azoheteroarene photoswitches where done by the groups of Fuchter,[237–239] Herges,[240] and Otsuki.[241] As the amount of nitrogen atoms can vary from one in simple pyrroles to four in tetrazoles and these heterocycles can be connected to the azo bond in different positions, a huge number of derivatives is possible. The introduction of methyl groups in the pseudo-*ortho* positions provides a further handle which influences the photochromic properties dramatically. In an illustrative example **88**$_E$ (λ_{max} = 425nm) undergoes efficient and almost quantitative conversion to **88**$_Z$ (λ_{max} = 441 nm) with 355 nm (PSS > 98%, Φ_{EZ} = 0.46) since **88**$_Z$ features an absorption gap at this wavelength (Figure 32). The back isomerization with light > 532 nm produces the E isomer as efficiently (PSS > 98%, Φ_{ZE} = 0.56) but also works thermally with a half-life of 10 d at 25 °C. Without the methyl groups in the pseudo-*ortho* positions in **89**$_E$ (λ_{max} = 417nm), the E to Z isomerization at 355 nm was even more efficient due to a similar absorption gap of **89**$_Z$ (λ_{max} = 403nm, Φ_{EZ} = 0.61, PSS > 98%). The photochemical back reaction at 532 nm reached a moderate PSS of 70% E (Φ_{ZE} = 0.6), but the thermal half-life increased to 1000 d (25 °C).[238]

88 **89**

Figure 32: Pyrazole based azoheteroarene photoswitches with high PSS and long thermal half-life.[238]

Instead of hetero aromatic substituents, bigger π-systems, such as naphthalene could be considered as well (Figure 33). In principle, larger π-systems cause a bathochromic shift of the π-π* band, resulting in an overlap of π-π* band and n-π* band. Furthermore, the proximity of the π-system and the azo bond, seems to cause an increased intensity and bathochromic shift of the n-π* band of the E isomer, resulting in a lower PSS for the Z to E isomerization. The 2,2'-azonaphthalene **90**$_E$ can be isomerized with 365 nm to the Z isomer (PSS = 92% Z) and reverts either thermally with a half-life of 150 min at 29 °C or photochemically with 578 nm light (PSS = 98% E). On the contrary, the 1,1'-azonaphthalene **91**$_E$ can be isomerized with 405 nm light (PSS = 95% Z) and reverts thermally with a half-life of 30 min at 13 °C. For the photochemical back reaction of **91**$_Z$, a suitable irradiation wavelength is missing as both spectra are quite similar for $\lambda > 500$ nm (PSS = 48% E at 578 nm).[242,243]

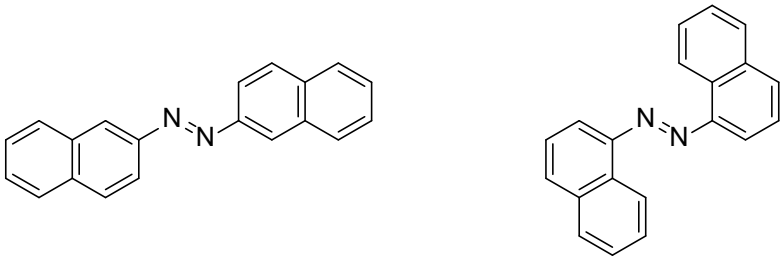

90 **91**

Figure 33: Azonaphthalenes connected either via the 1- or the 2-position.[242,243]

3.2.2 Motivation

Although the photochromism of azobenzene is known for decades, a general solution is missing to overcome some intrinsic issues. For most derivatives UV light is required for the E to Z isomerization, since the n-π* bands in the visible are highly overlapping. Furthermore, the n-π* bands suffer from low extinction coefficients for almost every azobenzene derivative, which makes high light intensities necessary for visible light switching. Despite these problems connected to the switching, a practical problem is the low water solubility, especially since the emerging field of photopharmacology relies almost exclusively on azobenzene switches. Here, a structural design is shown which intrinsically features two well separated bands in the visible region with high extinction coefficients for both isomers. The design is based on a charged moiety, allowing to tune the solubility by proper choice of the counterion, which leaves the photoswitch itself *untouched*.

3.2.3 Synthesis

The cyano-substituted cyclopentadienide was found during investigations on the reactivity of tetracyanoethylene **92**. Tetracyanoethylene **92** is easily reduced by a variety of reagents, of which mercaptoacetic acid was found to be the most convenient. The product tetracyanoethane **93** is precipitated from water, which in the original procedure is dried over anhydrous phosphorus pentoxide. However, since the material contains a huge amount of water, it was found advantageous to pre-dry the substance first, by sucking air through a frit which contains the precipitate for few hours. NaH deprotonates tetracyanoethane **93** rapidly two times, which is in contradiction to the literature. Since the subsequent intermolecular nucleophilic substitution only works when some monoanion is present, the equivalents have to be met carefully. The reaction to the hexacyanobutadienide **94** is easily followed by the intense coloration and precipitation of NaCN. It should be mentioned here, that this reaction highly depends on the quality of the NaH. It was sometimes necessary to add few droplets of methanesulfonic acid, when too much NaH caused complete deprotonation of the tetracyanoethane **93**. Protonation of the hexacyanobutadienide **94** causes cyclization *via* intramolecular addition to a cyano group. With strong acids, one of the nitrile groups is hydrolyzed and eliminated to yield the aminotetracyanocyclopentadienide **95**. For the isolation of the amine, the cyclization must be done under mild conditions such as protonation with an ion exchange resin. Either from the amine **95** or directly from the hexacyanobutadienide **94** a diazotation with acid and $NaNO_2$ gives the diazotetracyanocyclopentadiene **96**. Although diazotetracyanocyclopentadiene **96** is a stable solid, prolonged stirring of the diazotation reaction causes the loss of the diazo part which results in unsubstituted tetracyanocyclopentadiene (Scheme 61).[244]

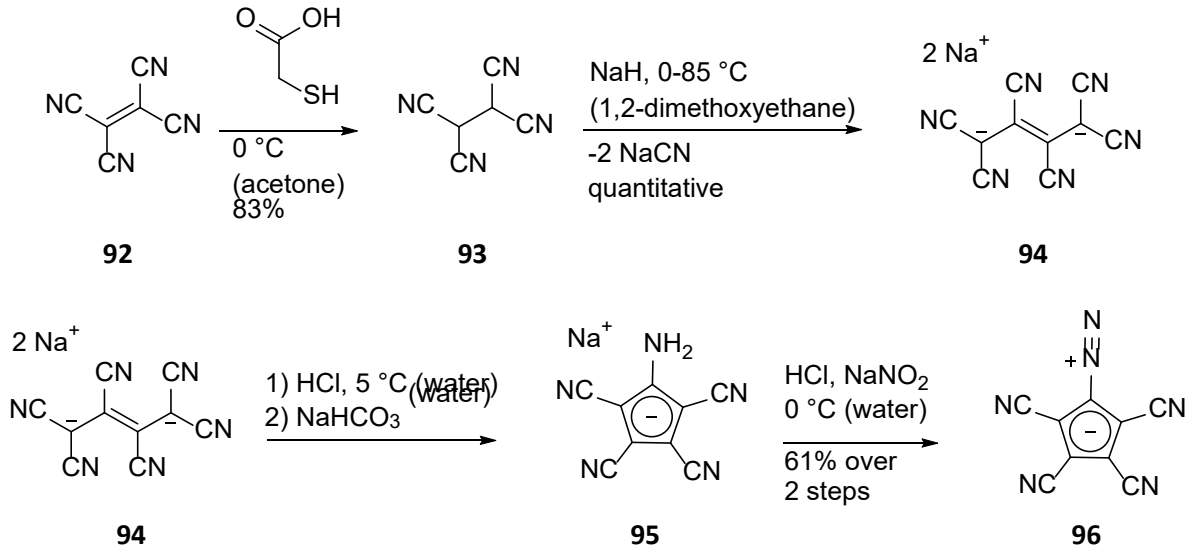

Scheme 61: Synthesis of diazotetracyanocyclopentadiene.[244–246]

3.2.4 Arylazotetracyanocyclopentadienides

The phenomenon of photochromism, a reversible photoreaction, has been observed on a huge variety of molecules.[192] Despite great effort to find new design principles for photoswitches, only few classes dominate the field, with azobenzenes probably being the most prominent one. On the one hand, azobenzenes have been applied to various fields, such as life science,[14] materials science,[10] catalysis,[12] and molecular machines.[13] On the other hand, tunability of the photochromic properties has seen many advances during the last decade, by exploring the effect of functional groups, especially in the *ortho* position,[222] heteroaromatic substituents,[237] and coordination[231]/protonation[229] of the azo bond.

Several problems still remain for many derivatives, namely most azobenzenes are limited to nonpolar solvents and require a solubilizing group if water is within the scope of the application. Furthermore, the low extinction coefficient of the n-π* band[247] often requires long irradiation times or high light intensities, which may result in the use of UV-light for switching *via* the much more intense π-π* transition. Usually the π-π* bands are well separated, allowing for efficient E to Z switching with UV-light, whereas the n-π* bands in the visible region largely overlap, resulting in lower photostationary states for the Z to E isomerization. Here, a new design for azobenzenes is introduced, which relies on the tetracyanocyclopentadienide (TCCp) substituent and does not suffer from the aforementioned drawbacks.

Webster found in 1965 that the dianion of hexacyanobutadiene **94** would cyclize with acid to form aminoTCCp **95**, which he treated with $NaNO_2$ to prepare the TCCp diazonium salt **96**. It is a remarkable compound in terms of thermal stability (decomposition > 200 °C) and dipole moment (11.4 D),[248] which can undergo azo coupling to electron-rich aromatic systems.[244]

Thereafter, the TCCp structural motive has been used in supramolecular chemistry,[249,250] but the photochromic properties of these azo dyes have not been reported, until now. The only compound where a cyclopentadienyl moiety is connected to an azo bond and for which photoreactions have been investigated is azoferrocene, where the isomerization to the Z isomer is irreversible.[251] It was surprising that the already known azo dye **97$_E$** undergoes a reversible photoreaction and hence this interesting class of molecules has been examined (Scheme 62 and Figure 34).

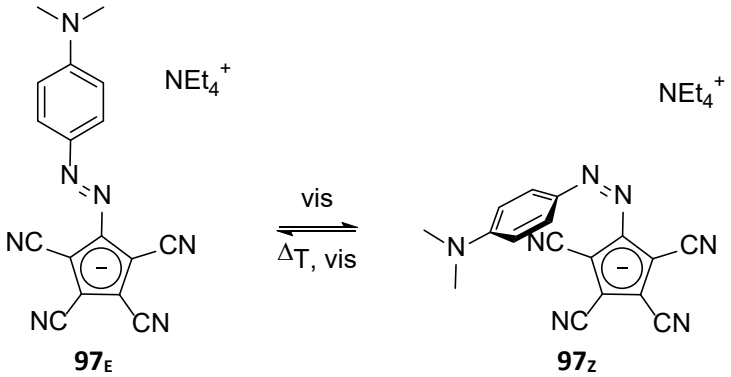

97$_E$ **97$_Z$**

Scheme 62: T-type photochromism of an arylazoTCCp switch.

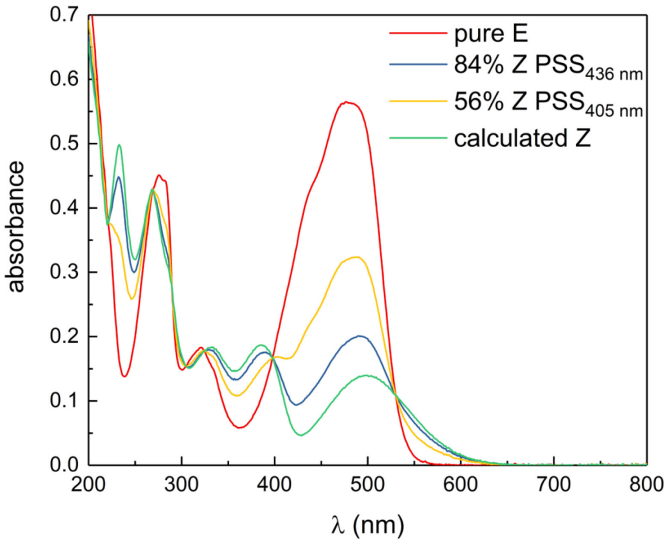

*Figure 34: UV/vis absorption spectra of **97E** and the PSS after irradiation with 405 nm and 436 nm in acetonitrile ($1.6 \cdot 10^{-5}$ M, −20 °C). The spectrum of **97Z** can be derived from the PSS spectra and the pure E spectrum according to the method developed by Fischer.[44]*

Mixing the TCCp diazonium salt **96** and an electron-rich aromatic molecule in acetonitrile usually results in quantitative azo coupling, while the main losses during synthesis result from purification by recrystallization, especially on a small scale. To enable a broader substrate scope, Mills coupling conditions have been investigated, which provide access to electron poor aromatic molecules, such as benzonitrile or nitrobenzene, as well (Scheme 63).

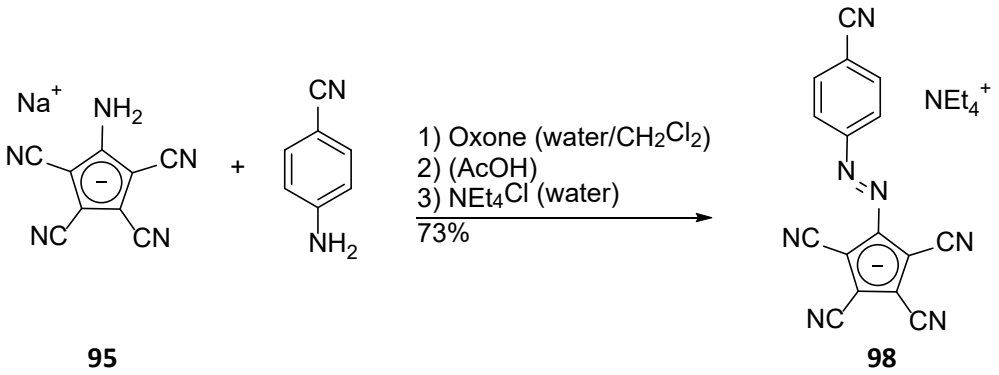

95 **98**

Scheme 63: Mills coupling reaction to introduce electron-deficient substituents.

Most of the arylazoTCCps are crystalline solids and single crystal structures for several derivatives have been obtained (Figure 35). For the potassium salt **103**, coordination of the potassium cation is found for methoxy O, azo N, and nitrile N. The latter is typical for pentacyanocyclopentadienide salts (Figure 36).[252]

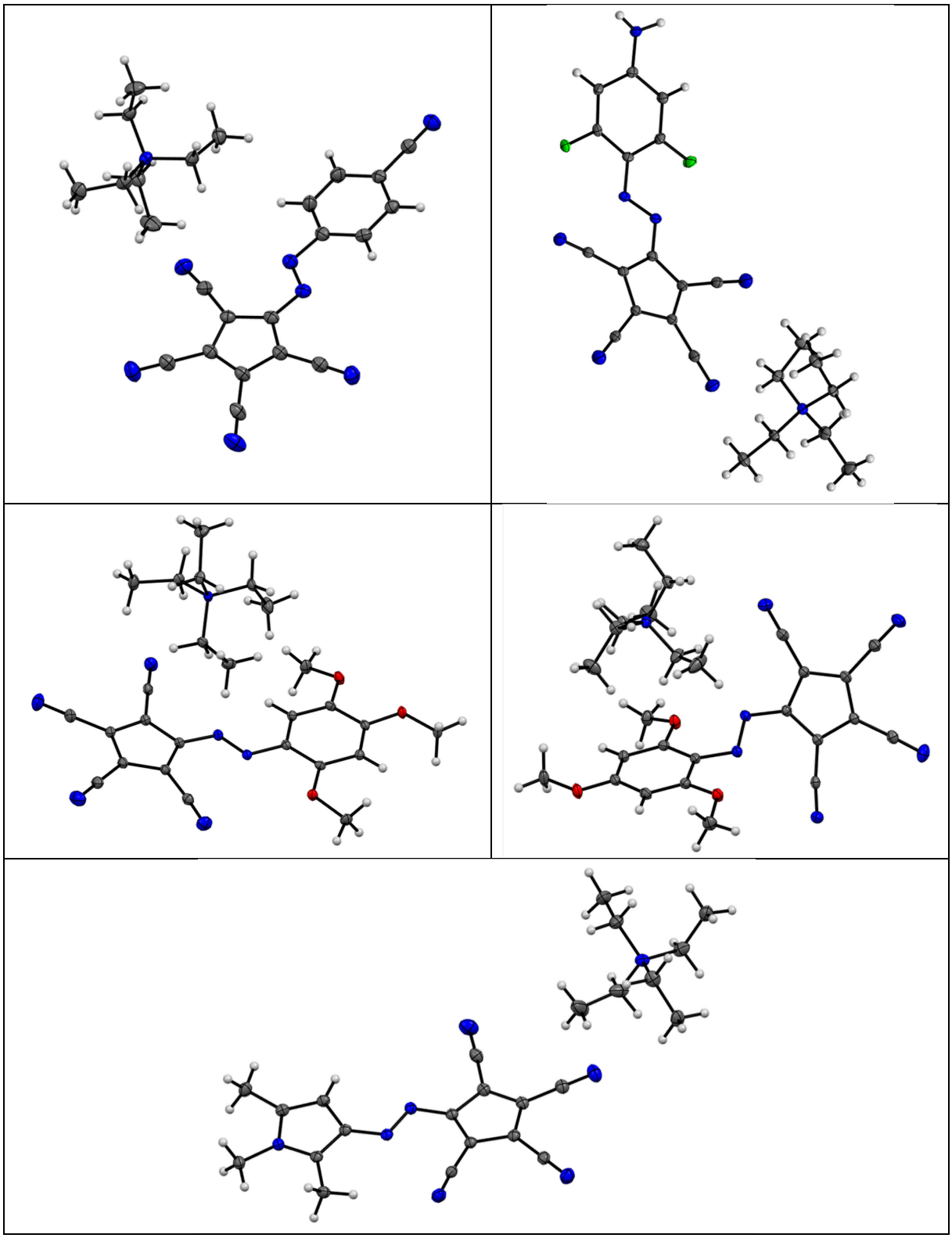

Figure 35: Molecular structures of some arylazoTCCp switches. Ellipsoids are set at a 50% probability. Top-left: ***98****; top-right:* ***99****; middle-left:* ***100****; middle-right:* ***101****; bottom:* ***102****.*[vi]

[vi] X-Ray analysis of **98**, **100**, and **102** performed by Florian Q. Römpp. X-Ray analysis of **99** and **101** performed by Bernd M. Schmidt.

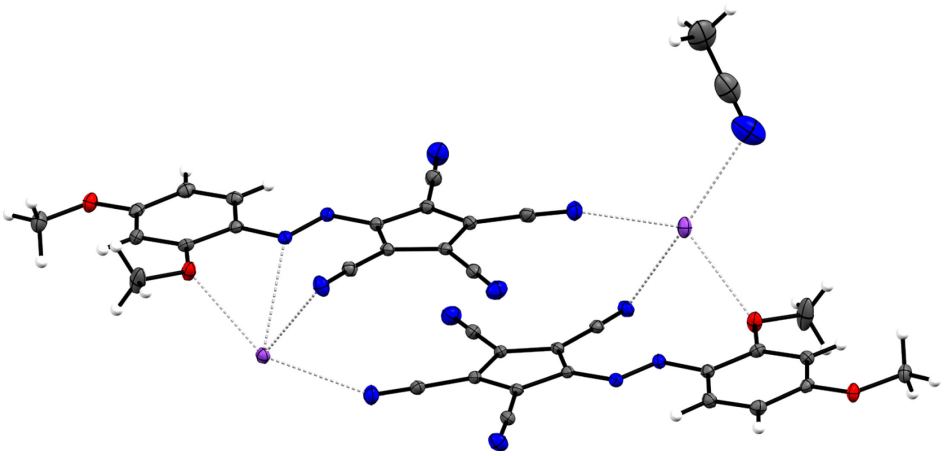

*Figure 36: Molecular structure of the potassium salt of **103**. Ellipsoids are set at a 50% probability.*[vii]

Since some of the newly synthesized photoswitches show positive photochromism in combination with a fast thermal back reaction, the standard methods (UV/vis in combination with NMR or HPLC) for obtaining the spectrum of the pure Z isomer are problematic to use, since they would have to be done at lower temperatures. To solve this classic problem of photochromism, the arylazoTCCp switches have been analyzed by applying the Fischer method[44] at temperatures, where the speed of the thermal back reaction is neglectable compared to the speed of the photoreaction. Assuming that the quantum yields for both isomerizations are independent of the irradiation wavelength, the spectrum of the pure Z isomer can be obtained from the pure E spectrum and the photostationary state (PSS) spectra at two different wavelengths. To verify the quantum yield assumption, three instead of two different wavelengths have been used for monochromatic irradiation (365, 405, and 436 nm), which resulted in similar Z spectra for each pair, with few exceptions due to intrinsic limitations of the method (see experimental section 5.3) or irradiation to a higher excited state.

Surprisingly, the TCCp unit leads to a large separation between the absorption maxima of the bands in the visible region for E and Z isomer of up to 80 nm. So far, only the bridged Z azobenzenes from the group of Herges show a similar large band separation.[234,235] For most azobenzenes the n-π* bands overlap, which makes the use of UV-light for switching *via* the π-π* band necessary. A large band separation is a prerequisite for a high PSS, since it allows to irradiate both isomers almost exclusively. In general, the Z isomers of arylazoTCCp switches show only little absorption around 405 nm, resulting in PSSs with 90% Z content. For the back reaction red light with a cut-off filter or heat can be used, allowing for almost full photoconversion in both directions.

Some of the photochromic properties are listed in Table 4 and some trends are found comparing to the benzene analogs: (1) All of the arylazoTCCps switch efficiently with visible light in both directions, resulting in a PSS around 90% for most derivatives. (2) The extinction coefficients of the E isomers in the visible are generally higher (> 20000 L $mol^{-1}cm^{-1}$) than for classic azobenzenes. (3) The E isomers show fine structure in the UV/vis spectrum, whereas the Z isomers lack such vibronic features. (4) The thermal half-lives are shorter compared to classic azobenzenes, ranging from few minutes to 14 h. (5) The quantum yields for both reactions are relatively high (0.2-0.7), typically the Z to E quantum yield being the higher one. (6) No fatigue was observed under prolonged irradiation, with the only exception being the free pyrrole derivative **111**. (7) The established design rules for azobenzene apply as well for TCCp azos: Strong donors (*N,N*-dimethylamino, **97**) or strong acceptors (nitro, **104**) lower the thermal

[vii] X-Ray analysis of **103** performed by Bernd M. Schmidt.

stability of the Z isomer.[253] Fluorine atoms in the *ortho*-position of the benzene ring can be used to increase the thermal half-life[254] (compare **97** vs **107** or **106** vs **99**), whereas hydroxyl groups, either in *ortho* or *para*, lead to low conversions under irradiation (**108**, **109**, **110**).[255]

It was possible to synthesize heteroarene azos, which resulted in longer thermal half-lives, *e.g.* 8 h for pyrrazole **112** or 13 h for *N*-methylpyrrole **102**. The free pyrrole **111** is found to be photochromic with a thermal half-life around 3 min, although prolonged irradiation led to side products, which prohibits a detailed analysis by the Fischer method.

Table 4: Photochromic properties of the new tetracyanocyclopentadienyl azo-compounds.[viii]

No.	aryl substituent	λ_{max} E (ε) λ_{max} Z (ε)	Φ_{EZ} Φ_{ZE}	$PSS_{405\ nm}$ %E $PSS_{436\ nm}$ %E PSS %Z (λ_{irr})	$t_{1/2}$[c] (min)
97	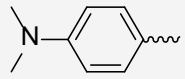	477 (35600)[a] 499 (8800)[a]	0.49[a] 0.62[a]	56%[a] 84%[a] 99% (579)[a]	2.4
98	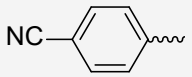	399 (22500)[b] 476 (3300)[b]	0.42[b] 0.61[b]	93%[b] 81%[b] 93% (> 550)[b]	39.6
104	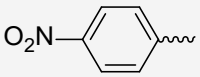	413 (26000)[a] 482 (4400)[a]	0.25[a] 0.62[a]	90%[a] 79%[a] 98% (> 550)[a]	6.6
105	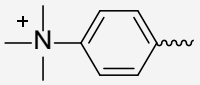	390 (20000)[c] 470 (3100)[c]	0.47[c] 0.68[c]	91%[c] 71%[c] 94% (> 500)[c]	150
106	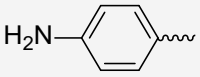	423 (27700)[b] 489 (6100)[b]	0.45[b] 0.56[b]	88%[b] 83%[b] 98% (> 550)[b]	5.1
107 acetonitrile	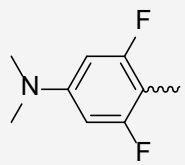	476 (27000)[b,d] 503 (7800)[b,d]	0.41[b] 0.58[b]	90%[b] 90%[b] 94% (> 550)[b]	29[d]
THF		466 (22000)[c,e]			91[e]
water		490 (29000)[c,d]			2.2 s[d]
[BMIM]BF4[f]		485 (27700)[c,d]			11.5[d]

[viii] Spectroscopy of **97**, **98**, **101**, **104**, **105**, and **106** together with Jonas Becker.

No.	aryl substituent	λ_{max} E (ε) λ_{max} Z (ε)	Φ_{EZ} Φ_{ZE}	$PSS_{405\ nm}$ %E $PSS_{436\ nm}$ %E PSS %Z (λ_{irr})	$t_{1/2}$[c] (min)
99	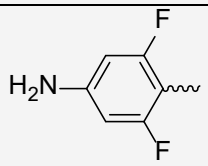	415 (30200)[b] 489 (7200)[b]	0.35[b] 0.48[b]	96%[b] 86%[b] 95% (> 550)[b]	67
100	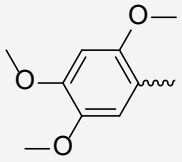	433 (20500)[b] 487 (5600)[b]	0.36[b] 0.27[b]	84%[b] 87%[b] 98% (> 590)[b]	5.1
101	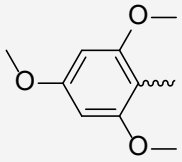	377 (34000)[c] 474 (8200)[c]	0.18[c] 0.30[c]	92%[c] 66%[c,g]	840
101-H$^+$	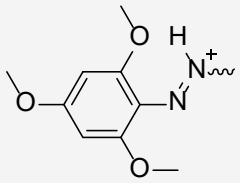	530 (46800)[a] 560 (24600)[a]	0.17[a] 0.26[a]	57% (546)[a] 43% (577)[a] 97% (> 610)[a]	2.1
108	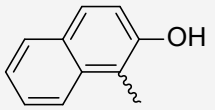	498 (15600)[c]			
109	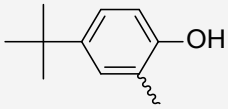	437 (17400)[c]			
110	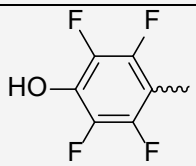	390 (18400)[c]			
111	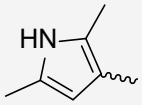	422 (20500)[a]			≈3
102	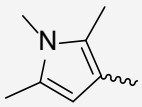	425 (20700)[c] 423 (2900)[c]	0.48[c] 0.69[c]	88%[c] 83%[c] 87% (> 500)[c]	770
112	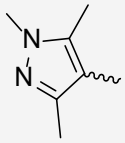	390 (21500)[c] 470 (4400)[c]	0.53[c] 0.61[c]	96%[c] 77%[c] 99% (> 500)[c]	485

λ_{max} in nm, ε in L mol^{-1}cm^{-1}; [a] –20 °C; [b] 0 °C; [c] 25 °C; [d] K$^+$-salt; [e] Bu_4N^+-salt; [f] 1-butyl-3-methylimidazolium tetrafluroborate; [g] No suitable wavelengths for the reverse reaction has been found, since the spectra show substantial overlap.

The common approach to solubilize a compound in a solvent where the solubility is low is the attachment of a solubilizing group. Depending on the polarity of the solvent one would choose different groups, *e.g.* alkyl chains for hexane and glyme for water. In general, this results in different molecules which are not necessarily comparable. The beauty of ionic compounds lies in the solubility tuning by proper choice of the counter-ion, leaving the functional part *untouched*. To exemplify the variety of applicable solvents, the K^+ salt as well as the Bu_4N^+ salt of **107** have been prepared and were investigated in nonpolar (THF) and polar (water) solvents, as well as in an ionic liquid (1-butyl-3-methylimidazolium tetrafluroborate, Figure 37). A small bathochromic shift is observed going to more polar solvents for both isomers. The band in the visible region seems to feature at least two different transitions, of which the lower energy transition has a higher extinction coefficient in polar solvents. The higher energy transition has a higher extinction coefficient in nonpolar solvents while the corresponding band only appears as a weak shoulder in water. This results in a larger band separation in nonpolar solvents. Furthermore, polar solvents accelerate the thermal back reaction, which allowed to tune the thermal half-life of **107** from 91 min (THF) to 2.1 s (water).

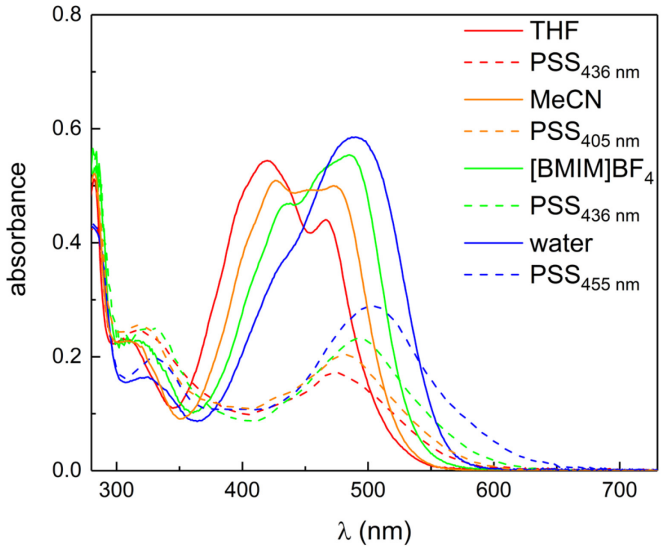

*Figure 37: UV/vis absorption spectra of **107** in various solvents before and under irradiation (normalized to $2 \cdot 10^{-5}$ M): A bathochromic shift is observed going from nonpolar to polar solvents for both isomers, $[BMIM]BF_4$ is 1-butyl-3-methylimidazolium tetrafluroborate.*

Covalent attachment of the cation to the aryl substituent would result in zwitterionic molecules. Zwitterions[256,257] are widely applied as solubilizing groups[258,259] and for the extraction of heavy metal ions from drinking water by chelation, as well as for sewage treatment, paper reinforcement, pigment retention, and formulation in shampoos or hair conditioners.[260] They also resist to nonspecific protein binding, which makes them applicable as nonfouling materials.[261–263] Such materials have various further microbiological applications[264] and can be utilized to produce "stealth" nanoparticles for drug delivery.[265] Zwitterionic compounds have proven to increase the conductivity in lithium metal batteries, by facilitating the dissociation of lithium ions from the polyelectrolyte and thereby increasing ion mobility.[266,267] The trimethylammonium switch **105**, which is easily obtained by methylation of the dimethylaniline derivative **97** with methyl iodide is a switchable zwitterion (Figure 38). Upon irradiation, the distance between positive and negative charge changes, which results in a change of the dipole moment and could be used in the context of some of the aforementioned applications.

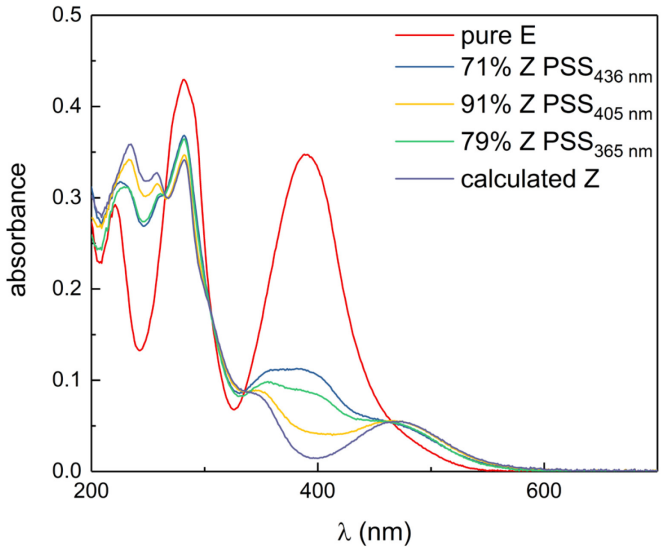

*Figure 38: UV/vis absorption spectra of **105E** and the PSS after irradiation with 365 nm, 405 nm and 436 nm in acetonitrile ($1.7 \cdot 10^{-5}$ M, 25 °C). The spectrum of **105Z** can be derived from the PSS spectra and the pure E spectrum according to the method developed by Fischer.[44]*

During their investigations on *ortho*-substituted azobenzenes, the group of Woolley found that the thermal half-life of photochromic azonium ions is in the range of microseconds to milliseconds when *ortho*-methoxy groups are introduced.[268] The arylazoTCCp derived from phloroglucinol trimethylether **101**, which bears two *ortho*-methoxy groups as well, exhibits a large hyperchromic and bathochromic shift upon protonation from 377 to 530 nm. The protonation supposedly occurs at the azo bond, given the extremely large pK_a value of the TCCp unit itself[269] and results in the zwitterionic (and therefore overall charge-neutral) azonium species (Scheme 64). Under irradiation with green light (546 nm) the Z isomer forms and reverts back with an astoundingly long thermal half-life of 2.1 min at room temperature. Furthermore, upon protonation a hyperchromic shift is observed for both isomers, which results in a surprisingly high extinction coefficient of the Z isomer (24600 L $mol^{-1}cm^{-1}$, Figure 39).

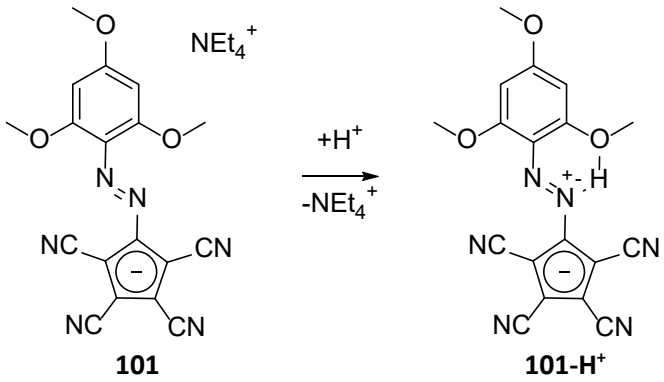

*Scheme 64: Protonation of **101** causes a bathochromic shift and results in surprisingly long thermal half-life of the Z isomer.*

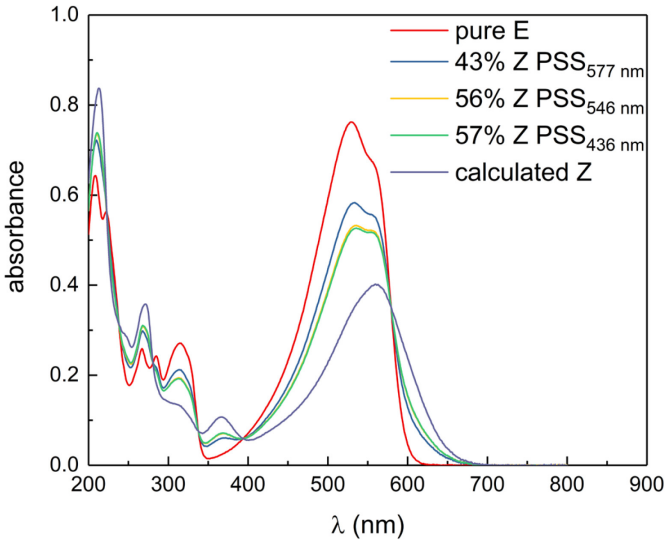

*Figure 39: Photochromism of **101-H**$^+$ in acetonitrile ($1.6 \cdot 10^{-5}$ M, −20 °C). An excess of methanesulfonic acid was added to assure complete protonation. The thermal half-life is 2.1 min (25 °C). The pure Z spectrum was calculated according to the method developed by Fischer.*[44]

In conclusion, the TCCp serves as a superb substitute for the benzene ring in azo-based photoswitches. A broad structural variation is possible, including electron-rich or electron poor benzene derivatives, as well as heterocycles. The TCCp unit provides a handle to overcome the problem of the poorly separated n-π* bands in the visible region, where band separations of up to 80 nm have been observed. The combination of absorption maxima with high extinction coefficients (> 20000 L mol^{-1}cm^{-1}) for the E isomer together with the absorption gap of the corresponding Z isomer at almost the same wavelength assures high photostationary states utilizing only visible light for both isomerization directions. Given the anionic nature of the TCCp unit, the solubility of the same switch can be tuned from THF to water (and even to ionic liquids), which is accompanied by a change of thermal half-life from 1.5 h to 2 s going to more polar solvents and may lead to applications in switchable ionic liquid crystals.[270] By covalent attachment of the cation to the aryl unit, a photochromic zwitterion has been shown to switch efficiently between both isomers, which has potential use in material and biological applications. Furthermore, the TCCp unit stabilizes the Z isomer of the corresponding azonium species in acidic media, giving rise to azo-based pK_a switches, which do not suffer from a fast thermal back reaction.

4 Conclusion and Outlook

Photoswitches are an ideal basis for smart materials, as they can be switched by light to alter their physical properties, which is advantageous since light is noninvasive, readily available, and offers the opportunity of good spatial and temporal resolution. However, from the huge number of reports on photochromism only a small quantity of different classes of photoswitches can be extracted, based on even fewer photoreactions. From all these classes the two most commonly applied photoreactions are E/Z isomerization and 6 π electrocylization, which have been investigated further, considerably improving the switching properties of dihydropyrenes and arylazotetracyanocyclopentadienides.

4.1 Dihydropyrenes

A series of 2,7-diaryldihydropyrenes has been synthesized and characterized in terms of their photochromic properties. The 6 π cycloreversion in dihydropyrene switches suffers from an activation barrier in the excited state, which results in low quantum yields for the ring opening. It has been shown in this work, how the symmetric extension of the π-system by two aryl units in the 2- and 7-position inhibits photoswitching, presumably increasing this barrier. On the contrary, substitution with donor and acceptor moieties reduces the barrier. This has led to a remarkable increase of the quantum yield rendering non-switches photochromic. Furthermore, the donor-acceptor substitution pattern causes a bathochromic shift of λ_{max} with high extinction coefficients and lowers the thermal half-life by reducing the ground state activation barrier as well.

The use of pyridine substituents enables protons as a second handle to modulate the photochromic properties. A catalytic amount of acid generates some pyridinium substituted dihydropyrenes which can be addressed selectively further in the red and have a higher quantum yield due to the reduced barrier. Since the majority of the open switches is deprotonated, they can take advantage of their longer thermal half-life resulting in higher conversions than the degree of protonation. Protonation of a second pyridine on the dihydropyrene erases the dipole and therefore increases the barrier again. This results in a lower quantum yield and conversion under the otherwise same conditions.

In general, a photoswitch has two different states but the combination of two photoswitches already results in four different states (or three if symmetric), which allows for a broader range of applications. Approaches to this goal were done in the groups of Branda[271] (**113** in Scheme 65) and Irie,[272] who combined two dithienylethenes in a conjugated fashion. Both observed that only one of the two positive photochromic switches would close with UV-light to give the colored open-closed isomer. Following Kasha´s rule,[197] all excitation energy goes to the lowest excited state, which belongs to the extended conjugated system of the closed part and therefore prevents closing of the remaining open switch.

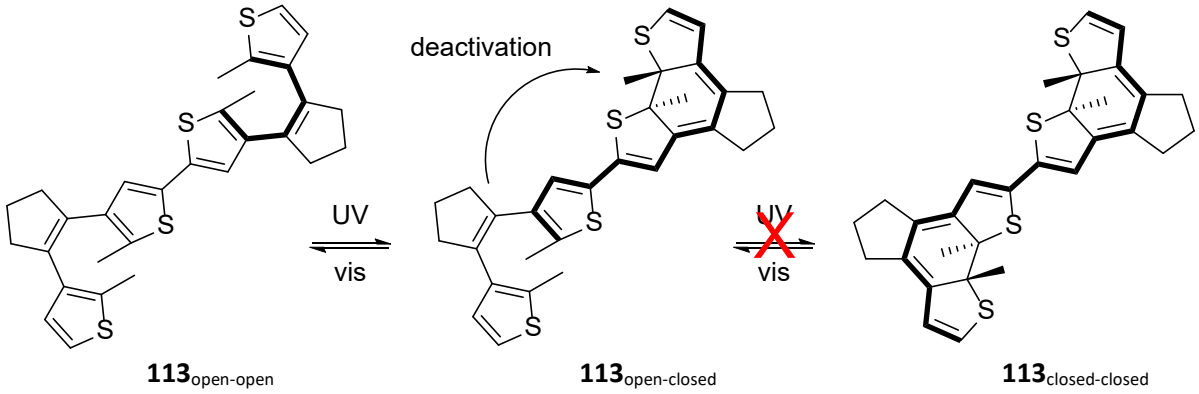

Scheme 65: Of conjugated positive photochromic switches only one isomerizes and a closed-closed derivative is not observed.

This issue can be solved using two conjugated dihydropyrenes, where the lowest excited state arises from the most extended π-system. Irradiation with visible light opens one switch and the new lowest excited state again arises from the longest π-system. This still includes the second dihydropyrene which opens upon further excitation with visible light. Since long π-systems generally disfavor light induced 6 π cycloreversions[208,273] and the π-system is shortened after the first dihydropyrene is opened, the second switching is assumed to be even more efficient. Although this positive cooperative effect has never been proven, several examples of multi photochromic molecules with conjugated dihydropyrenes have been published[49,274–278] and even a conjugated switchable copolymer of bithiophene and dihydropyrene is known.[279] The positive cooperative effect should be even more pronounced when the dihydropyrenes alternate with donor and acceptor linkers. In such a scenario, the attached donor and acceptor become stronger upon switching as they are not in conjugation with their former counterpart anymore. This should increase the dipole on the dihydropyrene, which is on the other side of the donor or acceptor and therefore lower the excited state activation barrier and enhance the quantum yield. A first example of two dihydropyrenes which are linked *via* an acceptor has been synthesized in a bachelor thesis and first irradiation experiments point to a cooperative switching effect (Scheme 66).[280]

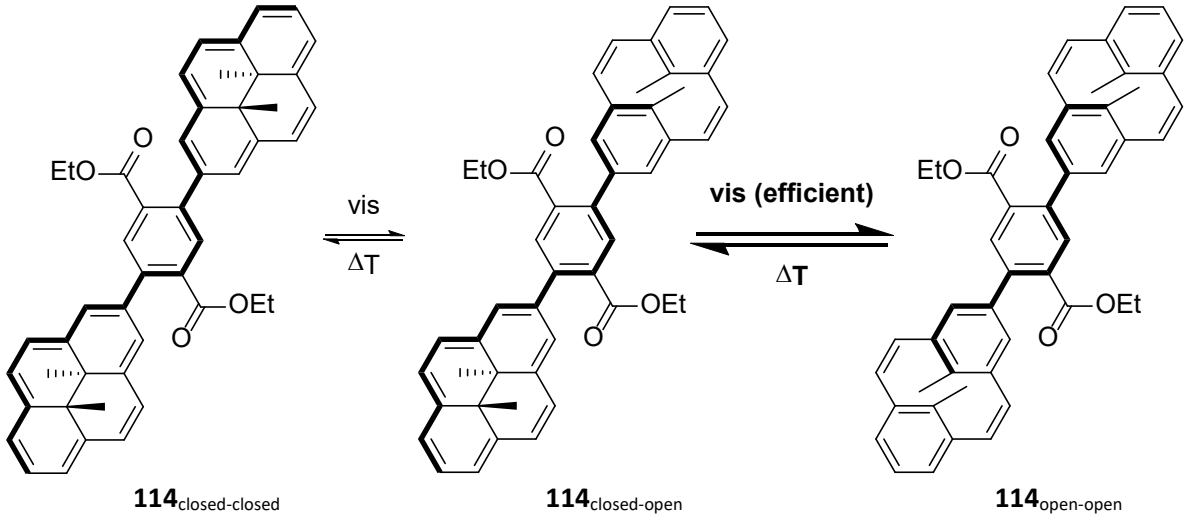

*Scheme 66: Dimeric **114** connects two dihydropyrenes via a conjugated linker.[280]*

Following the same argumentation, the combination of a colored metal complex and a further red absorbing dihydropyrene should still give a reasonable switch and indeed this was shown for several examples, although the switching efficiency was usually reduced compared to the free switch.[278,277,281–284] Therefore, deep red absorbing dihydropyrenes are ideal candidates for photoswitchable metal complexes which could be used to control transition metal catalysis. Initial switching experiments of the pyridine substituted dihydropyrenes **73** and **80** in the presence of excess zinc acetate revealed an increase of the quantum yield upon coordination of the metal to the switch (Scheme 67).

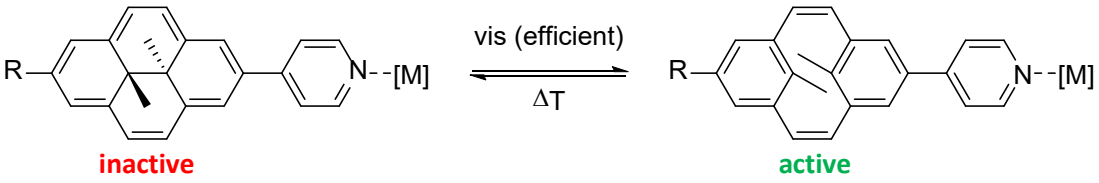

*Scheme 67: Photoswitchable metal complexes based on the pyridine substituted dihydropyrenes **73** (R=H) and **80** (R=anisole) with increased ring opening quantum yields, [M]=Zn.*

Further investigations will focus on device and solid-state applications, as crystal structures have been obtained and the switching in the crystalline state is not described sufficiently well for dihydropyrenes, although the minor geometrical changes should make them good candidates for switching in densely packed solid states.

4.2 Arylazotetracyanocyclopentadienides

A comprehensive library of arylazoTCCp derivatives has been synthesized and characterized with regard to their photochromic properties. The ionic nature of the TCCp unit facilitates crystallization and as a consequence several crystal structures have been obtained. The arylazoTCCps show high PSSs around 90% with visible light in both directions, which is due to the fact that the Z isomers have an absorption gap around 400 nm, where in most cases the E isomer shows its absorption maximum λ_{max}. Furthermore, especially the E isomers have extinction coefficients of $\varepsilon > 20000$ L mol^{-1}cm^{-1}, causing a dramatically increased absorptivity compared to ordinary azobenzenes. The ionic nature of the structures allows for tuning of the solubility by proper choice of the counter-ion leaving the chromophore *untouched*, which has been used to study solvent effects on the same anion in nonpolar and polar solvents as well as in water and an ionic liquid. Going to more polar solvents, λ_{max} of the E isomer is shifted further to the red and the thermal back reaction is accelerated from 90 min to 2 s for one isomer. In acetonitrile, the thermal half-life can be tuned from 3 min to 13 hours depending on the aryl substituent. While investigation of the photochromic properties of azonium ions usually requires flash photolysis techniques, due to their short thermal half-life in the range of microseconds to milliseconds, one of the arylazoTCCp derivatives could easily be protonated and switching of the (overall charge-neutral) azonium species showed a surprisingly long thermal half-life of more than 2 min. With some of these new azobenzenes in hand, several sophisticated applications in the life and material sciences are in reach.

Further development of the arylazoTCCp switches will include the synthesis of derivatives with long thermal half-lives. A candidate for this purpose could be **115**, since the pyrazole unit without *ortho*-methyl groups **89** is known to provide an exceptional long thermal half-life of 1000 d, when the other substituent is a benzene ring (Figure 40).[238]

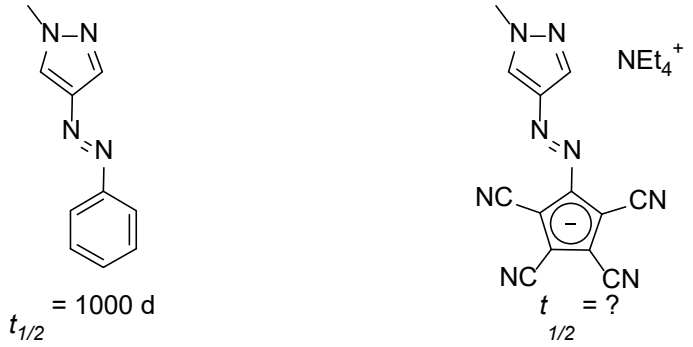

*Figure 40: Based on the phenylazopyrazol without ortho-methyl groups **89** a corresponding arylazoTCCp **115** could show an increased thermal half-life.*[238]

As azo based switches are usually applied to change the distance between two functional moieties, derivatives of the type of **116** could be developed. Transesterification or imide formation could then be used to substitute the cyclopentadienyl half of the switch (Scheme 68).

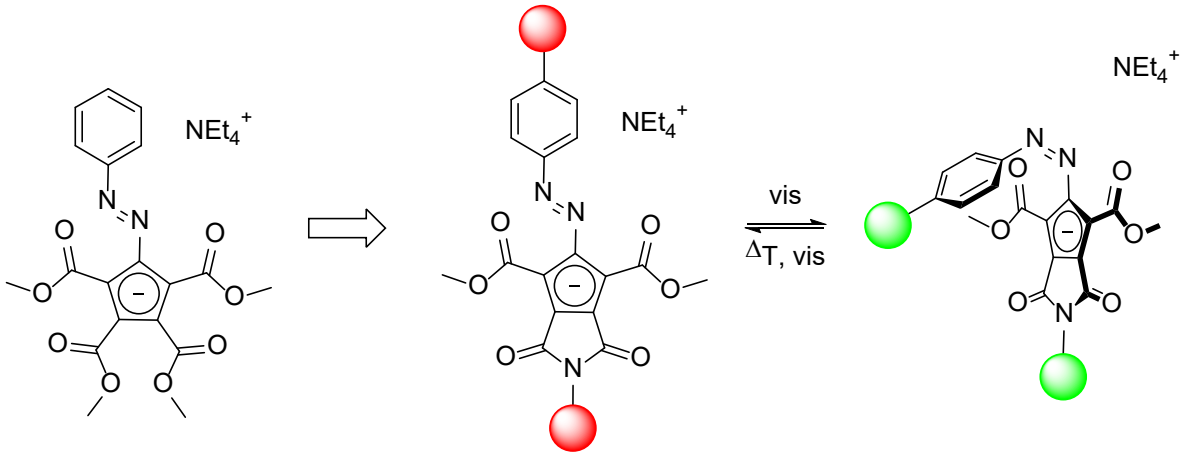

116

Scheme 68: Replacement of the cyano groups should allow for functionalization of the cyclopentadienide half, which opens the way for applications requiring a distance change of two moieties.

Application-wise, the zwitterionic structure **117** is easily synthesized on a larger scale and could be used to create photoswitchable micelles or membranes, as the dipole moment of the head group should change a lot and the tail can be easily varied since it is introduced in the last step of the synthesis. Other cationic aryl moieties are plausible as well, such as imidazolium **118** (Scheme 69), since protonated imidazole derived azoheteroarenes are known to be photochromic.[239]

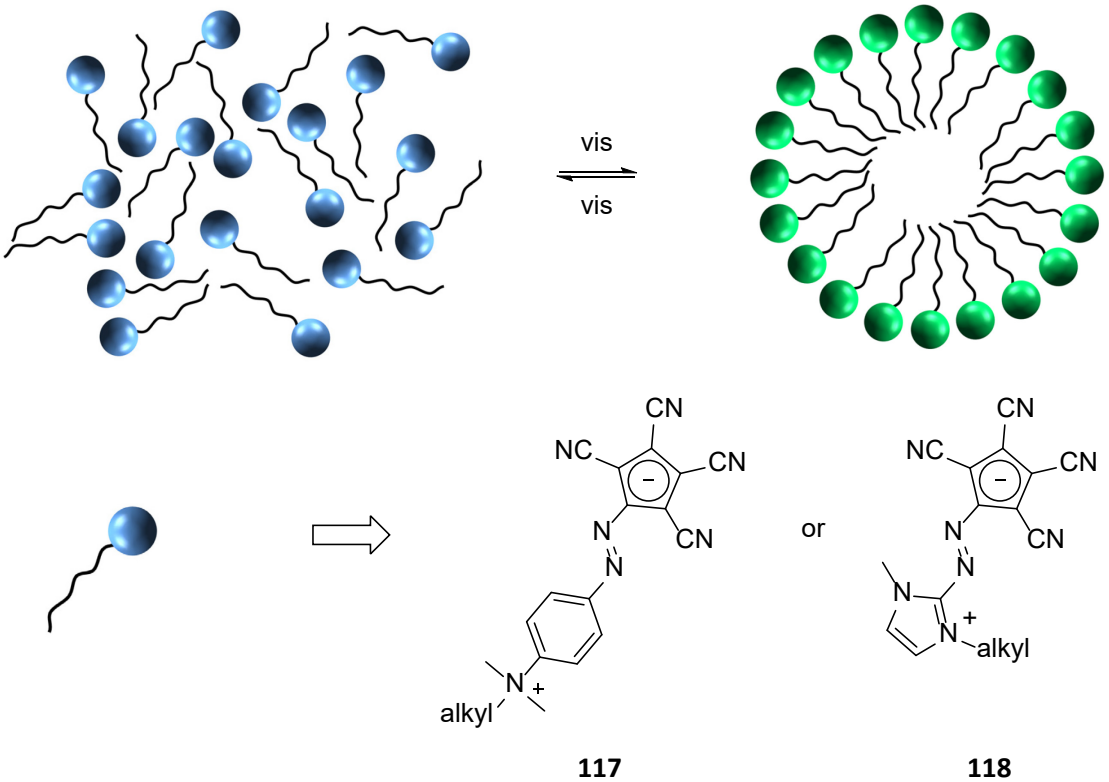

117 **118**

Scheme 69: Photoswitchable micelles based on zwitterionic arylazoTCCp amphiphiles.

The late alkylation forming a cationic aryl moiety also opens the possibility to anchor the dipole switch to surfaces or nanoparticles. This can be used to create photoswitchable devices, since the work

function of an inorganic semiconductor can be modulated *via* the dipole moment of a functional group attached to the surface.[285]

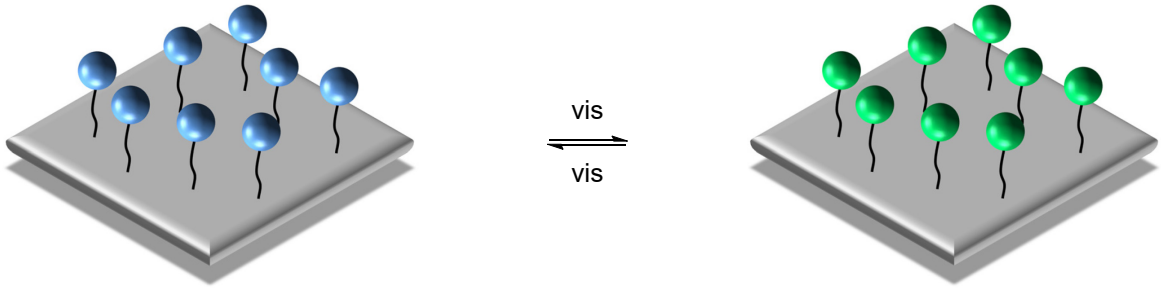

Scheme 70: Dipole switches on surfaces could be used to modulate the work function with light.

5 Experimental section

5.1 General Methods and Materials

Ethyl acetate, THF, dichloromethane, petroleum ether, methyl-*tert*-butyl ether, acetone, ethanol, and methanol were distilled before usage. All other starting materials were used as received. Dry solvents were taken from a Pure Solv Micro Solvent Purification System. NMR spectra were recorded on a Bruker DPX 300 Spectrometer (300 MHz for ^{1}H, 75 MHz for ^{13}C, and 282 MHz for ^{19}F) or Bruker DPX 500 Spectrometer (500 MHz for ^{1}H, 125 MHz for ^{13}C, and 471 MHz for ^{19}F) at 25 °C using residual protonated solvent signals as internal standard (^{1}H: δ($CHCl_3$) = 7.26 ppm; δ($CHDCl_2$) = 5.32 ppm; δ(DMSO-d_5) = 2.50 ppm; δ(CHD_2CN) = 1.94 ppm; ^{13}C: δ($CDCl_3$) = 77.16 ppm; δ(CD_2Cl_2) = 53.84 ppm; δ(DMSO-d_6) = 39.52 ppm; δ(CD_3CN) = 118.69 ppm) and $CFCl_3$ as external standard for ^{19}F-NMR spectra. For UPLC-MS a Waters UPLC Acquity with a Waters Alliance System (Waters Separations Module 2695, Waters Diode Array Detector 996 and Waters Mass Detector ZQ 2000) was used. Spectra and kinetic traces were recorded on a Cary60 equipped with a thermostated cell holder in a 10 mm x 10 mm 3 mL quartz cuvette with four clear sides. Irradiations were performed with a LOT-Oriel 500 W Hg(Xe) lamp connected to a LOT-Oriel MSH-300 monochromator and a LOT-Oriel time shutter. To enable simultaneous irradiation and recording of absorbance-time profiles the lamp setup was connected to the cell holder *via* an optical fiber in an orthogonal fashion. If not otherwise noted, experiments were performed with 3 mL of a 10^{-5} M solution of the switch at 25 °C in acetonitrile under efficient stirring. Preparative HPLC was performed on a Waters 600 equipped with a Waters 996 Photodiode Array Detector on a Phenomenex Luna 10 µm phenyl hexyl column (250 mm x 21 mm). For column chromatography silica gel (0.035-0.070 mm, 60 Å pore size) was used.

5.2 Spectroscopic Analysis of Dihydropyrenes

The spectrum of the photoproduct can be calculated from the initial spectrum and an irradiated spectrum by plotting $\frac{Abs_{irradiated}}{Abs_{initial}}$ versus λ, which gives a constant *b* in the red part of the visible region as illustrated in Figure 41. The spectrum of the open form can be calculated from:

$$Abs_{open} = \frac{Abs_{irradiated} - b \cdot Abs_{initial}}{1 - b}$$

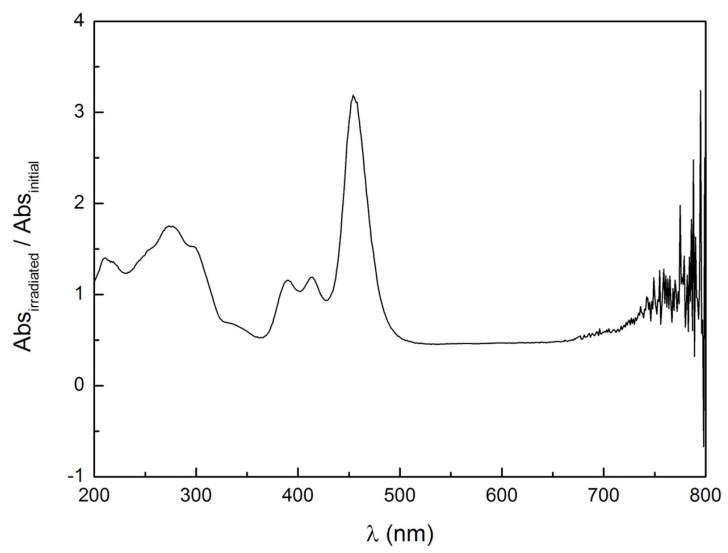

Figure 41: Plot of $\frac{Abs_{irradiated}}{Abs_{initial}}$ *versus λ for* ***74-Me₂²⁺.***

Note that this method is only applicable in cases where *b* is a constant over a certain range (which is the case for all dihydropyrenes in this work) and that the rate equation outlined in the following is only valid in this region. The assumption lying behind this is that there is no photoproduct formed whose absorption spectrum has the same shape in this region.

The photoreaction for ring opening with a thermal back reaction at a wavelength where only one isomer absorbs is described by the following rate equation:

$$\frac{d[DHP]}{dt} = -1000 \cdot I_0 \cdot \frac{1 - 10^{-Abs'}}{Abs'} \cdot \varepsilon_A \cdot d \cdot \Phi_{cl \rightarrow op} \cdot [DHP] + k_T \cdot ([DHP]_0 - [DHP])$$

with I_0 being the light intensity in mol $s^{-1}cm^{-3}$, *Abs'* being the absorbance at the irradiation wavelength, ε_A being the extinction coefficient at the irradiation wavelength in L $mol^{-1}cm^{-1}$, $\Phi_{cl->op}$ being the ring opening quantum yield, k_T being the rate constant for the thermal back reaction in s^{-1}, *d* being the optical path length in cm, and [DHP] being the concentration of the closed dihydropyrene switch in mol L^{-1} with $[DHP]_0$ being the initial dihydropyrene concentration.

Rate constants for the thermal back reactions were obtained separately by measuring spectra of an irradiated solution in defined time intervals and plotting ln(Abs_0−*Abs(t)*) vs time, with Abs_0 being the absorbance at the maximum in the visible region before irradiation and the slope being k_T. For **74** a protonated solution (methanesulfonic acid) was irradiated and deprotonated with triethylamine to obtain the rate constant. Irradiation experiments were carried out in a 10 mm x 10 mm fluorescence cuvette and a solution volume of 3 mL. Concentrations were chosen to be around 10^{-5} mol/L and ε_A was calculated according to the Beer-Lambert law from the absorbance before irradiation. The light intensity was determined using 1,2-bis(2,4-dimethyl-5-phenyl-3-thienyl)-3,3,4,4,5,5-hexafluoro-1-cyclopentene as an actinometer.[203] A solution of the actinometer in *n*-hexane was irradiated at 22 °C for approximately 5 min at 313 nm. The concentration of the closed form in solution was then determined from the absorbance at 562 nm and with that the extinction coefficient at the irradiation wavelength can be calculated. The ring opening reaction was performed at the wavelength, whose quantum yield was to be determined in time intervals of 30 s or 60 s. The absorbance at the irradiation wavelength was plotted to the following equation:

$$\log\left(10^{Abs'(t)} - 1\right) - \log\left(10^{Abs'(t=0)} - 1\right) = -1000 \cdot \varepsilon \cdot I_0 \cdot d \cdot \Phi_{cl\rightarrow op} \cdot t$$

Since the quantum yield for the ring opening is given for every wavelength, I_0 can be calculated from the slope.

By using a setup with the irradiation beam perpendicular to the probe beam of the spectrometer, the absorbance at the irradiation wavelength was recorded during irradiation.[286] The rate equation for the DHP opening was fitted to the obtained absorbance time profiles using an adapted Origin 8.5 fit-function based on the *Runge-Kutta* algorithm, taking into account that the absorbance is proportional to the DHP concentration. To exclude errors in the fit-function the method was first tested on 1,2-bis[2-methylbenzo[*b*]thiophen-3-yl]-3,3,4,4,5,5-hexafluoro-1-cyclopentene[203] whose quantum yield is described in the same reference as the applied actinometer using one of the two switches to determine the light intensity and then calculate the quantum yield of the other.

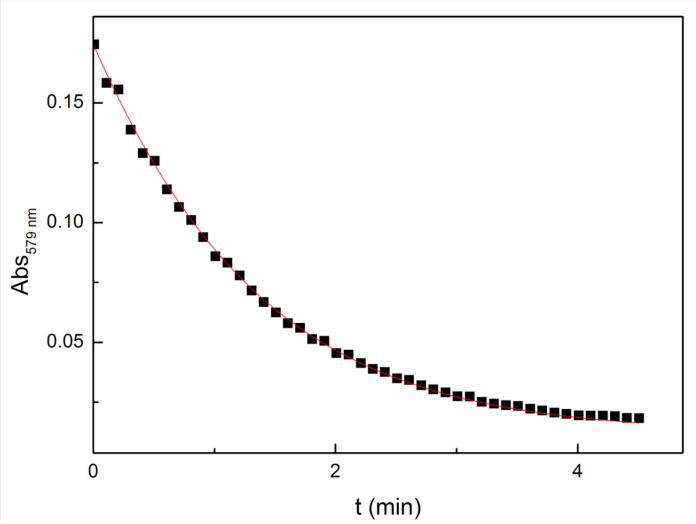

*Figure 42: Absorbance time profile of the irradiation of **73-Me**⁺ and fit of the corresponding rate equation.*

Alternatively, quantum yields can be calculated form the absorbance at the photo thermal equilibrium according to the following equation:

$$\Phi_{cl\rightarrow op} = \frac{k_T \cdot ([DHP]_0 - [DHP]_{PSS})}{1000 \cdot I_0 \cdot (1 - 10^{-Abs'})}$$

Both methods are in good agreement as long as in the PSS the difference in absorbance is > 0.03 and the residual absorbance is > 0.05. All quantum yields given in the manuscript where determined by fitting absorbance-time profiles.

To confirm the accuracy of this method, the complete procedure including sample preparation, irradiation experiment, and actinometry was performed six times with varying concentrations and light intensities on **73-Me**⁺. The results are given in Table 5 and it can be concluded that the relative error for the quantum yields given here is < 10%. No difference in the irradiation kinetics was found for degassed and non-degassed solutions of **73-Me**⁺.

*Table 5: Quantum yield of **73-Me**⁺ determined in 6 different runs.*

Run	1	2	3	4	5	6	Average
Φ	0.23401	0.22053	0.23528	0.2301	0.21826	0.23289	0.228512

Titration experiments were carried out in acetonitrile solutions of the corresponding switch (10^{-4} M) in a 0.3 mL cuvette with 1 mm path length by addition of methanesulfonic acid and subsequent volume correction. Lower concentrations of the switch gave inconsistent results due to auto protolysis effects of the solvent and residual water.

The proton catalysis experiments were carried out in a 3 mL cuvette with 1 cm path length with solutions containing the corresponding switch (10^{-5} M) and varying amounts of methanesulfonic acid. The degree of protonation was calculated from the absorbance at 546 nm or 585 nm. After irradiation to the PSS, excess NEt_3 was added to determine the amount of open form (after volume correction).

5.3 Spectroscopic Analysis of Arylazotetracyanocyclopentadienides

All spectra of the Z isomers were calculated according to a procedure developed by E. Fischer, where the spectrum of a photoproduct can be deduced from one spectrum containing only one isomer and two PSS spectra obtained from irradiation at two different wavelength.[44] The underlying assumptions are a) that the quantum yields for forward and backward reaction are independent of the irradiation wavelength, b) that no thermal back reaction is happening, and c) that no side reaction occurs. Therefore, the method is not applicable to switches, where a barrier in the excited state changes the quantum yield with the wavelength, *e.g.* for most diarylethenes. Furthermore, the irradiation should ideally occur in the same band, as concurrent deexcitation or reaction pathways from higher excited states could change the quantum yield. Since a thermal back reaction was observed at room temperature for all switches, the irradiation experiments where performed at lower temperatures, where the speed of the thermal back reaction was neglectable compared to the speed of the photoreaction.

To assure the quantum yield assumption, three instead of two different wavelengths where chosen for irradiation (365, 405, and 436 nm). Depending on which wavelength is set as wavelength 1 and 2 in the equations developed by Fischer, two spectra are obtained for each pair of PSS spectra, resulting in 6 over all spectra for the Z isomer. For few switches, the irradiation at 365 nm leads to a higher excited state, which produces side reactions or results in different quantum yields and is neglected in these cases. The method has intrinsic limitations, making some PSS spectra unsuitable for the determination of the Z isomer spectrum. This includes irradiation at a wavelength, where the absorbance is/becomes very low, which results in a bigger error in the absorbance measurement. A similar problem is observed for identical PSS spectra, where the ratio of the extinction coefficients at both irradiation wavelength is too similar.

The absorbance of the pure Z isomer at the irradiation wavelength can be calculated from:

$$Abs_{Z,\lambda 1} = Abs_{E,\lambda 1} + \frac{Abs_{PSS,\lambda 1} - Abs_{E,\lambda 1}}{a_{\lambda 1}}$$

The conversion α is calculated from the equation developed by Fischer:

$$\alpha_{\lambda 2} = \frac{\frac{Abs_{PSS,\lambda 1} - Abs_{E,\lambda 1}}{Abs_{E,\lambda 1}} - \frac{Abs_{PSS,\lambda 2} - Abs_{E,\lambda 2}}{Abs_{E,\lambda 2}}}{1 + \frac{Abs_{PSS,\lambda 1} - Abs_{E,\lambda 1}}{Abs_{E,\lambda 1}} - n \cdot \left(1 + \frac{Abs_{PSS,\lambda 2} - Abs_{E,\lambda 2}}{Abs_{E,\lambda 2}}\right)}$$

The ratio of both conversions is denoted by *n* and should be calculated from the absorbance change at a wavelength, where the absolute change in absorbance is biggest (to minimize errors):

$$n = \frac{Abs_{PSS,\lambda 1} - Abs_{E,\lambda 1}}{Abs_{PSS,\lambda 2} - Abs_{E,\lambda 2}}$$

With the extinction coefficients of both isomers the rate equation can be fitted in analogy to the dihydropyrene switches. The temperature was set low enough, so that the rate of the thermal back reaction was neglectable compared to the photoreaction. Since the extinction coefficient is temperature dependent and only known at low temperatures from the Fischer method, also the quantum yield measurement has to be performed at the low temperature. The underlying rate equation for the azos is then:

$$\frac{d[E]}{dt} = -1000 \cdot I_0 \cdot d \cdot \frac{1 - 10^{-Abs'}}{Abs'} \cdot (\varepsilon_E \cdot \Phi_{E \to Z} \cdot [E] - \varepsilon_Z \cdot \Phi_{Z \to E} \cdot [Z])$$

The rate equation was fitted as described for the dihydropyrenes and is depicted in Figure 43 for arylazoTCCp **100**.

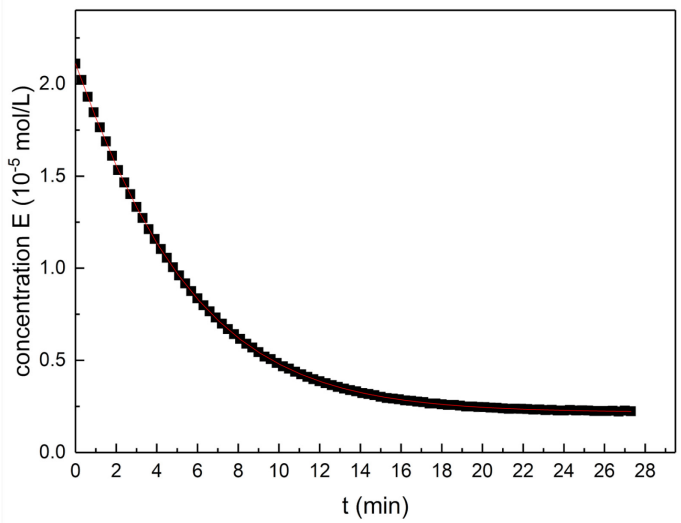

*Figure 43: Concentration time profile of the irradiation of **100** and fit of the corresponding rate equation.*

5.4 Synthesis

5.4.1 Dihydropyrenes

2,6-Biscyanotoluene (119)[202]

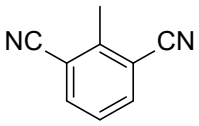

$K_4[Fe(CN)_6]*3H_2O$ (58.9 g, 139.5 mmol) was stirred at 80 °C under reduced pressure overnight. The flask was flushed with argon and $Pd(OAc)_2$ (487 mg, 2.17 mmol), di(1-adamantyl)-1-butylphosphine (2.33 g, 6.50 mmol), Na_2CO_3 (14.8 g, 139.5 mmol), 2,6-dichlorotoluene(50.0 g, 39.4 mL, 310 mmol), and dry NMP (500 mL) were added. The reaction mixture was stirred at 140 °C for 22 h and cooled to room temperature. Water (500 mL) was added and the mixture was extracted with ethyl acetate (3x 500 mL). The organic layer was washed with saturated NaCl solution (5x 500 mL) and evaporated under reduced pressure to a volume of about 500 mL. The residue was dried over anhydrous $MgSO_4$ and the solvent was evaporated under reduced pressure. The crude product was dissolved in 1 L of boiling ethanol and filtered hot. Crystallization in a fridge yielded 2,6-biscyanotoluene as brown crystals (33.2 g, 234 mmol, 75 %). The ^{1}H-NMR spectrum is in agreement with the literature,[287] whereas no ^{13}C-NMR spectrum was published.^{1}H-NMR (300 MHz, $CDCl_3$): δ [ppm]= 2.77 (s, 3H, C*H*$_3$), 7.43 (t, ^3J = 7.9 Hz, 1H, Ar-*H*), 7.82 (d, ^3J = 7.9 Hz, 2H, Ar-*H*). ^{13}C{^{1}H}-NMR (75 MHz, $CDCl_3$): δ [ppm]= 19.7, 115.0, 116.5, 127.4, 136.6, 145.9.

2-Methylisophthalic acid (120)[ix,288]

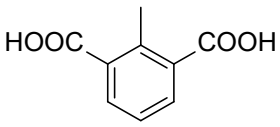

2-Methylisophthalic acid was prepared by an adapted protocol from the literature.[288] 2,6-Biscyanotoluene (27 g, 190 mmol) was suspended in aqueous KOH (44.9 g, 800 mmol in 100 mL) and stirred under reflux overnight. After cooling to room temperature, the mixture was filtered and acidified with concentrated aqueous HCl. The precipitate was filtered, taken up in ethanol and dried under reduced pressure to yield 2-Methylisophthalic acid as a white powder (32.6 g, 181 mmol, 95%).

2,6-Bis(hydroxymethyl)toluene (121)[ix,289]

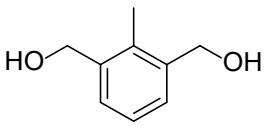

Under an argon atmosphere, $LiBH_4$ (15.7 g, 720 mmol) was suspended in dry THF (200 mL). The mixture was degassed by applying alternately vacuum and argon to the flask. The mixture was cooled to 0 °C and Me_3SiCl (183 mL, 1.44 mol) was added over 15 min with LiCl precipitating. 2-Methylisophthalic acid (32.4 g, 180 mmol) was dissolved in dry THF (250 mL) and added *via* a dropping funnel to the

[ix] Conditions for synthesis of **66** and **67** (Scheme 53) were developed by Jonas Becker.

mixture at 0 °C. The mixture was stirred at room temperature for 36 h until no more gas formation was observed. After cooling to 0 °C, the mixture was carefully quenched with methanol (500 mL) and the solvents were evaporated under reduced pressure. The residue was recrystallized from water and filtered. The mother liqueur was extracted with methyl-*tert*-butyl ether. The extract was dried over anhydrous $MgSO_4$ and the solvent was evaporated under reduced pressure. The combined fractions from crystallization and extraction gave the 2,6-Bis(hydroxymethyl)toluene (20.3 g, 133.5 mmol, 74%) as a grey solid of suitable purity for the next step.

9,18-Dimethyl-2,11-dithia[3.3]-*meta*-cyclophane (122)[171]

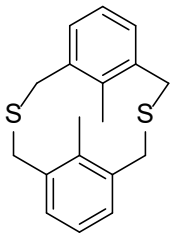

9,18-Dimethyl-2,11-dithia[3.3]-*meta*-cyclophane was prepared as mixed isomers from 2,6-biscyanotoluene according to the literature in 32% over 6 steps.[171]

***trans*-15,16-Dimethyldihydropyrene (49)**[49,174]

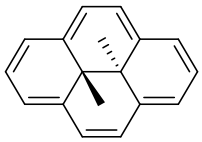

Under an argon atmosphere, mixed isomers of 9,18-dimethyl-2,11-dithia[3.3]-*meta*-cyclophane (5.60 g, 18.6 mmol) were dissolved in dry THF (100 mL) and cooled in an ice bath. *n*-BuLi (2.2 M in hexane, 21.1 mL, 46.5 mmol) was added dropwise over 15 min. After stirring of the black mixture for 5 min, MeI (13.2 g, 5.8 mL, 92.9 mmol) was added and stirring continued for 10 min. After addition of water, the mixture was extracted with dichloromethane and the combined organic layers were dried ($MgSO_4$). Evaporation of the solvents under reduced pressure and elution of the product from a silica gel column using dichloromethane yielded the product as a yellow solid (6.4 g) containing mixed Wittig isomers and a residue of dichloromethane directly used in the next step.

Trimethyl orthoformate (6.89 g, 7.1 mL, 64.9 mmol) was dissolved in dry dichloromethane (30 mL) and cooled to −30 °C, using an ethanol/ice bath that was cooled with liquid nitrogen to maintain the temperature. To this solution BF_3*Et_2O (9.34 g, 8.1 mL, 65.5 mmol) was added while stirring. After stirring for 45 min at 0 °C the mixture was cooled to −30 °C and the oil was washed with dichloromethane (2x 20 mL). The previously described mixture of Wittig isomers was suspended in dry dichloromethane (30 mL) and added to the oily Borch Reagent at −30 °C. After stirring at room temperature for 4 h, ethyl acetate (90 mL) was added and stirring continued for 2 h. Filtration of the precipitate afforded a white solid containing mixed methylated isomer salts (8.22 g) directly used in the next step.

The mixed methylated isomers (8.14 g) were added to a solution of KO*t*Bu (5.00 g, 44.6 mmol) in dry THF (200 mL) and heated to 80 °C for 4 h. After cooling to room temperature, water was added and

the mixture was extracted with dichloromethane. The combined organic layers were dried over anhydrous $MgSO_4$ and the solvents were evaporated under reduced pressure. Silica gel column chromatography of the crude product using petroleum ether yielded *trans*-15,16-dimethyldihydropyrene as a green crystalline solid (2.00 g, 8.6 mmol, 46 % over 3 steps). The ^{1}H-NMR and ^{13}C-NMR spectrum are in agreement with the literature.[171]

2-Bromo-*trans*-15,16-dimethyldihydropyrene (123)[290]

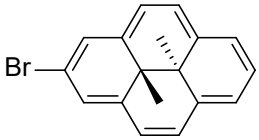

2-Bromo-*trans*-15,16-dimethyldihydropyrene was prepared from *trans*-15,16-dimethyldihydropyrene according to the literature in 89%.[290]

2,7-Dibromo-*trans*-15,16-dimethyldihydropyrene (124)[188]

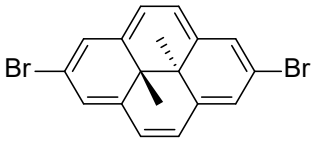

2,7-Dibromo-*trans*-15,16-dimethyldihydropyrene was prepared from *trans*-15,16-dimethyldihydropyrene according to the literature in 68%.[188]

2,7-Bis-(4-pyridyl)-*trans*-15,16-dimethyldihydropyrene (74)[189]

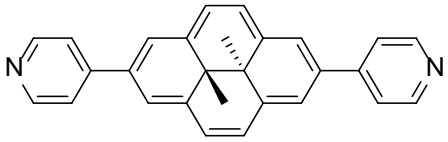

2,7-Dibromo-*trans*-15,16-dimethyldihydropyrene (400 mg, 1.03 mmol), 4-pyridineboronic acid (500 mg, 4.1 mmol), and Cs_2CO_3 (2.67 g, 8.2 mmol) were suspended in 90 mL of a mixture of THF/EtOH/DMF (4/4/1). The solution was degassed by applying 10 times alternately vacuum and argon to the flask. Pd(dppf)Cl_2*DCM (42 mg, 0.051 mmol) was added and the mixture was heated to 50 °C and stirred for 6 d. After cooling to room temperature, ethyl acetate was added and the mixture was washed with water. The organic layer was dried over anhydrous $MgSO_4$ and evaporated under reduced pressure. The product was obtained after silica gel column chromatography using ethyl acetate as eluent as a red crystalline solid (363 mg, 0.94 mmol, 92%). ^{1}H-NMR (500 MHz, CD_2Cl_2): δ [ppm]= −3.77 (s, 6H, C*H*$_3$), 8.04 (m, 4H, Py-*H*), 8.76 (s, 4H, DHP-*H*), 8.78 (m, 4H, Py-*H*), 8.96 (s, 4H, DHP-*H*). ^{13}C{^{1}H}-NMR (125 MHz, CD_2Cl_2): δ [ppm]= 15.4, 31.0, 122.8, 123.0, 126.4, 132.6, 138.7, 149.4, 151.0. ESI-MS $[M+H]^+$ *m/z* calculated for $C_{28}H_{29}N_2^+$: 387.186 found: 387.185.

2-(*N*-Methylpyridin-4-yl)-*trans*-15,16-dimethyldihydropyrene hexafluorophosphate (73-Me$^+$)

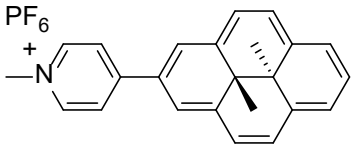

2-(4-Pyridyl)-*trans*-15,16-dimethyldihydropyrene (80 mg, 0.26 mmol) was dissolved in dichloromethane (70 mL) and iodomethan (1.6 mL, 26 mmol) was added. After stirring the solution at room temperature for 65 h, all liquids were evaporated under reduced pressure. The residue was dissolved in MeOH (30 mL) and NH_4PF_6 (1.27 g, 7.8 mmol) in water (25 mL) was added. After stirring for 30 min at room temperature, the mixture was filtered, washed with water, and dried in vacuo to yield the product as a deep blue crystalline solid (117 mg, 0.25 mmol, 96%). ^{1}H-NMR (500 MHz, DMSO-d_6): δ [ppm]= −3.99 (s, 3H, C*H*$_3$), −3.97 (s, 3H, C*H*$_3$), 4.36 (s, 3H, N-C*H*$_3$), 8.30 (t, ^3J = 7.7 Hz, 1H, DHP-*H*-*7*), 8.72 (d, ^3J = 7.7 Hz, 2H, Ar-*H*), 8.77 (d, ^3J = 7.8 Hz, 2H, Ar-*H*), 8.95 (d, ^3J = 7.7 Hz, 2H, Ar-*H*), 8.98 (d, ^3J = 7.1 Hz, 2H, Ar-*H*), 9.04 (d, ^3J = 7.1 Hz, 2H, Ar-*H*), 9.49 (s, 2H, Ar-*H*). ^{13}C{^{1}H}-NMR (125 MHz, DMSO-d_6): δ [ppm]= 14.3, 15.2, 29.1, 30.4, 46.7, 122.6, 124.0, 124.5, 124.6, 125.1, 127.0, 127.9, 135.7, 140.2, 145.1, 154.8. ^{19}F-NMR (470 MHz, DMSO-d_6): δ [ppm]= −70.69, −69.18. ESI-MS [M]$^+$ *m/z* calculated for $C_{24}H_{22}N^+$: 324.175 found: 324.175.

2,7-Bis-(*N*-Methylpyridin-4-yl)-*trans*-15,16-dimethyldihydropyrene hexafluorophosphate (74-Me$_2^{2+}$)

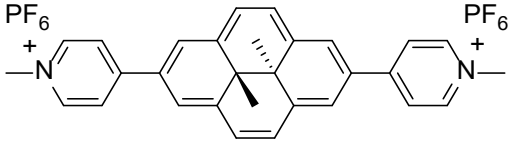

2,7-Bis-(4-pyridyl)-*trans*-15,16-dimethyldihydropyrene (100 mg, 0.26 mmol) was dissolved in dichloromethane (70 mL) and iodomethane (3.2 mL, 52 mmol) was added rapidly. The reaction mixture was heated to reflux for 3 h and then stirred at room temperature for 15 h. The product was filtered, washed with cold dichloromethane, and dried in vacuo to yield the crude iodine salt (170 mg, 0.255 mmol, 98%), which was used without further purification.

The iodine salt (101 mg, 0.15 mmol) was dissolved in MeOH (50 mL) and NH_4PF_6 (980 mg, 6 mmol) in water (10 mL) was added. More water (100 mL) was added, causing the precipitation of the product. The product was filtered and washed with water and small amounts of MeOH. After drying in vacuo, the product was obtained as a deep blue crystalline solid (56 mg, 0.08 mmol, 53%). ^{1}H-NMR (500 MHz, DMSO-d_6): δ [ppm]= −3.63 (s, 6H, C*H*$_3$), 4.39 (s, 6H, N-C*H*$_3$), 8.96 (s, 4H, DHP-*H*), 9.01 (d, ^3J = 7.1 Hz, 4H, Py-*H*), 9.12 (d, ^3J = 7.1 Hz, 4H, Py-*H*), 9.49 (s, 4H, DHP-*H*). ^{13}C{^{1}H}-NMR (125 MHz, DMSO-d_6): δ [ppm]= 15.6, 30.2, 47.0, 109.5, 124.5, 128.4, 128.5, 139.1, 145.4, 154.3. ^{19}F-NMR (282 MHz, DMSO-d_6): δ [ppm]= −71.09, −68.57. ESI-MS [M]$^{2+}$ *m/z* calculated for $C_{30}H_{28}N_2^+$: 208.112 found: 208.112.

2-(*N*-Methylpyridin-4-yl)- 7-(4-pyridyl)-*trans*-15,16-dimethyldihydropyrene hexafluorophosphate (74-Me$^+$)

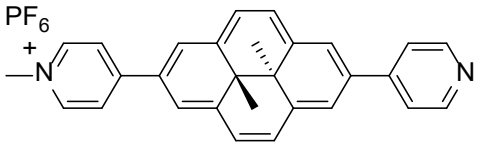

2,7-Bis-(4-pyridyl)-*trans*-15,16-dimethyldihydropyrene (100 mg, 0.26 mmol) was dissolved in dichloromethane (50 mL) and iodomethane (37 mg, 0.26 mmol) was added. The reaction mixture was stirred at room temperature for 72 h and filtered. The residue was dissolved in 10 mL of water and NH_4PF_6 (850 mg, 5.2 mmol) in water (10 mL) was added. The precipitate was filtered off and purified by preparative HPLC using acetonitrile/water (25/75) with 1vol% formic acid on a phenyl hexyl column. The product was obtained as a deep blue crystalline solid (45 mg, 0.08 mmol 32%). ^{1}H-NMR (300 MHz, DMSO-d_6): δ [ppm]= −3.73 (s, 3H, C*H*$_3$), −3.73 (s, 3H, C*H*$_3$)4.37 (s, 3H, N-C*H*$_3$), 8.28 (m, 2H, Ar-*H*), 8.82 (m, 2H, Ar-*H*), 8.88 (m, 2H, Ar-*H*), 8.97 (m, 4H, Ar-*H*), 9.06 (m, 2H, Ar-*H*), 9.25 (s, 2H, Ar-*H*), 9.46 (s, 2H, Ar-*H*). ^{13}C{^{1}H}-NMR (75 MHz, DMSO-d_6): δ [ppm]= 14.9, 15.6, 29.7, 30.3, 46.8, 109.6, 122.2, 122.7, 123.2, 124.1, 126.3, 126.4, 128.3, 133.5, 137.0, 140.1, 145.3, 147.2, 150.6, 154.6. ^{19}F-NMR (282 MHz, DMSO-d_6): δ [ppm]= −71.08, −68.56. ESI-MS [M]$^+$ *m/z* calculated for $C_{29}H_{25}N_2^+$: 401.201 found: 401.204.

2,7-Di(3,5-bis(trifluoromethyl)benzene)- *trans*-15,16-dimethyldihydropyrene (77)

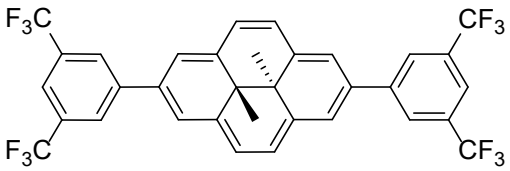

2,7-Dibromo-DHP (400 mg, 1 mmol), 3,5-bis(trifluoromethyl)phenylboronic acid (1.59 g, 6.1 mmol), and Cs_2CO_3 (4 g, 12.3 mmol) were suspended in a mixture of THF/EtOH/DMF (4/4/1, 90 mL). After alternately applying vacuum and argon to the flask for several times, Pd(dppf)Cl_2·DCM (42 mg, 0.05 mmol) was added and the reaction was stirred for 2.5 h. Ethyl acetate was added and the mixture was washed with water successively. The organic phase was dried over anhydrous $MgSO_4$ and evaporated under reduced pressure. Silica gel column chromatography (petroleum ether) yielded the product as a red solid (550 mg, 0.84 mmol, 84%). ^{1}H-NMR (500 MHz, $CDCl_3$): δ [ppm]= −3.78 (s, 6H, C*H*$_3$), 7.96-7.94 (m, 2H, Ar-*H*), 8.53 (s, 4H, Ar-*H*), 8.77 (s, 4H, Ar-*H*), 8.88 (s, 4H, Ar-*H*). ^{13}C{^{1}H}-NMR (126 MHz, $CDCl_3$) δ [ppm]= 15.2, 30.5, 120.8 (quin, ^3J= 4 Hz), 122.8, 123.7 (q, ^1J= 273 Hz), 126.1, 128.3 (d, ^3J= 3 Hz), 132.3, 132.6 (q, ^2J= 32 Hz), 138.2, 144.3. ^{19}F-NMR (471 MHz, $CDCl_3$): δ [ppm]= −62.84. ESI-MS [M]$^+$ *m/z* calculated for $C_{34}H_{21}F_{12}^+$: 656.1373 found: 656.1415.

2,7-Bis(4-cyanobenzene)-*trans*-15,16-dimethyldihydropyrene (76)

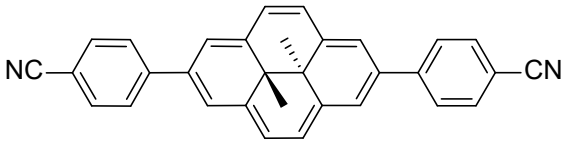

2,7-Dibromo-DHP (380 mg, 0.97 mmol), 4-cyanophenylboronic acid (855 mg, 5.82 mmol), and Cs_2CO_3 (3.8 g, 11.6 mmol) were suspended in a mixture of THF/EtOH/DMF (4/4/1, 90 mL). After alternately applying vacuum and argon to the flask for several times, Pd(dppf)Cl_2·DCM (40 mg, 0.05 mmol) was added and the reaction was stirred for 20 h. Dichloromethane was added and the mixture was washed with water successively. The organic phase was dried over anhydrous $MgSO_4$ and evaporated under reduced pressure. Silica gel column chromatography (dichloromethane/petroleum ether 5/5 to 9/1) yielded the product as a red solid (380 mg, 0.87 mmol, 90%). ^{1}H-NMR (500 MHz, $CDCl_3$): δ [ppm]= −3.76 (s, 6H, C*H*$_3$), 7.89 (d, ^3J = 8.5 Hz, 4H, Ph-*H*), 8.22 (d, ^3J = 8.5 Hz, 4H, Ph-*H*), 8.71 (s, 4H, DHP-*H*), 8.86 (s, 4H, DHP-*H*). ^{13}C{^{1}H}-NMR (126 MHz, $CDCl_3$): δ [ppm]= 15.3, 30.6, 110.9, 119.3, 122.9, 125.9, 128.8, 133.0, 133.1, 138.2, 146.4. ESI-MS $[M]^+$ *m/z* calculated for $C_{32}H_{22}N_2^+$: 434.1783 found: 434.1769.

2,7-Bisphenyl-*trans*-15,16-dimethyldihydropyrene (75)

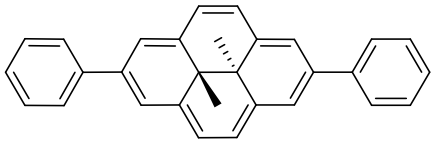

2,7-Dibromo-DHP (300 mg, 0.77 mmol), 4-cyanophenylboronic acid (563 mg, 4.62 mmol), and Cs_2CO_3 (3 g, 9.24 mmol) were suspended in a mixture of THF/EtOH/DMF (4/4/1, 90 mL). After alternately applying vacuum and argon to the flask for several times, Pd(dppf)Cl_2 DCM (31 mg, 0.04 mmol) was added and the reaction was stirred for 20 h. Ethyl acetate was added and the mixture was washed with water successively. The organic phase was dried over anhydrous $MgSO_4$ and evaporated under reduced pressure. Silica gel column chromatography (dichloromethane/petroleum ether 1/9) yielded the product as a red solid (250 mg, 0.72 mmol, 93%). ^{1}H-NMR (300 MHz, CD_2Cl_2): δ [ppm]= -3.80 (s, 6H, C*H*$_3$), 7.45 (t, ^3J = 7.4 Hz, 2H, Ph-*H*), 7.62 (dd, ^3J = 7.7 Hz, ^3J = 7.7 Hz, 4H, Ph-*H*), 8.15 (d, ^3J = 7.1 Hz, 4H, Ph-*H*), 8.69 (s, 4H, DHP-*H*), 8.90 (s, 4H, DHP-*H*). ^{13}C{^{1}H}-NMR (126 MHz, CD_2Cl_2): δ [ppm]= 15.2, 30.8, 123.0, 125.2, 127.9, 128.7, 129.7, 135.1, 138.2, 142.6. ESI-MS $[M]^+$ *m/z* calculated for $C_{30}H_{24}^+$: 384.1878 found: 384.1885.

2-(4-Cyanobenzene)-7-(4-methoxybenzene)-*trans*-15,16-dimethyldihydropyrene (78)

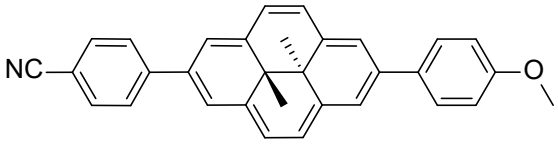

2-Bromo-7-(4-methoxybenzene)-DHP (169 mg, 0.41 mmol), 4-cyanophenylboronic acid (239 mg, 1.62 mmol), and Cs_2CO_3 (1.15 g, 3.25 mmol) were suspended in a mixture of THF/EtOH/DMF (4/4/1, 45 mL). After alternately applying vacuum and argon to the flask for several times, Pd(dppf)Cl_2·DCM (17 mg, 0.02 mmol) was added and the reaction was stirred for 20 h. Dichloromethane was added and the mixture was washed with water successively. The organic phase was dried over anhydrous $MgSO_4$

and evaporated under reduced pressure. Silica gel column chromatography (ethyl acetate/petroleum ether 10/90 to 25/75) yielded the product as a red solid (154 mg, 0.35 mmol, 86%). ^{1}H-NMR (500 MHz, $CDCl_3$): δ [ppm]= −3.77 (s, 3H, C*H*$_3$), −3.77 (s, 3H, C*H*$_3$), 3.95 (s, 3H, O-C*H*$_3$), 7.16 (d, ^{3}J = 8.8 Hz, 2H, Ar-*H*), 7.87 (d, ^{3}J = 8.5 Hz, 2H, Ar-*H*), 8.08 (d, ^{3}J = 8.8 Hz, 2H, Ar-*H*), 8.21 (d, ^{3}J = 8.4 Hz, 2H, Ar-*H*), 8.63 (d, ^{3}J = 7.8 Hz, 2H, Ar-*H*), 8.68 (d, ^{3}J = 7.7 Hz, 2H, Ar-*H*), 8.83 (s, 2H, DHP-*H*), 8.85 (s, 2H, DHP-*H*). ^{13}C{^{1}H}-NMR (126 MHz, $CDCl_3$): δ [ppm]=14.9, 15.4, 30.4, 30.5, 55.6, 110.4, 114.9, 119.5, 122.5, 122.6, 124.5, 125.8, 128.6, 129.5, 131.6, 132.9, 134.4, 135.7, 136.9, 138.9, 146.8, 159.7. ESI-MS $[M]^+$ *m/z* calculated for $C_{32}H_{25}NO^+$: 439.1936 found: 439.1964.

2-(4-Methoxybenzene)-7-(4-pyridine)-*trans*-15,16-dimethyldihydropyrene (80)

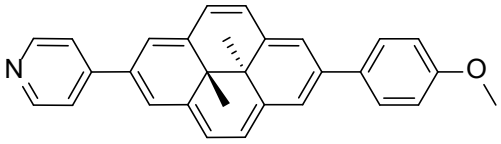

2-Bromo-7-(4-pyridine)-DHP (58 mg, 0.15 mmol), 4-methoxyphenylboronic acid (68 mg, 0.45 mmol), and Cs_2CO_3 (244 mg, 0.75 mmol) were suspended in a mixture of THF/EtOH/DMF (4/4/1, 45 mL). After alternately applying vacuum and argon to the flask for several times, Pd(dppf)Cl_2·DCM (6 mg, 0.008 mmol) was added and the reaction was stirred for 18 h. Ethyl acetate was added and the mixture was washed with water successively. The organic phase was dried over anhydrous $MgSO_4$ and evaporated under reduced pressure. Silica gel column chromatography (dichloromethane/methanol/trimethylamine 98.5/1/0.5) yielded the product as a red solid (55 mg, 0.13 mmol, 88%). ^{1}H-NMR (300 MHz, CD_2Cl_2): δ [ppm]= −3.79 (s, 3H, C*H*$_3$), −3.78 (s, 3H, C*H*$_3$), 3.94 (s, 3H, O-C*H*$_3$), 7.17 (d, ^{3}J = 8.9 Hz, 2H, Ar-*H*), 8.06 – 8.00 (m, 2H, Ar-*H*), 8.10 (d, ^{3}J = 8.8 Hz, 2H, Ar-*H*), 8.66 (d, ^{3}J = 7.8 Hz, 2H, Ar-*H*), 8.73 (d, ^{3}J = 7.8 Hz, 2H, Ar-*H*), 8.77 (d, ^{3}J = 5.5 Hz, 2H, Ar-*H*), 8.88 (s, 2H, DHP-*H*), 8.92 (s, 2H, DHP-*H*) . ^{13}C{^{1}H}-NMR (126 MHz, CD_2Cl_2): δ [ppm]=15.0, 15.7, 30.9, 30.9, 56.0, 115.2, 122.6, 122.7, 122.8, 124.8, 126.4, 129.8, 130.8, 134.6, 136.1, 137.2, 139.5, 149.8, 150.7, 160.3. ESI-MS $[M+H]^+$ *m/z* calculated for $C_{30}H_{26}NO^+$: 416.2009 found: 416.2030.

2-(4-Cyanobenzene)-7-(4-*N,N*-dimethylaminobenzene)-*trans*-15,16-dimethyldihydropyrene (79)

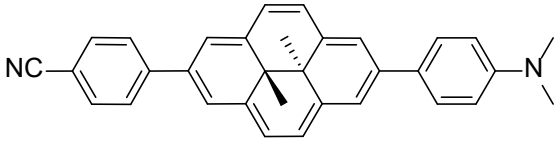

2-Bromo-7-(4-cyanobenzene)-DHP (82 mg, 0.2 mmol), 4-*N,N*-dimethylaminophenylboronic acid (100 mg, 0.6 mmol), and Cs_2CO_3 (391 mg, 1.2 mmol) were suspended in a mixture of THF/EtOH/DMF (4/4/1, 45 mL). After alternately applying vacuum and argon to the flask for several times, Pd(dppf)Cl_2·DCM (8 mg, 0.01 mmol) was added and the reaction was stirred for 2 h. Ethyl acetate was added and the mixture was washed with water successively. The organic phase was dried over anhydrous $MgSO_4$ and evaporated under reduced pressure. Silica gel column chromatography (dichloromethane/petroleum ether 45/55) yielded the product as a purple solid (60 mg, 0.13 mmol, 66%). ^{1}H-NMR (300 MHz, CD_2Cl_2): δ [ppm]= −3.74 (s, 3H, C*H*$_3$), −3.73 (s, 3H, C*H*$_3$), 3.09 (s, 6H, N-C*H*$_3$), 6.97 (d, ^{3}J = 9.0 Hz, 2H, Ar-*H*), 7.87 (d, ^{3}J = 8.5 Hz, 2H, Ar-*H*), 8.08 (d, ^{3}J = 8.9 Hz, 2H, Ar-*H*), 8.24 (d, ^{3}J = 8.5 Hz, 2H, Ar-*H*), 8.60 (d, ^{3}J = 8.0 Hz, 2H, Ar-*H*), 8.68 (d, ^{3}J = 7.7 Hz, 2H, Ar-*H*), 8.85 (s, 2H, DHP-*H*), 8.88 (s, 2H, DHP-*H*). ^{13}C{^{1}H}-NMR (126 MHz, CD_2Cl_2): δ [ppm]= 15.8, 15.8, 30.3, 30.9, 40.8, 107.6, 110.6,

113.5, 122.1, 122.8, 124.3, 126.2, 128.8, 129.2, 133.3, 136.6, 136.8, 139.6, 150.9. ESI-MS $[M+H]^+$ *m/z* calculated for $C_{33}H_{29}N_2^+$: 453.2325 found: 453.2326.

2-(4-Cyanobenzene)-*trans*-15,16-dimethyldihydropyrene (125)

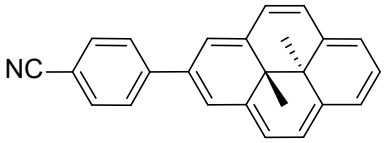

2-Bromo-DHP (150 mg, 0.48 mmol), 4-cyanophenylboronic acid (212 mg, 1.44 mmol), and Cs_2CO_3 (940 mg, 2.88 mmol) were suspended in a mixture of THF/EtOH/DMF (4/4/1, 90 mL). After alternately applying vacuum and argon to the flask for several times, $Pd(dppf)Cl_2$·DCM (20 mg, 0.024 mmol) was added and the reaction was stirred for 24 h. Ethyl acetate was added and the mixture was washed with water successively. The organic phase was dried over anhydrous $MgSO_4$ and evaporated under reduced pressure. Silica gel column chromatography (dichloromethane/petroleum ether 4/6) yielded the product as a yellow solid (70 mg, 0.21 mmol, 44%). ^{1}H-NMR (300 MHz, CD_2Cl_2): δ [ppm]= −4.01 (s, 3H, C*H*$_3$), −3.99 (s, 3H, C*H*$_3$), 7.88 (d, ^3J = 8.4 Hz, 2H, Ar-*H*), 8.12 (t, ^3J = 7.7 Hz, 1H, DHP-*H*), 8.22 (d, ^3J = 8.5 Hz, 2H, Ar-*H*), 8.59 (d, ^3J = 7.7 Hz, 2H, Ar-*H*), 8.64 (d, ^3J = 7.8 Hz, 2H, Ar-*H*), 8.72 (d, ^3J = 7.7 Hz, 2H, Ar-*H*), 8.89 (s, 2H, DHP-*H*). ^{13}C{^{1}H}-NMR (126 MHz, CD_2Cl_2): δ [ppm]= 14.7, 14.7, 30.0, 30.7, 110.5, 122.2, 124.3, 124.4, 124.4, 125.2, 128.8, 131.9, 132.9, 137.0, 138.2, 146.8. ESI-MS $[M]^+$ *m/z* calculated for $C_{25}H_{19}N^+$: 333.1517 found: 333.1502.

2-Bromo-7-(4-cyanobenzene)-*trans*-15,16-dimethyldihydropyrene (126)

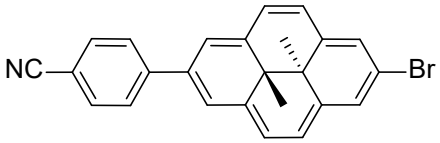

2-(4-Cyanobenzene)-DHP (67 mg, 0.2 mmol) was dissolved in dry DMF (30 mL). After adding *N*-bromosuccinimide (36 mg, 0.2 mmol) the reaction mixture was stirred for 24 h. Ethyl acetate was added and the mixture was washed with water successively. The organic phase was dried over anhydrous $MgSO_4$ and evaporated under reduced pressure. Silica gel column chromatography (dichloromethane/petroleum ether 3/7 to 4/6) yielded the product as a yellow solid, with minor contaminations of starting material (81 mg, 0.2 mmol, 98%). ^{1}H-NMR (500 MHz, $CDCl_3$): δ [ppm]= −3.89 (s, 3H, C*H*$_3$), −3.88 (s, 3H, C*H*$_3$), 7.88 (d, ^3J = 8.5 Hz, 2H, Ar-*H*), 8.21 (d, ^3J = 8.4 Hz, 2H, Ar-*H*), 8.56 (d, ^3J = 7.7 Hz, 2H, Ar-*H*), 8.69 (d, ^3J = 7.8 Hz, 2H, Ar-*H*), 8.70 (s, 2H, DHP-*H*), 8.87 (s, 2H, DHP-*H*). ^{13}C{^{1}H}-NMR (126 MHz, $CDCl_3$): δ [ppm]= 14.7, 14.9, 29.7, 30.2, 110.8, 119.3, 119.5, 123.3, 123.7, 126.3, 126.5, 128.7, 132.5, 133.0, 137.1, 137.9, 146.5. ESI-MS $[M]^+$ *m/z* calculated for $C_{25}H_{18}N^{81}Br^+$: 413.0602 found: 413.0612.

2-(4-Pyridine)-*trans*-15,16-dimethyldihydropyrene (73)

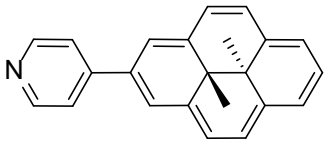

2-Bromo-DHP (218 mg, 0.7 mmol), 4-pyridineboronic acid (258 mg, 2.1 mmol), and Cs_2CO_3 (800 mg, 2.45 mmol) were suspended in a mixture of THF/EtOH/DMF (4/4/1, 90 mL). After alternately applying vacuum and argon to the flask for several times, Pd(dppf)Cl_2·DCM (29 mg, 0.035 mmol) was added and the reaction was stirred for 17 h at 50 °C. After cooling to room temperature, ethyl acetate was added and the mixture was washed with water successively. The organic phase was dried over anhydrous $MgSO_4$ and evaporated under reduced pressure. Silica gel column chromatography (ethyl acetate) yielded the product as a yellow solid (160 mg, 0.52 mmol, 74%). ^{1}H-NMR (300 MHz, CD_2Cl_2): δ [ppm]= −4.03 (s, 3H, C*H*$_3$), −4.01 (s, 3H, C*H*$_3$), 8.08-8.02 (m, 2H, Ar-*H*), 8.14 (t, ^3J = 7.7 Hz, 1H, DHP-*H*), 8.61 (d, ^3J = 7.7 Hz, 2H, Ar-*H*), 8.66 (d, ^3J = 7.8 Hz, 2H, Ar-*H*), 8.82 – 8.73 (m, 4H, Ar-*H*), 8.98 (s, 2H, DHP-*H*). ^{13}C{^{1}H}-NMR (126 MHz, CD_2Cl_2): δ [ppm]= 14.8, 15.0, 30.4, 31.1, 122.3, 122.8, 124.6, 124.7, 124.8, 125.8, 131.4, 137.4, 138.7, 149.6, 151.0. ESI-MS $[M+H]^+$ *m/z* calculated for $C_{23}H_{20}N^+$: 310.1590 found: 310.1605.

2-Bromo-7-(4-pyridine)-*trans*-15,16-dimethyldihydropyrene (127)

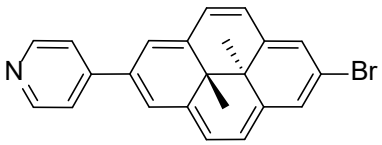

2-(4-Pyridine)-DHP (164 mg, 0.53 mmol) was dissolved in dry DMF (30 mL). After adding *N*-bromosuccinimide (94 mg, 0.53 mmol), the reaction mixture was stirred for 17 h. Ethyl acetate was added and the mixture was washed with water successively. The organic phase was dried over anhydrous $MgSO_4$ and evaporated under reduced pressure. Silica gel column chromatography (ethyl acetate) yielded a yellow fraction (62 mg, 0.16 mmol, 30%), which contained mostly the product and was used without further purification in the next step. ESI-MS $[M+H]^+$ *m/z* calculated for $C_{23}H_{19}N^{81}Br^+$: 390.0695 found: 390.0650.

2-Bromo-7-(4-methoxybenzene)-*trans*-15,16-dimethyldihydropyrene (128)

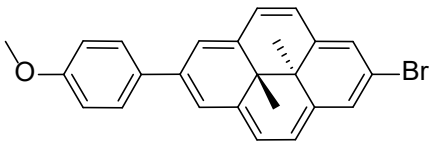

2,7-Dibromo-DHP (387 mg, 1 mmol), 4-methoxyphenylboronic acid (152 mg, 1 mmol), and Cs_2CO_3 (650 mg, 2 mmol) were suspended in a mixture of THF/EtOH/DMF (4/4/1, 180 mL). After alternately applying vacuum and argon to the flask for several times, Pd(dppf)Cl_2·DCM (25 mg, 0.03 mmol) was added and the reaction was stirred for 54 h. Dichloromethane was added and the mixture was washed with water successively. The organic phase was dried over anhydrous $MgSO_4$ and evaporated under reduced pressure. Silica gel column chromatography (dichloromethane/petroleum ether 1/9 to 3/7)

yielded a yellow solid (140 mg, containing debrominated species as well), which was used without further purification.

5.4.2 Arylazotetracyanocyclopentadienides

Unless otherwise noted, the counter-ion is tetraethylammonium.

General Procedure A for Coupling to Electron-rich Aryl Compounds.

The diazonium salt **96**[244] (192 mg, 1 mmol) was suspended in acetonitrile (5 mL) and the coupling partner (1 mmol) was added. After stirring overnight, methyl-*tert*-butyl ether was added to precipitate the protonated azo compound. The filtrate was washed with methyl-*tert*-butyl ether and dissolved in aqueous potassium hydroxide solution (200 mg, 2 mmol in 10 mL). After stirring for 10 min, the solution was filtered again and tetraethylammonium chloride in water (830 mg, 5 mmol in 5 mL) was added. After standing overnight, the resulting precipitate was filtered and washed with water, to yield the crude azo compound. The yield of the azo coupling is usually > 90%. To obtain material of high purity for spectroscopic analysis, further purification was achieved by recrystallization from water and precipitation by addition of methyl-*tert*-butyl ether to a concentrated acetonitrile solution of the azo compound.

General Procedure B for Coupling to Phenols.

The diazonium salt **96**[244] (192 mg, 1 mmol) and the phenol (1 mmol) were suspended in acetonitrile (5 mL). Potassium acetate (100 mg, 1 mmol) was added. After stirring overnight, methyl-*tert*-butyl ether was added to precipitate the potassium salt of the azo compound. The filtrate was washed with methyl-*tert*-butyl ether and water was added to dissolve most of the precipitate. The solution was filtered and added to tetraethylammonium chloride in water (830 mg, 5 mmol in 5 mL). After standing overnight, the resulting precipitate was filtered and washed with water, to yield the crude azo compound. The yield of the azo coupling was usually > 90%. To obtain material of high purity for spectroscopic analysis, further purification was achieved by recrystallization from water and precipitation by addition of methyl-*tert*-butyl ether to a concentrated acetonitrile solution of the azo compound.

General Procedure C for Coupling to Electron Poor Aryl Compounds.

To a solution of the electron poor arylamine (1.65 mmol) in dichloromethane (4 mL) was added oxone (500 mg, 3.3 mmol) in water (16 mL). After stirring overnight, the aqueous phase was discarded and the organic phase was washed with water. Tetraethylammonium aminotetracyano-cyclopentadienide[244] (170 mg, 0.55 mmol) was suspended in acetic acid (5 mL) and added to the solution of the nitroso species. The dichloromethane was removed under reduced pressure and the residue stirred overnight. Upon addition of water the product precipitated, was filtered and washed with water. Recrystallization from water and acetone/petroleum ether afforded the pure product.

4-(*N,N*-Dimethylamino)phenylazotetracyanocyclopentadienide (97)

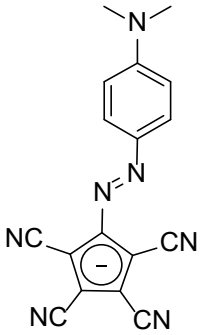

Compound **97** was synthesized as described in the literature.[244] ^{1}H-NMR (500 MHz, CD_3CN): δ [ppm]= 1.19 (tt, $^{3}J_{HH}$ = 7.3 Hz, $^{3}J_{NH}$ = 1.9 Hz, 12H), 3.06 (s, 6H), 3.13 (q, ^{3}J = 7.2 Hz, 8H), 6.81 (d, ^{3}J = 9.5 Hz, 2H), 7.74 (d, ^{3}J = 9.3 Hz, 2H). ^{13}C{^{1}H}-NMR (126 MHz, CD_3CN): δ [ppm]= 7.7, 40.5, 53.0, 53.0, 53.1, 92.3, 102.1, 112.7, 115.8, 116.7, 125.3, 143.8, 149.6, 153.8. ESI-MS $[M]^-$ *m/z* calculated for $C_{17}H_{10}N_7^-$: 312.1003 found: 312.0931.

4-Cyanophenylazotetracyanocyclopentadienide (98)

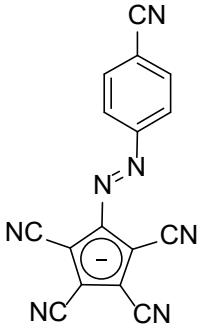

Compound **98** was synthesized according to general method C in 73% yield. ^{1}H-NMR (500 MHz, CD_3CN): δ [ppm]= 1.20 (tt, $^{3}J_{HH}$ = 7.3 Hz, $^{3}J_{NH}$ = 1.9 Hz, 12H), 3.15 (q, ^{3}J = 7.3 Hz, 8H), 7.85 (dt, ^{3}J = 8.6 Hz, ^{4}J = 1.9 Hz, 2H), 7.90 (dt, ^{3}J = 8.7 Hz, ^{4}J = 1.9 Hz, 2H). ^{13}C{^{1}H}-NMR (126 MHz, CD_3CN): δ [ppm]= 7.7, 53.0, 53.0, 53.1, 94.9, 104.1, 114.2, 115.1, 115.8, 119.4, 123.6, 134.5, 147.4, 155.7. ESI-MS $[M]^-$ *m/z* calculated for $C_{16}H_4N_7^-$: 294.0534 found: 294.0243.

2,6-Difluoro-4-aminophenylazotetracyanocyclopentadienide (99)

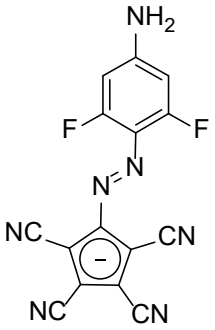

Compound **99** was synthesized according to general method A in 30% yield. ^{1}H-NMR (500 MHz, CD_3CN): δ [ppm]= 1.20 (tt, $^{3}J_{HH}$ = 7.3 Hz, $^{3}J_{NH}$ = 1.9 Hz, 12H), 3.15 (q, ^{3}J = 7.3 Hz, 8H), 5.20 (s, 2H), 6.32 (m, 2H). ^{13}C{^{1}H}-NMR (126 MHz, CD_3CN): δ [ppm]= 7.7, 53.0, 53.0, 53.1, 92.6, 98.2 (m), 102.7, 115.6, 116.3, 150.2, 153.1 (t, ^{2}J = 15.0 Hz), 159.3 (dd, ^{1}J = 257.2 Hz, ^{3}J = 7.7 Hz). ^{19}F-NMR (471 MHz, CD_3CN): δ [ppm]= −118.05 (d, ^{2}J = 12.5 Hz). ESI-MS $[M]^-$ *m/z* calculated for $C_{15}H_4N_7F_2^-$: 320.0502 found: 320.0274.

2,4,5-(Trimethoxy)phenylazotetracyanocyclopentadienide (100)

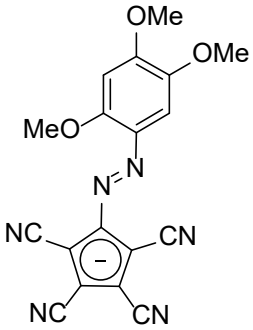

Compound **100** was synthesized according to general method A in 29% yield). ^{1}H-NMR (500 MHz, CD_3CN): δ [ppm]= 1.20 (tt, $^{3}J_{HH}$ = 7.3 Hz, $^{3}J_{NH}$ = 1.8 Hz, 12H), 3.14 (q, ^{3}J = 7.2 Hz, 8H), 3.78 (s, 3H), 3.92 (s, 3H), 3.98 (s, 3H), 6.75 (s, 1H), 7.32 (s, 1H). ^{13}C{^{1}H}-NMR (126 MHz, CD_3CN): δ [ppm]= 7.7, 53.0, 53.0, 53.1, 56.5, 56.8, 58.9, 92.9, 99.6, 100.4, 102.6, 115.7, 116.4, 136.2, 145.3, 149.5, 154.9, 155.0. ESI-MS $[M]^-$ *m/z* calculated for $C_{18}H_{11}N_6O_3^-$: 359.0898 found: 359.0707.

2,4,6-(Trimethoxy)phenylazotetracyanocyclopentadienide (101)

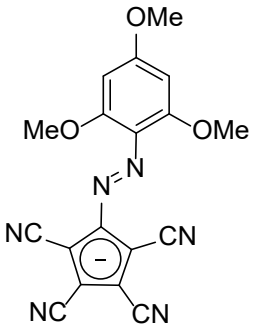

Compound **101** was synthesized according to general method A in 58% yield. ^{1}H-NMR (500 MHz, CD_3CN): δ [ppm]= 1.20 (tt, $^{3}J_{HH}$ = 7.2 Hz, $^{3}J_{NH}$ = 1.9 Hz, 12H), 3.15 (q, ^{3}J = 7.3 Hz, 8H), 3.82 (s, 6H), 3.87 (s, 3H), 6.31 (s, 2H). ^{13}C{^{1}H}-NMR (126 MHz, CD_3CN): δ [ppm]= 7.6, 53.0, 53.0, 53.1, 56.4, 57.1, 92.4, 92.9, 102.5, 115.7, 116.4. ESI-MS $[M]^-$ *m/z* calculated for $C_{18}H_{11}N_6O_3^-$: 359.0898 found: 359.0707.

3-(1,2,5-Trimethylpyrrolyl)-azotetracyanocyclopentadienide (102)

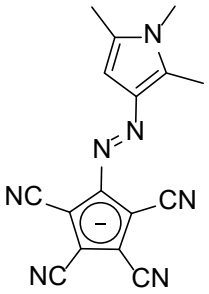

Diketone **111** (130 mg, 0.31 mmol) was dissolved in acetonitrile (5 mL). Methyl iodide (0.17 mL, 2.8 mmol) and tetraethylammonium hydroxide (35% aqueous solution, 0.23 mL, 0.56 mmol) were added and stirred overnight. Upon addition of water the product precipitated, was filtered and washed with water to yield a red solid (74 mg, 0.15 mmol, 50%). ^{1}H-NMR (500 MHz, CD_3CN): δ [ppm]= 1.20 (tt, $^{3}J_{HH}$ = 7.3 Hz, $^{3}J_{NH}$ = 1.9 Hz, 12H), 2.20 (d, ^{4}J = 1.0 Hz, 3H), 2.51 (s, 3H), 3.14 (q, ^{3}J = 7.3 Hz, 8H), 3.44 (s, 3H), 6.11 (q, ^{4}J = 1.1 Hz, 1H). ^{13}C{^{1}H}-NMR (126 MHz, CD_3CN): δ [ppm]= 7.7, 9.9, 12.4, 30.9, 53.0, 53.1, 53.1, 91.1, 95.4, 101.3, 116.1, 117.3, 132.9, 138.5, 140.5, 151.7. ESI-MS $[M]^-$ *m/z* calculated for $C_{16}H_{10}N_7^-$: 300.1003 found: 300.1086.

Potassium 2,4-(Dimethoxy)phenylazotetracyanocyclopentadienide (103)

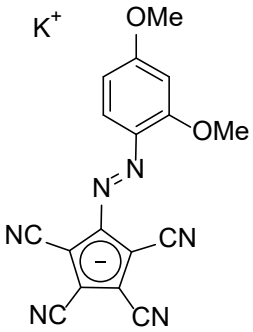

Compound **103** was synthesized according to general method A, without the cation exchange in 30% yield. ^{1}H-NMR (500 MHz, CD_3CN): δ [ppm]= 3.87 (s, 3H), 3.96 (s, 3H), 6.59 (dd, ^{3}J = 9.1, ^{4}J = 2.6 Hz, 1H), 6.68 (d, ^{4}J = 2.6 Hz, 1H), 7.65 (d, ^{3}J = 9.0 Hz, 1H). ^{13}C{^{1}H}-NMR (126 MHz, CD_3CN): δ [ppm]= 56.5, 57.3, 93.0, 100.4, 102.6, 107.5, 115.7, 116.4, 118.4, 137.5, 149.6, 159.9, 165.0. ESI-MS $[M]^-$ *m/z* calculated for $C_{17}H_9N_6O_2^-$: 329.0792 found: 329.0606.

4-Nitrophenylazotetracyanocyclopentadienide (104)

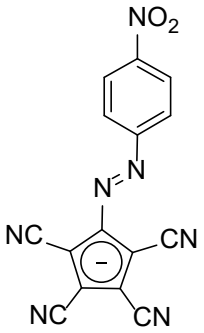

Compound **104** was synthesized according to general method C in 74% yield. ^{1}H-NMR (500 MHz, CD_3CN): δ [ppm]= 1.20 (tt, $^{3}J_{HH}$ = 7.3 Hz, $^{3}J_{NH}$ = 1.9 Hz, 12H), 3.15 (q, ^{3}J = 7.3 Hz, 8H), 7.95 (dt, ^{3}J = 9.1 Hz, ^{4}J = 2.4 Hz, 2H), 8.33 (dt, ^{3}J = 9.1 Hz, ^{4}J = 2.4 Hz, 2H). ^{13}C{^{1}H}-NMR (126 MHz, CD_3CN): δ [ppm]= 7.7, 53.0, 53.0, 53.1, 95.1, 104.3, 115.1, 115.8, 123.8, 125.9, 147.5, 149.5, 157.0. ESI-MS $[M]^-$ *m/z* calculated for $C_{15}H_4N_7O_2^-$: 314.0432 found: 314.0110.

4-(Trimethylammonium)phenylazotetracyanocyclopentadienide (105)

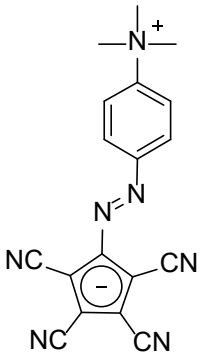

The N,N-dimethylaniline derivative **97** (110 mg, 0.25 mmol) and methyl iodide (0.39 mL, 6.25 mmol)) were dissolved in acetonitrile (10 mL) and stirred at 60 °C for 48 h. The product precipitated and was filtered after cooling to room temperature. Recrystallization from acetonitrile afforded a yellow solid (57 mg, 0.175 mmol, 70%). ^{1}H-NMR (500 MHz, DMSO-d_6): δ [ppm]= 3.66 (s, 9H), 7.93 (d, ^{3}J = 9.5 Hz, 2H), 8.18 (d, ^{3}J = 9.3 Hz, 2H). ^{13}C{^{1}H}-NMR (126 MHz, DMSO-d_6): δ [ppm]= 56.5, 93.2, 102.3, 114.0, 114.7, 122.2, 123.0, 146.1, 148.4, 152.1. ESI-MS $[M+HCO_2]^-$ *m/z* calculated for $C_{19}H_{14}N_7O_2^-$: 372.1214 found: 372.1214.

4-Aminophenylazotetracyanocyclopentadienide (106)

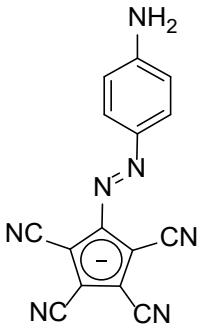

Compound **106** was synthesized according to general method A in 72% yield. ^{1}H-NMR (500 MHz, CD_3CN): δ [ppm]= 1.20 (tt, $^{3}J_{HH}$ = 7.3 Hz, $^{3}J_{NH}$ = 1.9 Hz, 12H), 3.14 (q, ^{3}J = 7.3 Hz, 8H), 4.84 (s, 2H), 6.73 (d, ^{3}J = 9.0 Hz, 2H), 7.65 (d, ^{3}J = 8.8 Hz, 2H). ^{13}C{^{1}H}-NMR (126 MHz, CD_3CN): δ [ppm]= 7.7, 53.0, 53.0, 53.1, 92.4, 102.2, 115.0, 115.8, 116.6, 125.6, 145.0, 149.3, 152.9. ESI-MS $[M]^-$ *m/z* calculated for $C_{15}H_6N_7^-$: 284.0690 found: 284.0629.

Potassium 2,6-difluoro-4-(*N,N*-dimethylamino)phenylazotetracyanocyclopentadienide (107)

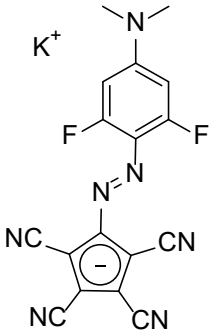

Compound **107** was synthesized according to general method A, without the cation exchange in 42% yield. ^{1}H-NMR (500 MHz, CD_3CN): δ [ppm]= 3.04 (s, 6H), 6.38 (m, 2H). $^{13}C\{^{1}H\}$-NMR (126 MHz, CD_3CN): δ [ppm]= 40.5, 92.4, 96.2 (m), 102.6, 115.7, 116.4, 150.5, 153.4 (t, ^{2}J = 14.7 Hz), 159.3 (dd, ^{1}J = 256.5 Hz, ^{3}J = 8.5 Hz). ^{19}F-NMR (471 MHz, CD_3CN): δ [ppm]= −117.49 (d, ^{2}J = 14.3 Hz). ESI-MS $[M]^-$ *m/z* calculated for $C_{17}H_8N_7F_2^-$: 348.0815 found: 348.0573.

1-(2-Hydroxynaphthyl)azotetracyanocyclopentadienide (108)

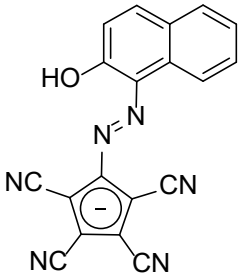

Compound **108** was synthesized according to general method B in 30% yield. ^{1}H-NMR (500 MHz, CD_3CN): δ [ppm]= 1.18 (tt, $^{3}J_{HH}$ = 7.2 Hz, $^{3}J_{NH}$ = 1.8 Hz, 12H), 3.13 (q, ^{3}J = 7.3 Hz, 8H), 7.15 (d, ^{3}J = 9.0 Hz, 1H), 7.44 (t, ^{3}J = 7.4 Hz, 1H), 7.58 (t, ^{3}J = 7.7 Hz, 1H), 7.81 (d, ^{3}J = 8.1 Hz, 1H), 7.88 (d, ^{3}J = 9.0 Hz, 1H), 8.77 (d, ^{3}J = 8.5 Hz, 1H), 14.05 (s, 1H). $^{13}C\{^{1}H\}$-NMR (126 MHz, CD_3CN): δ [ppm]= 7.6, 53.0, 53.0, 53.1, 92.5, 103.0, 115.3, 116.2, 120.7, 123.4, 125.7, 129.1, 129.1, 129.5, 130.8, 133.9, 136.2, 147.0, 154.3. ESI-MS $[M]^-$ *m/z* calculated for $C_{19}H_7N_6O^-$: 335.0687 found: 335.0464.

2-Hydroxy-5-*tert*-butylphenylazotetracyanocyclopentadienide (109)

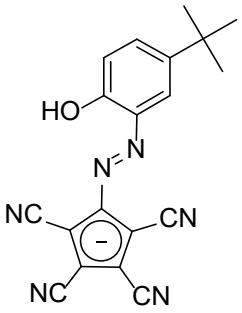

Compound **109** was synthesized according to general method B in 5% yield. ^{1}H-NMR (500 MHz, CD_3CN): δ [ppm]= 1.20 (tt, $^{3}J_{HH}$ = 7.2 Hz, $^{3}J_{NH}$ = 1.8 Hz, 12H), 1.34 (s, 9H), 3.15 (q, ^{3}J = 7.2 Hz, 8H), 6.96 (d, ^{3}J = 8.7 Hz, 1H), 7.48 (dd, ^{3}J = 8.7, 2.5 Hz, 1H), 7.76 (d, ^{3}J = 2.5 Hz, 1H), 11.10 (s, 1H). ^{13}C{^{1}H}-NMR (126 MHz, CD_3CN): δ [ppm]= 7.7, 31.5, 34.8, 53.0, 53.0, 53.1, 93.2, 103.2, 115.2, 116.1, 125.5, 132.0, 137.8, 144.3, 146.8, 152.1. ESI-MS $[M]^-$ *m/z* calculated for $C_{19}H_{13}N_6O^-$: 341.1156 found: 341.1376.

4-Hydroxy-2,3,5,6-tetrafluorophenylazotetracyanocyclopentadienide (110)

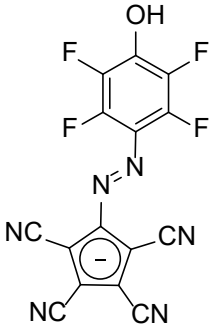

Compound **110** was synthesized according to general method B in 18% yield. ^{1}H-NMR (500 MHz, CD_3CN): δ [ppm]= 1.20 (tt, $^{3}J_{HH}$ = 7.3 Hz, $^{3}J_{NH}$ = 1.8 Hz, 12H), 3.15 (q, ^{3}J = 7.3 Hz, 8H). ^{13}C{^{1}H}-NMR (126 MHz, CD_3CN): δ [ppm]= 7.7, 53.0, 53.0, 53.1, 94.2, 103.9, 115.2, 115.7, 124.8 (m), 138.2 (m), 140.5 (m), 142.9 (m), 148.6. ^{19}F-NMR (471 MHz, CD_3CN): δ [ppm]= −164.08 (d, ^{3}J = 14.3 Hz), −152.38 (d, ^{3}J = 12.5 Hz). ESI-MS $[M]^-$ *m/z* calculated for $C_{15}HN_6OF_4^-$: 357.0153 found: 357.0074.

3-(2,5-Dimethylpyrrolyl)-azotetracyanocyclopentadienide (111)

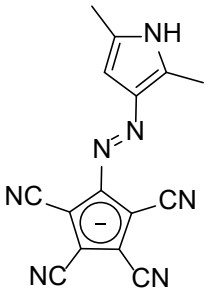

Compound **111** was synthesized according to general method A in 36% yield. ^{1}H-NMR (500 MHz, CD_3CN): δ [ppm]= 1.20 (tt, $^{3}J_{HH}$ = 7.3 Hz, $^{3}J_{NH}$ = 1.9 Hz, 12H), 2.19 (d, ^{4}J = 1.2 Hz, 3H), 2.49 (s, 3H), 3.13 (q, ^{3}J = 7.3 Hz, 8H), 6.04 (m, 1H), 9.28 (s, 1H). ^{13}C{^{1}H}-NMR (126 MHz, CD_3CN): δ [ppm]= 7.7, 10.5, 12.9, 53.0, 53.1, 53.1, 91.2, 95.5, 101.3, 116.1, 117.2, 130.9, 136.7, 141.2, 151.5. ESI-MS $[M]^-$ *m/z* calculated for $C_{15}H_8N_7^-$: 286.0847 found: 286.0844.

4-(1,3,5-Trimethyl-1*H*-pyrazolyl)-azotetracyanocyclopentadienid (112)

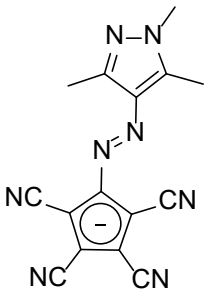

Diketone **129** (105 mg, 0.25 mmol) and methylhydrazine (0.13 mL, 2.5 mmol) were dissolved in ethanol (10 mL) and heated to 60 °C for 5 h. After cooling to room temperature, methyl-*tert*-butyl ether was added. The precipitate was filtered and washed with methyl-*tert*-butyl ether to yield a yellow solid (70 mg, 0.16 mmol, 65%). ^{1}H-NMR (500 MHz, CD_3CN): δ [ppm]= 1.20 (tt, $^{3}J_{HH}$ = 7.3 Hz, $^{3}J_{NH}$ = 1.9 Hz, 12H), 2.37 (s, 3H), 2.51 (s, 3H), 3.15 (q, ^{3}J = 7.3 Hz, 8H), 3.71 (s, 3H). ^{13}C{^{1}H}-NMR (126 MHz, CD_3CN): δ [ppm]= 7.7, 10.0, 14.4, 36.6, 53.0, 53.0, 53.1, 91.7, 101.7, 115.9, 116.8, 135.6, 141.3, 141.9, 150.9. ESI-MS $[M]^-$ *m/z* calculated for $C_{15}H_9N_8^-$: 301.0956 found: 301.0816.

2-Acetylacetonylhydrazonotetracyanocyclopentadienide (129)

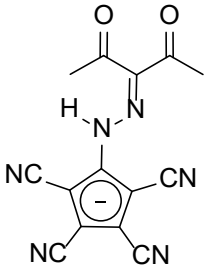

Compound **129** was synthesized according to general method B in ethanol/water 7/4 in 30% yield. ^{1}H-NMR (500 MHz, CD_3CN): δ [ppm]= 1.20 (tt, $^{3}J_{HH}$ = 7.3 Hz, $^{3}J_{NH}$ = 1.9 Hz, 12H), 2.41 (s, 3H), 2.51 (s, 3H), 3.16 (q, ^{3}J = 7.3 Hz, 8H), 15.02 (s, 1H). $^{13}C\{^{1}H\}$-NMR (126 MHz, CD_3CN): δ [ppm]= 7.7, 27.7, 31.7, 53.0, 53.0, 53.1, 85.7, 100.3, 115.6, 115.6, 134.2, 138.1, 198.0, 199.2. ESI-MS $[M]^-$ *m/z* calculated for $C_{14}H_7N_6O_2^-$: 291.0636 found: 291.0461.

5.5 Single-Crystal X-Ray Analysis

All derivatives were crystallized by vapor diffusion or slow evaporation of a concentrated solution. The prepared single-crystal was mounted using a microfabricated polymer film crystal-mounting tool (dual-thickness MicroMount, MiTeGen) using low viscosity oil (perfluoropolyalkylether; viscosity 1800 cSt, ABCR) to reduce the X-ray absorption and scattering. A Bruker D8 Venture single-crystal X-ray diffractometer with area detector using Mo-K_α (λ = 0.71073 Å) radiation was used for data collection at −173 °. Multiscan absorption corrections implemented in SADABS[291] were applied to the data. The structure was solved by intrinsic phasing (SHELXT-2013)[292] and refined by full-matrix least-squares methods on F^2 (SHELXL-2014).[293] The hydrogen atoms were placed at calculated positions and refined by using a riding model.

6 References

(1) Allan, R. *Manual of Mineralogy* **1834**.

(2) Lee, O. I. A New Property of Matter: Reversible Photosensitivity in Hackmanite from Bancroft, Ontario. *Am. Mineral.* **1936**, *21*, 764–776.

(3) Fritzsche, J. *J. C. R. Acad. Sci. Paris* **1867**, *69*, 78.

(4) Kawata, S.; Kawata, Y. Three-Dimensional Optical Data Storage Using Photochromic Materials. *Chem. Rev.* **2000**, *100*, 1777–1788.

(5) Corredor, C. C.; Huang, Z.-L.; Belfield, K. D. Two-Photon 3D Optical Data Storage *via* Fluorescence Modulation of an Efficient Fluorene Dye by a Photochromic Diarylethene. *Adv. Mater.* **2006**, *18,* 2910–2914.

(6) Zhang, J.; Zou, Q.; Tian, H. Photochromic Materials: More Than Meets The Eye. *Adv. Mater.* **2013**, *25*, 378–399.

(7) Kim, M.; Safron, N. S.; Huang, C.; Arnold, M. S.; Gopalan, P. Light-Driven Reversible Modulation of Doping in Graphene. *Nano Lett.* **2012**, *12*, 182–187.

(8) Ishii, N.; Abe, J. Fast Photochromism in Polymer Matrix with Plasticizer and Real-Time Dynamic Holographic Properties. *Appl. Phys. Lett.* **2013**, *102*, 163301.

(9) Todorov, T.; Nikolova, L.; Tomova, N.; Dragostinova, V. Photochromism and Dynamic Holographic Recording in a Rigid Solution of Fluorescein. *Opt. Quant. Electron* **1981**, *13*, 209–215.

(10) Zhou, H.; Xue, C.; Weis, P.; Suzuki, Y.; Huang, S.; Koynov, K.; Auernhammer, G. K.; Berger, R.; Butt, H.-J.; Wu, S. Photoswitching of Glass Transition Temperatures of Azobenzene-Containing Polymers Induces Reversible Solid-to-Liquid Transitions. *Nat. Chem.* **2017**, *9*, 145–151.

(11) Orgiu, E.; Samorì, P. 25th Anniversary Article: Organic Electronics Marries Photochromism: Generation of Multifunctional Interfaces, Materials, and Devices. *Adv. Mater.* **2014**, *26*, 1827–1845.

(12) Zhao, H.; Sen, S.; Udayabhaskararao, T.; Sawczyk, M.; Kučanda, K.; Manna, D.; Kundu, P. K.; Lee, J.-W.; Král, P.; Klajn, R. Reversible Trapping and Reaction Acceleration within Dynamically Self-Assembling Nanoflasks. *Nat. Nanotech.* **2016**, *11*, 82–88.

(13) Ragazzon, G.; Baroncini, M.; Silvi, S.; Venturi, M.; Credi, A. Light-Powered Autonomous and Directional Molecular Motion of a Dissipative Self-Assembling System. *Nat. Nanotech.* **2015**, *10*, 70–75.

(14) Broichhagen, J.; Frank, J. A.; Trauner, D. A Roadmap to Success in Photopharmacology. *Acc. Chem. Res.* **2015**, *48*, 1947–1960.

(15) Kawai, T.; Nakashima, Y.; Irie, M. A Novel Photoresponsive π-Conjugated Polymer Based on Diarylethene and Its Photoswitching Effect in Electrical Conductivity. *Adv. Mater.* **2005**, *17*, 309–314.

(16) Jochum, F. D.; zur Borg, L.; Roth, P. J.; Theato, P. Thermo- and Light-Responsive Polymers Containing Photoswitchable Azobenzene End Groups. *Macromolecules* **2009**, *42*, 7854–7862.

(17) Tamesue, S.; Takashima, Y.; Yamaguchi, H.; Shinkai, S.; Harada, A. Photoswitchable Supramolecular Hydrogels Formed by Cyclodextrins and Azobenzene Polymers. *Angew. Chem. Int. Ed.* **2010**, *49*, 7461–7464.

(18) Yamaguchi, H.; Kobayashi, Y.; Kobayashi, R.; Takashima, Y.; Hashidzume, A.; Harada, A. Photoswitchable Gel Assembly Based on Molecular Recognition. *Nat. Commun.* **2012**, *3*, 603.

(19) Fuhrmann, A.; Göstl, R.; Wendt, R.; Kötteritzsch, J.; Hager, M. D.; Schubert, U. S.; Brademann-Jock, K.; Thünemann, A. F.; Nöchel, U.; Behl, M.; et al. Conditional Repair by Locally Switching the Thermal Healing Capability of Dynamic Covalent Polymers with Light. *Nat. Commun.* **2016**, *7*, 13623.

(20) Kathan, M.; Kovaříček, P.; Jurissek, C.; Senf, A.; Dallmann, A.; Thünemann, A. F.; Hecht, S. Control of Imine Exchange Kinetics with Photoswitches to Modulate Self-Healing in Polysiloxane Networks by Light Illumination. *Angew. Chem. Int. Ed.* **2016**, *55*, 13882–13886.
(21) Amamoto, Y.; Kamada, J.; Otsuka, H.; Takahara, A.; Matyjaszewski, K. Repeatable Photoinduced Self-Healing of Covalently Cross-Linked Polymers through Reshuffling of Trithiocarbonate Units. *Angew. Chem. Int. Ed.* **2011**, *50*, 1660–1663.
(22) Lutsyk, P.; Janus, K.; Sworakowski, J.; Generali, G.; Capelli, R.; Muccini, M. Photoswitching of an N-Type Organic Field Effect Transistor by a Reversible Photochromic Reaction in the Dielectric Film. *J. Phys. Chem. C* **2011**, *115*, 3106–3114.
(23) Tseng, C.-W.; Huang, D.-C.; Tao, Y.-T. Electric Bistability Induced by Incorporating Self-Assembled Monolayers/Aggregated Clusters of Azobenzene Derivatives in Pentacene-Based Thin-Film Transistors. *ACS Appl. Mater. Interfaces* **2012**, *4*, 5483–5491.
(24) Zacharias, P.; Gather, M. C.; Köhnen, A.; Rehmann, N.; Meerholz, K. Photoprogrammable Organic Light-Emitting Diodes. *Angew. Chem. Int. Ed.* **2009**, *48*, 4038–4041.
(25) Willner, I.; Rubin, S.; Riklin, A. Photoregulation of Papain Activity through Anchoring Photochromic Azo Groups to the Enzyme Backbone. *J. Am. Chem. Soc.* **1991**, *113*, 3321–3325.
(26) Lee, W.-S.; Ueno, A. Photocontrol of the Catalytic Activity of a β-Cyclodextrin Bearing Azobenzene and Histidine Moieties as a Pendant Group. *Macromol. Rapid Commun.* **2001**, *22*, 448–450.
(27) Stoll, R. S.; Peters, M. V.; Kuhn, A.; Heiles, S.; Goddard, R.; Bühl, M.; Thiele, C. M.; Hecht, S. Photoswitchable Catalysts: Correlating Structure and Conformational Dynamics with Reactivity by a Combined Experimental and Computational Approach. *J. Am. Chem. Soc.* **2009**, *131*, 357–367.
(28) Peters, M. V.; Stoll, R. S.; Kühn, A.; Hecht, S. Photoswitching of Basicity. *Angew. Chem. Int. Ed.* **2008**, *47*, 5968–5972.
(29) Neilson, B. M.; Bielawski, C. W. Photoswitchable Organocatalysis: Using Light to Modulate the Catalytic Activities of *N*-Heterocyclic Carbenes. *J. Am. Chem. Soc.* **2012**, *134*, 12693–12699.
(30) Sud, D.; Norsten, T. B.; Branda, N. R. Photoswitching of Stereoselectivity in Catalysis Using a Copper Dithienylethene Complex. *Angew. Chem. Int. Ed.* **2005**, *44*, 2019–2021.
(31) Wei, Y.; Han, S.; Kim, J.; Soh, S.; Grzybowski, B. A. Photoswitchable Catalysis Mediated by Dynamic Aggregation of Nanoparticles. *J. Am. Chem. Soc.* **2010**, *132*, 11018–11020.
(32) Eisenreich, F.; Kathan, M.; Dallmann, A.; Ihrig, S. P.; Schwaar, T.; Schmidt, B. M.; Hecht, S. A Photoswitchable Catalyst System for Remote-Controlled (Co)Polymerization in Situ. *Nat. Catal.* **2018**, *1*, 516–522.
(33) Kassem, S.; Leeuwen, T. van; S. Lubbe, A.; R. Wilson, M.; L. Feringa, B.; A. Leigh, D. Artificial Molecular Motors. *Chem. Soc. Rev.* **2017**, *46*, 2592–2621.
(34) Ruangsupapichat, N.; Pollard, M. M.; Harutyunyan, S. R.; Feringa, B. L. Reversing the Direction in a Light-Driven Rotary Molecular Motor. *Nat. Chem.* **2011**, *3*, 53–60.
(35) Koumura, N.; Geertsema, E. M.; van Gelder, M. B.; Meetsma, A.; Feringa, B. L. Second Generation Light-Driven Molecular Motors. Unidirectional Rotation Controlled by a Single Stereogenic Center with Near-Perfect Photoequilibria and Acceleration of the Speed of Rotation by Structural Modification. *J. Am. Chem. Soc.* **2002**, *124*, 5037–5051.
(36) Hernández, J. V.; Kay, E. R.; Leigh, D. A. A Reversible Synthetic Rotary Molecular Motor. *Science* **2004**, *306*, 1532–1537.
(37) Stolik, S.; Delgado, J. A.; Pérez, A.; Anasagasti, L. Measurement of the Penetration Depths of Red and near Infrared Light in Human "Ex Vivo" Tissues. *J. Photochem. Photobio. B* **2000**, *57*, 90–93.
(38) Lerch, M. M.; Hansen, M. J.; van Dam, G. M.; Szymanski, W.; Feringa, B. L. Emerging Targets in Photopharmacology. *Angew. Chem. Int. Ed.* **2016**, *55*, 10978–10999.
(39) Velema, W. A.; Szymanski, W.; Feringa, B. L. Photopharmacology: Beyond Proof of Principle. *J. Am. Chem. Soc.* **2014**, *136*, 2178–2191.

(40) Klaue, K.; Garmshausen, Y.; Hecht, S. Taking Photochromism beyond Visible: Direct One-Photon NIR Photoswitches Operating in the Biological Window. *Angew. Chem. Int. Ed.* **2018**, *57*, 1414–1417.
(41) Boggio-Pasqua, M.; Bearpark, M. J.; Robb, M. A. Toward a Mechanistic Understanding of the Photochromism of Dimethyldihydropyrenes. *J. Org. Chem.* **2007**, *72*, 4497–4503.
(42) Blattmann, H.-R.; Schmidt, W. Über die Phototropie des *trans*-15,16-dimethyldihydropyrens und seiner Derivate. *Tetrahedron* **1970**, *26*, 5885–5899.
(43) Mitchell, R. H.; Chen, Y. Synthesis of the Elusive Dibenzannelated Dihydropyrene Dibenzo[e,l]dimethyldihydropyrene, a Molecular Photo-Switch. *Tetrahedron Letters* **1996**, *37*, 5239–5242.
(44) Fischer, E. Calculation of Photostationary States in Systems A ⇌ B When Only A is Known. *J. Phys. Chem.* **1967**, *71*, 3704–3706.
(45) Rau, H.; Greiner, G.; Gauglitz, G.; Meier, H. Photochemical Quantum Yields in the A ⇌ B System When Only the Spectrum of A is Known. *J. Phys. Chem.* **1990**, *94*, 6523–6524.
(46) Mauser, H. *Formale Kinetik*; Bertelsmann-Universitätsverlag, **1974**.
(47) Dürr, H.; Bouas-Laurent, H. *Photochromism: Molecules and Systems: Molecules and Systems*; Gulf Professional Publishing, **2003**.
(48) Robinson, S. G.; Sauro, V. A.; Mitchell, R. H. Oligothiophene Functionalized Dimethyldihydropyrenes I: Syntheses and Photochromicity. *J. Org. Chem.* **2009**, *74*, 6592–6605.
(49) Mitchell, R. H.; Ward, T. R.; Chen, Y.; Wang, Y.; Weerawarna, S. A.; Dibble, P. W.; Marsella, M. J.; Almutairi, A.; Wang, Z.-Q. Synthesis and Photochromic Properties of Molecules Containing [e]-Annelated Dihydropyrenes. Two and Three Way π-Switches Based on the Dimethyldihydropyrene−Metacyclophanediene Valence Isomerization. *J. Am. Chem. Soc.* **2003**, *125*, 2974–2988.
(50) Morimoto, M.; Irie, M. A Diarylethene Cocrystal That Converts Light into Mechanical Work. *J. Am. Chem. Soc.* **2010**, *132*, 14172–14178.
(51) Wang, M.-S.; Xu, G.; Zhang, Z.-J.; Guo, G.-C. Inorganic–Organic Hybrid Photochromic Materials. *Chem. Commun.* **2010**, *46*, 361–376.
(52) Nakai, H.; Isobe, K. Photochromism of Organometallic Compounds with Structural Rearrangement. *Coord. Chem. Rev.* **2010**, *254*, 2652–2662.
(53) Vollhardt, K. P. C.; Weidman, T. W. Synthesis, Structure, and Photochemistry of Tetracarbonyl(Fulvalene)Diruthenium. Thermally Reversible Photoisomerization Involving Carbon-Carbon Bond Activation at a Dimetal Center. *J. Am. Chem. Soc.* **1983**, *105*, 1676–1677.
(54) Boese, R.; Cammack, J. K.; Matzger, A. J.; Pflug, K.; Tolman, W. B.; Vollhardt, K. P. C.; Weidman, T. W. Photochemistry of (Fulvalene)Tetracarbonyldiruthenium and Its Derivatives: Efficient Light Energy Storage Devices. *J. Am. Chem. Soc.* **1997**, *119*, 6757–6773.
(55) Burger, P. [$Me_2C(\eta^5\text{-}C_5H_4)_2Ru_2(CO)_4$]—An Organometallic Thermo-Optical Switch. *Angew. Chem. Int. Ed.* **2001**, *40*, 1917–1919.
(56) Coppens, P.; Novozhilova, I.; Kovalevsky, A. Photoinduced Linkage Isomers of Transition-Metal Nitrosyl Compounds and Related Complexes. *Chem. Rev.* **2002**, *102*, 861–884.
(57) Smith, M. K.; Gibson, J. A.; Young, C. G.; Broomhead, J. A.; Junk, P. C.; Keene, F. R. Photoinduced Ligand Isomerization in Dimethyl Sulfoxide Complexes of Ruthenium(II). *Eur. J. Inorg. Chem.* **2000**, *2000*, 1365–1370.
(58) To, T. T.; Duke III, C. B.; Junker, C. S.; O'Brien, C. M.; Ross II, C. R.; Barnes, C. E.; Webster, C. E.; Burkey, T. J. Linkage Isomerization as a Mechanism for Photochromic Materials: Cyclopentadienylmanganese Tricarbonyl Derivatives with Chelatable Functional Groups. *Organometallics* **2008**, *27*, 289–296.
(59) Kobayashi, M.; Takashima, A.; Ishii, T.; Naka, H.; Uchiyama, M.; Yamaguchi, K. Reverse Photochromic Behavior of an Iron−Magnesium Complex. *Inorg. Chem.* **2007**, *46*, 1039–1041.
(60) White, D. M.; Sonnenberg, J. Oxidation of Triarylimidazoles. Structures of the Photochromic and Piezochromic Dimers of Triarylimidazyl Radicals. *J. Am. Chem. Soc.* **1966**, *88*, 3825–3829.

(61) Hayashi, T.; Maeda, K. Preparation of a New Phototropic Substance. *Bull. Chem. Soc. Jpn.* **1960**, *33*, 565–566.
(62) Kishimoto, Y.; Abe, J. A Fast Photochromic Molecule That Colors Only under UV Light. *J. Am. Chem. Soc.* **2009**, *131*, 4227–4229.
(63) Yamaguchi, T.; Hatano, S.; Abe, J. Multistate Photochromism of 1-Phenylnaphthalene-Bridged Imidazole Dimer That Has Three Colorless Isomers and Two Colored Isomers. *J. Phys. Chem. A* **2014**, *118*, 134–143.
(64) Hatano, S.; Horino, T.; Tokita, A.; Oshima, T.; Abe, J. Unusual Negative Photochromism via a Short-Lived Imidazolyl Radical of 1,1′-Binaphthyl-Bridged Imidazole Dimer. *J. Am. Chem. Soc.* **2013**, *135*, 3164–3172.
(65) Yamaguchi, T.; Kobayashi, Y.; Abe, J. Fast Negative Photochromism of 1,1′-Binaphthyl-Bridged Phenoxyl–Imidazolyl Radical Complex. *J. Am. Chem. Soc.* **2016**, *138*, 906–913.
(66) Herz, M. L. Photochemical Ionization of the Triarylmethane Leuconitriles. *J. Am. Chem. Soc.* **1975**, *97*, 6777–6785.
(67) Sporer, A. H. Photoionization of Triarylmethyl Leuconitriles. *Trans. Faraday Soc.* **1961**, *57*, 983–991.
(68) Knauer, K.-H.; Gleiter, R. Photochromism of Rhodamine Derivatives. *Angew. Chem. Int. Ed.* **1977**, *16*, 113–113.
(69) Tran-Thi, T.-H.; Gustavsson, T.; Prayer, C.; Pommeret, S.; Hynes, J. T. Primary Ultrafast Events Preceding the Photoinduced Proton Transfer from Pyranine to Water. *Chem. Phys. Lett.* **2000**, *329*, 421–430.
(70) Gliemeroth, G.; Mader, K.-H. Phototropic Glass. *Angew. Chem. Int. Ed.* **1970**, *9*, 434–445.
(71) Kamogawa, H.; Sato, S. Redox Photochromism of Arylviologen Crystals. *Bull. Chem. Soc. Jpn.* **1991**, *64*, 321–323.
(72) Nakagaki, R.; Kobayashi, T.; Nakamura, J.; Nagakura, S. Spectroscopic and Kinetic Studies of the Photochromism of N-Salicylideneanilines and Related Compounds. *Bull. Chem. Soc. Jpn.* **1977**, *50*, 1909–1912.
(73) Rawat, M. S. M.; Mal, S.; Singh, P. Photochromism in Anils - A Review. *Open Chem. J.* **2015**, *2*.
(74) Minkin, V. I.; Komissarov, V. N. Perimidmespirocyclohexadienones - a Novel Photo and Thermochromic System. *Mol. Cryst. Liq. Cryst. Sci. Tech. A.* **1997**, *297*, 205–212.
(75) Naumov, P.; Sekine, A.; Uekusa, H.; Ohashi, Y. Structure of the Photocolored 2-(2′,4′-Dinitrobenzyl)Pyridine Crystal: Two-Photon Induced Solid-State Proton Transfer with Minor Structural Perturbation. *J. Am. Chem. Soc.* **2002**, *124*, 8540–8541.
(76) Corval, A.; Kuldová, K.; Eichen, Y.; Pikramenou, Z.; Lehn, J. M.; Trommsdorff, H. P. Photochromism and Thermochromism Driven by Intramolecular Proton Transfer in Dinitrobenzylpyridine Compounds. *J. Phys. Chem.* **1996**, *100*, 19315–19320.
(77) Frej, A.; Goeschen, C.; Näther, C.; Lüning, U.; Herges, R. Synthesis and Properties of Di- and Trinitrobenzyl Substituted Pyridine Derivates. *J. Phys. Org. Chem.* **2010**, *23*, 1093–1098.
(78) Tochitsky, I.; Kienzler, M. A.; Isacoff, E.; Kramer, R. H. Restoring Vision to the Blind with Chemical Photoswitches. *Chem. Rev.* **2018**, *118*, 10748-10773.
(79) Moiseyev, G.; Chen, Y.; Takahashi, Y.; Wu, B. X.; Ma, J. RPE65 Is the Isomerohydrolase in the Retinoid Visual Cycle. *Proc. Nat. Acad. Sci.* **2005**, *102*, 12413–12418.
(80) Briggs, W. R.; Olney, M. A. Photoreceptors in Plant Photomorphogenesis to Date. Five Phytochromes, Two Cryptochromes, One Phototropin, and One Superchrome. *Plant Physiology* **2001**, *125*, 85–88.
(81) Li, J.; Li, G.; Wang, H.; Wang Deng, X. Phytochrome Signaling Mechanisms. *The Arabidopsis Book* **2011**.
(82) Rockwell, N. C.; Su, Y.-S.; Lagarias, J. C. Phytochrome Structure and Signaling Mechanisms. *Annu. Rev. Plant Biol.* **2006**, *57*, 837–858.
(83) Dugave, C.; Demange, L. Cis−Trans Isomerization of Organic Molecules and Biomolecules: Implications and Applications. *Chem. Rev.* **2003**, *103*, 2475–2532.

(84) Minnaard, N. G.; Havinga, E. Some Aspects of the Solution Photochemistry of 1,3-cyclohexadiene, (Z)- and (E)-1,3,5-hexatriene. *Recl. Trav. Chim. Pays-Bas* **1973**, *92*, 1315–1320.
(85) Richers, M. T.; Tran, D. D.; Wachtveitl, J.; Ellis-Davies, G. C. R. Coumarin-Diene Photoswitches for Rapid and Efficient Isomerization with Visible Light. *Chem. Commun.* **2018**, *54*, 4983–4986.
(86) Cammenga, H. K.; Emel'yanenko, V. N.; Verevkin, S. P. Re-Investigation and Data Assessment of the Isomerization and 2,2′-Cyclization of Stilbenes and Azobenzenes. *Ind. Eng. Chem. Res.* **2009**, *48*, 10120–10128.
(87) Waldeck, D. H. Photoisomerization Dynamics of Stilbenes. *Chem. Rev.* **1991**, *91*, 415–436.
(88) A. Muszkat, K.; Fischer, E. Structure, Spectra, Photochemistry, and Thermal Reactions of the 4a,4b-Dihydrophenanthrenes. *J. Chem. Soc. B* **1967**, 662–678.
(89) Guo, X.; Zhou, J.; Siegler, M. A.; Bragg, A. E.; Katz, H. E. Visible-Light-Triggered Molecular Photoswitch Based on Reversible E/Z Isomerization of a 1,2-Dicyanoethene Derivative. *Angew. Chem. Int. Ed.* **2015**, *54*, 4782–4786.
(90) Caia, V.; Cum, G.; Gallo, R.; Mancini, V.; Pitoni, E. A High Enthalpy Value in Thermal Isomerization of Photosynthesized Cis-9-Styrylacridines. *Tetrahedron Lett.* **1983**, *24*, 3903–3904.
(91) Bastianelli, C.; Caia, V.; Cum, G.; Gallo, R.; Mancini, V. Thermal Isomerization of Photochemically Synthesized (Z)-9-Styrylacridines. An Unusually High Enthalpy of Z → E Conversion for Stilbene-like Compounds. *J. Chem. Soc., Perk. Trans. 2* **1991**, 679–683.
(92) Wyman, G. M.; Brode, W. R. The Relation between the Absorption Spectra and the Chemical Constitution of Dyes XXII. Cis-Trans Isomerism in Thioindigo Dyes. *J. Am. Chem. Soc.* **1951**, *73*, 1487–1493.
(93) Huang, C.-Y.; Bonasera, A.; Hristov, L.; Garmshausen, Y.; Schmidt, B. M.; Jacquemin, D.; Hecht, S. *N*,*N*′-Disubstituted Indigos as Readily Available Red-Light Photoswitches with Tunable Thermal Half-Lives. *J. Am. Chem. Soc.* **2017**, *139*, 15205–15211.
(94) Petermayer, C.; Dube, H. Indigoid Photoswitches: Visible Light Responsive Molecular Tools. *Acc. Chem. Res.* **2018**, *51*, 1153-1163.
(95) Kink, F.; Collado, M. P.; Wiedbrauk, S.; Mayer, P.; Dube, H. Bistable Photoswitching of Hemithioindigo with Green and Red Light: Entry Point to Advanced Molecular Digital Information Processing. *Chem. Eur. J.* **2017**, *23*, 6237–6243.
(96) Dubonosov, A. D.; Bren, V. A. Inverse Photochromic Systems Based on Ketoenamine Derivatives. *Russ. Chem. Bull.* **2005**, *54*, 512–524.
(97) Fischer, E.; Frei, Y. Photoisomerization Equilibria Involving the C=N Double Bond. *J. Chem. Phys.* **1957**, *27*, 808–809.
(98) Coelho, P. J.; Castro, M. C. R.; Raposo, M. M. M. Reversible Trans–Cis Photoisomerization of New Pyrrolidene Heterocyclic Imines. *J. Photochem. Photobiol. A* **2013**, *259*, 59–65.
(99) Padwa, A. Photochemistry of the Carbon-Nitrogen Double Bond. *Chem. Rev.* **1977**, *77*, 37–68.
(100) Appenroth, K.; Reichenbächer, M.; Paetzold, R. Thermochromism and Photochromism of Aryl-Substituted Acyclic Azines II: Photokinetics. *J. Photochem.* **1980**, *14*, 39–50.
(101) Appenroth, K.; Reichenbächer, M.; Paetzold, R. Thermochromism and Photochromism of Aryl Substituted Acyclic Azines: Uncatalised and Acid-Catalised Thermal Isomerisation. *Tetrahedron* **1981**, *37*, 569–573.
(102) Sigeikin, G. I.; Lipunova, G. N.; Pervova, I. G. Formazans and Their Metal Complexes. *Russ. Chem. Rev.* **2006**, *75*, 885.
(103) R. Burns, G.; W. Cunningham, C.; McKee, V. Photochromic Formazans: Raman Spectra, X -Ray Crystal Structures, and ^{13}C Magnetic Resonance Spectra of the Orange and Red Isomers of 3-Ethyl-1,5-Diphenylformazan. *J. Chem. Soc. Perk. Trans. 2* **1988**, 1275–1280.
(104) Hausser, I.; Jerchel, D.; Kuhn, R. Über die Rot ⇌ Gelb-Umlagerung von Formazanen im Licht; Grenzfragen von Mesomerie und Isomerie. *Chem. Ber.* **1949**, *82*, 515–527.
(105) Kuhn, R.; Weitz, H. M. Photochemie des Triphenylformazans. *Chem. Ber.* **1953**, *86*, 1199–1212.
(106) Qian, H.; Pramanik, S.; Aprahamian, I. Photochromic Hydrazone Switches with Extremely Long Thermal Half-Lives. *J. Am. Chem. Soc.* **2017**, *139*, 9140–9143.

(107) van Dijken, D. J.; Kovaříček, P.; Ihrig, S. P.; Hecht, S. Acylhydrazones as Widely Tunable Photoswitches. *J. Am. Chem. Soc.* **2015**, *137*, 14982–14991.
(108) Engel, P. S.; Steel, C. Photochemistry of Aliphatic Azo Compounds in Solution. *Acc. of Chem. Res.* **1973**, *6*, 275–281.
(109) Engel, P. S. Mechanism of the Thermal and Photochemical Decomposition of Azoalkanes. *Chem. Rev.* **1980**, *80*, 99–150.
(110) Engel, P. S.; Melaugh, R. A.; Page, M. A.; Szilagyi, S.; Timberlake, J. W. Stable Cis Dialkyldiazenes (Azoalkanes): Cis-Di-1-Adamantyldiazene and Cis-Di-1-Norbornyldiazene. *J. Am. Chem. Soc.* **1976**, *98*, 1971–1972.
(111) Ege, S. N.; Sharp, R. R. Magnetic Shielding by the Azo-Group. A Nuclear Magnetic Resonance Study of Phenylazoalkanes. *J. Chem. Soc. B* **1971**, 2014–2020.
(112) Porter, N. A.; Marnett, L. J. Photolysis of Unsymmetric Azo Compounds. Cis Azo Compound Intermediates. *J. Am. Chem. Soc.* **1973**, *95*, 4361–4367.
(113) Conti, I.; Marchioni, F.; Credi, A.; Orlandi, G.; Rosini, G.; Garavelli, M. Cyclohexenylphenyldiazene: A Simple Surrogate of the Azobenzene Photochromic Unit. *J. Am. Chem. Soc.* **2007**, *129*, 3198–3210.
(114) Sieburth, S. M.; Cunard, N. T. The [4 + 4] Cycloaddition and Its Strategic Application in Natural Product Synthesis. *Tetrahedron* **1996**, *52*, 6251–6282.
(115) Woodward, R. B.; Hoffmann, R. Stereochemistry of Electrocyclic Reactions. *J. Am. Chem. Soc.* **1965**, *87*, 395–397.
(116) Woodward, R. B.; Hoffmann, R. The Conservation of Orbital Symmetry. *Angew. Chem. Int. Ed.* **1969**, *8*, 781–853.
(117) Dauben, W. G.; Cargill, R. L. Photochemical Transformations-VI: Isomerization of Cycloheptadiene and Cycloheptatriene. *Tetrahedron* **1961**, *12*, 186–189.
(118) Jones, G.; Turbini, L. J. Valence Photoisomerization of 1-Ethoxycarbonyl-1H-Azepine and Its Thermal Reversion. Quantitative Aspects Including Energy Surface Relations. *J. Org. Chem.* **1976**, *41*, 2362–2367.
(119) Kobayashi, T.; Hirai, T.; Tsunetsugu, J.; Hayashi, H.; Nozoe, T. Reversible Photo-Valence Isomerization of Troponoids. *Tetrahedron* **1975**, *31*, 1483–1489.
(120) Abraham, W.; Paulick, W.; Kreysig, D. Photochemie Substituierter Cycloheptatriene—VI: Diarylsubstituierte Cycloheptatriene *Tetrahedron* **1979**, *35*, 2269–2273.
(121) Abraham, W.; Paulick, W.; Kreysig, D. Photochemie Substituierter Cycloheptatriene. XI Cyclisierung und Cycloreversion. *J. Prak. Chem.* **1981**, *323*, 427–434.
(122) Trozzolo, A. M.; Leslie, T. M.; Sarpotdar, A. S.; Small, R. D.; Ferraudi, G. J.; Minh, T. D.; Hartless, R. L. Photochemistry of Some Three-Membered Heterocycles. *Pure and Appl. Chem.* **1979**, *51*, 261–270.
(123) Dürr, H. Perspectives in Photochromism: A Novel System Based on the 1,5-Electrocyclization of Heteroanalogous Pentadienyl Anions. *Angew. Chem. Int. Ed. 28*, 413–431.
(124) Thap Do Minh; Trozzolo, A. M. Photochromic Aziridines. I. Mechanism of Photochromism in 1,3-Diazabicyclo[3.1.0]Hex-3-Enes and Related Aziridines. *J. Am. Chem. Soc.* **1972**, *94*, 4046–4048.
(125) Bren', V. A.; Dubonosov, A. D.; Minkin, V. I.; Chernoivanov, V. A. Norbornadiene–Quadricyclane — an Effective Molecular System for the Storage of Solar Energy. *Russ. Chem. Rev.* **1991**, *60*, 451–469.
(126) Dubonosov, A. D.; Bren, V. A.; Chernoivanov, V. A. Norbornadiene–Quadricyclane as an Abiotic System for the Storage of Solar Energy. *Russ. Chem. Rev.* **2002**, *71*, 917–927.
(127) Lennartson, A.; Roffey, A.; Moth-Poulsen, K. Designing Photoswitches for Molecular Solar Thermal Energy Storage. *Tetrahedron Lett.* **2015**, *56*, 1457–1465.
(128) An, X.; Xie, Y. Enthalpy of Isomerization of Quadricyclane to Norbornadiene. *Thermochimica Acta* **1993**, *220*, 17–25.

(129) Doering, W. v. E.; Roth, W. R.; Breuckmann, R.; Figge, L.; Lennartz, H.-W.; Fessner, W.-D.; Prinzbach, H. Verbotene Reaktionen. — [2+2]-Cycloreversion Starrer Cyclobutane. *Chem. Ber.* **1988**, *121*, 1–9.
(130) Miki, S.; Asako, Y.; Yoshida, Z. Photochromic Solid Films Prepared by Doping with Donor–Acceptor Norbornadienes. *Chem. Lett.* **1987**, *16*, 195–198.
(131) Lainé, P.; Marvaud, V.; Gourdon, A.; Launay, J.-P.; Argazzi, R.; Bignozzi, C.-A. Electron Transfer through Norbornadiene and Quadricyclane Moieties as a Model for Molecular Switching. *Inorg. Chem.* **1996**, *35*, 711–714.
(132) Gray, V.; Lennartson, A.; Ratanalert, P.; Börjesson, K.; Moth-Poulsen, K. Diaryl-Substituted Norbornadienes with Red-Shifted Absorption for Molecular Solar Thermal Energy Storage. *Chem. Commun.* **2014**, *50*, 5330–5332.
(133) Dubonosov, A. D.; Galichev, S. V.; Chernoivanov, V. A.; Bren', V. A.; Minkin, V. I. Synthesis and Photoinitiated Isomerizations of 3-(4-Nitrophenyl)-and 3-(4-Aminophenyl)Bicyclo[2.2.1]Hepta-2,5-Diene-2-Carbaldehyde and -2-Carboxylic Acid Derivatives. *Russ. J. Org. Chem.* **2001**, *37*, 67–71.
(134) Nagai, T.; Fujii, K.; Takahashi, I.; Shimada, M. Trifluoromethyl-Substituted Donor–Acceptor Norbornadiene, Useful Solar Energy Material. *Bull. Chem. Soc. Jpn.* **2001**, *74*, 1673–1678.
(135) Hamada, T.; Iijima, H.; Yamamoto, T.; Numao, N.; Hirao, K.; Yonemitsu, O. Photochemical Formation of Strained Cage Compounds and Their Acid-Catalysed Reversion as a Preliminary Model for Light Energy Conversion. *J. Chem. Soc., Chem. Commun.* **1980**, *15*, 696–697.
(136) Morrison, H.; Curtis, H.; McDowell, T. Solvent Effects on the Photodimerization of Coumarin. *J. Am. Chem. Soc.* **1966**, *88*, 5415–5419.
(137) Bernstein, H. I.; Quimby, W. C. The Photochemical Dimerization of Trans-Cinnamic Acid. *J. Am. Chem. Soc.* **1943**, *65*, 1845–1846.
(138) Mustafa, A. Dimerization Reactions in Sunlight. *Chem. Rev.* **1952**, *51*, 1–23.
(139) Kawai, S.; Nakashima, T.; Atsumi, K.; Sakai, T.; Harigai, M.; Imamoto, Y.; Kamikubo, H.; Kataoka, M.; Kawai, T. Novel Photochromic Molecules Based on 4,5-Dithienyl Thiazole with Fast Thermal Bleaching Rate. *Chem. Mater.* **2007**, *19*, 3479–3483.
(140) Nakashima, T.; Atsumi, K.; Kawai, S.; Nakagawa, T.; Hasegawa, Y.; Kawai, T. Photochromism of Thiazole-Containing Triangle Terarylenes. *Eur. J. Org. Chem.* **2007**, 3212–3218.
(141) Yokoyama, Y.; Kurita, Y. Photochromism of Fulgides and Related Compounds. *Mol. Cryst. Liq. Cryst. Sci. Tech. A.* **1994**, *246*, 87–94.
(142) Yokoyama, Y. Fulgides for Memories and Switches. *Chem. Rev.* **2000**, *100*, 1717–1740.
(143) Herder, M.; Schmidt, B. M.; Grubert, L.; Pätzel, M.; Schwarz, J.; Hecht, S. Improving the Fatigue Resistance of Diarylethene Switches. *J. Am. Chem. Soc.* **2015**, *137*, 2738–2747.
(144) Schmidt, R.; Drews, W.; Brauer, H.-D. Die Entwicklung eines neuen Photochromen Strukturprinzips Basierend auf der Reversiblen Photo-Oxidation. *J. Photochem.* **1982**, *18*, 365–378.
(145) Brauer, H.-D.; Schmidt, R. Wavelength Effects on the Photocycloreversion Quantum Yield of some Photochromic Endoperoxides. *Photochem. Photobiol.* **1985**, *41*, 119–122.
(146) Ihmels, H. Synthesis, Fluorescence Properties, and Head-to-Tail Regioselectivity in the Photodimerization of a Donor–Acceptor-Substituted Anthracene. *Eur. J. Org. Chem.* **1999**, 1595–1600.
(147) Greene, F. D.; Misrock, S. L.; Wolfe, J. R. The Structure of Anthracene Photodimers. *J. Am. Chem. Soc.* **1955**, *77*, 3852–3855.
(148) Castellan, A.; Lapouyade, R.; Bouas-Laurent, H.; Lallemand, J. Y. Head-to-Head Mixed Photodimers between Monomesosubstituted Anthracenes; Control of Photocycloaddition Selectivity by Charge-Transfer and Dipole-Dipole Interactions. *Tetrahedron Lett.* **1975**, *16*, 2467–2470.

(149) McSkimming, G.; Tucker, J. H. R.; Bouas-Laurent, H.; Desvergne, J.-P. An Anthracene-Based Photochromic System That Responds to Two Chemical Inputs. *Angew. Chem. Int. Ed.* **2000**, *39*, 2167–2169.
(150) Castellan, A.; Lacoste, J.-M.; Bouas-Laurent, H. Study of Non-Conjugated Bichromophoric Systems, the so-Called 'Jaw Photochromic Materials'. Part 1. Photocyclomerization and Fluorescence of Bis-9-Anthrylmethyl Ethers. *J. Chem. Soc. Perk. Trans. 2* **1979**, 411–419.
(151) Goerner, H.; Fischer, C.; Gierisch, S.; Daub, J. Dihydroazulene/Vinylheptafulvene Photochromism: Effects of Substituents, Solvent, and Temperature in the Photorearrangement of Dihydroazulenes to Vinylheptafulvenes. *J. Phys. Chem.* **1993**, *97*, 4110–4117.
(152) Broman, S. L.; Petersen, M. Å.; Tortzen, C. G.; Kadziola, A.; Kilså, K.; Nielsen, M. B. Arylethynyl Derivatives of the Dihydroazulene/Vinylheptafulvene Photo/Thermoswitch: Tuning the Switching Event. *J. Am. Chem. Soc.* **2010**, *132*, 9165–9174.
(153) Tamai, N.; Miyasaka, H. Ultrafast Dynamics of Photochromic Systems. *Chem. Rev.* **2000**, *100*, 1875–1890.
(154) Irie, M.; Mohri, M. Thermally Irreversible Photochromic Systems. Reversible Photocyclization of Diarylethene Derivatives. *J. Org. Chem.* **1988**, *53*, 803–808.
(155) Erko, F. G.; Berthet, J.; Patra, A.; Guillot, R.; Nakatani, K.; Métivier, R.; Delbaere, S. Spectral, Conformational and Photochemical Analyses of Photochromic Dithienylethene: Cis-1,2-Dicyano-1,2-Bis(2,4,5-Trimethyl-3-Thienyl)Ethene Revisited. *Eur. J. Org. Chem.* **2013**, 7809–7814.
(156) Applequist, D. E.; Lintner, M. A.; Searle, R. Photocyclizations of Compounds Containing Two Anthracene Rings. *J. Org. Chem.* **1968**, *33*, 254–259.
(157) Celani, P.; Bernardi, F.; Olivucci, M.; Robb, M. A. Conical Intersection Mechanism for Photochemical Ring Opening in Benzospiropyran Compounds. *J. Am. Chem. Soc.* **1997**, *119*, 10815–10820.
(158) Gómez, I.; Reguero, M.; Robb, M. A. Efficient Photochemical Merocyanine-to-Spiropyran Ring Closure Mechanism through an Extended Conical Intersection Seam. A Model CASSCF/CASPT2 Study. *J. Phys. Chem. A* **2006**, *110*, 3986–3991.
(159) Klajn, R. Spiropyran-Based Dynamic Materials. *Chem. Soc. Rev.* **2013**, *43*, 148–184.
(160) Johns, V. K.; Peng, P.; DeJesus, J.; Wang, Z.; Liao, Y. Visible-Light-Responsive Reversible Photoacid Based on a Metastable Carbanion. *Chem. Eur. J.* **2014**, *20*, 689–692.
(161) Peng, P.; Strohecker, D.; Liao, Y. Negative Photochromism of a TCF Chromophore. *Chem. Commun.* **2011**, *47*, 8575–8577.
(162) Lerch, M. M.; Wezenberg, S. J.; Szymanski, W.; Feringa, B. L. Unraveling the Photoswitching Mechanism in Donor–Acceptor Stenhouse Adducts. *J. Am. Chem. Soc.* **2016**, *138*, 6344–6347.
(163) Helmy, S.; Leibfarth, F. A.; Oh, S.; Poelma, J. E.; Hawker, C. J.; Read de Alaniz, J. Photoswitching Using Visible Light: A New Class of Organic Photochromic Molecules. *J. Am. Chem. Soc.* **2014**, *136*, 8169–8172.
(164) Yamaguchi, T.; Kamihashi, Y.; Ozeki, T.; Uyama, A.; Kitai, J.; Kasuno, M.; Sumaru, K.; Kimura, Y.; Yokojima, S.; Nakamura, S.; et al. Photochromic Reaction of Diarylethenes Having Phenol Moiety as an Aryl Ring. *Bull. Chem. Soc. Jpn.* **2014**, *87*, 528–538.
(165) Kathan, M.; Eisenreich, F.; Jurissek, C.; Dallmann, A.; Gurke, J.; Hecht, S. Light-Driven Molecular Trap Enables Bidirectional Manipulation of Dynamic Covalent Systems. *Nat. Chem.* **2018**, *10*, 1031-1036.
(166) Sheepwash, M. A. L.; Mitchell, R. H.; Bohne, C. Mechanistic Insights into the Photochromism of Trans-10b,10c-Dimethyl-10b,10c-Dihydropyrene Derivatives. *J. Am. Chem. Soc.* **2002**, *124*, 4693–4700.
(167) Ayub, K.; Zhang, R.; Robinson, S. G.; Twamley, B.; Williams, R. V.; Mitchell, R. H. Suppressing the Thermal Metacyclophanediene to Dihydropyrene Isomerization: Synthesis and Rearrangement of 8,16-Dicyano[2.2]Metacyclophane-1,9-Diene and Evidence Supporting the Proposed Biradicaloid Mechanism. *J. Org. Chem.* **2008**, *73*, 451–456.

(168) Kishida, M.; Kusamoto, T.; Nishihara, H. Photoelectric Signal Conversion by Combination of Electron-Transfer Chain Catalytic Isomerization and Photoisomerization on Benzodimethyldihydropyrenes. *J. Am. Chem. Soc.* **2014**, *136*, 4809–4812.
(169) Boekelheide, V.; Phillips, J. B. 2,7-Diacetoxy-Trans-15,16-Dimethyl-15,16-Dihydropyrene. A Novel Aromatic System with Methyl Groups Internal to the π-Electron Cloud. *J. Am. Chem. Soc.* **1963**, *85*, 1545–1546.
(170) Boekelheide, V.; Phillips, J. B. trans-15,16-dimethyldihydropyrene: A new type of aromatic system having methyl groups within the cavity of the π-electron cloud. *Proc. Nat. Acad. Sci. U. S.* **1964**, *51*, 550–552.
(171) Mitchell, R. H.; Boekelheide, V. Transformation of Sulfide Linkages to Carbon-Carbon Double Bond. Syntheses of Cis- and Trans-15,16-Dimethyldihydropyrene and Trans-15,16-Dihydropyrene. *J. Am. Chem. Soc.* **1974**, *96*, 1547–1557.
(172) Mitchell, R. H. The Metacyclophanediene-Dihydropyrene Photochromic π Switch. *Eur. J. Org. Chem.* **1999**, 2695–2703.
(173) Tashiro, M.; Yamato, T. Selective Preparation 29. Preparation of 2,6-Bis(Chloromethyl)- and of 2,6-Bis(Mercaptomethyl)-4-Substituted-Tert-Butylbenzenes. *Org. Prep. Proc. Intern.* **1981**, *13*, 1–7.
(174) Tashiro, M.; Yamato, T. Metacyclophanes and Related Compounds. 4. Halogenations of 8,16-Dialkyl-Anti-5,13-Di-Tert-Butyl[2.2]Metacyclophan-1-Enes and 2,7-Di-Tert-Butyl-Trans-10b,10c-Dialkyl-10b,10c-Dihydropyrenes. *J. Am. Chem. Soc.* **1982**, *104*, 3701–3707.
(175) Phillips, J. B.; Molyneux, R. J.; Sturm, E.; Boekelheide, V. Aromatic Molecules Bearing Substituents within the Cavity of the π-Electron Cloud. Chemical Properties of Trans-15,16-Dimethyldihydropyrene. *J. Am. Chem. Soc.* **1967**, *89*, 1704–1709.
(176) Mitchell, R. H.; Zhou, P. The Synthesis and Trapping of the First [14]Annulyne with Benzyne like Reactivity. A Fast Route to Several Annelated Bridged Annulenes. *Tetrahedron Lett.* **1990**, *31*, 5277–5280.
(177) Ayub, K.; Mitchell, R. H. Syntheses of Dihydropyrene–Cyclophanediene Negative Photochromes Containing Internal Alkenyl and Alkynyl Groups and Comparison of Their Photochemical and Thermochemical Properties. *J. Org. Chem.* **2014**, *79*, 664–678.
(178) Mitchell, R. H. Measuring Aromaticity by NMR. *Chem. Rev.* **2001**, *101*, 1301–1316.
(179) Ayub, K.; Li, R.; Bohne, C.; Williams, R. V.; Mitchell, R. H. Calculation Driven Synthesis of an Excellent Dihydropyrene Negative Photochrome and Its Photochemical Properties. *J. Am. Chem. Soc.* **2011**, *133*, 4040–4045.
(180) Boekelheide, V.; Pepperdine, W. Aromatic Molecules Bearing Substituents within the Cavity of the π-Electron Cloud. XXII. Synthesis of Trans-1,3,15,16-Tetramethyl-15,16-Dihydro-2-Azapyrene. *J. Am. Chem. Soc.* **1970**, *92*, 3684–3688.
(181) Mitchell, R. H.; Iyer, V. S. Synthesis and Relative Diatropicity of a Remarkably Aromatic Thia[13]Annulene. *J. Am. Chem. Soc.* **1996**, *118*, 722–726.
(182) Straight, S. D.; Andréasson, J.; Kodis, G.; Bandyopadhyay, S.; Mitchell, R. H.; Moore, T. A.; Moore, A. L.; Gust, D. Molecular AND and INHIBIT Gates Based on Control of Porphyrin Fluorescence by Photochromes. *J. Am. Chem. Soc.* **2005**, *127*, 9403–9409.
(183) Lee, H.-W.; Robinson, S. G.; Bandyopadhyay, S.; Mitchell, R. H.; Sen, D. Reversible Photo-Regulation of a Hammerhead Ribozyme Using a Diffusible Effector. *J. Mol. Biol.* **2007**, *371*, 1163–1173.
(184) Bakkar, A.; Cobo, S.; Lafolet, F.; Saint-Aman, E.; Royal, G. A New Surface-Bound Molecular Switch Based on the Photochromic Dimethyldihydropyrene with Light-Driven Release of Singlet Oxygen Properties. *J. Mater. Chem. C* **2015**, *3*, 12014–12017.
(185) Cobo, S.; Lafolet, F.; Saint-Aman, E.; Philouze, C.; Bucher, C.; Silvi, S.; Credi, A.; Royal, G. Reactivity of a Pyridinium-Substituted Dimethyldihydropyrene Switch under Aerobic Conditions: Self-Sensitized Photo-Oxygenation and Thermal Release of Singlet Oxygen. *Chem. Commun.* **2015**, *51*, 13886–13889.

(186) Garmshausen, Y.; Klaue, K.; Hecht, S. Dihydropyrene as an Aromaticity Probe for Partially Quinoid Push–Pull Systems. *ChemPlusChem* **2017**, *82*, 1025–1029.
(187) Garmshausen, Y. Synthese Photoschaltbarer Terphenyle Und Neuer Sexiphenylderivate, Diploma Thesis, Humboldt-Universität Zu Berlin. **2013**.
(188) Mitchell, R. H.; Chen, Y.; Iyer, V. S.; Lau, D. Y. K.; Baldridge, K. K.; Siegel, J. S. Bond Fixation in a [14]Annulene: Synthesis, Characterization, and Ab Initio Computations of Furan Adducts of Dimethyldihydropyrene. *J. Am. Chem. Soc.* **1996**, *118*, 2907–2911.
(189) Haag, B. A.; Sämann, C.; Jana, A.; Knochel, P. Practical One-Pot Preparation of Magnesium Di(Hetero)Aryl- and Magnesium Dialkenylboronates for Suzuki–Miyaura Cross-Coupling Reactions. *Angew. Chem. Int. Ed.* **2011**, *50*, 7290–7294.
(190) Catalyst. In *IUPAC Compendium of Chemical Terminology*; Nič, M., Jirát, J., Košata, B., Jenkins, A., McNaught, A., Eds.; IUPAC: Research Triagle Park, NC, **2009**.
(191) Turro, N. J.; McVey, J.; Ramamurthy, V.; Lechtken, P. Adiabatic Photoreactions of Organic Molecules. *Angew. Chem. Int. Ed.* **1979**, *18*, 572–586.
(192) Bouas-Laurent, H.; Dürr, H. Organic Photochromism (IUPAC Technical Report). *Pure Appl. Chem.* **2001**, *73*, 639–665.
(193) Dulić, D.; Kudernac, T.; Pužys, A.; Feringa, B. L.; van Wees, B. J. Temperature Gating of the Ring-Opening Process in Diarylethene Molecular Switches. *Adv. Mater.* **2007**, *19*, 2898–2902.
(194) Kudernac, T.; Kobayashi, T.; Uyama, A.; Uchida, K.; Nakamura, S.; Feringa, B. L. Tuning the Temperature Dependence for Switching in Dithienylethene Photochromic Switches. *J. Phys. Chem. A* **2013**, *117*, 8222–8229.
(195) Nakamura, S.; Uchida, K.; Hatakeyama, M. Potential Energy Surfaces and Quantum Yields for Photochromic Diarylethene Reactions. *Molecules* **2013**, *18*, 5091–5103.
(196) Bohne, C.; Mitchell, R. H. Characterization of the Photochromism of Dihydropyrenes with Photophysical Techniques. *J. Photochem. Photobiol. C* **2011**, *12*, 126–137.
(197) Kasha, M. Characterization of Electronic Transitions in Complex Molecules. *Discuss. Faraday Soc.* **1950**, *9*, 14–19.
(198) Tashiro, M.; Yamato, T. Halogenation of 2,7-di-*tert*-butyl-*trans*-10b,10c-dialkyl-10b,10c-dihydropyrenes. *Chem. Lett.* **1980**, *9*, 1127–1130.
(199) Tashiro, M.; Yamato, T. Selective Preparation. 30. A Convenient Preparation of 5,13-Di-Tert-Butyl-8,16-Disubstituted-[2.2]Metacyclophanes and Their Trans-Tert-Butylation and Halogenation Reactions. *J. Org. Chem.* **1981**, *46*, 1543–1552.
(200) Harris, T.; Neuschwander, B.; Boekelheide, V. Synthesis of Trans-15-n-Butyl-16-Methyldihydropyrene. Synthetic Access to 1,2,3-Trisubstituted Benzene Derivatives via Direct Alkylation of 1,3-Bis(4',4'-Dimethyl-2'-Oxazolinyl)Benzene. *J. Org. Chem.* **1978**, *43*, 727–730.
(201) Murakami, S.; Tsutsui, T.; Saito, S.; Yamato, T.; Tashiro, M. Photochromism of 10b,10c-Dihydropyrene Derivatives with the *t*-Butyl Groups at 2,7-Positions. *Nippon Kagaku Kaishi* **1988**, *2*, 221–229.
(202) Schareina, T.; Zapf, A.; Mägerlein, W.; Müller, N.; Beller, M. A New Palladium Catalyst System for the Cyanation of Aryl Chlorides with $K_4[Fe(CN)_6]$. *Tetrahedron Lett.* **2007**, *48*, 1087–1090.
(203) Sumi, T.; Takagi, Y.; Yagi, A.; Morimoto, M.; Irie, M. Photoirradiation Wavelength Dependence of Cycloreversion Quantum Yields of Diarylethenes. *Chem. Commun.* **2014**, *50*, 3928–3930.
(204) Thurn, J.; Maier, J.; Pärs, M.; Gräf, K.; Thelakkat, M.; Köhler, J. Temperature Dependence of the Conversion Efficiency of Photochromic Perylene Bisimide Dithienylcyclopentene Triads Embedded in a Polymer. *Phys. Chem. Chem. Phys.* **2017**, *19*, 26065–26071.
(205) Russew, M.-M.; Hecht, S. Photoswitches: From Molecules to Materials. *Adv. Mater.* **2010**, *22*, 3348–3360.
(206) Dulić, D.; van der Molen, S. J.; Kudernac, T.; Jonkman, H. T.; de Jong, J. J. D.; Bowden, T. N.; van Esch, J.; Feringa, B. L.; van Wees, B. J. One-Way Optoelectronic Switching of Photochromic Molecules on Gold. *Phys. Rev. Lett.* **2003**, *91*, 207402.

(207) Kuldová, K.; Tsyganenko, K.; Corval, A.; Trommsdorff, H. P.; Bens, A. T.; Kryschi, C. Photo-Switchable Dithienylethenes: Threshold of the Photoreactivity. *Synth. Met.* **2000**, *115*, 163–166.
(208) Irie, M.; Eriguchi, T.; Takada, T.; Uchida, K. Photochromism of Diarylethenes Having Thiophene Oligomers as the Aryl Groups. *Tetrahedron* **1997**, *53*, 12263–12271.
(209) Irie, M.; Lifka, T.; Kobatake, S.; Kato, N. Photochromism of 1,2-Bis(2-Methyl-5-Phenyl-3-Thienyl)Perfluorocyclopentene in a Single-Crystalline Phase. *J. Am. Chem. Soc.* **2000**, *122*, 4871–4876.
(210) Cox, J. M.; Walton, I. M.; Patel, D. G. (Dan); Xu, M.; Chen, Y.-S.; Benedict, J. B. The Temperature Dependent Photoswitching of a Classic Diarylethene Monitored by in Situ X-Ray Diffraction. *J. Phys. Chem. A* **2015**, *119*, 884–888.
(211) Boggio-Pasqua, M.; Garavelli, M. Rationalization and Design of Enhanced Photoinduced Cycloreversion in Photochromic Dimethyldihydropyrenes by Theoretical Calculations. *J. Phys. Chem. A* **2015**, *119*, 6024–6032.
(212) Dewar, M. J. S. A Molecular Orbital Theory of Organic Chemistry. IV Free Radicals. *J. Am. Chem. Soc.* **1952**, *74*, 3353–3354.
(213) Stella, L.; Janousek, Z.; Merényi, R.; Viehe, H. G. Stabilization of Radicals by "Capto-Dative" Substitution -C-C Addition to Radicophilic Olefins. *Angew. Chem. Int. Ed.* **1978**, *17*, 691–692.
(214) Viehe, H. G.; Janousek, Z.; Merenyi, R.; Stella, L. The Captodative Effect. *Acc. Chem. Res.* **1985**, *18*, 148–154.
(215) Mitscherlich, Eilhard. Ueber das Stickstoffbenzid. *Annalen der Pharmacie* **1834**, *12*, 311–314.
(216) Hartley, G. S. The *Cis*-Form of Azobenzene. *Nature* **1937**, *140*, 281.
(217) Hamon, F.; Djedaini-Pilard, F.; Barbot, F.; Len, C. Azobenzenes—Synthesis and Carbohydrate Applications. *Tetrahedron* **2009**, *65*, 10105–10123.
(218) Vetráková, Ľ.; Ladányi, V.; Anshori, J. A.; Dvořák, P.; Wirz, J.; Heger, D. The Absorption Spectrum of Cis -Azobenzene. *Photochem. Photobiol. Sci.***2017**, *16*, 1749–1756.
(219) Sekkat, Z.; Knoll, W. *Photoreactive Organic Thin Films*; Elsevier, **2002**.
(220) Yager, K. G.; Barrett, C. J. Novel Photo-Switching Using Azobenzene Functional Materials. *J. Photochem. Photobiol. A* **2006**, *182*, 250–261.
(221) Rabek, J. F.; Scott, G. W. *Photochemistry and Photophysics*; CRC Press, **1989**.
(222) Dong, M.; Babalhavaeji, A.; Samanta, S.; Beharry, A. A.; Woolley, G. A. Red-Shifting Azobenzene Photoswitches for in Vivo Use. *Acc. Chem. Res.* **2015**, *48*, 2662–2670.
(223) Bléger, D.; Hecht, S. Visible-Light-Activated Molecular Switches. *Angew. Chem. Int. Ed.* **2015**, *54*, 11338–11349.
(224) Sadovski, O.; Beharry, A. A.; Zhang, F.; Woolley, G. A. Spectral Tuning of Azobenzene Photoswitches for Biological Applications. *Angew. Chem. Int. Ed.* **2009**, *48*, 1484–1486.
(225) Samanta, S.; Beharry, A. A.; Sadovski, O.; McCormick, T. M.; Babalhavaeji, A.; Tropepe, V.; Woolley, G. A. Photoswitching Azo Compounds in Vivo with Red Light. *J. Am. Chem. Soc.* **2013**, *135*, 9777–9784.
(226) Beharry, A. A.; Sadovski, O.; Woolley, G. A. Azobenzene Photoswitching without Ultraviolet Light. *J. Am. Chem. Soc.* **2011**, *133*, 19684–19687.
(227) Samanta, S.; M. McCormick, T.; K. Schmidt, S.; S. Seferos, D.; Andrew Woolley, G. Robust Visible Light Photoswitching with ortho-Thiol Substituted Azobenzenes. *Chem. Commun.* **2013**, *49*, 10314–10316.
(228) Bléger, D.; Schwarz, J.; Brouwer, A. M.; Hecht, S. o-Fluoroazobenzenes as Readily Synthesized Photoswitches Offering Nearly Quantitative Two-Way Isomerization with Visible Light. *J. Am. Chem. Soc.* **2012**, *134*, 20597–20600.
(229) Dong, M.; Babalhavaeji, A.; J. Hansen, M.; Kálmán, L.; A. Woolley, G. Red, Far-Red, and near Infrared Photoswitches Based on Azonium Ions. *Chem. Commun.* **2015**, *51*, 12981–12984.
(230) Dong, M.; Babalhavaeji, A.; Collins, C. V.; Jarrah, K.; Sadovski, O.; Dai, Q.; Woolley, G. A. Near-Infrared Photoswitching of Azobenzenes under Physiological Conditions. *J. Am. Chem. Soc.* **2017**, *139*, 13483–13486.

(231) Yang, Y.; Hughes, R. P.; Aprahamian, I. Visible Light Switching of a BF_2-Coordinated Azo Compound. *J. Am. Chem. Soc.* **2012**, *134*, 15221–15224.
(232) Yang, Y.; Hughes, R. P.; Aprahamian, I. Near-Infrared Light Activated Azo-BF_2 Switches. *J. Am. Chem. Soc.* **2014**, *136*, 13190–13193.
(233) Paudler, W. W.; Zeiler, A. G. Diazocine Chemistry. VI. Aromaticity of 5,6-Dihydrodibenzo[b,f][1,2]Diazocine. *J. Org. Chem.* **1969**, *34*, 3237–3239.
(234) Siewertsen, R.; Neumann, H.; Buchheim-Stehn, B.; Herges, R.; Näther, C.; Renth, F.; Temps, F. Highly Efficient Reversible Z−E Photoisomerization of a Bridged Azobenzene with Visible Light through Resolved S_1(n-π*) Absorption Bands. *J. Am. Chem. Soc.* **2009**, *131*, 15594–15595.
(235) Sell, H.; Näther, C.; Herges, R. Amino-Substituted Diazocines as Pincer-Type Photochromic Switches. *Beilstein J. Org. Chem.y* **2013**, *9*, 1–7.
(236) Hammerich, M.; Schütt, C.; Stähler, C.; Lentes, P.; Röhricht, F.; Höppner, R.; Herges, R. Heterodiazocines: Synthesis and Photochromic Properties, Trans to Cis Switching within the Bio-Optical Window. *J. Am. Chem. Soc.* **2016**, *138*, 13111–13114.
(237) Calbo, J.; Weston, C. E.; White, A. J. P.; Rzepa, H. S.; Contreras-García, J.; Fuchter, M. J. Tuning Azoheteroarene Photoswitch Performance through Heteroaryl Design. *J. Am. Chem. Soc.* **2017**, *139*, 1261–1274.
(238) Weston, C. E.; Richardson, R. D.; Haycock, P. R.; White, A. J. P.; Fuchter, M. J. Arylazopyrazoles: Azoheteroarene Photoswitches Offering Quantitative Isomerization and Long Thermal Half-Lives. *J. Am. Chem. Soc.* **2014**, *136*, 11878–11881.
(239) Weston, C. E.; Richardson, R. D.; Fuchter, M. J. Photoswitchable Basicity through the Use of Azoheteroarenes. *Chem. Commun.* **2016**, *52*, 4521–4524.
(240) Wendler, T.; Schütt, C.; Näther, C.; Herges, R. Photoswitchable Azoheterocycles via Coupling of Lithiated Imidazoles with Benzenediazonium Salts. *J. Org. Chem.* **2012**, *77*, 3284–3287.
(241) Otsuki, J.; Suwa, K.; Narutaki, K.; Sinha, C.; Yoshikawa, I.; Araki, K. Photochromism of 2-(Phenylazo)Imidazoles. *J. Phys. Chem. A* **2005**, *109*, 8064–8069.
(242) Frankel, M.; Wolovsky, R.; Fischer, E. Geometrical Isomerism of the Azonaphthalenes. *J. Chem. Soc.* **1955**, 3441–3445.
(243) Fischer, E.; Frankel, M.; Wolovsky, R. Wavelength Dependence of Photoisomerization Equilibria in Azocompounds. *J. Chem. Phys.* **1955**, *23*, 1367–1367.
(244) Webster, O. W. Diazotetracyanocyclopentadiene. *J. Am. Chem. Soc.* **1966**, *88*, 4055–4060.
(245) Middleton, W. J.; Heckert, R. E.; Little, E. L.; Krespan, C. G. Cyanocarbon Chemistry. III Addition Reactions of Tetracyanoethylene. *J. Am. Chem. Soc.* **1958**, *80*, 2783–2788.
(246) Webster, O. W. Hexacyanobutadiene. *J. Am. Chem. Soc.* **1964**, *86*, 2898–2902.
(247) Rau, H. Spectroscopic Properties of Organic Azo Compounds. *Angew. Chem. Int. Ed.* **1973**, *12*, 224–235.
(248) Webster, O. W. Diazotetracyanocyclopentadiene and Its Conversion to Tetracyanocyclopentadienide and Pentacyanocyclopentadienide. *J. Am. Chem. Soc.* **1965**, *87*, 1820–1821.
(249) Bacsa, J.; Less, R. J.; Skelton, H. E.; Soracevic, Z.; Steiner, A.; Wilson, T. C.; Wood, P. T.; Wright, D. S. Assembly of the First Fullerene-Type Metal–Organic Frameworks Using a Planar Five-Fold Coordination Node. *Angew. Chem. Int. Ed.* **2011**, *50*, 8279–8282.
(250) J. Less, R.; C. Wilson, T.; McPartlin, M.; T. Wood, P.; S. Wright, D. Transition Metal Complexes of the Pentacyanocyclopentadienide Anion. *Chem. Commun.* **2011**, *47*, 10007–10009.
(251) Kurihara, M.; Matsuda, T.; Hirooka, A.; Yutaka, T.; Nishihara, H. Novel Photoisomerization of Azoferrocene with a Low-Energy MLCT Band and Significant Change of the Redox Behavior between the *Cis*- and *Trans* -Isomers. *J. Am. Chem. Soc.* **2000**, *122*, 12373–12374.
(252) Less, R. J.; Wilson, T. C.; Guan, B.; McPartlin, M.; Steiner, A.; Wood, P. T.; Wright, D. S. Solvent Direction of Molecular Architectures in Group 1 Metal Pentacyanocyclopentadienides. *Eur. J. Inorg. Chem.* **2013**, 1161–1169.

(253) Rau, H.; Rötger, D. Photochromic Azobenzenes Which Are Stable in the Trans and Cis Forms. *Mol. Cryst. Liq. Cryst. Sci. Tech. A.* **1994**, *246*, 143–146.
(254) Namkung, M. J.; Naimy, N. K.; Cole, C. A.; Ishikawa, N.; Fletcher, T. L. Fluorinated Azo Dyes. II. Synthesis and Spectral Properties of 2,6-Difluoro-4 and 2,3,5,6-Tetrafluoro-4-Aminoazobenzene and Their N-Methylated and 4'-Ethyl Derivatives. *J. Org. Chem.* **1970**, *35*, 728–733.
(255) Emond, M.; Le Saux, T.; Maurin, S.; Baudin, J.-B.; Plasson, R.; Jullien, L. 2-Hydroxyazobenzenes to Tailor PH Pulses and Oscillations with Light. *Chem. Eur. J.* **2010**, *16*, 8822–8831.
(256) Shao, Q.; Jiang, S. Molecular Understanding and Design of Zwitterionic Materials. *Adv. Mater.* **2015**, *27*, 15–26.
(257) Beverina, L.; Pagani, G. A. π-Conjugated Zwitterions as Paradigm of Donor–Acceptor Building Blocks in Organic-Based Materials. *Acc. Chem. Res.* **2014**, *47*, 319–329.
(258) Wei, H.; Insin, N.; Lee, J.; Han, H.-S.; Cordero, J. M.; Liu, W.; Bawendi, M. G. Compact Zwitterion-Coated Iron Oxide Nanoparticles for Biological Applications. *Nano Lett.* **2012**, *12*, 22–25.
(259) Page, Z. A.; Duzhko, V. V.; Emrick, T. Conjugated Thiophene-Containing Polymer Zwitterions: Direct Synthesis and Thin Film Electronic Properties. *Macromolecules* **2013**, *46*, 344–351.
(260) Lowe, A. B.; McCormick, C. L. Synthesis and Solution Properties of Zwitterionic Polymers. *Chem. Rev.* **2002**, *102*, 4177–4190.
(261) Schlenoff, J. B. Zwitteration: Coating Surfaces with Zwitterionic Functionality to Reduce Nonspecific Adsorption. *Langmuir* **2014**, *30*, 9625–9636.
(262) Chen, S.; Jiang, S. An New Avenue to Nonfouling Materials. *Adv. Mater.* **2008**, *20*, 335–338.
(263) Jiang, S.; Cao, Z. Ultralow-Fouling, Functionalizable, and Hydrolyzable Zwitterionic Materials and Their Derivatives for Biological Applications. *Adv. Mater.* **2010**, *22*, 920–932.
(264) Mi, L.; Jiang, S. Integrated Antimicrobial and Nonfouling Zwitterionic Polymers. *Angew. Chem. Int. Ed.* **2014**, *53*, 1746–1754.
(265) Cao, Z.; Jiang, S. Super-Hydrophilic Zwitterionic Poly(Carboxybetaine) and Amphiphilic Non-Ionic Poly(Ethylene Glycol) for Stealth Nanoparticles. *Nano Today* **2012**, *7*, 404–413.
(266) Tiyapiboonchaiya, C.; Pringle, J. M.; Sun, J.; Byrne, N.; Howlett, P. C.; MacFarlane, D. R.; Forsyth, M. The Zwitterion Effect in High-Conductivity Polyelectrolyte Materials. *Nat. Mater.* **2004**, *3*, 29–32.
(267) Byrne, N.; Howlett, P. C.; MacFarlane, D. R.; Forsyth, M. The Zwitterion Effect in Ionic Liquids: Towards Practical Rechargeable Lithium-Metal Batteries. *Adv. Mater.* **2005**, *17*, 2497–2501.
(268) Samanta, S.; Babalhavaeji, A.; Dong, M.; Woolley, G. A. Photoswitching of ortho-Substituted Azonium Ions by Red Light in Whole Blood. *Angew. Chem. Int. Ed.* **2013**, *52*, 14127–14130.
(269) Webster, O. W. Polycyanation. The Reaction of Cyanogen Chloride, Cyclopentadiene, and Sodium Hydride. *J. Am. Chem. Soc.* **1966**, *88*, 3046–3050.
(270) Binnemans, K. Ionic Liquid Crystals. *Chem. Rev.* **2005**, *105*, 4148–4204.
(271) Peters, A.; Branda, N. R. Limited Photochromism in Covalently Linked Double 1,2-Dithienylethenes. *Adv. Mater. Opt. Electron.* **2000**, *10*, 245–249.
(272) Kaieda, T.; Kobatake, S.; Miyasaka, H.; Murakami, M.; Iwai, N.; Nagata, Y.; Itaya, A.; Irie, M. Efficient Photocyclization of Dithienylethene Dimer, Trimer, and Tetramer: Quantum Yield and Reaction Dynamics. *J. Am. Chem. Soc.* **2002**, *124*, 2015–2024.
(273) Bens, A. T.; Frewert, D.; Kodatis, K.; Kryschi, C.; Martin, H.-D.; Trommsdorff, H. P. Coupling of Chromophores: Carotenoids and Photoactive Diarylethenes – Photoreactivity versus Radiationless Deactivation. *Eur. J. Org. Chem.* **1998**, 2333–2338.
(274) Mitchell, R. H.; Ward, T. R.; Wang, Y.; Dibble, P. W. Pi-Switches: Synthesis of Three-Way Molecular Switches Based on the Dimethyldihydropyrene−Metacyclophanediene Valence Isomerization. *J. Am. Chem. Soc.* **1999**, *121*, 2601–2602.
(275) Mitchell, R. H.; Bandyopadhyay, S. Linked Photoswitches Where Both Photochromes Open and Close. *Org. Lett.* **2004**, *6*, 1729–1732.

(276) Mitchell, R. H.; Bohne, C.; Wang, Y.; Bandyopadhyay, S.; Wozniak, C. B. Multistate π Switches: Synthesis and Photochemistry of a Molecule Containing Three Switchable Annelated Dihydropyrene Units. *J. Org. Chem.* **2006**, *71*, 327–336.
(277) Zhang, P.; Berg, D. J.; Mitchell, R. H.; Oliver, A.; Patrick, B. Platinum Complexes of Alkynyl-Substituted Dimethyldihydropyrenes. *Organometallics* **2012**, *31*, 8121–8134.
(278) Zhang, P.; Brkic, Z.; Berg, D. J.; Mitchell, R. H.; Oliver, A. G. Cobalt Complexes Containing Dimethyldihydropyrene-Substituted Cyclobutadiene Ligands. *Organometallics* **2011**, *30*, 5396–5407.
(279) Marsella, M. J.; Wang, Z.-Q.; Mitchell, R. H. Backbone Photochromic Polymers Containing the Dimethyldihydropyrene Moiety: Toward Optoelectronic Switches. *Org. Lett.* **2000**, *2*, 2979–2982.
(280) Becker, J. Synthese Multiphotochromer Dihydropyrenderivate, Bachelor Thesis, Humboldt-Universität Zu Berlin. **2015**.
(281) Muratsugu, S.; Kishida, M.; Sakamoto, R.; Nishihara, H. Comparative Study of Photochromic Ferrocene-Conjugated Dimethyldihydropyrene Derivatives. *Chem. Eur. J.* **2013**, *19*, 17314–17327.
(282) Muratsugu, S.; Kume, S.; Nishihara, H. Redox-Assisted Ring Closing Reaction of the Photogenerated Cyclophanediene Form of Bis(Ferrocenyl)Dimethyldihydropyrene with Interferrocene Electronic Communication Switching. *J. Am. Chem. Soc.* **2008**, *130*, 7204–7205.
(283) Vilà, N.; Royal, G.; Loiseau, F.; Deronzier, A. Photochromic and Redox Properties of Bisterpyridine Ruthenium Complexes Based on Dimethyldihydropyrene Units as Bridging Ligands. *Inorg. Chem.* **2011**, *50*, 10581–10591.
(284) Mitchell, R. H.; Brkic, Z.; Sauro, V. A.; Berg, D. J. A Photochromic, Electrochromic, Thermochromic Ru Complexed Benzannulene: An Organometallic Example of the Dimethyldihydropyrene−Metacyclophanediene Valence Isomerization. *J. Am. Chem. Soc.* **2003**, *125*, 7581–7585.
(285) Lange, I.; Reiter, S.; Pätzel, M.; Zykov, A.; Nefedov, A.; Hildebrandt, J.; Hecht, S.; Kowarik, S.; Wöll, C.; Heimel, G.; et al. Tuning the Work Function of Polar Zinc Oxide Surfaces Using Modified Phosphonic Acid Self-Assembled Monolayers. *Adv. Funct. Mater.* **2014**, *24*, 7014–7024.
(286) Maafi, M.; Maafi, M. Useful Spectrokinetic Methods for the Investigation of Photochromic and Thermo-Photochromic Spiropyrans. *Molecules* **2008**, *13*, 2260–2302.
(287) Skeean, R. W.; Goel, O. P. Convenient Syntheses of 1,3-Dihydro-1-Oxo-4-Isobenzofurancarboxylic Acid, 1,3-Dihydro-3-Oxo-4-Isobenzofurancarboxylic Acid, and the Homologous Acetic Acids. *Synthesis* **1990**, 628–630.
(288) Lindsay, W. S.; Stokes, P.; Humber, L. G.; Boekelheide, V. Syntheses of 4,12-Dimethyl[2.2]Metacyclophane. *J. Am. Chem. Soc.* **1961**, *83*, 943–949.
(289) Giannis, A.; Sandhoff, K. $LiBH_4(NaBH_4)/Me_3SiCl$, an Unusually Strong and Versatile Reducing Agent. *Angew. Chem. Int. Ed.* **1989**, *28*, 218–220.
(290) Mitchell, R. H.; Iyer, V. S.; Khalifa, N.; Mahadevan, R.; Venugopalan, S.; Weerawarna, S. A.; Zhou, P. An Experimental Estimation of Aromaticity Relative to That of Benzene. The Synthesis and NMR Properties of a Series of Highly Annelated Dimethyldihydropyrenes: Bridged Benzannulenes. *J. Am. Chem. Soc.* **1995**, *117*, 1514–1532.
(291) Sheldrick, G. M. SADABS, Program for Empirical Absorption Correction of Area Detector Data. *University of Göttingen: Germany* **1996**.
(292) Sheldrick, G. M. SHELXT-2013, Program for Crystal Structure Solution. *University of Göttingen: Germany* **2013**.
(293) Sheldrick, G. M. SHELXL-2014, Program for Crystal Structure Refinement. *University of Göttingen: Germany* **2014**.

7 Appendix

7.1 Abbreviations

CPD	*meta*-cyclophanediene
DCM	dichloromethane
DHP	dihydropyrene
DIBALH	diisobutylaluminium hydride
DMF	*N,N*-dimethylformamide
ESI	electrospray ionization
HOMO	highest occupied molecular orbital
HPLC	high performance liquid chromatography
LED	light-emitting diode
LUMO	lowest unoccupied molecular orbital
MS	mass spectrometry
NBS	*N*-bromosuccinimide
NMP	*N*-methyl-2-pyrrolidone
NMR	nuclear magnetic resonance
OFET	organic field effect transistor
OLED	organic light emitting device
PES	potential energy surface
PSS	photostationary state
TCCp	tetracyanocyclopentadienide
THEXI	thermally relaxed excited state
THF	tetrahydrofuran
UPLC	ultra performance liquid chromatography
UV	ultraviolet
vis	visible

7.2 Selbstständigkeitserklärung

Hiermit erkläre ich, die Dissertation selbstständig und nur unter Verwendung der von mir angegebenen Hilfsmittel angefertigt zu haben. Ich habe mich nicht anderweitig um einen Doktorgrad in dem Promotionsfach beworben und besitze keinen entsprechenden Doktorgrad. Die Promotionsordnung der Mathematisch-Naturwissenschaftlichen Fakultät, veröffentlicht im Amtlichen Mitteilungsblatt der Humboldt-Universität zu Berlin Nr. 42 am 11. Juli 2018, habe ich zur Kenntnis genommen.

Yves Garmshausen

7.3 Peer Reviewed Publications

[7] J. Niederhausen, Y. Zhang, F. Cheenicode Kabeer, Y. Garmshausen, B. M. Schmidt, Y. Li, K.-F. Braun, S. Hecht, A. Tkatchenko, N. Koch, S. W. Hla: "Subtle Fluorination of Conjugated Molecules Enables Stable Nanoscale Assemblies on Metal Surfaces" *J. Phys. Chem. C* **2018**, *122*, 18902-18911.

[6] K. Klaue, Y. Garmshausen, S. Hecht: "Taking Photochromism Beyond Visible: Direct One-Photon NIR Photoswitches Operating in the Biological Window" *Angew. Chem*. *Int. Ed.* **2018**, *57*, 1414-1417; *Angew. Chem.* **2018**, *130*, 1429-1432.

[5] C.-Y. Huang, A. Bonasera, L. Hristov, Y. Garmshausen, B. Schmidt, D. Jacquemin, S. Hecht: "N,N'-Disubstituted Indigos as Readily Available Red-Light Photoswitches with Tunable Thermal Half-Lives" *J. A. Chem. Soc.* **2017**, *139*, 15205-15211.

[4] Y. Garmshausen, K. Klaue, S. Hecht: "Dihydropyrene as an Aromaticity Probe for Partially Quinoid Push-Pull Systems" *ChemPlusChem* **2017**, *82*, 1025-1029.

[3] J. Meyer, A. Nickel, R. Ohmann, Lokamani, C. Toher, D. A. Ryndyk, Y. Garmshausen, S. Hecht, F. Moresco, G. Cuniberti: "Tuning the formation of discrete coordination nanostructures" *Chem. Commun.* **2015**, *51*, 12621-12624.

[2] M. Sparenberg, A. Zykov, P. Beyer, L. Pithan, C. Weber, Y. Garmshausen, F. Carla, S. Hecht, S. Blumstengel, F. Henneberger, S. Kowarik: "Controlling the growth mode of para-sexiphenyl (6P) on ZnO by partial fluorination" *Phys. Chem. Chem. Phys.* **2014**, *16*, 26084-26093.

[1] Y. Garmshausen, J. Schwarz, J. Hildebrandt, B. Kobin, M. Pätzel, S. Hecht: "Making Non-symmetrical Bricks: Synthesis of Insoluble Dipolar Sexiphenyls" *Org. Lett.* **2014**, *16*, 2838-2841.